The Government of
The Republic of the Union of Myanmar
Ministry of Education

Department of Higher Education

Universities Research Journal

Vol. 12, No. 2 December, 2020

The Government of
The Republic of the Union of Myanmar
Ministry of Education

Department of Higher Education

Universities Research Journal

Vol. 12, No. 2 December, 2020

Universities Research Journal 2019
Vol.12, No. 2
Chemistry, Mathematics, Computer Science, Industrial Chemistry, Marine Science

Editorial Board

Editors in Chief

Editors

Contents

I. Chemistry

Preparation, Characterization and Application of Wollastonite from Rice Husk Based-Nanosilica

Hsu Mon Kyaw Shwe[1], San San Myint[2] & Kyaw Naing[3]

Abstract

In this research, wollastonite was prepared from nanosilica and calcium oxide by hydrothermal method. At first, rice husk ash was prepared from rice husk by calcination at 650 °C for 6 h. Then nanosilica powder was prepared from rice husk ash. Wollastonite is used for treatment of acidic soil. Wollastonite can reduce the acidity of the soil. In this research, treatment of acidic soil with wollastonite was studied. Decades of acidic deposition is believed to have caused the loss of substantial amounts of calcium from forest soils. The process of 'calcium depletion' affected the chemistry of drainage waters in the region and may have impacted forest health. To study this phenomenon, one can applied wollastonite ($CaSiO_3$). The soil samples were collected from North Dagon Township. Before the treatment with wollastonite, the soil properties such as moisture content, pH, available K_2O and Fe, CEC, exchangeable Ca^{2+}, Mg^{2+}, K^+ , Al^{3+} and Na^+ were determined. The pH of the soil samples were increased 4.8 (zero day), 5.7 (after two weeks) and 6.5 (after four weeks). Therefore acidic soil can be treated with wollastonite prepared from rice husk. Cation exchange capacity (CEC) of soil was increased significantly after wollastonite application in the soil studied, primarily on the strength of the increased exchangeable Ca. After wollastonite addition to soil samples, the pH and exchangeable Ca concentration in the soils increased significantly. Exchangeable acidity and Al decreased significantly, thought the magnitudes of these decreases were less than the increases in exchangeable Ca and CEC.

Keywords: nanosilica, wollastonite, hydrothermal, soil acidity, calcination

Introduction

Rice husk is one of the major by-products derived in the milling of paddy rice. The quantity of rice husk depends on the kinds of paddy, grain type, soil and climate condition in which the paddy is cultivated and type of rice milled used (Lyenagbe and Mamat, 2012). The utilization of any rice husk will depend on its composition (FAO, 1997). Rice husk consists of

[1] Lecturer, Department of Chemistry, University of Yangon
[2] Associate Professor, Department of Chemistry, Pyay University
[3] Deputy Permanent Secretary, Dr, Ministry of Education, Myanmar

about 40% cellulose, 30% lignin group and 20% silica (Khemthong *et al.*, 2007). When rice husk is burnt approximately one fifth of the original weight is obtained as by product. Rice husk ash contains over 80% of silica and a small proportion of impurities such as K_2O, Na_2O and Fe_2O_3, which can be removed by acid leaching (Amutha, 2010).

Wollastonite is a chemically simple mineral named in honour of English mineralogist and chemist Sir W.H Wollaston. It is composed of calcium (Ca), silicon and oxygen (SiO_2, silica) with the chemical formular, $CaSiO_3$. It can contain some iron, magnesium, manganese, aluminium, potassium, sodium or strontium substituting for calcium in the mineral structure (Virta and Van Gosen, 2000). Wollastonite crystallizes in three polymorphic forms, low temperature triclinic, monoclinic or so called para-wollastonite and a high temperature form pseudo-wollastonite which occurs in a pseudo-hexagonal form (Yazdani *et al.***,** 2010).

Acidic deposition, primarily in the form of sulphuric and nitric acid, has resulted in the acidification of soil and surface water of the north-eastern United States, and many other regions of the world. There is a growing consensus that this acidification has resulted in the depletion of available calcium from many base poor soils. To study these relationships, calcium was added to the soil in the form of wollastonite ($CaSiO_3$), to replace the calcium believed to have been lost from the soil during the period of time (Johnson *et al.*, 2010).

Figure 1. Photograph of rice husk sample

Figure 2. Photograph of rice husk ash sample

Materials and Methods

In this work, the hydrothermal method was applied for synthesis of wollastonite by using nanosilica from rice husk. The rice husk samples were collected from Aung Mindalar Rice Mill, Insein Township, Yangon Region. Figure 3 shows the teflon-lined stainless steel autoclave (hydrothermal method). Characterization of wollastonite was carried out by using XRD

and SEM techniques. Then, the soil samples were collected from North Dagon Township, Yangon Region. Finally, the treated soil samples with wollastonite were determined by the physicochemical properties (pH, moisture, potassium, calcium, magnesium, iron, aluminium, available K_2O,cation exchange capacity (CEC) and sodium.

Figure 3. Teflon-lined stainless steel autoclave (hydrothermal method)

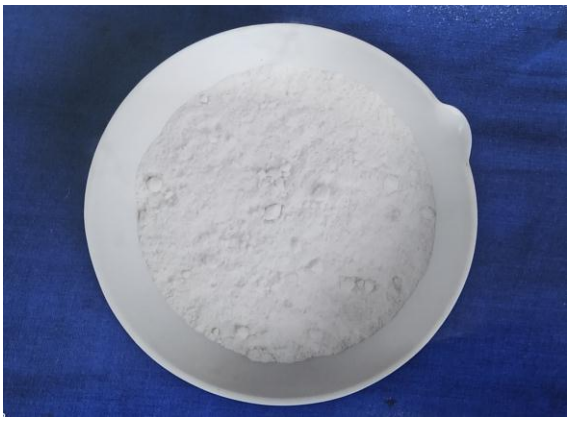

Figure 4. Photograph of nanosilica sample from rice husk

Results and Discussion

Characterization of the nanosilica sample from rice husk

Figure 5 shows XRD diffractogram of the nanosilica sample from rice husk. Formation of nanosilica was confirmed by the XRD diffractogram. All peaks of miller indices 101, 111, 220, 211, 212, 203, 301, 312, 214 and 321 of nanosilica samples were matched with standard library of JCPDS (82-1404). The XRD data of the synthesized nanosilica showed the crystalline nature free from impurities. Table 1 shows XRD data of nanosilica sample from rice husk. By using Scherrer equation, the crystalline size of nanosilica was found to be 22.83 nm. The micro structure of the prepared nanosilica from rice husk was studied by SEM. The SEM micrograph of the prepared nanosilica is described in Figure 6. So, it can be seen that the prepared nanosilica showed porous nature. There are some large size particles cubic structure in this figure, consisting of rice husk.

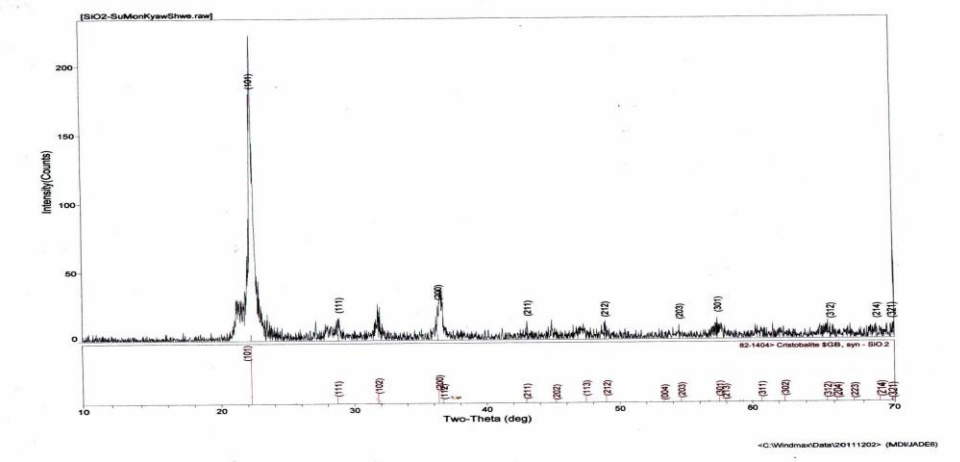

Figure 5. XRD diffractogram of the nanosilica sample from rice husk

Table 1. XRD Data of Nanosilica Sample from Rice Husk

#	2-Theta	d(Å)	(h k l)	BG	Height	Height%	Area	Area%	FWHM	XS(Å)	P/N
1	22.262	3.9900	(1 0 1)	0	180	100.0	4174	100.0	0.394	212	6.7
2	28.816	3.0957	(1 1 1)	0	16	8.9	222	5.3	0.236	384	2.0
3	36.344	2.4699	(2 0 0)	0	25	13.9	721	17.3	0.490	174	2.5
4	43.085	2.0977	(2 1 1)	0	13	7.2	155	3.7	0.203	484	1.8
5	48.889	1.8614	(2 1 2)	0	12	6.7	199	4.8	0.282	331	1.7
6	54.497	1.6824	(2 0 3)	0	10	5.6	131	3.1	0.223	449	1.6

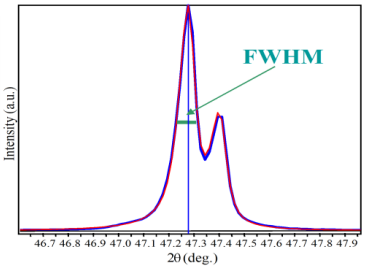

Scherrer Equation

$$t = \frac{K\lambda}{B\cos\theta}$$

Full Width at Half Maximum (FWHM) the width of the diffraction peak, in radians, at a height half-way between background and the peak maximum

t = crystalline size in nanometers
K = Scherrer constant
θ = Diffraction angle of the peak under consideration at FWHM (°)
λ = wavelength (Å)
B = the broading solely due to small crystalline size (FWHM radians)
t = 22.83 nm

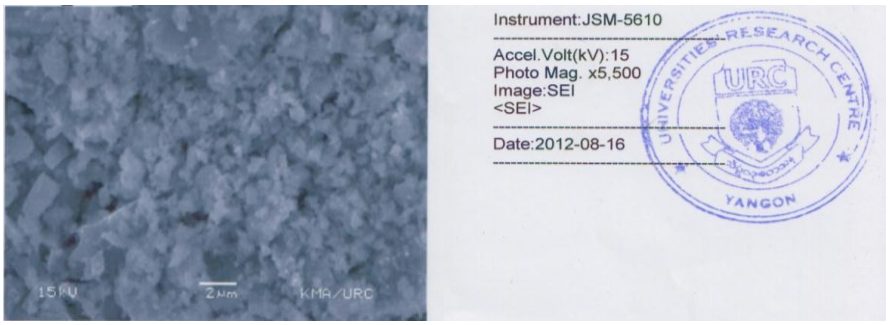

Figure 6. SEM micrograph of the nanosilica sample from rice husk

Characterization of the wollastonite from nanosilica and calcium oxide

Figure 7 shows XRD diffractogram of the wollastonite from nanosilica and calcium oxide. The XRD data of the synthesized the wollastonite from nanosilica and calcium oxide showed the larnite structure (Ca_2SiO_4). Larnite has a composition very close to wollastonite. This is compatible with XRD patterns of calcined samples. It can be seen that the intensity of larnite have increased, but the increase in the amount of wollastonite is more noticeable (Yazdani *et al.*, 2010). Figure 8 shows SEM microphotograph of the wollastonite from nanosilica and calcium oxide.

SEM microphotograph of the wollastonite at 1000 °C for 5 h were found to be acicular (needle) shape morphology.

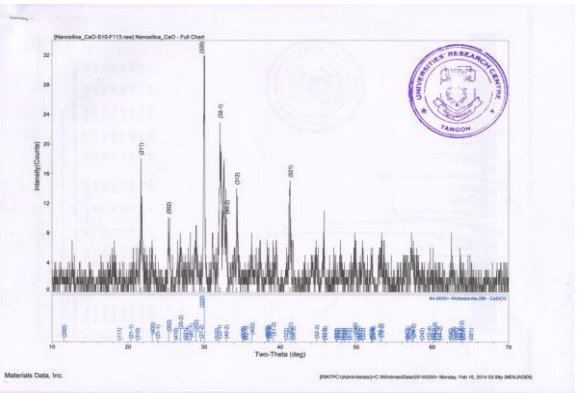

Figure 7. XRD diffractogram of the wollastonite from nanosilica and calcium oxide

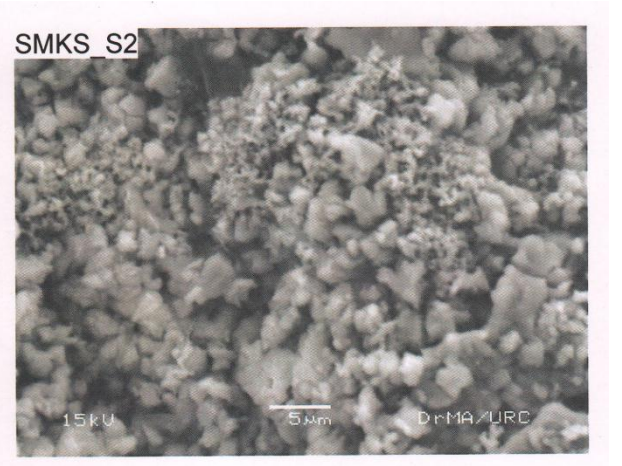

Figure 8. SEM microphotograph of the wollastonite from nanosilica and calcium oxide

The effect of pH and moisture content of the soil samples

Table 2 shows the physical properties (pH and moisture) of the soil samples. The soil pH is a measure of active acidity. When, soil pH decreases and soils become more acidic (Ulrich, 2009). The values of the pH were found to be 4.8 for pre-treatment, 5.7 for after two weeks and 6.5 for after four weeks. It was found that, the pH of the soil samples treated

with wollastonite for four weeks was neutralized. The moisture content of soil samples was found to be 0.45 % for pre-trement, 0.47 % for after two weeks and 0.49 % for after four weeks.

Determination of K^+, Ca^{2+}, Mg^{2+}, Fe, Al^{3+}, K_2O, CEC and Na^+

Table 3 shows changes in soil samples (before and after with wollastonite treated to soil samples). Nutrients such as calcium, magnesium, potassium, sodium and many other soil elements are cations. Nutrients retained by CEC are prevented from leaching out of the rooting zone, yet are held loosely enough to be available to growing plants. Cation exchange capacity (CEC) of soil was increased significantly after wollastonite application in the soil studied, primarily on the strength of the increased exchangeable Ca. After wollastonite addition to soil samples, the pH and exchangeable Ca concentration in the soils increased significantly. Exchangeable acidity and Al decreased significantly, thought the magnitudes of these decreases were less than the increases in exchangeable Ca and CEC.

Table 2. Physical Properties (pH and moisture) of the Soil Samples

No.	Soil Samples	pH	Moisture (%)
1.	Pre-treatment	4.8	0.45
2.	After two weeks	5.7	0.47
3.	After four weeks	6.5	0.49

Table 3. Changes in Soil Samples (before and after with wollastonite treated to soil samples)

Property	Pre-treatment	Post-treatment after two weeks	After four weeks
Exch.Ca (mmol/100g)	9.14	24.4	54.86
Exch.Mg (mmol/100g)	1.52	4.94	6.10

Property	Pre-treatment	Post-treatment after two weeks	After four weeks
Exch.K (mmol/100g)	0.22	0.23	0.24
Exch.Na (mmol/100g)	0.33	0.44	0.57
Fxch.Al (ppm)	1.13	0.86	0.84
Available K_2O (ppm)	10.24	10.43	10.85
Available Fe (ppm)	236.40	131.17	153.80
CEC (mmol/100g)	18.0	21.52	72.61

Conclusion

In this research, wollastonite was prepared from nanosilica and calcium oxide by hydrothermal method. Then nanosilica powder was prepared from rice husk ash. The treatment of acidic soil with wollastonite was studied. Before the treatment with wollastonite, the soil properties such as moisture content, pH, available K_2O and Fe, CEC, exchangeable Ca^{2+}, Mg^{2+}, K^{+}, Al^{3+} and Na^{+} were determined. Then 5 g of wollastonite mixed thoroughly with 10 g of soil samples and put into the pot. After two and four weeks' soil samples were taking out from the pot and analyzed. The pH of the soil samples was increased 4.8 (zero day), 5.7 (after two weeks) and 6.5 (after four weeks). Therefore, acidic soil can be treated with wollastonite prepared from rice husk. Cation exchange capacity (CEC) of soil was increased significantly after wollastonite application in the soil studied, primarily on the strength of the increased exchangeable Ca. After wollastonite addition to soil samples, the pH and exchangeable Ca concentration in the soils increased significantly. Exchangeable acidity and Al decreased significantly, thought the magnitudes of these decreases were less than the increases in exchangeable Ca and CEC. Wollastonite is used for treatment of acidic soil. Wollastonite can reduce the acidity of the soil. Therefore, wollastonite prepared from rice husk based-nanosilica was used for the treatment of acidic soil.

Acknowledgements

The author would like to express my deep appreciation to professor and head Dr Ni Ni Than, Department of Chemistry, University of Yangon, for her kind provision of the research paper. I also wish to express my profound gratitude to Dr Myint Myint Khine, Dr Myat Kyaw Thu and Dr Cho Cho, Professors, Department of Chemistry, University of Yangon, for their close supervision, kind and comments offered to me during the course of this research work.

References

Amutha, K., Ravibaskar, R., and Sivakumar, G., (2010), "Extraction, Synthesis and Characterization of Nanosilica from Rice Husk Ash", *International Journal of Nanotechnology and Applications*, **4**, 61-66

FAO, (1997), "Rice By- products in Asia", RAP Publication, The UN.RAP, Bangkok

Johnson, C. E., Driscoll, C.T., and Cho, Y., (2010), "Changes in Soil Chemistry Following a Watershed-Scale Application of Wollastonite ($CaSiO_3$) at Hubbard Brook", New Hampshire USA, 19th World Congress of Soil Science, Soil Solutions for a Changing World.

Khemthong, P., Prayoonpokarach, S., and Wittayakun, J., (2007), "Synthesis and Characterization of Zeolite LSX from Rice Husk Silica", *Suranaree J. Sci. Techno*l, **14**, 367-379

Lyenagbe, U., B., and Mamat, O., (2012), "Hydro Thermo-Baric Processing and Properties of Nano Silica from Rice Husk", *Applied Mechanics and Materials,* **152,** 177-182

Virta, R.L., and Van Gosen, B.S., (2000), "Wollastonite-AVersatile Industrial Mineral",U.S. Geological Survey, **4**, 1119-1128

Yazdani, A., Rezaie, H.R., and Ghassai, H., (2010), "Investigation of Hydrothermal Synthesis of Wollastonite Using Silica Nanosilica at Different Pressure", *Journal of Ceramic Processing Research*, **11,** 348-353

Study on the Effect of Media and pH on the Growth Rate of *Spirulina platensis* in Natural Seawater

Sit Thu Aung[1] & Min Oo[2]

Abstract

Spirulina platensis is the most important microalgae for human and animal as healthy food. In this experiment the growth rates of *S. platensis* were tested at five different media (F-2, Z-1, Z-2, urea and T-super, and PES) with different three pH values (9.0, 9.5 and 10.0) and salinity 30‰. The culture was started at the optical density (OD) 0.20 and the experimental period was ended after 10 days in the laboratory room. Among the media, urea and T-super with sodium bicarbonate was recorded the best. The optimum growth of *S. platensis* (OD 0.69) was observed at pH 10 in urea and T-super with sodium bicarbonate. The minimum OD 0.39 was recorded in F-2 medium.

Keywords: *Spirulina platensis*; media; pH; seawater

Introduction

Spirulina were the dominance of life on earth for more than 3.5 billion years ago. The name "Spirulina" is derived from the Latin word for "helix" or "spiral" denoting the physical configuration of the organism when it forms swirling, microscopic stands. Spirulina is a "Superfood."

Spirulina is not a nitrogen fixing blue-green algae. It has a long history of safe human consumption, known to be safe and nutritious. It can play an important role in human and animal nutrition, environmental protection through wastewater recycling and energy conservation. Spirulina is rich in proteins (60-70%), vitamins and minerals used as protein supplement in diets of undernourished poor children in developing countries. One gram of Spirulina protein is equivalent to one kilogram of assorted vegetables (Usharani et.al 2012).

There are about 1.386 x 1012 (one trillion three hundred eighty six billion) cubic meters of water on Earth. About 97% of it is in the oceans and seas, and, therefore too salty for human consumption. Of the remaining water, about 3% is fresh water. Nearly 70% of that fresh water is frozen in

[1] U, Assistant Lecturer, Department of Marine Science, Pathein University.
[2] U, Lecturer, Department of Marine Science, Pathein University.

icecaps of Antarctica and Greenland. Most of the remainder is present as soil moisture, or lies in deep underground aquifers not accessible to human use. Of the 1% fresh water, agriculture (including irrigation) uses 70%, industry 20% and other 10% including drinking water for 7 billion people. In the year 2025 at least 2.5 billion people won't have enough water to drink (Gershwin & Belay 2007). So, we will have to use seawater for agriculture.

The advantages of *S. platensis* production in seawater medium are: (1) lower fertilizer cost; (2) saving farm land by using waste sea beach; (3) seawater culture is not easily polluted by heavy metals and contaminations. The utilization of seawater media for the cultivation of *S. platensis* will be reduced the production cost considerably (Wu *et al*., 1993).

High pH and temperature are the key factors for large scale *S. platensis* culture indoors. The optimum water temperature for *S. platensis* culture is in the range of (28-33°C). In addition *S. platensis* requires relatively high pH values between 9.5 and 9.8, which effectively inhibit the contamination of most algae in the culture. *S. platensis* is the edible microorganisms which grow naturally in tropical regions inhabiting alkaline lakes containing sodium carbonate or sodium bicarbonate other materials and a source of fixed nitrogen of tropical and subtropical regions. These lakes are found near volcanoes or even within the caldera of the volcano. In nature lakes of the world, the limited supply of nutrients usually regulates growth cycles. New nutrients come from an upwelling from inside the earth, when rains wash soils into the lakes, or from pollution. The alga grows rapidly and reaches a maximum density, and then dies off when nutrients are exhausted. A new seasonal cycle begins when decomposed algae release their nutrients when more nutrients flow into the lake (Henrikson, 2010).

Spirulina was known to grow naturally in the Lake Bodu (Chard, Africa), Lake Chad (Chard, Africa), Lake Johann (Chard, Africa), Lake Rombu (Chard, Africa), Lake Aranguadi (Chard, Africa), Lake Elementia (Ethiopia, Africa), Lake Nakuru (Kenya, Africa) Lake Rudolf (Kenya, Africa), Lake TaungPyauk (Myanmar, Asia), Lake Twyn Ma (Myanmar, Asia), Lake Twyn Taung (Myanmar, Asia), Lake Ye Kharr (Myanmar, Asia), Lake Chenghai (China, Asia), Lake Texcoco (Mexico, North America) and Lake Buccacina (Peru, South America).The aims of this present study are to observe the best salinity, light quality and light intensity for *S. platensis* culture in natural seawater.

Materials and methods

Research Site and Facilities

S. platensis cultivation was studied in the laboratory of the Marine Science Department of Pathein University. The sample was collected from Ye Kharr Lake in Sagaing Township, Sagaing Region. Strain of *S. platensis* with 20 ‰ of salinity and 10.3 of PH value transported to the laboratory in plastic bottles. In the laboratory, the stock algal culture was maintained in one litter plastic bottles. The culture bottles were placed on the shelf and illuminated with 40 watt fluorescent lamps. Aeration was accomplished using aeration pump. Growth of algae was estimated by measuring the optical density (OD) of the culture. Determination of cell densities was made by using Digital Photocolorimeter. For the culture experiments, the natural seawater was collected from Chaung Tha coast. Seawater was boiled and then filtered with Whatman No. 540 filter paper. During the experimental period, the laboratory apparatus (refractometer, pH meter, pipettes, conical flasks, beakers) and drinking plastic bottles were used for culture. Four digits digital balance was also used to measure chemical nutrients for dilution media. *S. platensis* were cultivated in three different pH values (9.0, 9.5 and 10.0) which were adjusted by using sodium bicarbonate with modified F-2 medium (Table- 1), two of modified Zarrouk's media: Z-1medium (Table - 2) and Z-2 medium (Table – 3), Provasoli's enriched seawater (PES) medium (Table –4) and urea & T-super medium. The nutrient urea & T-super medium was prepared as the ratio 5:1 that 10 g of urea and 2 g of T-super were separately soluted with each one liter of distil water which 10 ml of each nutrient solution was daily feed into the culture bottles.

Table 1. Chemical composition of modified F-2 medium.

Nutrient Elements	**g/L of seawater**
$NaNO_3$	0.075
$NaH_2PO_4.2H_2O$	0.005
$Na_2SiO_3.9H_2O$	0.030
Thiamine HCl (B_1)	0.0001
Biotin (B_6)	0.0000005
Vitamin (B_{12})	0.0000005

Table 2. Chemical composition of modified Zarrouk's (Z-1) medium

Nutrient Elements	**g/L of seawater**
K_2SO_4	1.148
$NaNO_3$	2.500
NaH_2PO_4	0.344
KOH	0.227
Na_2EDTA	0.080

Table 3. Chemical composition of modified Zarrouk's (Z-2) medium

Nutrient Elements	**g/L of seawater**
K_2SO_4	1.148
$NaNO_3$	2.400
NaH_2PO_4	0.344
KOH	0.227
$Mg(NO_3)_2.6H_2O$	0.192
Na_2EDTA	0.080

Table 4. Provasoli's Enriched Seawater Medium (PES Medium).

Nutrient Elements	**g/L**	*** Fe (EDTA: 1:1 molar)**	**Amount**
		Distilled water	**500 ml**
$NaNO_3$	0.7	$Fe(NH_4)_2(SiO_4)_2.6H_2O$	0.351 g
NaH_2PO_4 . $6H_2O$	0.1	Na_2EDTA	0.3 g
Fe (EDTA: 1:1 molar)*	0.05	** **P II metal solution**	Amount
P II metal**	0.05	Distilled water	100 ml
Tris Buffer	0.001	H_3BO_3	114.0mg
Vitamin B_{12}	0.00002	Na_2EDTA	100 mg
Biotin (B_6)	0.00001	$MnSO_4.4H_2O$	16.4 mg

Nutrient Elements	g/L	* Fe (EDTA: 1:1 molar)	Amount
		Distilled water	**500 ml**
Thiamine HCl (B_1)	0.000001	$FeCl_2$.6H2O	4.9 mg
Distilled water	1000 ml	$ZnSO_4.7H_2O$	2.2 mg
		$COSO_4.7H_2O$	0.48

Results

Scientific Classification

Phylum: Cyanophyta

Class : Cyanophyceae

Order : Nostocales

Family : Oscillatoriaceae

Genus : *Spirulina*

Species: *S. platensis*

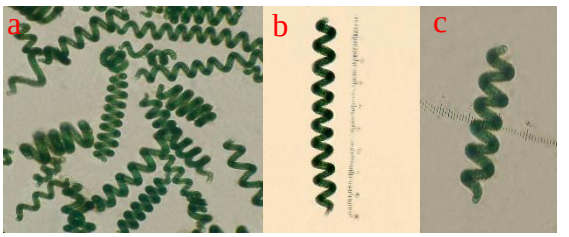

Figure1. *S. platensis* Geitler in the Laboratory Culture. (a) Habitat of *S. platensis*, (b) Length of *S. platensis* and (c) Width of

Description: The length of cell is 125-225 µm and the cell's width is 25-30 µm (Fig. 1). Ends of trichomes are not or very slightly attenuated, terminal cells broadly rounded. Cells of trichomes are 10-12µm in diameter and 2-5 µm long. The filaments are motile, gliding along their axis and have no heterocyst. Reproduction is accomplished by fragmentation of a mature trichome into a number of shorter segments through destruction of specialized multiple intercalary cells.

Effects of modified F-2 medium at salinity 30‰

Growth rates of *S. platensis* in F-2 medium at different pH values were illustrated in Fig. 2. Cell densities both increased and decreased within age for all different pH values at salinity 30‰ with initial OD 0.20 in F-2 medium.

In pH value 9.0, the growth was gradually increased for seven days and nearly steadied at maximum OD 0.40 and then slowly reduced during the experimental period.

In pH value 9.5, the growth of *S. platensis* was gradually increased within the experiment and steadied at 6th and 7th days, and then slowly reduced at the end of the experiment. The maximum OD was 0.43 and the colour was pale-green at the end of the culture.

In pH value 10.0, *S. platensis* growth was increased within the experiment for eight days and then slowly reduced in last two days. Double time was observed within 4th day. The culture of *S. platensis* was light-green in colour and the maximum OD was 0.47.

In this culture, the maximum growth rates were found on 7th and 8th days. Doubling times were occurred on day 7 in pH 9.0 and on day 6 in other pH. The reducing time was occurred on 8th day in pH 9.0 and on 9th day in other pH. If the pH value was increased, the growth of *S. platensis* was good and the best pH was 10.0. This result suggested that *S. platensis* may be to survive in high pH values.

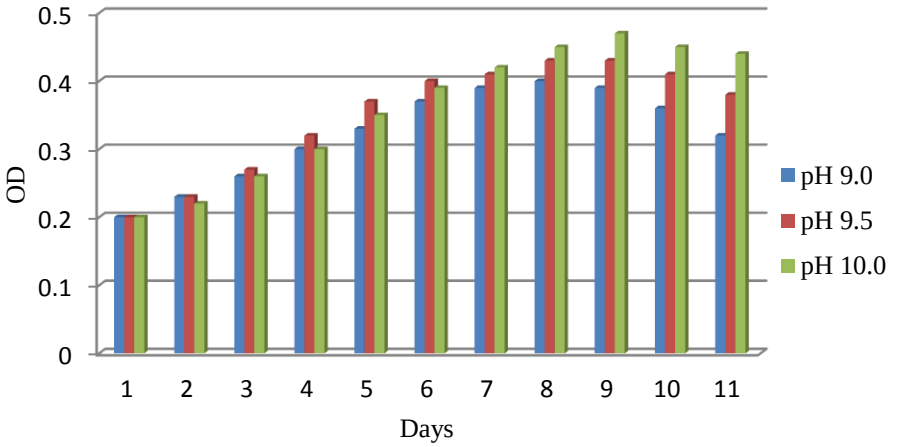

Figure 2. Comparison of the growth of *S. platensis* in different pH with modified F-2 medium.

Effects of Z-1 medium at salinity 30‰

Growth rates of *S. platensis* in Z-1 medium at different pH values were shown in Fig. 3. Cell densities increased with age for all pH values with initial optical density 0.20 in Z-1 medium.

In pH value 9.0, the growth of *S. platensis* was gradually increased and maximum OD 0.55 was reached at the end of the culture period. The culture of *S. platensis* was dark-green in colour.

In pH value 9.5, *S. platensis* growth was gradually increased within the experiment and over doubling time was observed 5th day of the experiment. The maximum OD 0.57 was reached within 10 days of the experiment. The colour was dark-green at the end of the culture.

In pH value 10.0, the growth of *S. platensis* was gradually increased and nearly doubling time was observed 4th day of the experiment. The colour was dark-green and the maximum OD 0.62 was reached within 10 days of the experiment.

In this test, *S. platensis* grew up the culture end. Over doubling times started from day 5. If the pH value was increased, the growth of *S. platensis* was also increased. This experiment suggested that *S. platensis* may be to survive in high pH values.

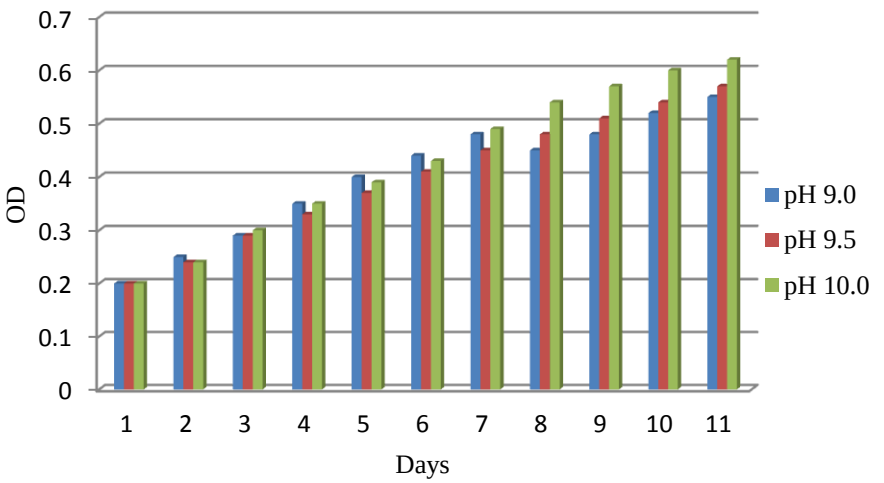

Figure 3. Comparison of the growth of *S. platensis* in different pH with Z-1 medium.

Effects of Z-2 medium at salinity 30‰

Growth rates of *S. platensis* in Z-2 medium at different pH values were as shown in Fig. 4. Cell densities increased with age for all different

pH values at salinity 30‰ with initial optical density 0.20 in Z-2 medium. The culture of *S. platensis* was dark-green in color at the end of the experiment.

In pH value 9.0, the growth of *S. platensis* was gradually increased and double time was observed 5th day of the experiment. The cell culture was dark-green in colour and the maximum point of OD was 0.53.

In pH value 9.5, *S. platensis* growth was gradually increased within the experiment and nearly double time was observed 4th day of the experiment. The maximum OD 0.59 was reached within 10 days of the experiment. The colour was dark-green at the end of the culture.

In pH value 10.0, the growth of *S. platensis* was gradually increased and over doubling time was observed 4th day of the experiment. The maximum OD 0.61 was reached within 10 days of the experiment.

In this experiment, the reducing time was not occurred during the culture period. Over tripling times were occurred in pH 10.0. This result suggested that *S. platensis* survive in high pH values. If the pH value was increased, the growth of *S. platensis* was good.

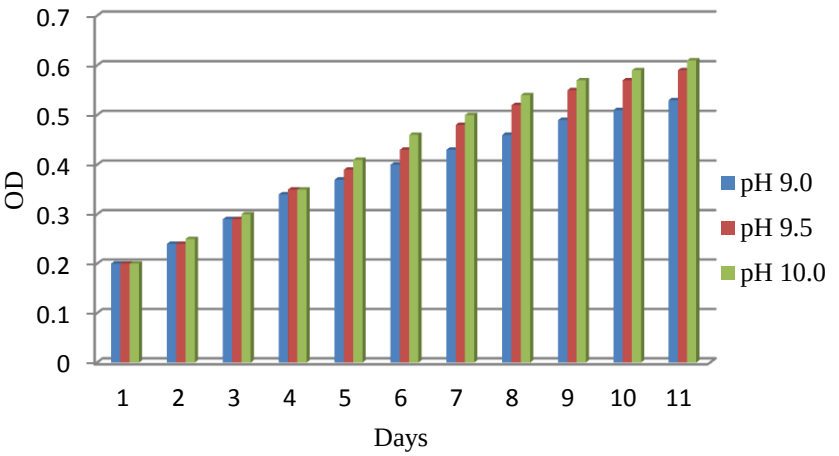

Figure 4. Comparison of the growth of *S. platensis* in different pH with Z-2 medium.

Effects of PES medium at salinity 30‰

Growth rates of *S. platensis* in PES medium at different pH values were as shown in Fig. 5. Cell densities increased with age for all different pH values at salinity 30‰ with initial OD 0.20 PES medium. The culture of *S. platensis* was dark-green in colour at the end of the experiment.

In pH value 9.0, the growth of *S. platensis* was gradually increased and maximum point of OD 0.56 was reached at the end of the experiment.

In pH value 9.5, *S. platensis* growth was gradually increased within the experiment and the maximum OD 0.67 was reached within 10 days of the experiment.

In pH value 10.0, the growth of *S. platensis* was rapidly increased and over doubling time was observed 4th day of the experiment. The maximum OD 0.61 was reached within 10 days of the experiment.

In this culture, the maximum growth rates were found on 8th, 9th and 10th days. Over doubling times were occurred in all pH values. The reducing date was not occurred during culture period. Thus *S. platensis* may be to survive from pH 9.0-10.0 but the best pH was 10.05. If the pH value was increased, growth rate of *S. platensis* was increased.

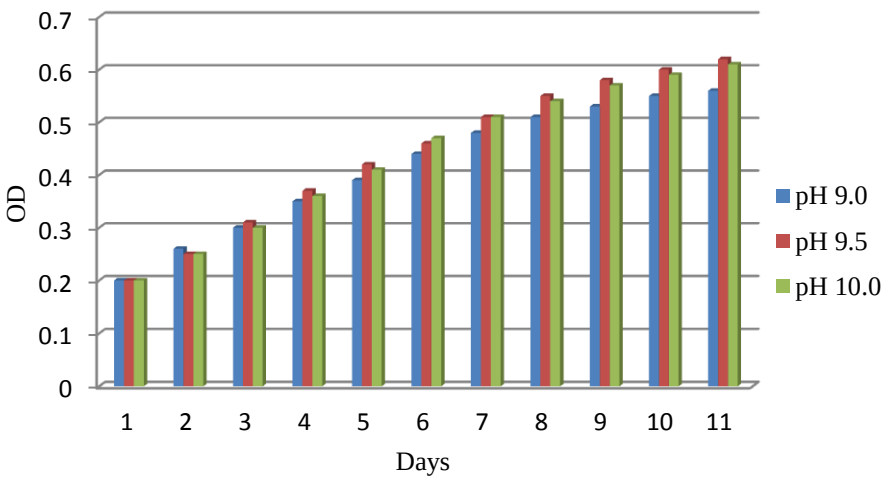

Figure 5. Comparison of the growth of *S. platensis* in different pH with PES medium.

Effects of Urea and T-super medium at salinity 30‰

Growth rates of *S. platensis* in urea and T-super medium at different pH values were as shown in Fig. 6. Cell densities increased with age for all different pH values with initial optical density 0.20 in urea and T-super medium. The culture of *S. platensis* was dark-green in color at the end of the experiment.

In pH value 9.0, the growth of *S. platensis* was gradually increased and maximum point of OD was three time of the initial. The culture of *S. platensis* was dark-green in colour.

In pH value 9.5, *S. platensis* growth was gradually increased within the experiment and nearly double time was observed 4th day of the experiment. The maximum OD 0.67 was reached within 10 days of the experiment. The colour was dark-green at the end of the culture.

In pH value 10.0, the growth of *S. platensis* was gradually increased and over doubling time was observed 5th day of the experiment. The colour was dark-green and the maximum OD 0.69 was reached within 10 days of the experiment.

In this experiment, *S. platensis* grew up the culture end. Over doubling times started from day 5. If the pH value was increased, the growth of *S. platensis* was also increased. This experiment suggested that *S. platensis* may be to survive in high pH values.

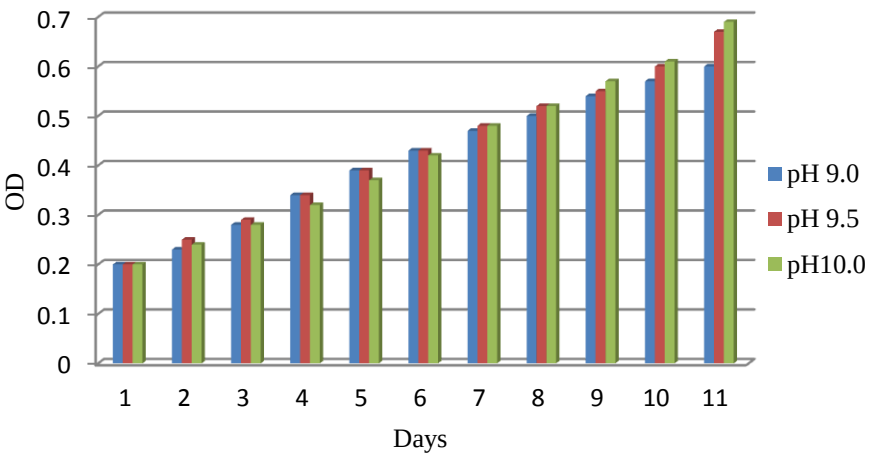

Figure 6. Comparison of the growth of *S. platensis* in different pH with Urea and T-super medium.

Discussion and Conclusion

S. platensis is a filamentous and photoautotrophic cyanobacterium which grows naturally in tropical regions inhabiting alkaline lakes containing sodium carbonate or sodium bicarbonate, other materials and a source of fixed nitrogen of tropical and subtropical regions. This cyanobacterium blooms in bicarbonate-rich environments and has gained a significant position in recent years as a source of proteins and pigments in the food, pharmaceutical, and cosmetic industries.

S. platensis production plants for mass cultivation could be done in areas with suitable climatic conditions, particularly with the sunshine throughout the year. It is difficult to have an ideal growth due to different environmental factors like solar radiation, rain, wind, temperature fluctuation, etc. In this research *S. platensis* was studied in small laboratory culture.

According to the report of Mahadevaswamy and Venkataraman (1987), pH values between 8.5 and 9.5 decreased *S. platensis* growth due to the contamination of bacteria and protozoa. Richmond (1982) stated that *S. platensis* grow well at pH values between 9 and 11 and specific growth rate is also independent of pH between 8.5 and 10.5. Hill (1980) found that the growth of predators can be prevented by maintaining pH levels near 10.5. May Yu Khaing (1987) stated that the optimum pH for the growth of *S. platensis* biomass was 8.5 to 9.5.

In the present study, the effects of culture media on the growth of *S. platensis* in seawater were studied in different three pH values (9.0, 9.5, and 10.0) at salinity 30‰. Among this experiment, the highest optimum density (OD 0.69) was observed in urea and T-super nutrient medium at pH 10.0 at the end of culture. The lowest was in modified F-2 medium at pH 9.0. Therefore *S. platensis* possesses a high tolerance to alkaline pH for cultivation.

In all media urea and T-super obtained the highest growth rate and followed by PES medium and Z-1. This may be the effect of feeding method. In this experiment urea and T-super was fed daily. So the plants obtained the nutrients for growth. In other culture media the increasing growth rates gradually slow down due to the exhausted nutrients.

Khin Mar Soe (2009) studied the growth of *S. platensis* on seawater-based Provasoli (PES) medium, seawater-urea medium, seawater-based

medium I and seawater-based medium II and seawater-based medium III. The optimal growth was found in seawater-based medium III which contained a low concentration of phosphate, a small amount of bicarbonate, nitrate and Fe-EDTA, for the optimal growth of *S. platensis* in laboratory culture.

PES and Z-1 media are suitable for culturing in seawater but the treatments of *S. platensis* are expensive. Others, Z-2 and F-2, are not suitable to use in seawater culture because the growth rates of *S. platensis* in them were poor and the costs are expensive. Therefore, urea and T-super medium with $NaHCO_3$ was the most suitable medium in seawater.

It may be concluded that urea and T-super medium was the most suitable medium in seawater for the best growth of *S. platensis* because the nutrients are cheaper than other media. Therefore *S. platensis* culture with pH 10.0 at salinity 30‰ by using urea and T-super medium was the most suitable condition in natural seawater. The results were to provide good ideas for mass cultivation in natural seawater.

Acknowledgement

The author greatly appreciates Rector and Pro-rectors of Pathein University for their kind permission to do this research work. I also greatly thank to Dr. Cherry Aung, Professor and Head of Marine Science Department, Pathein University for supporting. Special thanks go to Dr. Htay Aung, Professor (Retired), Marine Science Department of Pathein Uniersity for his suggestions and necessary helps.

References

Gershwin, M. E. & Belay, A. 2007. *Spirulina in Human Nutrition and Health*. Taylor & Francis Group, an informa business, Boca Raton London New York. 312 pp.

Henrikson, R. 2010. *Spirulina World Food*. Ronore Enterprises, Inc., Hana, Maui, Hawaii. 187 pp.

Hill, G. 1980. *The secret of Spirulina*. University of Tree Press. California. 218 pp.

Khin Mar Soe. 2009. Studies on the culture of *Spirulina platensis* (Nordstedt) Geitler using seawater medium. Unpublished Master of Research Thesis, Department of Marine Science, Mawlamyine University, Myanmar.

Mahadevaswamy, M. and Venkataraman, L. V. 1987. Bacterial contaminants in blue green alga *Spirulina* produced for use as biomass protein. *Archiv. For Hydrobologie*, **10**(4): 623-630.

May Yu Khaing. 1987. Studies on laboratory culture of *Spirulina*. Unpublished Master of Science Thesis, Department of Marine Science, Mawlamyine University, Myanmar.

Richmond, A., Hkarg, S. and Boussiba, S. 1982. Effect of bicarbonate and carbondioxide on the competition between *Chlorella vulgaris* and *Spirulina platensis*, plant and cell physiology. 23:1411-1417.

Usharani, G., Saranraj, P. and Kanchana, D. 2012. *Spirulina* Cultivation: A Review. *International Journal of Pharmaceutical & Biological Archives*. **3**(6): 1327-1341.

Wu, B., Tseng, C.K, and Xiang, W. (1993). Large- scale cultivation of *Spirulina* in seawater based culture medium. *Bot. Mar.*, **36**; 99-102.

Morphology and Distribution of Triton Shell (Family Ranellidae) in Mon Coastal Area

Naung Naung Oo*

Abstract

The *Cymatium* Röding, 1798 is a small-to large-sized marine gastropod genus belonging to family Ranellidae Gray, 1854 and it is widely distributed in the tropical seas. A total of six species, namely *Cymatium aquatile* (Reeve, 1844), *C. caudatum* (Gmelin, 1791), *C. gutturnium* (Röding, 1798), *C. hepaticum* (Röding, 1798), *C. pfeifferianum* (Reeve, 1844) and *C. pileare* (Linnaeus, 1758) were collected by hand picking from Mon coastal area. This is the part of seashells study to report the distribution of these six species from Mon coastal areas, providing a detailed characteristics of the species with the illustrations for the shell morphology.

Keywords: Distribution, family Ranellidae, Mon coastal area, shell morphology, triton shell.

Introduction

The *Cymatium* Röding, 1798 is a small to large-sized marine gastropod genus, with its size ranging from a few cm to nearly 20 cm (Lee *et.al* 2012). It comprises of about one hundred species, of which majority are found in tropical waters (Henning and Hemmen 1993). The genus *Cymatium* is carnivorous that usually prey on diverse invertebrate species, such as tube worms, ascidians, bivalve molluscs (Houbrick and Fretter 1969; Littlewood 1989; Govan 1995).

The shell morphology of this genus is characterized by having a club-shaped body whorl with an ornamentation of knob, spiral ribs and axial varices (Soe Thu 1980). Although surveys on the molluscan fauna of Mon coastal areas were periodically conducted in the past few years, thus far, only six species of this genus have been reported from these areas (Naung Naung Oo 2012). Recently, several unrecorded species of marine gastropods were collected during an ecological study in the intertidal zones on the north to south coasts of Mon coastal shoreline. Here in this study report the records of genus *Cymatium* in Mon coastal areas with species characteristics and illustration for the shell morphology. This study adds a

* Dr., Assistant Lecturer, Department of Marine Science, Mawlamyine University

new geographic locality to their originally reported distribution ranges. The aim of this study is to identify and collate existing information on *Cymatium* species and to know the distribution ranges of these species in Mon coastal area.

Materials and Methods

In this study, triton shell of the genus *Cymatium* Röding, 1798 was collected in the forms of drift and live specimens living in intertidal and shallow subtidal areas of 1) Kyaikkhami (Lat. 16° 04′ N, Long. 97° 33′ E), 2) Sinpone (Lat. 16° 03′ N, Long. 97° 33′ E), 3) Kayinthaung (Lat. 15° 56′ N, Long. 97° 37′ E), 4) Yathaetaung (Lat. 15° 55′ N, Long. 97° 40′ E), 5) Hnitkayin (Lat. 15° 34′ N, Long. 97° 45′ E), 6) Kawdut (Lat. 15° 32′ N, Long. 97° 45' E), 7) Pagoda Point (Lat. 15°12' N, Long. 97°46' E), 8) Sitaw (Lat. 15° 11' N, Long. 97° 48' E) and 9) Kabyarwa (Lat. 15° 04' N, Long. 97° 48' E) in Mon coastal area from January 2015 to May 2019 (Fig. 1).

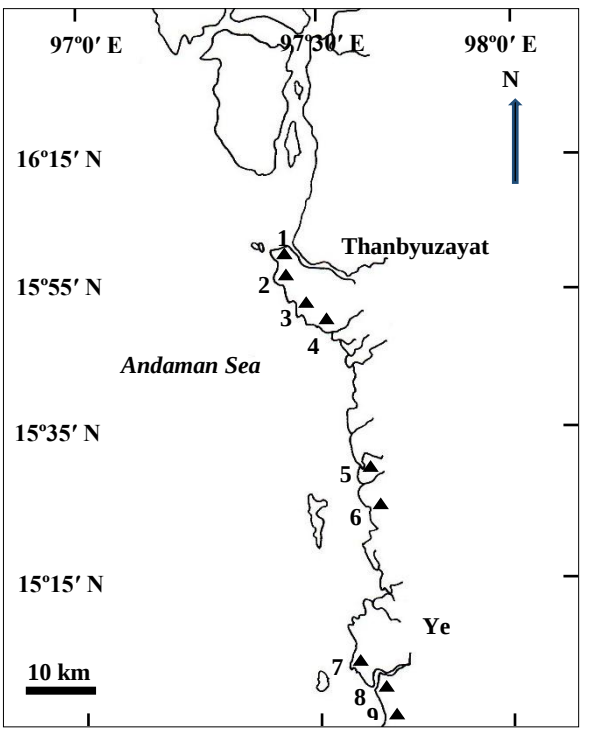

Figure 1. Map showing the collection sites of the samples in Mon coastal area

All collections were preserved in 10 % formalin in seawater, and then cleaned, washed, dried, and ready for storage, they are lightly rubbed with a small amount of oil applied with a brush to make them fresh-looking in a slight luster to the surface, and aid in presenting the delicate colouring for further study. The specimens were identified to species level and verified following Poutiers (1998), Carpenter (2002), Dance (2002), Subba Rao (2003), Oliver (2004), Poppe (2008), Rosenberg (2009) and WoRMS (World Register of Marine Species, 2018).

Results and Discussion

Of the 35 specimens collected, six species namely *Cymatium aquatile* (Reeve, 1844), *C. caudatum* (Gmelin, 1791), *C. gutturnium* (Röding, 1798), *C. hepaticum* (Röding, 1798), *C. pfeifferianum* (Reeve, 1844) and *C. pileare* (Linnaeus, 1758) belonging to the family Ranellidae were identified (Fig. 2). The detailed classification of each species are given below.

Classification of Triton shell in Mon coastal area

Phylum: Mollusca Linnaeus, 1758

Class: Gastropoda Cuvier, 1795

Order: Mesogastropoda Thiele, 1929

Family: Ranellidae (= Cymatiidae) Gray, 1854

Genus: *Cymatium* Röding, 1798

Species
(1) *C. aquatile* (Reeve, 1844)
(2) *C. caudatum* (Gmelin, 1791)
(3) *C. gutturnium* (Röding, 1798)
(4) *C. hepaticum* (Röding, 1798)
(5) *C. pfeifferianum* (Reeve, 1844)
(6) *C. pileare* (Linnaeus, 1758)

Genus *Cymatium* Röding, 1798

This genus is periostracum often conspicuous, fibrous to hairy, aperture without a posterior canal. Shell spindle shape or fusiform, varices white, aperture oval and coloured inside.

Distinct characters of triton shell: Shell ovate to fusiform, thick and solid, with a raised spire and strong sculpture composed of nodules, spiral ribs and axial varices. Periostracum frequently well developed and fibrous to hairy. Aperture with a short to long siphonal canal anteriorly. Outer lip prominently thickened, often denticulate inside. Inner lip commonly wrinkled and with a columellar callus. Operculum thick and corneous, rounded to trigonal. Head with a moderately stout, extensible snout and filiform tentacles bearing eyes on protuberances of their outer bases. Foot rather short, somewhat truncated posteriorly (Table 1 A and B).

Habitat, biology, and fisheries: Active predators, living on sandy or rocky bottoms from the intertidal zone to depths of a few hundred meters. Ranellidae have a variety of diets including molluscs (bivalves and gastropods), echinoderms (starfishes and sea urchins) or even ascidians, depending upon the species. Prey is often first paralysed with an acidic salivary secretion, then devoured. Sexes separate, fertilization internal. Eggs laid on the substrate in large capsules clustered in masses. Planktonic larval stage sometimes very long, hence the very wide geographical distribution of some species. Since ancient times, certain species of Ranellidae have been fished, in the area as well as in other parts of the world, for their beautiful shell or their edible flesh, the large shells of genus *Charonia* being traditionally used as a kind of horn.

Key to the species of genus *Cymatium* in Mon coastal area

1.a. Outer sculpture relatively rough ……***C. aquatile***

1.b. Outer sculpture relatively fine ……...**2**

2.a. Apex of shell is rounded ……..***C. pileare***

2.b. Apex of shell is moderately sharp ……**3**

3.a. Siphonal canal is moderately long ……...***C. pfeifferianum***

3.b. Siphonal canal is short and curved backward ……...**4**

4.a. Shell surface is beaded with strong spiral cords ……***C. hepaticum***

4.b. Shell surface is nodules, spiral ribs and cords ……...**5**

5.a. Body whorl is ovate ……***C. gutturnium***

5.b. Body whorl is ovate to fusiform ……***C. caudatum***

Table 1.(A) Characteristics of Triton shell in Mon coastal area

Characteristics	***C. aquatile* (Reeve, 1844)**	***C. caudatum* (Gmelin, 1791)**	***C. gutturnium* (Röding, 1798)**
Common name	Triton shell	Triton shell	Triton shell
Local name	Kha-yu-hmway	Kha-yu-hmway	Kha-yu-hmway
FAO name	Aquatile hairy triton	Long siphonal triton	Wavy thick-lip triton
Measurement (mm)	25	47	33
Form of shell	thick, solid	thick, solid	thick, solid
Shape of body whorl	fusiform	ovate to fusiform	ovate
Shape of apex	moderately blunt	rounded	broken off
Surface structure	relatively rough	nodules, spiral ribs and cords, axial varices	nodules, spiral ribs and axial varices
Shape of aperture	small, short	long	small, narrow, trigonal in shape
Siphonal canal	anterior canal short	anterior canal moderately long	anterior canal moderately long
Umbilicus	present	present	covered by strong callus
Style of columella	covered with regular teeth	present	wide
Type of	thick,	thick, corneous	thick, corneous

Characteristics	*C. aquatile* (Reeve, 1844)	*C. caudatum* (Gmelin, 1791)	*C. gutturnium* (Röding, 1798)
operculum	corneous		
Structure of base	thick, short	thick, short	thick, long
Form of suture	deep	deep	deep
Colour of shell surface	brown	yellowish brown, grayish white	yellowish brown
Habitat	rocky hard substratum	sandy bottoms	rocky hard substratum

Table 1.(B) Characteristics of Triton shell in Mon coastal area

Characteristics	*C. hepaticum* (Röding, 1798)	*C. pfeifferianum* (Reeve, 1844)	*C. pileare* (Linnaeus, 1758)
Common name	Triton shell	Triton shell	Triton shell
Local name	Kha-yu-hmway	Kha-yu-hmway	Kha-yu-sue-yit
FAO name	Liver triton	Pfeifferi triton	Common hairy triton
Measurement (mm)	20	33	23
Form of shell	thick, solid	thick, solid	thick, solid, small
Shape of body whorl	fusiform	fusiform	fusiform
Shape of apex	blunted	moderately sharp	rounded
Surface structure	beaded with strong spiral cords and concentric lines	beaded spiral cords and varices	nodules, spiral ribs and cords, axial varices
Shape of	small, oval shape	rather oval in	small, long

Characteristics	***C. hepaticum* (Röding, 1798)**	***C. pfeifferianum* (Reeve, 1844)**	***C. pileare* (Linnaeus, 1758)**
aperture		shape	
Siphonal canal	Short and curved backward	anterior canal moderately long	anterior canal moderately long
Umbilicus	present	present	present
Style of columella	absent	strong	thin, covered with many teeth
Type of operculum	thick, corneous	thick, corneous	thick, corneous
Structure of base	thick, strong	slightly long	thick, short
Form of suture	deep	deep	deep
Colour of shell surface	white, brown and pale yellowish base	yellowish brown	dark brown, orange, yellowish white
Habitat	rocky and coarse sandy bottoms	sandy mud bottoms	on hard and coarse detritus bottoms

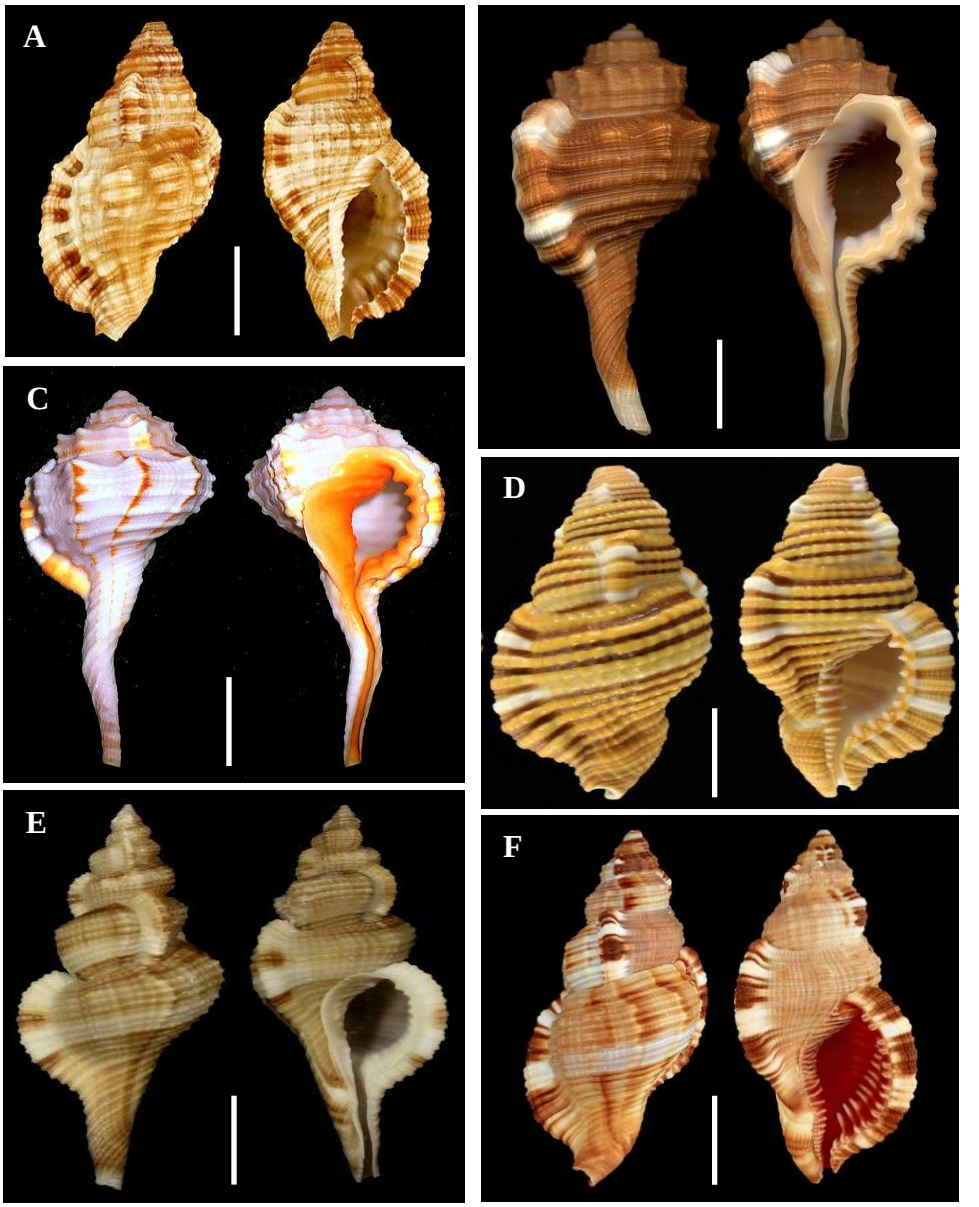

Figure 2. (A-F): **Triton shell in Mon coastal area:** (A) *Cymatium aquatile* (Reeve, 1844); (B) *C. caudatum* (Gmelin, 1791); (C) *C. gutturnium* (Röding, 1798); (D) *C. hepaticum* (Röding, 1798); (E) *C. pfeifferianum* (Reeve, 1844); (F) *C. pileare* (Linnaeus, 1758). Scale bars = 3 cm.

Table 2. Local distribution of Triton shell in Mon coastal area

Sampling sites	Species					
	C. aquatile	*C. caudatum*	*C. gutturnium*	*C. hepaticum*	*C. pfeifferianum*	*C. pileare*
Kyaikkhami			+	+		
Sinpone	+	+			+	
Kayinthaung			+			+
Yathaetaung		+		+		
Hnitkayin			+			+
Kawdut	+			+	+	
Pagoda Point	+		+			+
Sitaw	+	+			+	
Kabyarwa			+	+		

World distribution records of Triton shells

Cymatium aquatile (Reeve, 1844): Circumtropical (Indo-West Pacific, East Central Pacific, West and East Central Atlantic). Widespread in the Indo-West Pacific, from East Africa, including Madagascar and the Red Sea, to eastern Polynesia; north to southern Japan and Hawaii, and south to Queensland and New Caledonia. (Source: Poutiers 1998)

C. caudatum (Gmelin, 1791): Indo-West Pacific, from East Africa to Polynesia; north to Japan and Hawaii, and south to Queensland. (Source: Poutiers 1998)

C. gutturnium (Röding, 1798): Widespread in the Indo-West Pacific, from East Africa to eastern Polynesia north to Japan and Hawaii, and south to Queensland. Also in the western and eastern tropical Atlantic. (Source: Poutiers 1998)

C. hepaticum (Röding, 1798): The global distribution of *Cymatium hepaticum* is reported to be from Philippines to Polynesia (western and central Pacific Ocean) (Cernohorsky, 1967). There are no previous reports from mainland India or from the Andaman and Nicobar Islands. (Source: Franklin *et.al* 2015)

The species *C. hepaticum* very closely resembles its congener *C. rubeculum*, but the transverse black bands (3-5 nos.) are limited to the body whorl of the latter species. In addition the interstices of the labial denticles are coloured white in *C. rubeculum*, whereas in *C. hepaticum* it is reddish orange.

C. pfeifferianum (Reeve, 1844): Widespread in the Indo-West Pacific, from East Africa to eastern Polynesia; north to Japan and Hawaii, and south to New South Wales. (Source: Poutiers 1998)

C. pileare (Linnaeus, 1758): Widespread in the Indo-West Pacific, from East and South Africa, including Madagascar and the Red Sea, to eastern Polynesia; north to southern Japan and Hawaii, and south to southern Queensland. (Source: Poutiers 1998)

The species *C. pileare* has a wide distribution along the north and south Atlantic (amphi-atlantic distribution) (Magno and Frietas, 2009). However, *C. martinianum* (d'Orbigny, 1847), a closely similar species distributed in the Indo-Pacific was earlier considered as distinct species based on the shell morphological characters (Nordseick and Talavera, 1979). Nevertheless, recent revisions (Beu, 1986; Beu and Alison, 1988; Bouchet, 2013) of the genus *Cymatium* Röding, 1798 have merged both the species. Presently, *C. martinianum* (d'Orbigny, 1847) is considered as a synonym of *C. pileare* (Linnaeus, 1758).

The present study conducted that six species namely, *Cymatium aquatile* (Reeve, 1844), *C. caudatum* (Gmelin, 1791), *C. gutturnium* (Röding, 1798), *C. pileare* (Linnaeus, 1758), *C. pfeifferianum* (Reeve, 1844) and *C. hepaticum* (Röding, 1798) as new records to the Mon coastal area. Distribution of 6 species of triton shells were recorded from Kyaikkhami, Sinpone, Kayinthaung, Yathaetaung, Hnitkayin, Kawdut, Pagoda Point, Sitaw and Kabyarwa in Mon coastal area. Of these species *C. gutturnium* was highly distributed in study areas (Table 2). At present, the estimated total number of *Cymatium* species occur in the Indian seas is 18 (Hylleberg and Kilburn, 2002) and from the Andaman and Nicobar Islands

is 13 (Subba Rao and Dey, 2000) reported. This number is less when compared with other parts of the world oceans. The identification of tritons are challenging as they closely resemble Murexes.

However, a typical difference is that only two prominent varices are found on a whorl and those on adjacent whorls rarely connect in tritons. The major ecological significance of this genus *Cymatium* is the presence of long planktonic larval period. Marine snail species exhibit a range (modes) of larval development (Thorson, 1950; Krug, 2011). The different developmental modes are characterized by very different amounts of time spent as plankton. The genus *Cymatium* spends several months as plankton that allows the larvae to travel long distances and to reach new territories. This is one of the key factors that impact the broad geographic distribution of this genus *Cymatium* in the tropical seas.

Conclusion

Shells are moderately small, solid and stout, conical-ovate in shape with a moderately high, stepped spire, inflated body whorl and relatively long siphonal canal. Outer sculpture strong, with thick axial varices and heavy, nodulose axial ridges crossed by irregularly granulose spiral ribs and grooves. Body whorl with about 6 larger spiral ribs, thickening on axial varices and ridges that become almost spiny at shoulder. Periostracum thick and prominently bristled. Aperture ovate, calloused at periphery. Outer lip thickened and marginally dentate, with 6 or 7 folds, often more or less divided in 2 series by a shallow axial groove. Inner lip almost smooth centrally and extensively calloused over ventral side of body whorl. Anterior siphonal canal rather slender, bent dorsalward, its ventral side narrowly open. The triton shells are found on sand and coarse detritic rock bottoms, usually associated with coral reefs in intertidal, sublittoral and shelf zones, to a depth of about 100 m. Most common between tide marks and in shallow subtidal waters. Locally collected for food and shell trade by hand, where common, by native people of the Mon coastal areas. Appears also in local markets of the southern Mon coastal areas, often mixed with small species of Strombidae.

Acknowledgements

I am indebted to Dr Aung Myat Kyaw Sein, Rector of Mawlamyine University and Dr Mie Mie Sein and Dr San San Aye, Pro-Rectors of Mawlamyine University, for their encouragement and supports in preparing this work. I am very grateful to Dr San Tha Tun, Professor and Head of the Department of Marine Science, Mawlamyine University, for his valuable suggestions and constructive criticisms on this study. I would like to express my sincere thanks to the local people who kindly help me in many ways during my field trips. Many thanks go to Daw Lwin Lwin, Retired Lecturer of the Department of Marine Science, Mawlamyine University, for her assistance in preparations of the manuscript.

References

Beu, A. G. 1986. Taxonomy of gastropods of the families Ranellidae (= Cymatiidae) and Bursidae. Part 2. Descriptions of 14 new modern Indo-West Pacific species and subspecies, with revisions of related taxa. *N. Z. J. Zool*., **13**: 273-355.

Beu, A. G. and Alison Kay, E. 1988. Taxonomy of gastropods of the families Ranellidae (= Cymatiidae) and Bursidae. Part IV. The Cymatium pileare complex. *J. R. Soc. N. Z.* **18**: 185-223.

Bouchet, P. 2013. *Monoplex pilearis* (Linnaeus, 1758). Accessed through: World Register of Marine Species at http://www.marinespecies.org/ on 2014-01-31.

Carpenter, A. 2002. Population of the Muricidae from Indo-pacific region. *J. Mar. Biol. Ass., UK*. **11**:51-76.

Cernohorsky, W. O. 1967. The Bursidae, Cymatiidae and Colubrariidae of Fiji: (Mollusca: Gastropoda). *The Veliger*. **9**(3): 310-329.

Dance, S. P. 2002. *Shells*. Dorling Kindersley, Inc. New York, 256 pp.

Franklin, B. J., Venkateshwaran, P., Vinithkumar, N. V. and Kirubagaran, R. 2015. First record of three tritons (Gastropoda: Tonnoidea: Ranellidae) from the Andaman Islands, India. *J. Mar. Biol. Ass. India*. **57**(1): 47-51.

Govan, H. 1995. *Cymatium muricinum and other ranellid gastropods: major predators of cultured tridacnid clams*. International Center for Living Aquatic Resources Management, Manila, 136 pp.

Henning, T. and Hemmen, J. 1993. *Ranellidae and Personidae of the World*. V. C. Hemmen, Wiesbaden, Germany. 263 pp.

Houbrick, J. R. and Fretter, V. 1969. Some aspects of the functional anatomy and biology of *Cymatium* and *Bursa*. *Proc. Malacol. Soc. Lond*. **38**:415-429.\

Hylleberg, J. and Kilburn, R. N. 2002. Annotated inventory of molluscs from the Gulf of Mannar and vicinity. *Spec. Publ. Phuket Mar. Biol. Cent*. **26**: 19-79.

Krug, P. J. 2011. Patterns of speciation in marine gastropods: a review of the phylogenetic evidence for localized radiations in the sea. *Am. Malacol. Bull*., **29**:169-86.

Lee, J., Lee, H. S., Lee, J. and Park, J. K. 2012. A New Record of *Cymatium encausticum* (Ranellidae: Tonnoidea: Gastropoda) from Korea. *Anim. Syst. Evol. Divers*. **28**(3): 212-214.

Littlewood, D. T. J. 1989. Predation on cultivated *Crassostrea rhizophorae* (Guilding) by the gastropod *Cymatium pileare* (Linnaeus). *J. Mollus. Stud*. **55**:125-127.

Magno, N. and Frietas, B. 2009. On the occurrence of *Cymatium martinianum* (d'Orbigny, 1847) (gastropoda, Ranellidae) in the islands of Madeira (Ne Atlantic Ocean). *Bocagiana*. **224**:1-6.

Naung Naung Oo. 2012. Study on the marine gastropods from Mon coastal areas. Unpublished MRes Thesis. Department of Marine Science, Mawlamyine University. Myanmar.

Nordseick, F. and Talavera, F. G. 1979. Molluscos marinos de Canarias y Madeira (gastropoda). *Aula de Cultura de Tenerife*, 208 pp. XLVIpls.

Oliver, A. P. H. 2004. *Guide to sea shells of the world*. Philip's a division of Octopus Publishing Group Ltd, London, 320 pp.

Poppe, G. T. 2008. *Philippine marine mollusks*. Vol. 1 (Gastropoda - Part 1). Conch Books. 759 pp.

Poutiers, J. M. 1998. Gastropods. *In*: Carpenter KE, Niem VH. (Eds.), FAO Species Identification Guide for Fishery Purposes. The Living Marine Resources of the Western Central Pacific. Volume 1. Seaweeds, Corals, Bivalves and Gastropods. Food and Agriculture Organization, Rome: 363-649 pp.

Rosenberg, G. 2009. Malacolog 4.1.1: A Database of Western Atlantic Marine Mollusca. http://www.malacolog.org/.

Soe Thu. 1980. Taxonomy and distribution of Burmese marine gastropods. Unpublished MSc Thesis, Department of Zoology, Art and Science University, Rangoon.

Subba Rao, N. V. 2003. *Indian Seashells* (Part-I): *Polyplacophora and Gastropoda*, *Rec. zool. Surv. India*, Occ. Paper No. 192: i-x, 1-416. (Published: Director, *Zool. Surv. India*, Kolkata)

Thorson, G. 1950. Reproductive and larval ecology of marine bottom invertebrates. *Biol. Rev*. **25**:1-45.

WoRMS. Available Source: http://www.marinespecies.org. 2018.

Mantis Shrimp Fishery of Min Khaung Shay, Myeik Archipelago

Khin May Chit Maung[1], Ei Thal Phyu[2] & Zin Lin Khine[3]

Abstract

Six mantis shrimps species (Order Stomatopoda) collected from the trammel net fishery were identified as *Harpiosquilla harpax*, *H. raphidea*, *Dictyosquilla foveolata*, *Erugosquilla woodmasoni*, *Miyakea nepa*, and *Oratosquillina interrupta*. The identification is based on their external morphological characters. Species of *Harpiosquilla harpax* and *H. raphidea* are the most commonly abundant species and adequate to have fishery potential.

Keywords: Mantis shrimps, Stomatopoda, trammel net.

Introduction

Mantis shrimps are shrimp-like or lobster-like crustacean with triramous antennules, a large abdomen supported by stiltlike uropods, full pleopods adorned with plumose gills, 3 pairs of walking legs and 5 pairs of maxillipeds (Ahyong, 2001). They are commonly known as mantis shrimps and locally known as Kin-pazun in Myanmar and Pa-Kann or Pa-Kann-Taunk in Myeik. The common name 'mantis shrimp' is derived from the large and powerful raptorial appendages. They belong to the order Stomatopoda. There are 17 families of mantis shrimps in the world wide (Ahyong, 2001).

Ecologically, mantis shrimps are one of the most conspicuous members of large-sized benthic animals living in soft sediment. Also, they are available in the local and foreign markets because of their delicacy and richness in vitamins. Mantis shrimps fishery is very popular among small-scaled fishermen in Min Khaung Shay village which is located in the southern part of Myeik. Except for the study on morphometric characters of two mantis shrimps species *Harpiosquilla raphidea* and *Miyakea nepa* in Myeik coastal water by Myo Nander Myint (2012), there was no data

[1] Dr. Assistant Lecturer, Department of Marine Science, Myeik University.
[2] Demonstrator, Department of Marine Science, Myeik University.
[3] Dr. Lecturer, Department of Marine Science, Myeik University.

concerning the species diversity and fishery of Mantis shrimps in Min Khaung Shay water area. Thus, the present study attempted to investigate the mantis shrimp diversity and fishery status of the Min Khaung Shay water area.

Materials and methods

Mantis shrimps samples were collected from the trammel net operated in Min Khaung Shay water area (Lat 12° 11'N and Long 98° 36'E) during May – July 2018 (Fig 1 and 2).

Figure 1. Map showing the study area

Coloration and distinctive characters of Mantis shrimps were firstly recorded in fresh condition. Species identification was done according to the classification systems of Manning 1998, Ahyong 2001 and Ahyong *et al.* 2008. Based on the distinctive morphological characters, it was found that propodus claw with small spines or blunt pectination, posterolateral corner of carapace excavate or rounded, the presence or absence of spine on the intermediate carinae of thoracic somites, the presence or absence of

anterior bifurcation on the median carina and the lateral pattern of 5th thoracic somites.

The total length (the distance from the apex of the rostral plate to the end of the telson teeth), carapace length (the distance from the behind of the rostral plate to the posterior of the carapace along the midline) were measured by using a ruler to the nearest 0.1cm (Fig 3). Then total weight was measured by using an electronic balance to the nearest 0.1g. Sex was determined by the presence or absence of a penis located at the base of a pair of third pereiopods on the eighth thoracic segment. The samples were photographed during the study.

After that, some specimens were preserved in 10% formalin and deposited in the museum of Marine Science Department, Myiek University for further study. The information attained on the fishing method, season and market value mantis shrimps were gathered from the local fishermen and dealers.

Figure 2. A) Fishing boat; B) Trammel net; C) Float and D) Lead

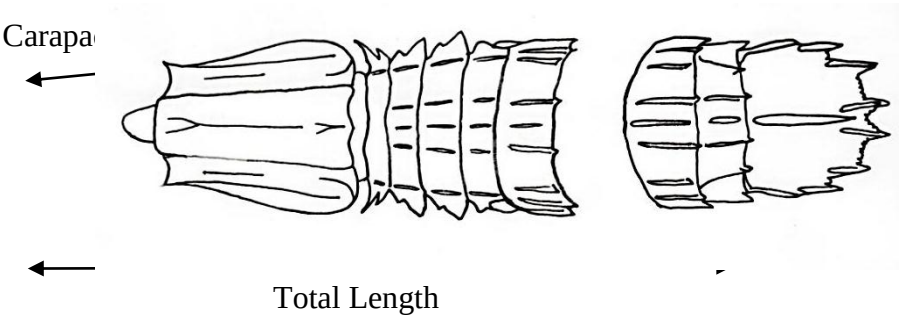

Figure 3. Measurements of carapace length and total length used in the present study

Results

Six mantis shrimps species belonging to the five genera of the 2 families which are identified as *Harpiosquilla harpax*, *H. raphidea*, *Dictyosquilla foveolata*, *Erugosquilla woodmasoni*, *Miyakea nepa*, and *Oratosquillina interrupta* were constituted in the mantis shrimp fishery of Min Khaung Shay (Table 1 and Figure 4).

Table 1. Classified lists of mantis shrimps recorded in the present study

Phylum	**Class**	**Order**	**Family**	**Genus**	**Species**
Arthropoda	Malacostraca	Stomatopoda	Harpiosquillidae	*Harpiosquilla*	*Harpiosquilla harpax* (De Hann,1844)
					Harpiosquilla raphidea(Fabricius,1798)
			Squillida	*Dictyosquilla*	*Dictyosquilla foveolata* (Wood-Mason,1895)

Phylum	Class	Order	Family	Genus	Species
				Erugosquilla	*Erugosquilla woodmasoni*(Kemp,1911)
				Miyakea	*Miyakea nepa* (Latreille,1828)
				Oratosquillina	*Oratosquillina interrupta* (Kemp,1911)

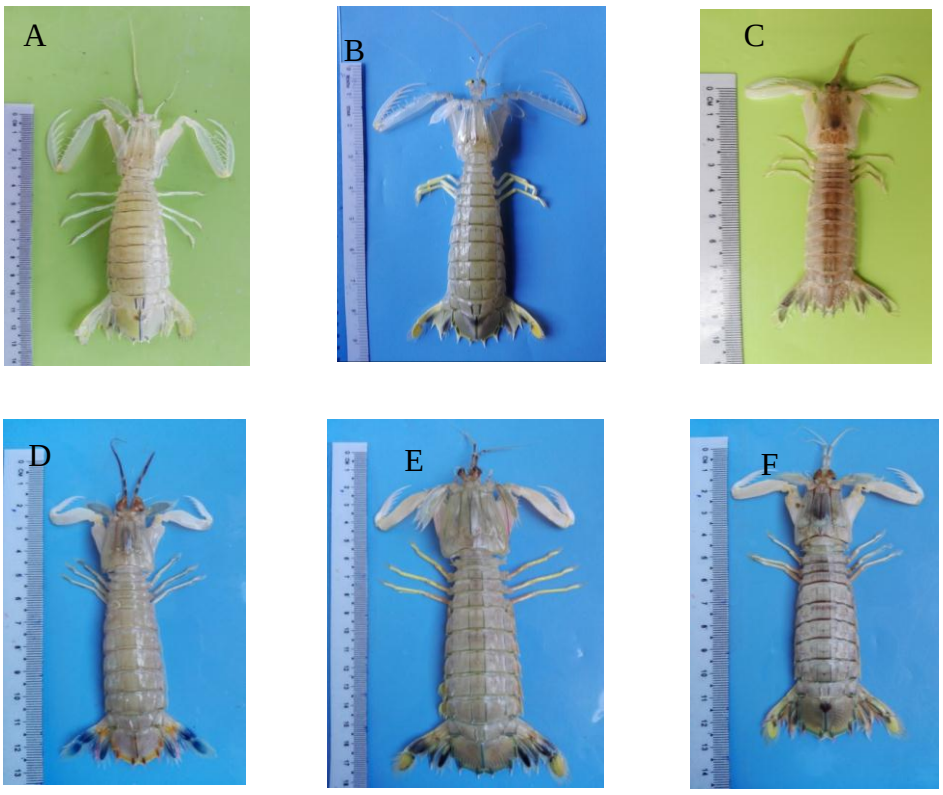

Figure 4. Mantis shrimps: A) *Harpiosquilla harpax*; B) *H. raphidea*; C) *Dictyosquilla foveolata*; D) *Erugosquilla woodmasoni*; E) *Miyakea nepa* and F) *Oratosquillina interrupta*

Fishery status

Mantis shrimps fishery is the main fishery of Min Khaung Shay village. There were about 50 mantis shrimp fishing boats in this village. The size of the fishing boat, engines, and the number of fishermen varied according to the financial ability of fishermen. Commonly, the size of the mantis shrimps fishing boat used in Min Khaung Shay village was about 13-15m long and 2-2.5m wide, with 10 engine horsepower motor. The fishing areas in the study are particularly around the water areas of Min Khaung Shay village.

The fishermen used the trammel net to catch the mantis shrimp. Trammel net has three panels of netting suspended from a common row of floats and attached to a single bottom line. The two outside walls of netting have a larger mesh size (7cm) than interior netting (2cm). The length of the net was 28 m and the depth was 2 m. Mantis shrimps fishing was conducted twice a day during the neap tide. During the neap tide, the fishermen set the net up at 18-50 m in depth across the water current at night and hauled up the net after 15 to 20 hours later. According to the local fishermen interviews, the fishery was conducted throughout the year and the highest catch of mantis shrimp was recorded during the rainy season.

There are six species of mantis shrimps: *Harpiosquilla harpax, H. raphidea, Dictyosquilla foveolata, Erugosquilla woodmasoni, Miyakea nepa*, and *Oratosquillina interrupta* were constituted in the mantis shrimp fishery. Among these species, *Harpiosquilla harpax* and *H. raphidea* are the largest mantis shrimp and economically important species for local and export markets. So these two species are caught as a target by local fishermen.

Live *Harpiosquilla raphidea* and *H. harpax* species ranging from 100 g to 300 g in weight can be sold in the market and exported to China and Thailand. The prices vary from 1,000 kyats to 12,000 kyats depending on the size and weight. The death and small-sized mantis shrimps caught in trammel net were discarded or sold in the village.

The recorded size ranges of mantis shrimps were 11-13.5 cm in total length, 2.4-2.9 cm in carapace length and 12.75-15.40 g total weight for *Harpiosquilla harpax*, 18-30 cm TL, 4-6.5 cm CL and 79-320 g TW for *Harpiosquilla raphidea*, 8-9.5 cm TL, 2-2.5 cm CL and 7-8.5 g TW for *Dictyosquilla foveolata*, 8.6-10.2 cm TL, 2.2-2.7 cm CL and 10.73-14.82 g

TW for *Erugosquilla woodmasoni*, 6.5-15.5 cm TL, 1.5-3.6 cm CL and 12.5-44.7 g TW for *Miyakea nepa* and 9-10.7 cm TL, 2.3-2.6 cm CL and 9.32-13.5 g TW for *Oratosquillina interrupta*.

Discussion

The mantis shrimp fishery plays a very important role in the economy of small scale fishermen in Min Khaung Shay village, Myeik Archipelago. Six species of mantis shrimps belonging to 5 genera under the two families: Harpiosquillidae and Squillidae were recorded from the trammel net fisheries during the study. The different characters between the two families were the morphology of carapace and the pattern of propodus of raptorial claw.

The family Harpiosquillidae is characterized by the excavated posterolateral corner of carapace and propodus of raptorial claw lined with erect spines. There are nine species of *Harpiosquilla* genera was mentioned under the family Harpiosquillidae from Western Central Pacific by Manning (1998). Ahyong (2001) reported 8 species of *Harpiosquilla* from Australian water. Only one species *Harpiosquilla raphidea* was reported from San Khan Thit, Ye Kan Aw, Kyat Chaung, and The Chaung by Myo Nandar Myint (2012). Two species of *Harpiosquilla harpax* and *H. raphidea* were recorded in the present study and identified based on the presence or absence of the spine on 5th thoracic somites. The present specimens of these two species were similar to the description and color pattern of *Harpiosquilla harpax* and *H. raphidea* mentioned by Manning (1998) and Ahyong (2001). Manning (1998) recorded the maximum total length of about 25cm for *Harpiosquilla harpax* and more than 33 cm for *H. raphidea*. The size range of the total length for *Harpiosquilla harpax* and *H. raphidea* recorded in the present study were 11-13.5 cm and 18-30 cm respectively. Taylor and Haddy (2005) stated that the mean carapace length of *Harpiosquilla harpax* from Moreton Bay, Queensland was 4.5 cm. The recorded carapace length range of *Harpiosquilla harpax* in the present study was 2.4-2.9 cm.

The family Squillidae is characterized by the rounded posterolateral corner of carapace and propodus of raptorial claw lined blunt pectinations. Manning (1998) mentioned eight genera of squillid under the family Squillidae. Only four genera: *Dictyosquilla*, *Erugosquilla*, *Miyakea*, and

Oratosquillina were recorded under the family Squillidae in the present study.

Dictyosquilla is unique in the Squillidae in bearing having the entire mid-dorsal surface covered with mesh-like reticulated carinae. Ahyong (2001) reported that two species: *Dictyosquilla foveolata* and *D. tuberculata* included in this family. Only one species of *Dictyosquilla foveolata* was reported from the survey around Singapore by Ahyong (2016). In the present study, only one species of *Dictyosquilla foveolata* was recorded in the Min Khaung Shay water area.

The genus *Erugosquilla* is easily distinguished by its lacking trace of an anterior bifurcation on the median carina of the dorsal carapace. The distinctive character between the genus *Miyakea* and *Oratosquillina* is the form of bifurcation in which bifurcation on the median carina of the carapace is posterior to dorsal pit in *Miyakea* and bifurcation on the median carina of the carapace is anterior to dorsal pit and interrupted at the base of bifurcation in *Oratosquillina*.

With regard to the genus *Erugosquilla*, only one species of *Erugosquilla woodmasoni* (Smooth squillid mantis shrimp) was recorded in the present study. This species is diagnosed by its lacking bifurcation of median carina on the carapace. The description on the diagnostic characters of *Erugosquilla woodmasoni* collected in the present study generally agreed well with the taxonomy of Manning (1998) and Ahyong (2001). The reported maximum total length of *Erugosquilla woodmasoni* was 15cm (Manning, 1998) while the maximum total length range of 8.6-10.2 cm was only observed during the study period.

In the present study, only one species of *Miyakea nepa* (Small eyed squillid mantis shrimp) was recorded under the genus *Miyakea.* The distinctive character of this species is the posterior bifurcation of median carina on the carapace. The general morphological description of *Miyakea nepa* resembled those of *Miyakea nepa* mentioned by Manning (1998) and Ahyong (2001). Manning (1998) reported the maximum total length of *Miyakea nepa* as 17cm. The small size range of total length was only observed in the present study.

Under the genus *Oratosquillina*, only one species of *Oratosquillina interrupta* was recorded in the present study. *Oratosquilla interrupta* is easily distinguished by the median carina of carapace with interrupted at the

base of bifurcation. The diagnostic characters that occurred in the species resembled those of the description of *Oratosquilla interrupta* mentioned by Ahyong (2001) and Ahyong (2016). The total length of *Oratosquilla interrupta* ranged from 9-10.7 cm in the present study. However, the maximum total length of *O. interrupta* reported by Ahyong 2001 was 3.8-15.5 cm in males and 6.6-16 cm in females.

Mantis shrimps were found to be highly caught in the rainy season during the present study. But annual landings of mantis shrimp from Moreton Bay were lowest in winter and peaked between late summer and early autumn (Taylor and Haddy, 2005). And the high catch of mantis shrimp in summer and low in winter from the trawl catch of the eastern Ligurian Sea was reported by Rossetti *et al*. 2005. This situation could be due to some differences in the Spatio-temporal distribution of the fishing effort.

There are about 50 mantis shrimp fishing boats in Min Khaung Shay village. The market demand of foreign countries on mantis shrimp (*Harpiosquilla harpax* and *H. raphidea*) is high. So, high market demand and the high price of mantis shrimp may lead to the increased fishing effort in this species in this area. Although the fishery potential on mantis shrimp is high in Min Khaung Shay village, there is no data on its fishery status. So, it is necessary to record the regular fishery data for stock assessment which is important for the management of any fishery.

Conclusion

Mantis shrimps are commercially caught as a target by trammel net in the Min Khaung Shay village, Myeik Archipelago. Six species: *Harpiosquilla harpax*, *H. raphidea*, *Dictyosquilla foveolata*, *Erugosquilla woodmasoni*, *Miyakea nepa*, and *Oratosquillina interrupta* constituted in this fishery. Moreover, fishing is important and profitable for small scale fishermen of Min Khaung Shay village because of the high market price of mantis shrimp. So, this situation may lead to the increase in fishing pressure on this species which in turn could lead to stock decline which could possibly result in the total collapse of the stock. Therefore, it is still necessary to the information about the stock structure, abundance, life history, and reproductive rate of species for sustainable utilization on this species.

Acknowledgements

We would like to express our special thanks, to Dr. Ni Ni Oo and Dr. Win Win Than, Pro-Rectors of Myeik University for their permission to carry out this research. We are very grateful to Dr. Nyo Nyo Tun, Professor, and Head of Marine Science Department, Myeik University for her critical suggestions and permission to use the laboratory facilities. Thanks are also due to local people from Min Khaung Shay Village for helping during the samples and data collection of mantis shrimps species. The first author also would like to thank her beloved parents, U Chit Maung and Daw May Lwin, for their physical moral and financial support throughout this study.

References

Ahyong, S.T. 2001. Revision of the Australian Stomatopod Crustacea. Records of the Australian Museum, Supplement 26:1-326.

Ahyong, S.T. 2016. Results of the Comprehensive Marine Biodiversity Survey International Workshops 2012 and 2013: Stomatopod Crustacea. *Raffles Bulletin of Zoology.* (34): 455-469.

Ahyong, S.T., Chan, T.Y and Liao, Y.C. 2008. A Catalog of the Mantis Shrimps (Stomatopoda) of Taiwan. National Taiwan Ocean University. 199pp.

Manning, R.B. 1998. Stomatopods. In K. E. Carpenter and Niem, FAO species identification guide for fishery purposes. The living marine resources of the Western Central Pacific. Vol.2. Cephalopods, Crustaceans, Halothurians and Sharks. FAO, Rome. Pp. 827-849.

Myo Nandar Myint. 2012. Study of the morphometric characters and length weight relationship of *Harpiosquilla raphidae* (Mantis Shrimp) in Myeik Coastal waters. M.SC (Thesis). Department of Marine Science Myeik University. Myanmar.

Rossetii, I., Sartor, P., Francesconi, B. and Belcari, P. 2005. Fishery and biology of mantis shrimp, *Squilla mantis* (L., 1758), exploited with “rapido” trawl in the eastern Ligurian Sea. *Biologia Marina mediterranea*, 12: 585-588.

Taylor, J. and Haddy, J. A. 2005. Species composition, spatial distribution, relative abundance and reproductive biology of mantis shrimps in Moreton Bay, Queensland. 177-194pp.

General Quality Assessment of Mangroves in Mawtin Coast

Tin Tin Kyu[1], Moe Lwin Lwin[2], Chaw Su Lwin[3] & Yin Yin Htay[4]

Abstract

The survey was conducted in the mangrove forests of Nga Pu Taw Township and Ngwe Saung Township, Ayeyarwady Region during January 2018. A total of 25 true mangroves and 5 species of mangrove associates were recorded. Among true mangroves, 4 species were reported as Nearly Threatened, Endangered or Critically Endangered, and one in mangrove associates as Nearly Threatened. The species composition, vegetation community, degradation level and overall threats to mangrove forests were also presented.

Keywords: Degradation, Mawtin Coast, Nearly Threatened, species composition, vegetation community

Introduction

Mangroves are found in the tidal areas of three coastal regions along Myanmar Coastline; 46% in Ayeyarwady, 37% in Tanintharyi and 17% in Rakhine respectively. Myanmar stands at 3rd position in Southeast Asia and 8th position in world mangroves. Mangrove ecosystems play an important role in livelihood of coastal communities. They provide not only good source of timber, fuel and fodder, but also potential source for recreation and tourism.

Mangroves also play a critical role in protecting lives and property in low-lying coastal areas from storm surges, which are expected to increase due to global warming. They also stabilize shorelines and improve water quality. They protect shorelines from destructive storms and floods. They stabilize the balance of carbon dioxide. They can filter out pollutants like nitrates, phosphates and petroleum based products that are present in run-off.

The mangroves in Mawtin Coast are the area which is not conserve for sustainability. The impact on the forests seems primarily due to the

[1,2,3] Assistant Lecturers, Department of Marine Science, Myeik University
[4] Lecturer, Dr., Department of Marine Science, Myeik University

extraction of mangrove materials for local and household needs. The communities in the study areas rely primarily on fishing, a beginning tourist industry to survive and the extraction of mangroves for timber and wood.

The specific objectives were to undertake habitat surveys of the mangrove forests of the Mawtin Coast including species composition, the vegetation community, densities and canopy heights and degradation level.

Materials and Methods

Study Areas

This survey was carried out in three forests along the Mawtin Coast in Ayeyarwady Region during January 2018. They are the mangrove forest of:

1) Tuu Myaung, near the Nga Yoke Kaung village, Nga Pu Taw Township,
2) Tazin village, Ngwe Saung Township and
3) Yay Thoe river, Ngwe Saung Township (Fig. 1).

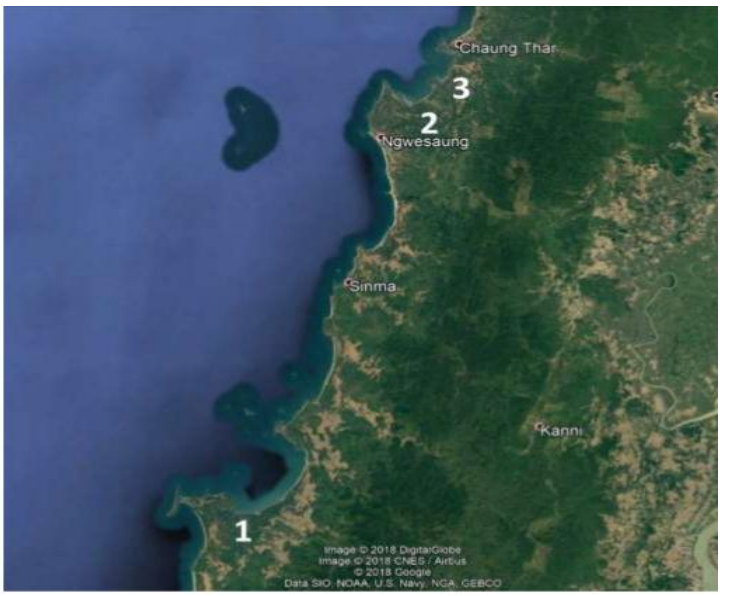

Figure 1. Map of the three study areas in Mawtin Coast

Method for Quality Assessment of Mangroves

The date, time, village and mangrove zone were systematically recorded. The GPS system was used for data collection. The start and end point of the transects were marked at a minimum. Point-Centre-Quarter-Method (PCQM) (Cintron and Schaeffer-Novelli, 1984, Dahdouh-Guebas and Koedam, 2006) was used, as it produces standard forestry measures such as basal area/hector, tree density/ha and average height etc.

The transects were laid in these three mangrove forests in Mawtin Coast. According to the google map, the number of transects was selected. Along each transect, at least 15 center points were set at distances depending on the length of the whole transect. Each center point was divided into four (5 × 5) quadrants in the adjacent mangrove area. In each quadrant, an adult mangrove plant closet to this center point is chosen to measure. The species of the tree, its height, its circumference at breast height (CBH130) and its distance to the center point are also measured. In two of the four quadrants defined, cut stumps of between 130 and 35 mm diameter, the number of saplings and of juvenile trees were counted, and hemispherical photography (using an Olympus Tough TG-5 Compact Digital Camera equipped with a FCON-T01 Fisheye Converter and tripod) was used to assess canopy quality, through the sky/leaf coverage ratio over the sampling quadrant. The lower the ratio, the healthier the mangrove, since a closed canopy provides a pristine habitat for the floral and faunal components of these forests. The salinity of pore water was recorded using a portable refractometer.

The main method utilized for measuring the tree height was the use of clinometers (SUUNTO PM-5/360 PC) and, for small trees, the use of metal tape measure (5 m long). Tape measures having various lengths (2m, 30m and 50m) were also used to measure the distance of the measured trees from the center point and its CBH130. All the above data were recorded directly on a data sheet printed on waterproof paper.

Apart from this quantitative sampling, the data outside the sampled quadrants were recorded. The species were classified as Critically Endangered (CE), Endangered (EN), Vulnerable (VU) or Nearly Threatened (NT) in the IUCN Red List of Threatened Species (http://www.iucnredlist.org/).

Data Analyses

The data recorded on the inventory data sheets were transferred to Microsoft Excel files. The PCQM data analysis excel programme 'P-Data Pro 1000', developed by Dahdouh- Guebas and Koedam (2006), was used. The output from this excel of average tree height (m), tree density/ hectare and basal area (m^2/hectare) from the measurements of tree height, tree distance from sample point and circumference were studied.

Results and Discussion

Twenty-five species of true mangroves and (5) mangrove associates were recorded. Among true mangroves, (4) species were reported as Nearly Threatened, Endangered or Critically Endangered, and one in mangrove associates as Nearly Threatened. (Table 1)

At all study areas, the human impacts on mangroves were conspicuous, with some areas almost completely degraded and no visible sign of any community-based or government effort for sustainable management. Many areas formerly dominated by mangroves are now dominated by the Finlayson's creeper, *Finlaysonia obovata*. This species grows dense aggregations, impeding the natural recruitment and establishment of mangrove propagules, and overgrow mature mangrove trees.

Mangroves at Nga Yoke Kaung village, Nga Pu Taw Township

Five transects were laid in the mangroves at Nga Yoke Kaung; each two in the downstream area of the estuary and the intermediate area, and one in the upstream area (Fig. 2). At all transects, 15 points were marked and a total of 60 sub-quadrants were recorded.

It is found that at all sites, mangroves were strongly impacted, as shown by the low mean tree height at all sites (Table 2). An almost pristine and untouched area was only found on the landward of T5, where trees of *A. officinalis* up to 10 m tall were frequent. The Complexity Index was extremely low in T2, T3 and T4, while it was slightly higher at T1 (mainly due to healthy *N. fruticans* palms) and T5 (mainly dominated by *A. officinalis*) although still not finding as a pristine situation.

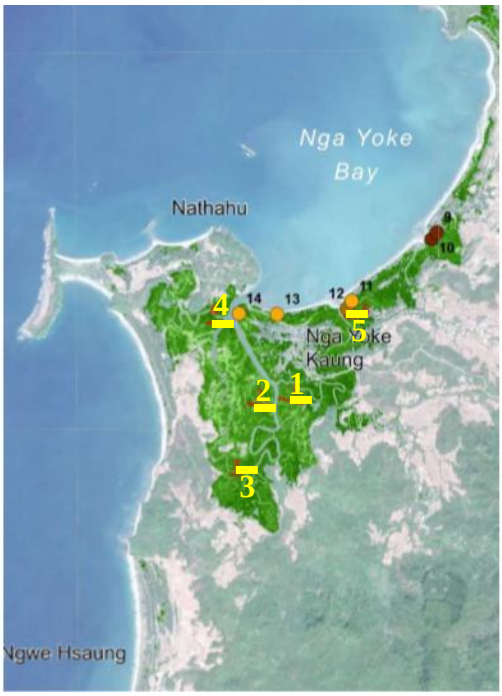

Figure 2. Map of the position of yellow five transects in Nga Yoke Kaung mangrove forest

The Degradation Index was in between 2 and 3 in all transects. The two transects in the intermediate area were very different. The former one was co-dominated by *C. decandra* (26.8%), *A. officinalis* (23.2%), *R. apiculata* (19.6%) and *N. fruticans* (17.9%) and the latter one was strongly dominated by *R. apiculata* (60.3%). This showed that the intermediate area of this forest is spatially heterogeneous. The upstream T3 was dominated by *R. apiculata* (57.6%) and *B. gymnorhiza* (15.1%), while two transects of downstream were dominated by *E. agallocha* (39.8% in T4 and 20.3% in T5, respectively) and *A. officinalis* (23% in T4 and 27.1% in T5, respectively). These transects, or parts of them were influenced by freshwater as shown by their salinities. The number of juveniles in the sub-quadrants of all transects was low except T5, where high number of recently recruited saplings with a higher variability was found.

The number of rare or endangered species were also recorded. Adult trees of *S. griffithii* (IUCN Red List Critically Endangered) were fairly

common near T1, T2 and T3, although most showed some degrees of human impacts, such us cut stems. Only one plant of *E. indica* was found, near the end of T1. The (5) plants of *A. rodundifolia* sparsely distributed near T5 were recorded.

Table 1. List of mangrove species commonly found in Mawtin Coast

True Mangroves			
Species	**Common Name**	**Family**	**IUCN Cat.**
Acanthus ilicifolius	Lilac-flowered Holy Mangrove	Acanthaceae	LC
Acrosticum aureum	Golden Mangrove Fern	Pteridaceae	LC
Aegialitis rotundifolia	Northern Club Mangrove	Plumbaginaceae	NT
Aegiceras corniculatum	Southern River Mangrove	Myrsinaceae	LC
Avicennia alba	White Grey Mangrove	Avicenniaceae	LC
Avicennia marina	Grey Mangrove	Avicenniaceae	LC
Avicennia officinalis	Round-leafed Grey Mangrove	Avicenniaceae	LC
Bruguiera cylindrica	Reflexed Orange Mangrove	Rhizophoraceae	LC
Bruguiera gymnorhiza	Large-leafed Orange Mangrove	Rhizophoraceae	LC
Bruguiera sexangula	Upriver Orange Mangrove	Rhizophoraceae	LC
Ceriops decandra	Western Clumped Yellow Mangrove	Rhizophoraceae	NT
Ceriops tagal	Rib-fruited Yellow Mangrove	Rhizophoraceae	LC
Dolichandrone spathacea	Trumpet Mangrove	Bignoniaceae	LC
Excoecaria agallocha	Common Milky Mangrove	Euphorbiaceae	LC
Heritiera fomes	Sundri Mangrove	Sterculiaceae	En
Heritiera littoralis	Keeled-pod Mangrove	Sterculiaceae	LC
Lumnitzera littorea	Red-flowered Black Mangrove	Combretaceae	LC
Nypa fruticans	Mangrove Palm	Palmae	LC
Rhizophora apiculata	Corky Stilt Mangrove	Rhizophoraceae	LC
Rhizophora mucronata	Upstream Stilt Mangrove	Rhizophoraceae	LC
Sonneratia alba	White-flowered Apple Mangrove	Sonneratiaceae	LC
Sonneratia apetala	Asian Apple Mangrove	Sonneratiaceae	LC
Sonneratia caseolaris	Red-flowered Apple Mangrove	Sonneratiaceae	LC
Sonneratia griffithii	Griffith's Apple Mangrove	Sonneratiaceae	CE
Xylocarpus granatum	Cannonball Mangrove	Meliaceae	LC

True Mangroves			
Species	**Common Name**	**Family**	**IUCN Cat.**
Mangrove Associates			
Aglaia cucullata	Pacific Maple	Meliaceae	DD
Excoecaria indica	Spiny Milky Mangrove	Euphorbiaceae	DD
Phoenix paludosa	Mangrove Date Palm	Arecaceae	NT
Talipariti tiliaceum	Native Hibiscus	Malvaceae	NL
Volkameria inermis		Lamiaceae	NL
Vines			
Derris trifoliata	Common Derris	Leguminosae	NL
Finlaysonia obovate	Finlayson's creeper	Asclepiadaceae	NL

LC, Least Concerned; NT, Nearly Threatened; En, Endangered;
CE, Critically Endangered, NL, Not Listed, DD, Data Deficient.

Table 2. The forestry and ecological parameters at Nga Yoke Kaung mangroves.

Nga Yoke Kaung

	T1	**T2**	**T3**	**T4**	**T5**
Number of tree species	8	9	7	8	9
Mean height (m)	3.7	3.9	3.4	4.0	5.3
Total forest density (trees 0.1 ha^{-1})	174.4	116.5	222.9	233.6	203.6
Total basal area (m^2 $0.1ha^{-1}$)	7.1	1.3	0.3	0.74	4.23
Complexity Index	36.8	5.5	1.7	5.5	40.8
Degradation Index	2.2	2.7	2.3	2.5	3.5
Mean salinity(± St. Dev.)	31.8±2.3	31.9 ±3.5	30.0 ± 0	32.0±2.5	30.0 ± 0
No. of juveniles (± St. Dev.)	3.4 ±3.2	5.2 ± 6.3	1.3 ±3.2	2.3±2.5	8.3±21.2

Mangroves of Ngwe Saung

Two mangrove estuaries, the Tazin River (T1) and the Yay Thoe estuary (T2 and T3) were studied (Fig. 3). One transect was marked 15 points and 60 sub-quadrants at each one. The large portions of the Yay Thoe mangroves seem to be managed as extensive mangrove crab aquacultures. These areas were delimited by fences, made of mud and stones, and ditches were dug to control the water level in the enclosure.

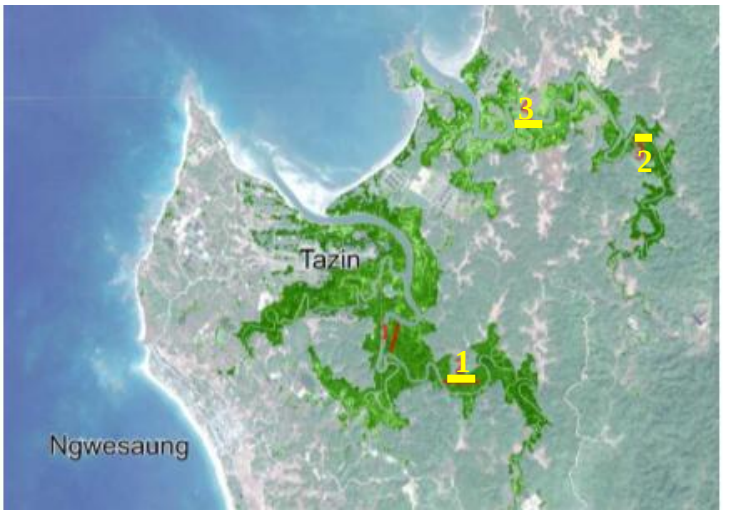

Figure 3. Map of the position of yellow transects in Ngwe Saung mangrove forest

The ecological status of these mangroves is even more degrading than those at Nga Yoke Kaung. At the Yay Thoe estuary, the large portions cannot influence by the natural tidal fluctuation because they are enclosed in fences, and the human impact is strong everywhere. At T3 in Yay Thoe, mangroves were completely destroyed, with not a single tree in 42 out of the 60 sub-quadrants. And, the other transects showed extensive ecological degradation, as shown in Table 3. No mature trees were recorded in the transects. The mean height of trees was less than 3 m. Both Complexity and Degradation Indexes are at their lowest range. The figures for basal area show that trees were very sparse and much lower than the norm. In this destruction, at Tazin, the most abundant species were *R. apiculata* (42.9%) and *C. decandra* (21.4%) at T2. At T3 and T4, the dominant species were *R. apiculata* and *C. decandra* (22.9% and 22.9%; 42.9% and 21.4%) respectively.

S. griffithii was also found in this area. They are in lesser quantity and smaller in size than plants at Nga Yoke Kaung. In the elevated intertidal area of both estuaries, the endangered species *H. fomes* was commonly found. However, nearly all the trees at Ngwe Saung mangroves were heavily impacted; there are the remains of stems which have been cut.

Table 3. The forestry and ecological parameters at Ngwe Saung mangroves. Ngwe Saung

	T1	**T2**	**T3**
Number of tree species	7	8	6
Mean height (m)	3.3	2.8	2.3
Total forest density (trees 0.1 ha^{-1})	214.9	327.6	290.5
Total basal area (m^2 0.1ha^{-1})	0.1	0.5	2.0
Complexity Index	4.3	3.7	8.2
Degradation Index	2.1	2.1	1.1
Mean salinity (± St. Dev.)	30.0 ± 0	28.7 ± 1.1	34.3 ± 4.8
No. of juveniles (± St. Dev.)	8.0 ± 13.2	4.7 ± 8.9	3.0 ± 3.8

Species composition, vegetation community, degradation level and overall threats to mangroves of the Mawtin Coast

In the previous years, the mangrove forest communities in Mawtin Coast were very diverse in all study sites, because a very high number of species were recorded. However, these were recorded by single adult trees or trees regeneration in many cases. These communities were once rich and healthy because the notable presence of a number of Nearly Threatened, Endangered species and one Critically Endangered species, together with two very uncommon mangrove-associates.

At all sites, the mangroves were deeply impacted, with almost all by either young plants or trees recovering from major cut. The mangrove area at Yay Thoe Estuary is destroyed, and it may be a very scarce probability of return to a healthy and functional forests. Some ecological functions and

there are no more services commonly provided by healthy mangrove forests. At many sites along the transects, soil erosion is clearly detected. In these areas, ecological functions such as soil retention and habitat providing for mangrove associated fauna have gone, with very little probability of restoration. The degradation of the mature mangrove communities has led to the rapid colonization of vines and mangrove associated species. In particular, the vine *F. obovata* forms quite dense associations preventing the recolonization of those area by the propagules of *Rhizophora* spp., *Bruguiera* spp. and *Ceriops* spp., changing the overall ecological balance of the forest. This vine is also fiercely growing on the few mature remaining trees, strangling them and shading their leaves, so that the trees may not grow well.

Local people seem to be used the species which they need for livelihoods at both sites. All species of the genera *Rhizophora* and *Bruguiera*, as well as *Xylocarpus granatum* show major damage. These species are known to provide the best timber and firewood among the mangrove trees and are heavily exploited throughout the tropics (Dahdouh-Guebas *et al*., 2006). *Ceriops* spp., *Sonneratia* spp. and *N. fruticans* are still impacted, but at a lower level than the previous ones.

On the other hand, all the species belonging to the genus *Avicennia* and *Excoacaria* are rarely cut or destroyed and, since they colonize together specific areas with abundant freshwater and sandy soil, those areas look really healthy and pristine. *Avicennia* spp. wood is not the best option for construction, but it is widely used for charcoal production in all Eastern Africa. It is not easy to understand at this stage why these trees were relatively untouched on the sites visited. *E. agallocha*, when cut, exudes a latex which is mildly toxic and it is never the preferred option for the timbermen.

At Nga Yoke Kaung, there were no ditches or dams, as well as very few evidence of industrial pollution. Thus, at that site, the source of mangrove destruction is the extraction of mangrove material for building purposes, firewood and charcoal production performed by local communities. At Ngwe Saung, it is certain that extraction of mangrove wood and leaves for building and household purposes is a major threat to mangroves. However, a large portion of this site is dammed for extensive crab aquaculture and its overall hydrology is also compromised. It can be considered that this situation represents a serious threat to the whole

estuary. That some chemicals could also be used for aquaculture purposes which may have other negative impacts to the forests. Nga Yoke Kaung and Tazin estuaries, the hydrology was not altered and there is no sign of heavy pollution. Thus, even though there is replantation programs, natural recolonization will be highly possible in these areas, where the exploitation may be strongly reduced. The public awareness and community run projects to preserve the mangrove forests for local community benefit, are essentially needed at the Mawtin Coast. The ecological status of the mangrove areas of Mawtin Coast has not been reported in recent years, thus the habitat survey is necessary to design a long-term monitoring plan for these forests.

Conclusions

The mangrove forest communities in Mawtin Coast are definitely not sustainably managed. They are strongly impacted due to the overexploitation of mangrove materials for local and household needs. Clearly, whatever the mangrove management model being used is (e.g. centralized or local community-based), it is not working. The exploitation of the mangroves in these areas is not sustainable and a better definition for such an overexploitation should be 'destruction'. A socio-economic survey involving local communities themselves will be of great help to understand how the mangrove forests could be protected. An in-depth understanding of the use of mangrove products is definitely needed. Again, some indications about the management of the aquaculture infrastructures would be important to understand if they are community-based facilities and how they are controlled and managed.

Acknowledgements

We are indebted to Dr. Ni Ni Oo, Rector and Dr. Win Win Than, Pro-rector, Myeik University, for their encouragement throughout this project. We are grateful to Professor Dr. Nyo Nyo Tun, Head of Department of Marine Science, Myeik University, for her kind support, encouragement and valuable advice. We would also like also to express our deep gratitude to Associate Professor Dr. Stefano Cannicci from Swire Institute of Marine Science, University of Hong Kong for sharing about mangrove quality assessment throughout the survey. Our special thanks also go to Fauna and Flora International (FFI) for supporting this survey. Finally, we would also like to express our deep gratitude to Associate Professor Dr. Yin Yin Aye, Head of English Department, Myeik University, for her help with English skills in this paper.

References

Cintron, G. & Schaeffer-Novelli, Y., 1984. Methods for studying mangrove structure. The Mangrove Ecosystem: Research Methods (S.C.Snedaker &J.G.Snedaker) (eds), pp. 91–113. UNESCO, Paris.

Dahdouh-Guebas, F. & Koedam, N., 2006. Empirical estimate of the reliability of the use of the Point-Centred Quarter Method (PCQM): Solutions to ambiguous field situations and description of the PCQM+ protocol. Forest Ecology and Management, 228, 1–18.

Dahdouh-Guebas, F., Collin, S., LoSeen, D., Rönnbäck, P., Depommier, D., Ravishankar, T. & Koedam, N., 2006 Analyzing ethnobotanical and fishery-related importance of mangroves of the East-Godavari Delta (Andhra Pradesh, India) for conservation and management purposes. Journal of ethnobiology and ethnomedicine, 2, 24.

Reproductive Biology of *Sillago sihama* in Myeik Coastal Area

Chaw Su Lwin[1], Tin Tin Kyu[2], Moe Lwin Lwin[3] & Hnin Hnin Maw[4]

Abstract

Fish samples were collected fortnight at Myeik Water Areas and its adjacent islands during the period from June 2013 to February 2014. Their maturity stages were recorded and the gonadosomatic index (GSI) was calculated. The monthly average GSI for both sexes fluctuated throughout the study period. The highest value of average GSI in male was 1.52 and it was 2.27 in female. This species showed a long spawning period and the spawning reached its peak during September and November. The male to female ratio was found that 1:1. According to the maturity stages of gonads, the size at first maturity stages was found above 15-16 cm and onwards was mature.

Keywords*:* gonadosomatic index, Sex ratio, maturity, reproduction

Introduction

Reproduction is the processes by which species are perpetuated. Information about reproduction of fish is also important in aquaculture. The availability of quality seeds and the ability to control fish reproduction are limiting factors in the farming of any commercial species. Most fishes lay a large number of eggs, fertilized in the aquatic environment.

Studies of reproduction and growth of many species indicated that the rate of reproduction depends particularly on temperature, the length of the day and food supply. The environmental factors greatest influence on the gonadol development initiation and fecundity of the species.

Fish belong to the family Sillaginidae (order-perciformes) commonly known as lady fish /whiting can be found all along the coast line and they contribute considerably to the coastal line and estuarine fisheries.

[1,2,3,4] Assistant Lecturers, Department of Marine Science, Myeik University

This species has great potential for brackish water fish culture because of its faster growth rate and high market price (Annappaswamy, *et al* 2008).This species inhabit sandy and /or muddy substrates in inshore areas, feeding mainly on benthic invertebrates including polychaetes, shrimps and crabs (Sano *et.al* 2006). The objective of this study is to know the spawning season of *S. sihama* in Myeik coastal area.

Materials and Methods

Fish samples were collected fortnighty at Myeik Water Areas and its adjacent islands from June 2013 to February 2014. Fish were dissected to examine sex after their length and weight had been recorded. Stages of gonads were determined on the basis of morphological appearance (macroscopic observation) the colour and the size of gonads in relation to body cavity and also microscopic appearance.

After that the gonads were dissected out and their weights were measured after removing the surface moisture by tissue paper.

The spawning season was determined on the basis of the distribution of different maturity stages of male and female during the study period. The gonadosomatic index (GSI) was calculated by using the formula,

$$GSI = \frac{\text{weight of gonad}}{\text{weight of fish}} \times 100$$ (Shamsan, 2008)

Fecundity was studied by examining 24 mature preserved ovaries. To determine fecundity, a sub–sample of 0.1 g was taken out from the mature ovary and the ovaries were tested out and dispersed in a small amount of ova was computed based on the total weight of the ovary using the following formula (Grimes and Huntsman, 1980).

$$Fecundity = \frac{\text{total weight of gonad}}{\text{sub} - \text{sample weight}} \times \text{No. of ova in the sub-sample}$$

Monthly sex ratio was worked out. The size of the fish was divided into 12 classes and the class interval between them was 1. The observed sex ratios were tested against an expected 1:1 ratio by the method of Chi-square (Banerjee, 2004).

Spawning season

Spawning season was determined on the basis of occurrence of different maturity stages of males and females in each month during the period from June 2013 to February 2014. The female in stage III with mature gonads appeared all the months. Both females and males with immature stage I and stage II gonads were observed all the months which indicated a protracted behavior. And then, females stage IV gonads were observed all the months, the highest percentage occurred in July. But, male's stage IV gonads were found from August to February and they were not found in June and July. Similarly, females' stage V gonads were found from August to February and were not occurred in June and July. Male's stage V gonads were not observed during this period. The ripe gonads were observed the highest in September, October, November and December. Therefore, the major spawning season was between September and November.

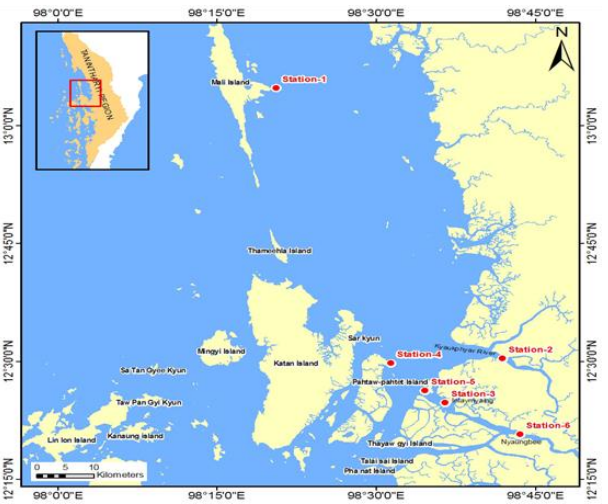

Figure 1 Map showing the study area of Myeik Coastal region.

Results and Discussions

Maturity stages in Male

Stage I (Immature): Testes are small, thin, and thread-like in shape. (Male)

Ovaries are small, thin, occupying less than ½ of the abdominal cavity. They are usually translucent pink or glassy. (Female)

Stage II (Maturing): Testes are semitransparent, dark, grey and extending up to less than ½ of the abdominal cavity. As testes developed they became moderately thick, slightly flattened, and gray-whitish extending up to ½ of the abdominal cavity. (Male)

The ovaries developed in size to occupy about ½ -2/3 of the body cavity. They appear as a semi translucent to clear yellow and oval in shape. It showed withdrawal of a batch of ova. (Female)

Stages III (Mature): Testes are large, opaque, well developed and white or ivory in color. They are ribbon shaped, occupying about 2/3-3/4 of the body cavity. (Male)

As more oocyts developed and turn opaque, the ovaries turn to pale yellow or apricot colour. At this stage ovaries extending up to more than ¾ of the body cavity (Female)

Stage IV (Ripe): They look like mature testes thick, flat but more swollen, creamy white, extending in the entire body cavity. (Male)

Ovaries are very large and swollen; filling the entire body cavity. Colour is orange with a prominent network of blood vessels. (Female)

I II III IV V

Figure 2. Ovaries of *S.sihama* in different maturity stages

I II III IV

Figure 3. Testes of *S. sihama* in different maturity stages

Percentage occurrence of different maturity stages

Table 1. Percentage occurrence of different maturity stages of *S.sihama* during the study period (females).

	Stages of maturity				
Month	**I**	**II**	**III**	**IV**	**V**
June(2013)	21.05	36.34	32.09	10.52	0
July	16.65	22.23	22.23	38.89	0
August	13.04	21.74	34.78	26.09	4.35
September	13.34	8.14	33.33	33.33	11.86
October	14.28	23.39	20.05	28	14.28

	Stages of maturity				
Month	**I**	**II**	**III**	**IV**	**V**
November	6.66	20	26.67	26.67	20
December	6.67	13.33	13.33	26.67	40
January(2014)	28.57	14.29	21.43	21.43	14.28
February	9.09	36.36	36.36	9.1	9.09

Table 2. Percentage occurrence of different maturity stages of *S.sihama* during the study period (Males).

	Stages of maturity				
Month	**I**	**II**	**III**	**IV**	**V**
June	31.25	50	18.75	0	0
July	27.27	45.46	27.27	0	0
August	36.37	27.27	27.27	9.09	0
September	10	40	20	30	0
October	10	40	20	30	0
November	20	10	35	35	0
December	12.5	37.5	19	31	0
January	33.11	40	15.78	11.11	0
February	40	40	6.67	13.33	0

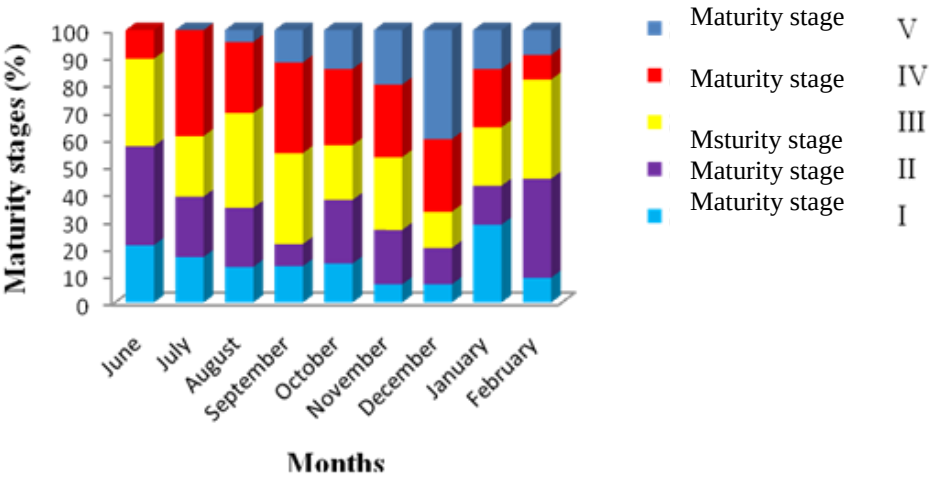

Figure .3 Percentage of different stages of gonad in female.

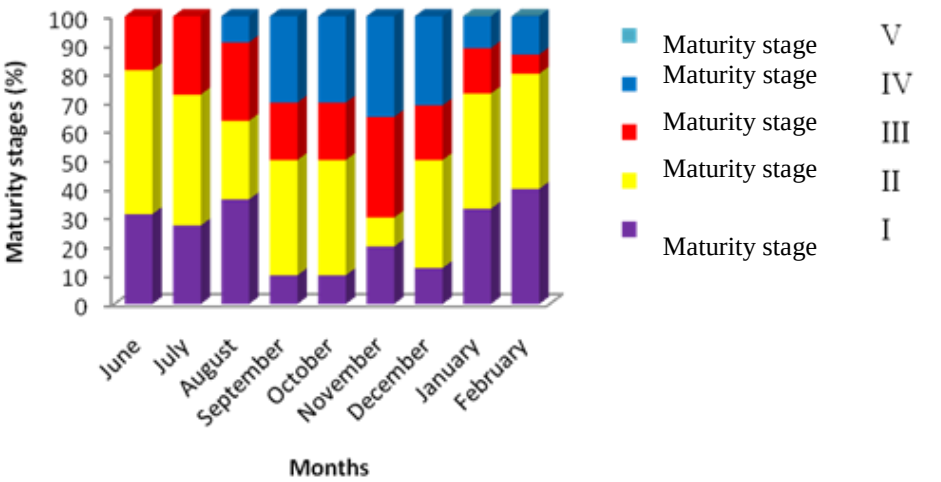

Figure 4. Percentage of different stages of gonad in male.

Sex ratio

Sex ratio was calculated for different months and size groups of the fish. The sex ratio was tested for equality months using Chi-square test. The sex ratio is presented in table.3 and 4. The difference was significant in all months. The numbers of female and male were not the same but the test showed the ratio of male to female is 1:1.

Table 3. Monthly variation in sex ration of *S. sihama* during June 2013 to February 2014

Months	Total no. of fish	No .of Males	No .of Females	Ratio M : F	X^2
June	35	16	19	0.84 : 1	0.05
July	33	15	18	0.83 : 1	0.06
August	34	11	23	0.47 : 1	1.78
September	25	9	15	0.60 : 1	0.72
October	31	11	20	0.55 : 1	1.03
November	35	20	15	0.80 : 1	0.23
December	21	13	18	0.72 : 1	0.26
January	32	18	14	1.29 : 1	0.14
February	26	15	11	1.37 : 1	0.17

Table 4. Variation in sex ratio of different size groups during June 2013 to February 2014.

Size class	Total no. of fish	No. of males	No. of female	Ratio M : F	$X^{\wedge}_2$
11-12	24	13	11	1.18 :1	0.02
12-13	22	10	12	0.8 : 1	0.01
13-14	19	8	11	0.72 : 1	0.10
14-15	28	15	13	1.15 :1	0.03
15-16	40	17	23	1.17 :1	0.31

Size class	Total no. of fish	No. of males	No. of female	Ratio M : F	$X^{\wedge}_2$
16-17	40	22	18	0.67 :1	0.05
17-18	15	6	9	0.67 :1	0.01
18-19	19	11	8	1.4 :1	0.10
19-20	20	8	12	0.67 :1	0.23
20-21	16	5	11	0.5 :1	0.78
21-22	19	8	11	0.9 :1	0.10
22-23	20	7	13	0.53 :1	0.62

Gonado Somatic Index (GSI)

Monthly GSI of male and female was described in Fig. 5.The mean monthly GSI. in male fluctuated between 0.26 in February to 1.52 in November and in female from 0.75 in October to 2.27 in September. The two values of GSI distinct peaks in September and November in both sexes.

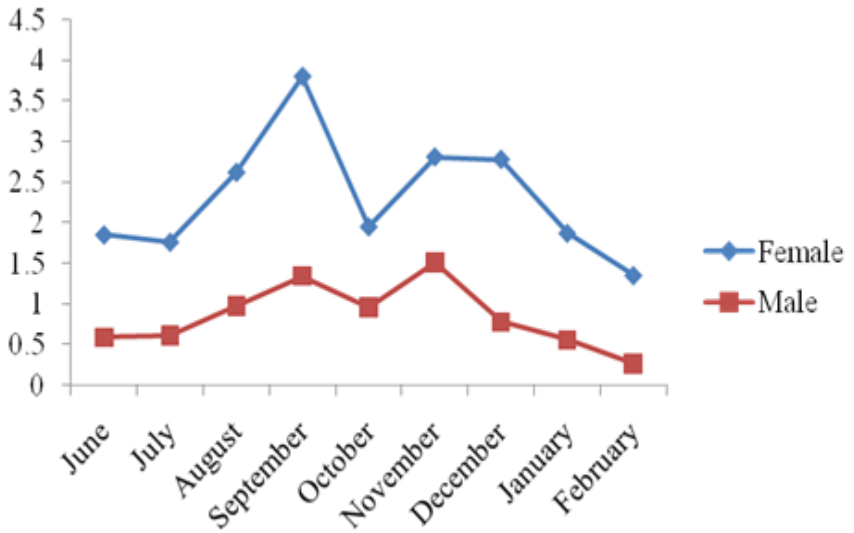

Figure 5. Monthly average gonadosomatic index (GSI) of *S. sihama*

Fecundity

Determination of the fecundity of *S. sihama* was investigated base on twenty four females (at Stage from III to VI). The fecundity of this species ranged from 12,376 to 1,126,000 for fish length that ranged from 15.5 to 22.5cm. The positive relationship was found between Fecundity and total length of fish, weight of fish and weight of gonads.

Size at first maturity

To determine the size at which the fish attain the first sexual maturity a total of 131 males and 150 females were used. The percentage occurrence of matured individuals was plotted against different size group in male and female was presented in Figure 6. It shows that both sexes became matured at the size group 14-15 cm for male and 15-16 cm for females. Therefore, both sexes are fully mature at the size groups 16-17 cm and onwards.

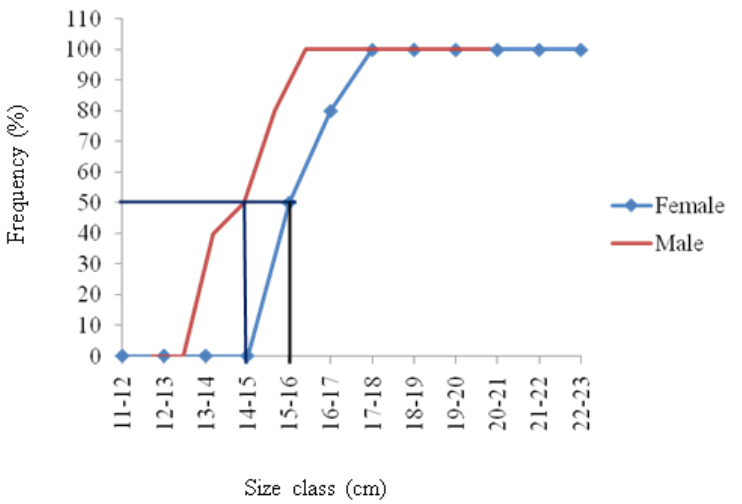

Figure 6. Percentage occurrence of male and female *S. sihama* in different size groups

The immature and mature gonads were found throughout the research. However, the frequency of mature gonads of female *S. sihama* was high in July, September, August, November and December. Spent stage was observed during the period from August to February and the highest percentage was found in December. The mature stage of the male of *S.*

sihama was observed during August –February and the highest percentage was found in November. This suggests that *S. sihama* has a prolonged spawning season. The major spawning may be between September and November. This observation corroborates the earlier reports of Annappaswamy *et.al* (2008) and Shamsan (2008).

The fecundity is a major part for fish culture. The total number of eggs produced by a fish during a year is important in determining the spawning potential of the fish. In the present study, the fecundity range of *S. sihama* was found from 12376 to 1126000 per female with the fish length from 15.5 cm to 22.5 cm. The earlier reports by Annappaswamy *et.al* (2008) for the fecundity of *Sillago sihama* from the estuarine of Mulki, Netravathi- Gurpur, Paranje and Shambavi rivers was 57,685 to 1,347,340 eggs for mature individuals measuring 130 to 330mm. And Shamsan (2008) reported that the fecundity of *S. sihama* from Zuari Estuary 11,376 to 103,695 eggs for mature individuals measuring from 150mm to 342 mm. Mirzaei *et.al* (2013) also described the fecundity estimation *S. sihama* as 21,345-73,781 eggs for specimens at 13-24 cm length. Krishnamurthy and Kaliyamurthy (1978) reported that the fecundity of the species measuring 227-313 mm in length varied from 31,678 to 28,800 eggs per female. Therefore, the fecundity of *S. sihama* varies with the condition of environment.

In general, fecundity increase with the increase in the size of female which can be expressed by $F= al^b$ (Bengal 1978). This formula refers to larger fish produced more eggs than the smaller fishes. In the present study, *S. sihama* showed the linear relationship between the fecundity and the length of the fish, the weight of the fish and the ovary weight of the fish. The linearity in such relationship has also proved by previous scientists Mirzaei *et.al* (2013); Ansari and Shamsan (2010); Annappaswamy *et.al* (2008) and Shamsan (2008).

Sex ratio indicates the proportion of male and female in the population and is expected to 1:1 in nature. This ratio show that the dominance of one sex over the other. This happens because of differential behavior of sexes, environmental conditions, fishing, etc (Bal and Roa 1984). In all months during the study period the numbers of males and females were not the same but the Chi-square value did not show any significant difference indicating equal distribution of both sexes. Mairzaei (2013) reported a sex ratio of 1.2:1 of *S. sihama* from Persian Gulf and

Oman Sea; Shamsan (2008) reported a sex ratio of 1:1.17 from Zuari Estuary; Ansari and Shamsan (2010) reported a sex ratio of *S. sihama* was 1:1.13 from Goa estuaries and Gowda *et.al* (1988)b reported a sex ratio of 1:1.45 from landing centre at Mangalore. The above ratio was significant from the hypothetical distribution.

In the present study, the size at first maturity of *S. sihama* was observed as 15-16 cm for female and 14-15 cm for male. Therefore above the 16 cm was considered as fully mature for both sexes. Slightly different values regarding the size of *S. sihama* was found by Mirzaei *et.al* (2013), the size at first maturity for females 138 mm and for males 132mm. And then, Annappaswamy *et.al* (2008) reported the size at first maturity was 212 mm for males and 226 mm for females. Shamsan (2008) described the size at first maturity 155-164 mm at both sexes and Krishnamurthy and Kakiyamurthy (1978) described the size at first maturity of this fish at 140-145 mm. The results of present study was closer to the values reported by Shamsan (2008) and Krishnamurthy and Kaliyamurthy (1978) but slightly different from that of Annappaswamy *et.al* (2008). This is because the size at first maturity of fish depends on the nature of the environment in which the population concern live.

Conclusion

The study of the relationship between the fecundity and the total length of fish, total weight of fish in Myeik Area indicates that this species was in good condition. *Sillago sihama* has a prolonged spawning season. The maturity stage is observed throughout the research. Therefore, the limitation of the size of fish in the catch especially not fishing the fish smaller than the size at first maturity and not fishing during the peak of spawning season may improve the condition of the *S. sihama* population. Moreover, the dynamite fishing should be prohibited because it effects negatively not only the fish population but also the main food of this species.

Acknowledgements

We wish to express thanks to Rector, Dr. Ni Ni Oo, and Pro-Rector, Dr. Win Win Than of Myeik University, for kind permission to conduct this study. We are very grateful to Dr. Nyo Nyo Tun, Professor, and Head of Marine Science Department, for permitting us to do this research.

References

Annappaswamy, T. S., Reddyandt, H. R. V. and Nages, T.S. 2008. Reproductive biology of Indian Sandwhiting, *Sillago sihama* from estuaries of Dakshina Kannada, southwest coast of Indian. *J.* Inland fish. Soc. India 40 (1): 44-49.

Ansari, Z. A and Shamsan, E. F. 2010. Study of age and growth of India sand whiting, Sillago sihama (Forsskal) from Zuari estuary, Goa. *Indian Journal of Marine Sciences*. Vol.39 (1) 68-73 pp.

Banerjee, P. K. 2004. *Introduction to Biostatistics (A Textbook of Biometry)*. S. Chand & Company Ltd. Ram Nagar, New Delhi, 200 pp.

Gowda, H. H., Joseph, P. S. and Joseph, M. M. 1988b. Growth, Condition and Sexuality of the Indian Sandwhiting *Sillago sihama*.

Grimes, C. B and Huntsman, G. R. 1980. Reproductive biology of the vermillion sanpper, *Rhomboplites aurorubens*, from North and South Caroilina. Fish.Bull.**78**:137-146.

Krishnamurthy, K. N and Kaliyamurthy, M. 1978. Studies on the age and growth of Indian Sandwhiting *sillago sihama* from Pulicat Lake with observation on its biology and fishery; Indian J fish; 84-97.

Mirzaei, M. R., Valinasalo, T., Yasin, Z. and Hwai, T.S. 2013. Reproduction characteristics of length –weight relationship of the sand whiting *(sillago sihama*) in the south coastal of Iran (Persian Gulf and Oman Sea). Annals of Biological Research, 4 (5): 269-278.

Sano, M., Kurokura, H. and Tongnunui, P. 2006. Reproductive biology of two sillaginid fishes, *Sillago sihama* and S.aeolus, in tropical coastal waters of Thailand. La mer 44: 1-16.

Shamsan, E. F. S. 2008. Ecobiology and fisheries of an economically important estuarine fish, *Sillago sihama* (Forsskal). Unpublished PhD Dissertation. Goa University-National Institute of Oceanography, Goa, India.

Treatment of River Water Collected from Hlaing River near Insein Township for Potable Purposes

Phyu Phyu Mon[1], Ko Win[2] & Tin Moe Moe Myint Zaw[3]

Abstract

The current water supply services of Yangon city are not sufficient in terms of both water quality and quantity. To solve these problems, the treatment of river water by less cost-effective conventional methods such as coagulation and sand filtration were studied. River water sample from Hlaing river near Insein township was collected and analysed for a number of water quality parameters such as temperature, pH, color, odor, turbidity, electrical conductivity, salinity, total solids, suspended solids, total dissolved solids, dissolved oxygen, biochemical oxygen demand (BOD), chemical oxygen demand (COD), total bacteria, *E.coli*, arsenic, cadmium, lead and absorbances at 272 nm, 465 nm, 665 nm wavelengths. The ratio of absorbances of dilute aqueous solutions of humic materials at 465 and 665 nm (called the E4/E6 ratio) has commonly been used to characterize humic materials. Water sample was treated by coagulation with alum and PAC (Polyaluminum Chloride) and by filtration with sand and rice husk char. The effectiveness of coagulation and filtration on the river water was studied by investigating the quality of treated water and it was also assessed by WHO guideline.

Keywords: alum, PAC, sand, rice husk char

Introduction

Surface water quality is affected by various natural processes and anthropogenic activities. In Myanmar, wastewater is discharged into the bodies of water which can assimilate and dilute the harmful constituents of the effluents. Hence, municipal and industrial demand for freshwater rises, as effluents of low quality are increasingly disposed without appropriate treatment into the bodies of water resulting in further degradation of their water quality. Potable water is suitable for public water supply. River water sample from Hlaing river near Insein township was collected. Some physical, chemical and biological characteristics of raw water was

[1] Demonstrator, Department of Industrial Chemistry, Dagon University
[2] Professor, Department of Industrial Chemistry, Dagon University
[3] Associate Professor, Department of Industrial Chemistry, West Yangon University

determined and water sample was treated by coagulation with alum and PAC (Polyaluminum Chloride) and by filtration using sand and rice husk char. Characteristics of raw and treated water sample were determined and compared with WHO guideline.

Materials and Methods

Sample Collection and Preparation

Hlaing river was selected for the collection of water sample during the rainy season. Water sample was collected from the place located near Insein Township. Sample collection point was presented on the sampling map of study area is shown in Figure (4). River water sample was collected at a distance of about 10 m from the river-bank and at a depth of 1 m below the surface of the river by using water sampler. After collection, raw water sample was promptly transported with a cool-box to the laboratory of Industrial Chemistry Department, Dagon University where most of the examinations were performed according to the standard methods for examination of water and wastewater (APHA, AWWA, 1989). The water sample was tested for initial values of pH using a pH meter HANNA HI98127 Waterproof Tester, dissolved oxygen using a HANNA HI9146 dissolved oxygen meter, conductivity and total dissolved solids (TDS) using a Mi306 Automatic and logging on TDS/conductivity meter, turbidity using a portable HACH 2100Q turbidity meter and color using a HACH test kit color model co-1 colorimeter. Temperature using a digital thermometer attached to the pH Meter.

Treatment of Water Sample by Coagulation using Alum

One liter of water sample was placed in a beaker and left on the table for 24 hr to settle out by gravity. Then, the water sample was decanted carefully, making sure that the settled particles were not disturbed. Then, 5 mg of alum was added to the beaker. The contents of the beaker were stirred and held quiescently on a table for 24 hr. The supernatant solution was then decanted into another beaker. After coagulation, treated water sample was collected. The water sample was treated by coagulation with Alum as shown in Figure (1). The effectiveness of the treatment system using plain sedimentation followed by coagulation were studied by investigating the pH, TDS, UV_{272}, E4/E6 ratio (calculated from the UV_{465}/UV_{665}) of the water sample and the results are shown in Table (2). The same procedure

was repeated for different amounts of Alum such as 10 mg, 15 mg, 20 mg and 25 mg and their respective data are tabulated in Table (2).

Treatment of Water Sample by Coagulation using PAC

The same procedure as mentioned in using Alum was carried out but coagulant (PAC) was used. The water sample was treated by coagulation with PAC as shown in Figure (2). The effectiveness of treatment system using plain sedimentation followed by coagulation with PAC with different doses of (5 mg, 10 mg, 15 mg, 20 mg, 25 mg) was studied by investigating the pH, TDS, UV_{272}, E4/E6 ratio (calculated from the UV_{465}/UV_{665}) of the water sample and the results are shown in Table (2).

Preparation of Sand and Rice Husk Char Filter for Filtration

A glass column of 5 cm in diameter and 60 cm in height was used. The filter medium was made with sand [effective size of 0.35 - 1.18 mm (14 mesh)] and was supported by gravels. Gravels [effective size of 12.5 – 25.4 mm] were filled into the column up to 15 cm in height from the base of the glass column. Above the gravel medium, sand was filled up to 15 cm into the column. The filtration column is shown in Figure (3). After packing into the column, the filter medium was washed with distilled water until clear water was discharged. Then the water sample was filtered through the sand filtration column.

A glass column of 5 cm in diameter and 60 cm in height was used. The filter medium was made with rice husk char and was supported by gravels. Gravels were filled into the column up to 15 cm in height from the base of the glass column. Above the gravel medium, rice husk char was filled up to 15 cm into the column. The filtration column is shown in Figure (3). After packing into the column, the filter medium was washed with distilled water until clear water was discharged. Then, the water sample was filtered through the rice husk char filtration column.

Treatment of Water Sample by Sand Filtration

One liter of water sample was placed in a beaker and left on the table for 1 hr to settle out by gravity. After 1 hr sedimentation, the supernatant liquid was carefully decanted into a beaker. After sedimentation, water sample was passed through sand filtration column to remove contaminants in the water. After filtration, treated water sample was collected. The effectiveness of the treatment system using plain sedimentation followed by filtration was studied by investigating of the

water sample before and after treatment and the results are shown in Table (3).

Treatment of Water Sample Filtration using Rice Husk Char

The same procedure as mentioned in sand filtration was carried out but rice husk char filter was used. The effectiveness of treatment system using plain sedimentation followed by filtration using rice husk char was studied by investigating the water sample before and after treatment and the results are shown in Table (3).

Combined Treatment Method

The combined method consisted of coagulation using PAC followed by filtration using rice husk char. One liter of water sample was placed in a beaker and left on the table for 24 hr to settle out by gravity. After that, the water sample was carefully decanted and optimum amount of PAC (20 mg) was added to this beaker and left on the table for 24 hr to settle the sludge. The supernatant solution was then carefully decanted into another beaker. Next, this water sample was passed through the rice husk char filter. The treated water was stored in PET bottles and the characteristics of the sample were determined. These results are shown in Table (4).

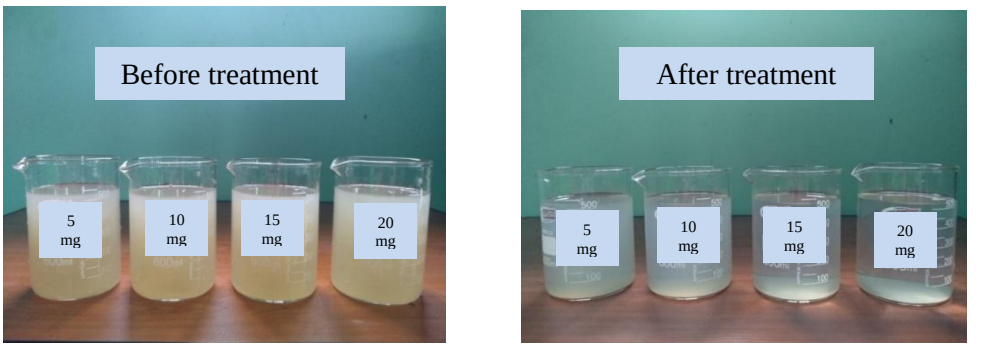

Figure 1. Coagulation with alum

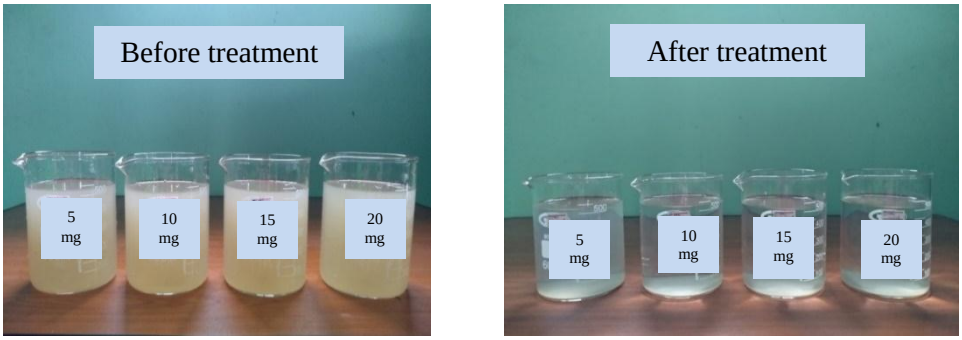

Figure 2. Coagulation with PAC

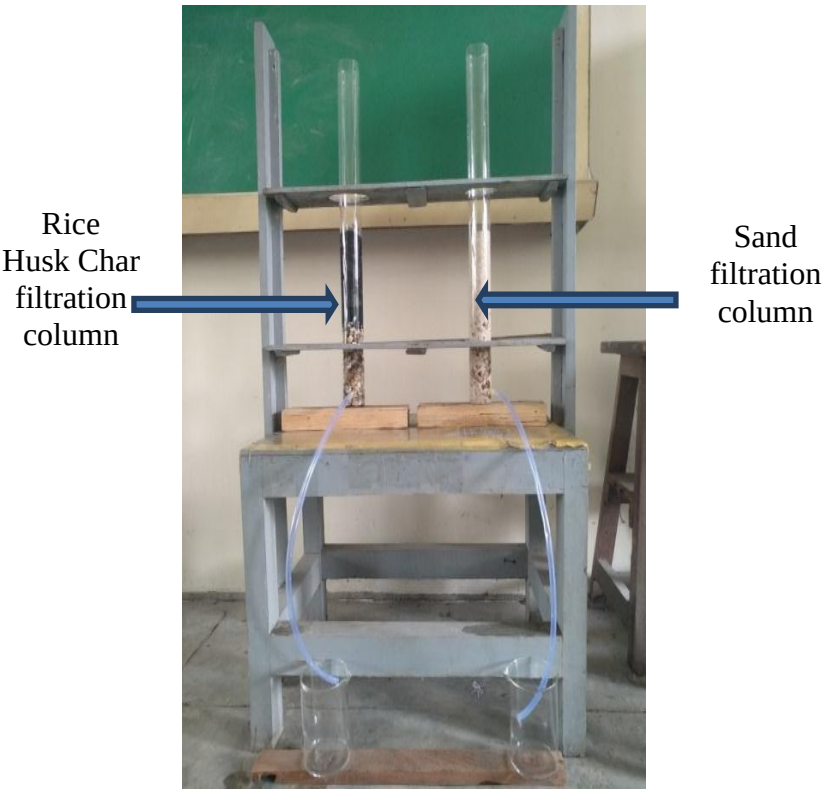

Figure 3. Sand and rice husk char filtration column

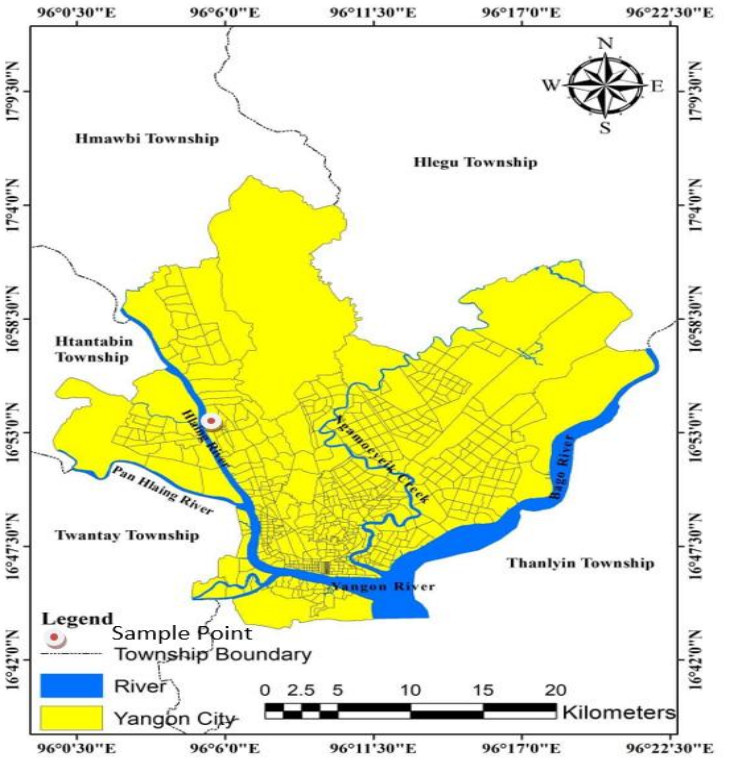

Figure 4. Sampling map of study area

Results and Discussion

The characteristics of river water sample from Hlaing river near Insein Township were determined. These results are expressed in Table (1) and compared with WHO drinking water standard. Some of the characteristics of river water sample were higher than WHO drinking water standard and unsuitable for potable purpose. The results indicated that water sample was required appropriate water treatment by physical, chemical and biological water treatment methods. The river water sample was treated by coagulation and filtration.

Table (2) shows that river water was treated by coagulation using various doses (5, 10, 15, 20 and 25 mg) of Alum and PAC. The organic substance content of water sample was determined by the use of UV absorbance at wavelengths of 272 nm (Szerzyna1.S et al., (2017). The ratio of absorbances of dilute aqueous solutions of humic materials at 465 and

665 nm (called the E4/E6 ratio) was commonly used to characterize humic materials. E4/E6 ratios for humic acids was determined to be in the 5.44 - 5.7 range and for fulvic acids in the 8.88 - 9.9 range (Chen et.al, 1977). The E4/E6 ratio of water sample was found between 1.0 and 1.2. These values were much lower than reference. According to the results, the water sample did not contain significant amount of humic and fulvic acids. Absorbance decreased with increasing amount of Alum and PAC. If Alum and PAC were more than 20 mg, both absorbance and pH decreased. However, if Alum and PAC dosages were less than 20 mg, the water was turbid. At 20 mg of Alum and PAC dosage, percent removal of TDS was the highest. It was noted that the optimum dose of Alum and PAC were 20 mg.

Table (3) shows that characteristics of river water before and after treatment. The river water sample was treated by coagulation (Alum and PAC) and filtration using sand and rice husk char. According to these results, the electrical conductivity of the water slightly decreased. This parameter indicates the presence of dissolved salts in the water. Color and turbidity of the river water sample was significantly reduced. The color in the water was generally due to the presence of colored organic material in the soils, which is principally composed of fulvic and humic acids. The turbidity of the water was due to the presence of particulate materials in suspension in the water, such as finely divided organic and inorganic materials and other microscopic organisms (Emanuelle.C, et.al, 2016). But the results of removal of total bacteria and *E.coli* by coagulation and filtration were found to be unsatisfactory.

Figure (5) shows the comparisons of efficiency of individual water treatment processes against % removal of water quality parameters. According to these results, % removal of color, turbidity, TS, SS, TDS, total bacteria and *E.coli* by using PAC was higher than Alum and also the rice husk char filter was more effective than sand filter.

Therefore, the combination of sedimentation, coagulation and filtration was applied for the treatment of water sample. After 24 hr sedimentation time, water sample was treated by coagulation with the suitable amount of coagulant (20 mg PAC) and then filtered by using rice husk char filter. According to the Table (4), pH, color, turbidity, TS, SS, TDS fall in the range of WHO Standard whereas BOD, COD, total bacteria and *E.coli* do not fall in the range of WHO Standard. The combined method (coagulation followed by filtration) was not sufficient to reduce BOD,

COD, total bacteria and *E.coli*. So, another effective water treatment methods should be used.

Table 1. Characteristics of Raw Water

Sr. No.	Parameter	Raw Water	WHO Drinking Water Standards	
			Desirable	Permissible
1	pH*	7.1	7-8.5	6.5-9.2
2	Color** (TCU)	160	5	25
3	Odor*	Nil	Unobject	Unobject
4	Turbidity** (NTU)	280	5	25
5	Temperature* (°C)	29	-	<25
6	Electrical Conductivity*(µS/cm)	76.2	100	750
7	Total Solids* (TS) (mg/L)	170	500	1500
8	Suspended Solids* (SS) (mg/L)	131.5	30	500
9	Total Dissolved Solids* (TDS) (mg/L)	38.5	450	1000
10	Dissolved Oxygen* (DO) (mg/L)	6.32	-	>5
11	Salinity* (%)	0.2	-	-
12	Biochemical Oxygen Demand** (BOD) (mg/L)	20	-	<5
13	Chemical Oxygen Demand** (COD) (mg/L)	64	-	10
14	Arsenic**** (mg/L)	0	0.01	0.01
15	Cadmium**** (mg/L)	ND	0.003	0.003
16	Lead**** (mg/L)	ND	0.01	0.01

Sr. No.	Parameter	Raw Water	WHO Drinking Water Standards	
			Desirable	Permissible
17	Total Bacteria*** (CFU/ml)	9×10^2	-	100
18	*E.coli**** (CFU/ml)	22×10^6	ND	ND

ND=Not Detected

* The samples were analysed at the laboratory of Department of Industrial Chemistry, Dagon University.

** The samples were analysed at the laboratory of ISO TECH, Insein Township, Yangon.

*** The samples were analysed at the laboratory of Pharmaceutical Research Department, Insein, Gyo Gone.

**** The samples were analysed at the laboratory of Ecological Laboratory, ALARM, Kan Street, Hlaing Township, Yangon.

Table 2. Treatment of River Water by Coagulation using Various Doses of Alum and PAC Volume of sample = 1Liter

Sr. No.	Dose (mg)	Alum				PAC			
		pH	TDS	UV_{272}	E4/E6	pH	TDS	UV_{272}	E4/E6
1	0	7.1	38.5	0.517	1.182	7.1	38.5	0.517	1.182
2	5	6.9	30.1	0.093	1.076	6.9	34.1	0.095	1.102
3	10	6.9	33.4	0.093	1.105	6.9	31.0	0.089	1.105
4	15	6.8	29.8	0.093	1.105	6.8	28.6	0.086	1.166
5	*20	6.8	28.7	0.089	1.166	6.8	26.3	0.083	1.083
6	25	6.5	29.5	0.087	1.083	6.9	26.0	0.080	1.083

*Optimum dose

Table 3. Characteristics of River Water Before and After Treatment

Sr. No.	Parameter	Before Treatment	After Treatment			
			Coagulation		Filtration	
			Alum	PAC	Sand	Rice Husk Char
1	pH	7.1	6.8	6.8	7.3	7.3
2	Color (TCU)	160	Nil	Nil	10	Nil
3	Odor	Nil	Nil	Nil	Nil	Nil
4	Turbidity (NTU)	280	3	4	21	4
5	Electrical Conductivity (µS/cm)	76.2	68.6	66.7	67.6	66.9
6	Total Solids (mg/L)	170	50	45	58.1	53.2
7	Suspended Solids (mg/L)	131.5	21.3	18.7	23.6	18.5
8	Total Dissolved Solids (mg/L)	38.5	28.7	26.3	33.5	33.4
9	Total Bacteria (CFU/ml)	9×10^{2}	5×10^{2}	7×10^{2}	7×10^{2}	2×10^{2}
10	*E.coli* (CFU/ml)	22×10^{6}	3×10^{6}	2×10^{6}	6×10^{6}	2×10^{6}

Table 4. Treatment of River Water by Coagulation using 20 mg of PAC followed by Filtration using Rice Husk Char

Sr. No.	Parameter	Raw Water	Treated Water	WHO Drinking Water Standards	
				Desirable	Permissible
1	pH	7.1	7.1	7-8.5	6.5-9.2
2	Color (TCU)	160	Nil	5	25
3	Odor	Nil	Nil	Unobject	Unobject
4	Turbidity (NTU)	280	2	5	25

Sr. No.	Parameter	Raw Water	Treated Water	WHO Drinking Water Standards	
				Desirable	Permissible
5	Temperature (°C)	29	28.1	-	<25
6	Electrical Conductivity (µS/cm)	76.2	72.8	100	750
7	Total Solids (mg/L)	170	57	500	1500
8	Suspended Solids (mg/L)	131.5	20.6	30	500
9	Total Dissolved Solids (mg/L)	38.5	36.4	450	1000
10	Dissolved Oxygen (DO) (mg/L)	6.32	5.70	-	>5
11	Salinity (%)	0.2	0.2	-	-
12	Biochemical Oxygen Demand (BOD) (mg/L)	20	6	-	<5
13	Chemical Oxygen Demand (COD) (mg/L)	64	32	-	10
14	Arsenic (mg/L)	0	0	0.01	0.01
15	Cadmium (mg/L)	ND	ND	0.003	0.003
16	Lead (mg/L)	ND	ND	0.01	0.01
17	Total Bacteria (CFU/ml)	9×10^{2}	1×10^{2}	-	100
18	*E.coli* (CFU/ml)	22×10^{6}	1×10^{6}	ND	ND

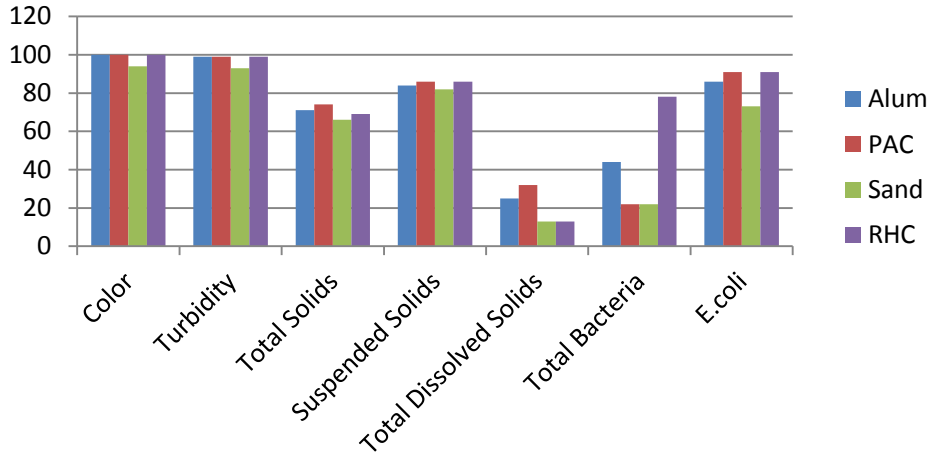

Figure 5. Comparisons of efficiency of individual water treatment processes against % removal of water quality parameters

Conclusion

In this research work, the contaminated river water from Hlaing river near Insein Township was not suitable for drinking due to the presence of color, turbidity, BOD, COD, bacteria and *E.coli*. So, water sample was treated by coagulation with different doses of Alum and PAC respectively. According to the results of this study, it can be concluded that Alum and PAC partially reduced BOD, COD, total bacteria and *E.coli*, so treatment by coagulation alone is not sufficient but PAC was more effective than Alum. In filtration, both sand filter and rice husk char filter were used and percent removal of contaminants by using the rice husk char filter was higher than by using sand filter. After a combination of sedimentation, coagulation and filtration operation, pH, color, odor, turbidity, electrical conductivity, total solids, suspended solids, total dissolved solids of water sample was found to acceptable for potable purposes according to WHO Drinking Water Standard. But total bacteria and *E.coli* do not fall in the range of WHO Drinking Water Standard. So for potable purpose, effective water treatment method for removal of total bacteria and *E.coli* should be attempted.

Acknowledgements

I would like to express my greatest appreciation to Dr. Khin Hla Mon, Professor and Head, Department of Industrial Chemistry, Dagon University for her permission to submit this research paper, reviewing the manuscripts and suggestions. I wish to express my profound respect and deepest gratitude to Dr. Yin Shwe, Part-time Professor, Department of Industrial Chemistry, Dagon University, for her constructive advice, valuable suggestions, encouragement, support and inspiration throughout my research work.

References

Chen, Y., N. Senesi, and M. Schnitzer, 1977. Information Provided on Humic Substances by E4/E6 Ratios, Soil Sci. soc. Am. J., 41:352-358.

Emanuelle.C, Wilmar.J, Mourad K, July 2016. Using Rice Husks in Water Purification in Brazil, International Journal of Environmental Planning and Management Vol. 2, No. 3, 2016, pp. 15-19.

APHA, AWWA, 1989. Standard Methods for the Examination of Water and Wastewater, 17th Edition.

Szerzyna1.S et al., 2017. Absorbance based water quality indicators as parameters for treatment process control with respect to organic substance removal. DOI:10.1051/e3sconf /20171700091.

W.H.O, 2008. Guideline for Drinking Water Quality. VoL.1 Geneva.

W.H.O, 2011. Guideline for Drinking Water Quality. WHO/SDE/WSH/ 03.04/ 09/Rev/1.

Study on the Preparation of Coconut Soft Drink

Phyu Phyu Cho[1], Ohnmar Kyi [2] & Seinn Lei Lei Phyu[3]

Abstract

This study is based on the preparation of low-fat coconut milk due to increasing the potential value in the market. Coconut soft drink can be used as a food beverage that includes coconut milk flavor. The fundamental objectives of this study were to examine the methods for coconut soft drink preparation and comparison of its quality with raw coconut milk. Coconut soft drink can be prepared by separating fat, adding sodium carboxymethyl cellulose, xanthan gum, sugar, potassium metabisulfite and potassium sorbate, homogenizing with magnetic stirrer at 85 °C and 1000 rpm for 45 minutes and then UHT sterilizing at 140 °C for 4 seconds. In this preparation, the addition of the sodium carboxymethyl cellulose and xanthan gum could obviously raise the stability of coconut milk emulsion and increased the viscosity of coconut soft drink. Coconut soft drink had higher specific gravity than the higher-fat samples. The physical and chemical characteristics such as pH, soluble solids, specific gravity, viscosity, taste, odour, colour, moisture content, ash content, protein content, fat content, fiber content, carbohydrate, energy value, minerals content of prepared coconut soft drink at the optimum condition and raw coconut milk were determined. *Escherichia coli* (E coli) of prepared coconut soft drink was also determined.

Keywords: coconut soft drink, sodium carboxymethyl cellulose, xanthan gum

Introduction

Coconut milk has been as a vital ingredient in a variety of Asian foods and desserts especially in China, India and Southeast Asia. In general, coconut milk is milky white juice prepared by pressing grated coconut flesh with or without added water. The composition of fresh coconut milk typically contains aqueous 55 ± 3%, fat 37 ± 2% and protein 8 ± 2% (Seow & Gwee, 1997). According to its composition, coconut milk is an oil-in

[1] Demonstrator, Department of Industrial Chemistry, West Yangon University.
[2] Professor (Retd.), Department of Industrial Chemistry, West Yangon University.
[3] Associate Professor, Department of Industrial Chemistry, Yangon University.

water emulsion which is stabilized by natural emulsifiers such as globulins and albumins proteins and phospholipids (Onsaard *et al*., 2005).

Fat is considered as a key component because it effects on the appearance and sensorial attributes of coconut milk products and the food that applied them as an ingredient. Although, most food that requires coconut milk as an ingredient prefers the coconut milk that contains fat content in the range of 17- 22%, the low-fat coconut milk is also interesting merchandise that should be able to the marketplace. It is because during the last decade, the trend of food product development has been spotlighted on the healthy food. A myriad of people avoid consuming fat for the reason that it leads to obesity and several diseases such as high blood pressure and coronary heart disease. Aqueous coconut products, coconut milk with fat content of less than 3.75 % are classified as "skim coconut milk". The skim coconut milk can be used as an ingredient in either food or sweet that requires coconut milk flavor but not the high fat. Skim coconut milk can be prepared by separating cream or oil from the raw coconut milk (Marina *et al*., 2009).

In order to preserve the quality and extend the storage life of coconut milk, a number of thermal processing methods can be applied such as pasteurization, sterilization and ultra-high temperature or heat (UHT) treatment. The UHT processing would be an attractive method due to kill microorganisms while maintaining the product quality (Wattanapahu *et al.*, 2012).

Coconut milk contains medium-chain triglycerides (MCTs) and it stimulates energy through a process called thermogenesis of heat production. MCTs work to reduce body weight and waist size. The objective of this study is to prepare coconut milk soft drink and to determine its physico-chemical characteristics. The research is preferred to produce low fat content coconut products which effect on body weight loss and health tonic.

Materials and Methods

Raw Materials

Mature coconuts were purchased from Bokalay, Ayeyarwaday Region. Sugar was purchased from Sanpya market. Sodium carboxylmethyl cellulose (England made), xanthan gum, potassium metabisulfite and

potassium sorbate (Analar grade) were purchased from Academy chemical group, (28th) Street, Pabedan Township, Yangon Region.

Experimental Procedure of Coconut Soft Drink

Preparation of Coconut Milk

Firstly, the coconut was dehusked and deshelled. The deshelled coconut was pared off to obtain coconut testa. The resulting coconut pieces were washed and then grated. The fine grated coconut was squeezed with muslin cloth and then filtered. The fresh coconut milk was pasteurized in a stainless steel pot using gas stove at 85°C for 5 minutes.

Fat Separation

The pasteurized coconut milk was separated into cream layer and milk according to the difference in specific gravity. Because of the specific gravity, cream layer is lighter than coconut milk laye, it was decanted from the beaker. Due to the extremely high fat content in the separated cream, the coconut milk after separation was to be lower fat content in the separated coconut milk sample.

Addition of Emulsifier and Stabilizer

Sodium carboxymethyl cellulose (SCMC) and xanthan gum were used as stabilizer and emulsifier respectively. Sodium carboxymethyl cellulose and xanthan gum (0.15 and 0.15 %, w/v) were used. In order to facilitate the dissolution of these additives, the coconut milk and coconut water were warmed to approximately 80 ºC before adding stabilizer and emulsifier.

Homogenization

The mixture of coconut milk, coconut water, sodium carboxymethyl cellulose (0.15 %, w/v), xanthan gum (0.15 %, w/v), sugar (2.5 %, w/v), potassium metabisulfite (0.15 %, w/v) and potassium sorbate (0.1 %, w/v) were stirred by using magnetic stirrer at 1000 rpm and 85°C. It takes 45 minutes in order to homogenize.

UHT Sterilization

The UHT sterilization was carried out at 140 °C for 4 seconds in the hot air oven. The UHT treated sample was filled into the pasteurized glass bottles and kept at refrigerator.

Characterization of Coconut Soft drink

Determination of pH

The pH value was measured by using pH meter (pH 300, HANA). About 2g of sample was added into 150 mL beaker and dissolved in 100 mL of distilled water. The glass electrode assembly was first standardized by using buffer solution of pH 4 and pH 7 and the pH meter was adjusted to those values. After the pH meter was calibrated, the pH value of coconut soft drink was measured.

Determination of Soluble Solids Content

The soluble solids content was measured by using a refractometer. A small quantity of the prepared coconut soft drink was placed on the prism of refractometer. Then, the prism was closed and the instrument was directed towards a light source. The soluble solids content (°Brix) was read at the line which divides the light and dark parts of the surface on the vertical scale.

Determination of Specific Gravity [AOAC method 2000(9.009)]

The specific gravity of coconut soft drink at 15/15 may be defined as the ratio of the weight of a given volume of coconut soft drink at 15 °C to the weight of an equal volume of water at 15 °C. The specific gravity of the coconut soft drink was determined by using a specific gravity bottle (25 mL). A specific gravity bottle was cleaned, dried and weight and its weight were noted. The bottle was first filled with distilled water at room temperature and the stopper was inserted in such a way that no entrapment of air bubbles took place. Then outside of the bottle was wiped thoroughly with a tissue paper. It was then weighed and its weight was recorded. The difference in weight gave the weight of distilled water. The bottle was then emptied and washed with acetone and allowed to dry. It was filled with sample and the bottle was carefully wiped with a tissue paper. The bottle and the contents were weighed at room temperature. The weight was noted. The weight of sample was determined as above. The specific gravity was calculated by using the following expression;

$$\text{Specific gravity} = \frac{\text{wt. of a volume of coconut soft drink}}{\text{wt. of an equal volume of water}}$$

Determination of Viscosity

The viscosities of the coconut soft drink were measured by Rotating Viscometer (DV- E, Spain), using a specially designed cylindrical shaped beaker (6 cm diameter and 10 cm height). A Rotating viscometer was employed in conjunction with spindle PB/PC at a controlled speed of 5rpm at 24 ºC. The reading shown by Viscometer was viscosity value expressed as cP.

Emulsion Stability

To evaluate the stability, the pasteurized samples were kept at 4°C for 3days and determined the stability of emulsion. The emulsion stability can be calculated by the following formula:

$$\% \text{ Emulsion stability} = \frac{\text{Height of cream phase}}{\text{Height of whole coconut milk}} \times 100$$

Sensory Evaluation

The sensory evaluation was performed at the West Yangon University, with a staff of 10 non-trained volunteer panelists. The participants in the sensory analysis received the coconut soft drink sample and a questionnaire containing two questions to answer. For the overall evaluation of the sample, the judges used the hedonic scale, anchored at the ends with ‘like extremely’ (9) to ‘dislike extremely’(1) as the acceptance test (Queiroz & Treptow, 2006; Meilgaard, civille & Carr,1991).

(a) **(b)** **(c)** **(d)**

Figure 1. (a) Mature Coconut
(b) Dehusked Coconut
(c) Deshelled Coconut
(d) Grated Coconut

Figure 2. Coconut Soft Drink

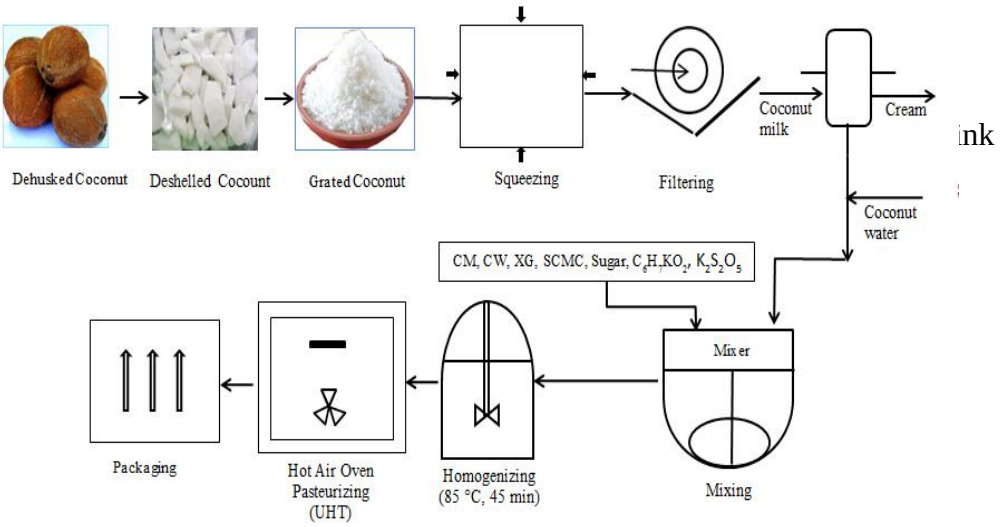

Figure 3. Schematic Diagram for the Preparation of Coconut Soft Drink

Results and Discussion

In the preparation of coconut soft drink, the main constituents were the coconut milk and coconut water. Table (1) shows coconut milk and coconut water (1:1, 3:2, 7:3 and 4:1 v/v) were used. Amount of sugar, xanthan gum and sodium carboxymethyl cellulose were varied in the

samples. The amount of sugar (1.0, 1.5, 2.0 and 2.5) g was added to the mixture of coconut milk and coconut water. Xanthan gum and carboxymethyl cellulose were used as emulsifier and stabilized agent. The effects of concentration of stabilizing agent were observed. The amount of xanthan gum (0.05, 0.10, 0.15 and 0.20) g and the amount of carboxymethyl cellulose (0.05, 0.10, 0.15 and 0.20) g were added to the samples. Their amounts were affected to the emulsion stability and viscosity of coconut soft drink.

The effects of emulsifier and stabilizing agent were not observed for the color change of the samples after heat treatment. Among samples (16), sample no (III and IV) were stable and the other samples were unstable and separated into the two layers. The emulsion stability was evaluated by applying the separation on standing method. In this evaluation, the height of cream layers were measured and calculated. According to this result, sample no (III and IV) were not separated into two layers within two weeks. The other samples were separated within one week.

The viscosity is an important characteristic of coconut soft drink because its effect on the appearance and the consumer favorite. The viscosities of all samples were conducted. It was found that the viscosities of samples (I to IV) were in the range between 11.5-13.2 cP as shown in Table (1). In these samples, the coconut milk and coconut water were same amount. The amount of xanthan gum and carboxymethyl cellulose were also same. It was observed that xanthan gum (2.0 g) and carboxymethyl cellulose (0.2 g) was more viscosity than other samples.

In samples (V to VII), the coconut milk and coconut water (3:2) was used. The viscosities of samples were observed in the range between 25.6-25.8 cP and emulsion stability of these samples was 90%.In samples (IX to XII), the coconut milk and coconut water (7:3) was used. The viscosities of samples were examined in the range between 27.1-27.5 cP and emulsion stability of these samples was 80%. In samples (XIII to XIV), the coconut milk and coconut water (4:1) was used. The viscosities of samples were examined in the range between 33.2-33.7 cP and emulsion stability of these samples was 75%.It was found that the more amount of coconut milk, the more viscosity of the samples and the less emulsion stability.

In this study, coconut milk contains the fat content (10.27%), useful source of iron and potassium. The fat separation was carried to lower the fat content. And the coconut water was mixed with lower fat coconut milk. The

coconut water is a natural fat free drink, low in sugar and calories and rich in essential electrolytes and vitamins.

Emulsifier and stabilizing agent (xanthan gum and carboxymethyl cellulose) was used to improve the emulsion stability but the viscosity is also an essential fact. Xanthan gum is adsorbed to the surface of fat droplets preventing the aggregation of fat droplets. Sodium carboxymethyl cellulose caused to increase the viscosity of continuous phase because it retards the gravitational separation of the droplets.

Homogenization process with the addition of emulsifier and stabilizer is necessary to prevent fat separation. UHT treatment is criteria to the storage life of the product. Potassium metabisufite and potassium sorbate are used as an antioxidant and a preservative. Therefore, the shelf-life of the product increased up to three months.

In nature, the pH of coconut milk and coconut water is 6.1-7.0. The pH of the samples was within 5.72-5.80. It was found when coconut milk was used more than coconut water, the soluble solid was decreased.

Specific gravity is a fundamental for the purpose of packaging of product. The specific gravity of the all samples was 1.01 because their main composition was water. It was detected that the coconut soft drink samples had higher specific gravity than higher fat samples. It is because the fat has lower density than water. These results are shown in Table (1).

The prepared coconut soft drink was presented to volunteers for sensory analysis and the acceptance test result was 7.00±1.09, where 7 mean 'like moderately'. A total of 66% of panelists chose 'like' or 'like moderately' for coconut soft drink, indicating that the product was not rejected by the panelists.

Table (2) shows the characteristics of raw coconut milk. Table (3) shows the characteristics of coconut soft drink and M & S product was compared. Coconut soft drink includes the minerals (calcium, magnesium, potassium and iron). The composition of *Escherichia coli* (E.coli) was conducted for the shelf life coconut soft drink. It was investigated the amount of *Escherichia coli* (E.coli) (<1 cfu per mL). This composition is acceptable amount and safe for the consumer.

Table 1. Effect of Ingredients Composition on Physical Properties of Coconut Soft Drink (Taguchi Design Calculation)

Sample	Amount of Coconut Milk (mL)	Amount of Coconut Water (mL)	Amount of Sugar (g)	Amount of Xanthan Gum(g)	Amount of Sodium carboxymethyl Cellulose(g)	Physical properties				
						pH	Soluble Solids (°Brix)	Specific Gravity	Viscosity (cP)	Emulsion Stability (%)
I.	50	50	1.0	0.05	0.05	5.79	13.3	1.01	11.5	85
II.	50	50	1.5	0.10	0.10	5.78	13.5	1.01	12.3	95
III.*	50	50	2.0	0.15	0.15	5.77	13.8	1.01	12.8	100
IV.	50	50	2.5	0.20	0.20	5.72	14.2	1.01	13.2	98.5
V.	60	40	1.0	0.10	0.15	5.76	10.8	1.01	25.6	90
VI.	60	40	1.5	0.05	0.20	5.77	10.9	1.01	25.8	90
VII.	60	40	2.0	0.20	0.05	5.75	11.1	1.01	25.8	90
VIII.	60	40	2.5	0.15	0.10	5.75	11.7	1.01	25.6	90
IX.	70	30	1.0	0.15	0.20	5.80	10.7	1.01	27.2	80
X.	70	30	1.5	0.20	0.15	5.79	10.6	1.01	27.5	80
XI.	70	30	2.0	0.05	0.10	5.80	10.5	1.01	27.3	80
XII.	70	30	2.5	0.10	0.05	5.79	11.6	1.01	27.1	80
XIII.	80	20	1.0	0.20	0.10	5.78	9.7	1.01	33.6	75
XIV.	80	20	1.5	0.15	0.05	5.78	9.7	1.01	33.2	75
XV.	80	20	2.0	0.10	0.20	5.78	9.8	1.01	33.7	75
XIV.	80	20	2.5	0.05	0.15	5.78	9.9	1.01	33.5	75

* the acceptable condition

Table 2. Characteristics of Raw Coconut Milk

Sr. No.	Characteristics	Raw Coconut Milk (per 100g)	*Literature Value
1.	Moisture content (%w/w)	86.73	87.3
2.	Ash content (% w/w)	0.22	0.52
3.	Protein content (% w/w)	0.08	1.88
4.	Fat content (% w/w)	10.27	10.0
5.	Fiber content (% w/w)	N.D	-
6.	Carbohydrate (% w/w)	1.26	4.53
7.	Energy value (kcal)	97.79	115.64

N.D = Not Detected

Table 3. Characteristics of Coconut Soft Drink and M & S Product (UK made)

Sr. No.	Characteristics	Coconut Soft Drink (per 100g)	M & S Product (UK made)
1.	Moisture content %w/w)	93.63	94.7
2.	Ash content (% w/w)	0.34	-
3.	Protein content (% w/w)	N.D	0.2
4.	Fat content (% w/w)	0.62	1.9
5.	Fiber content (% w/w)	N.D	1.0
6.	Carbohydrate (% w/w)	4.93	2.2
7.	Energy value (kcal)	25.30	29
8.	Calcium (mg/100mL)	92.43	-
9.	Magnesium (mg/100mL)	40.22	-
10.	Potassium (mg/100mL)	353.49	-

Sr. No.	Characteristics	Coconut Soft Drink (per 100g)	M & S Product (UK made)
11.	Iron (mg/100mL)	0.51	-
12.	Phosphate (mg/100mL)	Nil	-
13.	*Escherichia coli* (E.coli)	< 1 cfu per mL	-

Conclusion

In this present work, the coconut soft drink with remaining fat content of lower than 1 % can be obtained by effective cream separation. The addition of emulsifier and stabilizer is necessary for the stability of coconut milk emulsion. From the experiments, the ratio of coconut milk and coconut water (1:1% v/v), the ratio of xanthan gum and carboxymethyl cellulose (0.15:0.15 % w/v) and the amount of sugar (2.0 g) were the most suitable composition for the preparation of coconut soft drink. The prepared coconut milk was slightly viscous than the raw coconut milk samples. Besides, the sensorial attributes of coconut soft drink showed that it was more palatable than raw coconut milk. The coconut soft drink was long shelf-life for the suitable amount of potassium metabisulfite and potassium sorbate was used.

Acknowledgement

Firstly, I would like to express my gratitude to Dr. Thin Thin Khaing, Professor and Head of the Department of Industrial Chemistry, West Yangon University, for her kind provision of the research facilities and giving permission to this research.

I would like to convey my profound regard and deep sense of respect to my supervisor Dr. Ohnmar Kyi, Professor, Department of Industrial Chemistry, West Yangon University, for her guidance and supervision from the beginning to the completion of this work.

I would also like to express my profound respect and grateful appreciation to my co-supervisor, Dr. Seinn Lei Lei Phyu, Lecturer, Department of Industrial Chemistry, West Yangon University for her valuable suggestions, constructive direction, affectionate encouragement and kind co-operation at every step throughout the period of the research.

References

Marina, A.M., Che Man, y.B., & Amin, I. (2009). Virigin coconut oil: emerging functional food oil. *Trends Food Sci. Technol*., 20, 481-487.

Meilgaard, M., Civille, G. V. & Carr, B. T. (1991). Sensory evaluation techniques. (2a ed.). Boca Raton: CRC Press.

Queiroz, M. I., & Treptow, R. O. (2006). Rio Grande. RS: Furg.

Onsaard, E., Vittayanont, M., Sringam, S., & McClements, D.J. (2005). Properties and stability of oil-in-water emulsion stabilized by coconut skim milk protein. *J. Agri. Food Chem*., 53 (14), 5747- 5753.

Seow, C.C., & Gwee, C.N.(1997). Coconut milk:chemistry and technology, Int. J. Food Sci. Technol., 32, 189-201.

Wattanapathu S., Suwonsichon, T., Jirapakkul, W and Kasermsumran, S. (2012). Categorization of coconut milk products by their sensory characteristics. Kasetsart J. (Nat Sci),46, 944-954.

Study on the Preparation of Biodiesel from High Acidity Oils

Khin Moh Moh Zaw[1], Cho Mar Kyi[2] & Khin Htwe Nyunt[3]

Abstract

Biodiesel is one of the new possible substitutes of regular fuel for engines and it can be made from different vegetable oils or animal fats. Vegetable oils or animal fats with high acidity could not be directly used for making biodiesel. In this research, three methods of deacidification such as neutralization, extraction and esterification were being investigated for the reduction of acidity of some vegetable oils such as palm kernel and palm oils having different acidities. In this study, two samples of pretreated palm kernel oil and palm oil samples having acid value 19.8 were collected. In neutralization method, it was found that the acid values of respective oils were reduced to 0.48 and 0.5 but only gave 62.3 and 58.5 percent yield. In extraction method, pretreated various oils were extracted by using 95% ethanol solution at 70°C. It could be observed that pretreated palm kernel oil sample having AV 19.8 gave 71.8 percent yield and AV 1.35 after extraction. Pretreated palm oil sample having AV 19.8 gave 68.5 percent yield and AV 1.42. In esterification method, the effect and significance of parameters involved in the reaction, oil to ethanol ratio (1:2, 1:2.5 and 1:3) for dried crude palm oil were studied. It was observed that oil to 95 % ethanol ratio of 1:2.5, reaction temperature 200°C gave the lowest AV 1.5 and the more yield percent 80 % v/v for dried crude palm oil having AV 19.8. The direct esterification reaction of palm oil followed by transesterification to biodiesel was also studied. Yield of biodiesel from oil at optimal potassium hydroxide catalyst concentration 1%, reaction temperature 60°C, reaction time 2 hours was 88.5 %. The fuel properties of palm oil biodiesel, namely, kinematic viscosity, specific gravity, acid value were found to be within the limits of American Society for Testing and Materials (ASTM) specifications.

Keywords: Deacidification, transesterification, AV (acid value), ASTM

Introduction

The high energy demand in the industrialized world as well as in the domestic sector and pollution problems initiated due to the widespread use of fossil fuels make it increasingly necessary to develop the renewable

[1] Lecturer, Department of Industrial Chemistry, West Yangon University
[2] Associate Professor, Department of Industrial Chemistry, West Yangon University
[3] Professor and Head (Retired), Department of Industrial Chemistry, West Yangon University

.

energy sources of limitless duration and smaller environmental impact than the traditional one. One possible alternative to fossil fuel is the use of oils of plant origin like vegetable oils and tree borne oil seeds. This alternative diesel fuel can be termed as biodiesel. Biodiesel is a promising source of energy. It is a renewable and biodegradable diesel fuel with less harmful emissions than petroleum-based diesel fuel.

Chemically, the oils or fats consist of triglyceride molecules of three long chain fatty acids that are ester bonded to a single glycerol molecule. Alkaline catalysts such as NaOH and KOH are the most commonly used in transesterification reaction is much faster than an acid-catalyzed reaction. If high free fatty acid (FFA) feedstock such as fryer grease is used, the reaction is then partially driven to saponification which partially employs catalysts and produces soap. The use of alkaline catalyzed transesterification could be more suitable to produce biodiesel from high FFA feedstock. During this process, the vegetable oil reacted with alcohol such as methanol or ethanol in the presence of base or acid catalyst, resulted in biodiesel and glycerine as valuable by product. Soap formation reduces catalyst efficiency, causes an increase in viscosity, leads of gel formation and makes the separation of glycerol difficult. To complete the alkaline catalyzed reaction, a free fatty acid (FFA) value lower than 3% is needed. The oils used in transesterification should be substantially anhydrous (0.06% w/w).

The main objective of this research work is to study the methods of reduction of acidity of palm kernel oil and palm oil, to extract the most suitable method of reduction of acidity of these oil samples with the highest yield percentage and the lowest acidity and to prepare biodiesel using direct esterification of free fatty acid followed by transesterification reaction.

Materials and Methods

Materials

Dried palm kernel and dried crude palm oil samples with different acidities were obtained from Soap Factory No. (1), Hlaing Township, Yangon Region. Potassium hydroxide (BDH, Annular grade), phenolphthalein indicator (Laboratory chemicals, May & Baker Ltd.), and ethyl alcohol (95% absolute alcohol) 96% sulfuric acid solution (conc:),

95% ethanol (Technical grade), 95% methanol (Technical grade), Hot water (90ºC), concentrated phosphoric acid were used.

Experimental Procedure

The contents of free fatty acid of dried palm kernel and crude palm oil samples were determined by neutralization methods. Then the two samples with different acidities were pretreated by filtration, degumming and winterization. The pretreated crude oil samples with different acidities were deacidified by using caustic soda solution (20˚Be) and 95% ethanol. The deacidified sample of dried palm oil was esterified using various ratio of oil to 95% ethanol at 200˚C. After that, the preparation of biodiesel from dried palm oil was carried out by esterification following by transesterification. The fuel characteristics such as kinematic viscosity and specific gravity of palm oil were also determined.

Determination of Free Fatty Acid

The acid value is defined as the number of milligrams of potassium hydroxide required to neutralize the free fatty acid in one gram of oil. 1gm of oil was placed into a 100 ml conical flask and dissolved in 30 ml of 1:1 v/v mixture of previously neutralized ethanol and diethyl ether solution. While shaking, it was titrated with 0.1 N ethanolic potassium hydroxide solution until the pink colour did not change for at least 30 sec. The acid value of the oil sample was calculated as follows.

$$AV = \frac{V \times F \times 5.61}{\text{Weight of Sample}}$$

Where, V = Volume of 0.1 N KOH solution

F = Factor of 0.1 N KOH solution

The same procedure of the calculated acid values of palm kernel oil and crude palm oil were recorded and shown in Table (1).

Deacidification of Pretreated Oils

The pretreated crude oil samples with different acidities were deacidified by using caustic soda solution (20˚Be) and 95% ethanol.

Neutralization of Pretreated Oils

100 ml of pretreated (filtered, fully degummed and winterized) palm kernel oil sample with known acidity was preheated to 90ºC. A calculated amount of caustic soda solution (20ºBe) prepared was gradually added and the sample was kept under constant agitation at 300 rpm for 15 min. The soap and neutral oil formed were separated in the centrifugal separator. Refined oil was washed with hot water. The washed solution was constantly checked with phenolphthalein indicator to ensure that the neutral oil was free from soap. The washed oil was dried in the oven at 110ºC. The acidity and the yield percentage of neutralized, washed and dried oil sample were determined. The same experiments for pretreated palm kernel and palm oil samples with different acidities were also carried out. The results are shown in Table (2).

Extraction of Pretreated Oils

50 ml of pretreated (filtered, fully degummed and winterized) palm oil sample having an acidity of AV 19.8 was extracted with 95% ethanol using the oil to solvent ratio of 1:10. After addition of ethanol, the sample was kept under constant agitation at 300 rpm for 1 hour. The sample was transferred into a separating funnel. When two layers were formed sharply, the bottom fraction was drawn off. After distilling off the ethanol, the acidity of oil was then determined.

The same experiments were also carried out for pretreated palm kernel and palm oil samples respectively. The yield percentage and the acidity of the oil sample before and after extraction were determined. The results are shown in Table (3).

Esterification of Oils

The deacidified sample of dried palm oil was esterified using various ratio of oil to 95% ethanol at 200˚C. After that, the preparation of

biodiesel from dried palm oil was carried out by esterification following by transesterification.

Transesterification of the Preparation of Biodiesel

100 g of dried palm oil having known acidity was boiled and 50 g of 95% ethanol, 2 ml of concentrated sulphuric acid were gradually added. After 4 hr boiling, formed ester was separated and then washed with hot water. The neutral washed oil was dried in the oven at 110ºC.

Transesterification of esterified palm oil with methanol at 60ºC was then carried out. The catalyst, 1 g of potassium hydroxide which had already been mixed with 20 g of 99.9% methanol was gradually added and then stirred. After 2 hours, when the reaction was complete, the reaction mixture was transferred into a separating funnel. When two layers were formed sharply, the bottom glycerine layer was drawn off as the glycerin phase is much more dense than biodiesel phase.

The biodiesel was purified by washing gently with warm water to remove residual catalysts or soaps. The washed solution was checked with phenolphthalein indicator to ensure that the biodiesel was free from residual catalysts or soaps. The washed biodiesel was dried in an oven at 110ºC to remove residual methanol. The viscosity and yield of biodiesel were measured as shown in Table (6).

Determination of Physicochemical Properties of Fuel Oils

The physicochemical properties of kinematic viscosity, specific gravity and acid value of crude palm oil, diesel palm oil and biodiesel were also determined. The results are shown in Table (7).

Results and Discussion

In this research, two types of oils: palm kernel oil and palm oil were obtained from Soap Factory No. (1), Hlaing Township, Yangon Region. In this work, studies were conducted with these two oil samples, with high acidities, corresponding to developments made for producing of biodiesel. If free fatty are present, they can be removed or transformed into biodiesel using special pretreatment technologies. The yield of biodiesel produced is higher if the oil is dried and pretreated first. In this study, pretreatment including filtration, degumming and winterization were carried out. Two

samples of palm kernel oil samples having acid value 8.69 and 22.10, palm oil samples having acid value 10.91 and 23.93 were collected from Soap Factory No.(1), Hlaing Township.

The results of Table (1) showed the yield percent and acid value of pretreated oil respectively. After filtration the acid values of filtered oil were found to increase slightly. The filtrates were observed more clearly than before filtration. The degumming process involves heating the oil and adding hot water, 2.5% of the volume of oil. After the degumming process, all water had been removed, or it will lead to soap formation in the oil. Data on degumming of filtered oils with 2.5% of hot water followed by 0.1% phosphoric acid at 90ºC are given in Table 4.1. It was found that the increase in acidity for all oil samples after degumming.

Winterizing was carried out for the partial removal of saturated glycerides. These glycerides have relatively high melting points and possess only a limited solubility in the unsaturated glycerides. It was observed that the acidity also increases after winterization for all oil samples.

In this work, deacidification methods: neutralization and extraction were being explored for the reduction of acidity of some vegetable oils such as palm kernel and palm oils. In Table (2) showed that neutralization of pretreated oils with 20ºBe caustic soda solution at 90˚C. It was found that AV decreased from 19.8 to 0.48 for palm kernel oil and from 19.8 to 0.50 for palm oil and the yield of neutral palm kernel oil and neutral palm oil obtained were 62.3 and 58.5% respectively. The data were obtained from (Khin Htwe Nyunt, *et al.* 2010).

Deacidification of pretreated palm kernel and palm oils by using 95% ethanol solution at 70°C was shown in Table (3). It could be observed that pretreated palm kernel oil sample having AV 19.8 gave 71.8 percent yield and AV 1.35 after extraction. Pretreated palm oil samples having AV 19.8 gave 68.5, percent yield and AV 1.42 respectively. It was found that although pretreated palm kernel oil AV 30.48 and pretreated palm oil having AV 32.5 could not be economically refined using neutralization the reduction in their acidities could be made by stepwise extraction methods.

In Table (4) showed the data on esterification of dried crude palm oil having AV 19.8 using various ratio of oil to 95 % ethanol (1:2, 1:2.5 and 1:3). After esterification 1:3 ratio of oil to 95 % ethanol used showed the lowest AV of 1.68 but gave the yield percent (76 % v/v) lower than the

1:2.5 ratio used (80% v/v). It was found that the oil was not completely extracted with oil to solvent ratio less than 1:2. It was observed that 200°C gave the lowest AV after esterification. The reaction temperature 200°C, the oil to 95 % ethanol ratio (1:2.5) used was found the suitable condition for dried crude palm oil.

Table (5) showed the comparison in yield percent of palm kernel oil and crude palm oil samples for neutralization, extraction and esterification. It was found that the esterification gave more yield percent than the other two methods and acid value reduced by esterification to 2.3 may be suitable for biodiesel preparation. It was found that ethanol and sulfuric acid were suitable to perform not only the transesterification reaction but also the direct esterification reaction to increase biodiesel production of the process.

In this research work, Table (6) showed the data on transesterification of esterified palm oil. After transesterification AV and viscosity of esterified palm oil were reduced from 19.8 to 0.65 and 42.5 to 4.35 respectively. In Table (7) showed the data on the comparison of physico-chemical properties of crude palm oil, diesel palm oil and biodiesel. The characterization of the prepared palm oil biodiesel reveals that the kinematic viscosity at 40°C of 4.35 cSt, specific gravity of 0.8751, acid value (mg KOH /g oil) of 0.65 were obtained. The data were determined at the Research and Quality Control Department of No. (1) Refinery, Thanlyin, Ministry of Energy. It shows that the acid value , specific gravity and viscosity at 40ºC of palm oil biodiesel meet the specifications of 100% biodiesel (B 100) based on ASTM D 6751 (US biodiesel standard).

Table 1. Yield Percent and Acid Value of Pretreated Oil

Degumming of Filtered Oils with 2.5% Hot Water at 90°C
Degumming of Filtered, Partially degummed Oil with 0.1 % Phosphoric Acid at 90ºC
Winterization at 12ºC

Agitation time (min.) - 15
Agitation rate -300 rpm

Crude Oils / Characteristics	Palm Kernel Oil*		Palm Oil*	
	Sample 1	**Sample 2**	**Sample 3**	**Sample 4**
AV before filtration (mg KOH /g oil)	8.69	22.10	10.91	23.93
AV after filtration (mg KOH /g oil)	10.36	23.92	12.73	25.75
AV before hot water degumming (mg KOH /g oil)	10.36	23.92	12.13	25.75
AV after hot water degumming (mg KOH /g oil)	11.95	25.65	14.35	27.30
AV before phosphoric acid degumming (mg KOH /g oil)	11.95	25.65	14.35	27.30
AV after phosphoric acid degumming (mg KOH /g oil)	13.90	27.58	16.20	29.50
AV before winterization (mg KOH /g oil)	13.90	27.58	16.60	29.50
AV after winterization (mg KOH /g oil)	19.8	30.48	19.8	32.5
% Yield (v/v)	95.5	92.3	95.4	92.3

Table 2. Neutralization of Pretreated Oil with 20°Be Caustic Soda Solution at 90°C

Characteristics \ Crude Oils	Palm Kernel Oil*	Palm Oil*
	Sample 1	Sample 2
Vol. of Oil before Neutralization (ml)	100	100
Vol. of Oil after Neutralization (ml)	62.3	58.5
AV before Neutralization (mg KOH /g oil)	19.8	19.8
AV after Neutralization (mg KOH /g oil)	0.48	0.50
% Yield (v/v)	62.3	58.5

Table 3. Extraction of Pretreated Various Oils by Using 95% Ethanol

Oils	Extraction	Before Deacidification		After Deacidification		Yield* (% v/v)
		Volume of Oil (ml)	Acid Value of Oil (mg KOH /g oil)	Volume of Oil (ml)	Acid Value of LAV Fraction (mg KOH /g oil)	
Palm Kernel Oil Sample 1	First	100	19.8	71.80	1.35	71.8
Palm Kernel Oil Sample 2	First	100	30.48	60.0	6.50	60.0
	Second	60.0	6.50	56.0	1.60	56.0

Oils	Extraction	Before Deacidification		After Deacidification		Yield* (% v/v)
		Volume of Oil (ml)	Acid Value of Oil (mg KOH /g oil)	Volume of Oil (ml)	Acid Value of LAV Fraction (mg KOH /g oil)	
Palm Oil Sample 3	First	100	19.8	72.0	6.28	72.0
	Second	72.0	6.28	68.5	1.42	68.5
Palm Oil Sample 4	First	100	32.5	68.5	6.35	68.5
	Second	68.5	6.35	65.0	1.42	65.0

Table 4. Esterification of Dried Crude Palm Oil Using Various Ratio of Oil to 95 % Ethanol at 200°C

Oil to 95% Ethanol Ratio	Before Deacidification		After Deacidification		AV Reduced (% v/v)	Yield (%v/v)
	Volume of Oil (ml)	Acid Value of Oil (mg KOH/g oil)	Volume of Oil (ml)	Acid Value of Oil (mg KOH/g oil)		
1:2	50	19.8	44	2.4	73.6	88
1:2.5*	50	19.8	40	1.5	80.2	80
1:3	50	19.8	38	1.68	83.5	76

* = The most suitable condition

Table 5. Comparison in Acidity Reduced of Palm Kernel Oil and Crude Palm Oil by Different Deacidification Methods

Characteristics	Neutralizaton*	Extraction*	Esterification**
AV of PKO (before)	19.8	19.8	19.8
AV of PKO (after)	0.48	1.35	2.3
Yield (%v/v) of PKO	62.3	71.8	90
AV reduced percent of PKO(%v/v)	97.0	91.8	74.2
AV of CPO (before)	19.8	19.8	19.8
AV of CPO (after)	0.50	1.42	1.5
Yield (%v/v) of CPO	58.5	68.5	80
AV reduced percent of CPO(%v/v)	97.4	92.8	73.6

Table 6. Transesterification of Esterified Palm Oil

Parameter	Esterified Palm Oil
Amount of dried palm oil (g)	100
AV before transesterification (mg KOH /g oil)	1.5
AV after transesterification (mg KOH /g oil)	0.65
Viscosity at 40ºC before transesterification (cSt)	42.5
Viscosity at 40ºC after transesterification (cSt)	4.35
Yield (% w/w)	88.5

Table 7. The Comparison of Physico-chemical Properties of Crude Palm Oil, Diesel Palm Oil and Biodiesel

Property	**CPO***	**Palm Oil Diesel***	**100 % Biodiesel (B100) ****
Acid Value (mg KOH /g oil)	19.8	0.65	0.8
Specific gravity	0.91	0.8751	0.88
Viscosity at 40ºC (cSt)	42.5	4.35	1.9 to 6.0

Conclusion

The research investigation was to study the methods of reduction of acidity of palm kernel oil and palm oil, the most suitable method of reduction of acidity of palm kernel oil and palm oil with the highest yield percentage and the lowest acidity and to prepare biodiesel using direct esterification of free fatty acid followed by transesterification reaction. The experiments were performed in a range of operating conditions to screen out the most suitable operating parameters for the deacidification of palm kernel oil and palm oil to produce biodiesel from pretreated palm kernel and palm oils. The results show that oil with a higher yield percentage and that FFA can be effectively removed by esterification. It was then observed that oil to 95 % ethanol ratio of 1:2.5, reaction temperature 200°C gave the lowest AV-1.5 and the more yield percent 80 % v/v for dried crude palm oil having AV-19.8. The direct esterification reaction of palm oil followed by transesterification to biodiesel was also studied. Characterization of the prepared palm oil biodiesel reveals that the kinematic viscosity at 40°C of 4.35 cSt, specific gravity of 0.8751, acid value (mg KOH /g oil) of 0.65 were obtained. The palm oil biodiesel was compared with the international standard (ASTM D- 6751) and the result was in good agreement. The results compared fairly with reference quality specifications for diesel fuel standard showing that the high acidity oil is useful for biodiesel production.

Acknowledgements

The author would like to thank the Department of Higher Education (Lower Myanmar), Ministry of Education and Rector Dr. Myo Thein Gyi, West Yangon University for allowing us to carry out this research programme. The author wish deepest gratitude and profound regards are extended to Dr. Khin Htwe Nyunt, Professor and Head (Rtd.) of Department of Industrial Chemistry, West Yangon University, not only for her encouragement but also for meticulous comments and suggestions to accomplish this work. Moreover, the authors are thankful to the staff members of Quality Control and Research Laboratory of Soap Factory No. (1), Hlaing Township, Ministry of Industry (1) in providing crude oils with different acidities, U Htun Myint, Assistant General Manager, Research and Quality Control Department of No. (1) Refinery, Thanlyin, Ministry of Energy for providing the research facilities in measuring biodiesel properties.

References

Bailey, A.E. (1964) *Industrial Fat and Oil Products*, Third Edition.

Dorado, *et al*. (2002) "Transesterificaiton of Karanja (Pongamia Pinnata) Oil by Solid Basic Catalysts" *Am. Soc. Agr. Biol. Engs*., vol. 45(3), pp. 525-529.

Guo, Y. and Y.C.Leung (2003) "Analysis on the Biodiesel Production Using Grease Trap Oils form Restaurants" *Jpn. Macro Eng. Soc*., vol. 16, pp. 421-426.

Khin Swe Oo (2009) Production of Biodiesel. Ph.D Thesis, Department of Industrial Chemistry, Yangon University.

Linden,D. and G.Lorient (2000) *New Ingredients in Food Processing, Biochemistry and Agriculture*. CRC Press LLC.

Mattil, *et al.* (1964*) Bailey's Industrial Oil and Fat Products.*

Websites

http://www.tomze @fea.unicamp.br

http://www.academicjournals.Org / IJPS

http://www. pennwalt. com/ vegetable oil refining. html

http://encyclopedia.quickseek.com/Biodiesel/

http://www.unh.edu/p2/biodiesel/media/NHSTA-handout.doc

Effect of Process Parameters on Osmotic Dehydration and Quality Aspects of Meat (Mutton)

Phyu Phyu Khine[1], Thin Thin Naing[2] & Pansy Kyaw Hla[3]

Abstract

Osmotic dehydration is the incomplete removal of water from a food product by means of an osmotic solution. Osmotic dehydration has received greater attention in recent years as an effective method for preservation of foods. Osmotic dehydration of meat (mutton) was conducted by using the fabricated reactor. The process was conducted by varying the process parameters such as types of osmotic solution, size of the samples, immersion time, osmotic temperature, and sample to osmotic solution ratio. The osmo-treated dried mutton was analysed with respect to their weight reduction (WR), solute gain (SG), water loss (WL), and dehydration efficiency index (DEI). Physico-chemical characteristics of osmo-treated dried mutton were also determined. The total plate counts (TPC) of osmo-treated dried and sun-dried samples were determined. These results prove that the process of osmotic dehydration has an important influence on the reduction of total number of microbes in the samples. The organoleptic properties of products were also determined by the 9-Point Hedonic Scale Rating Test. The results of scores were greater than 7, thus the osmotic dehydrated mutton was good quality product. The morphology of osmo-treated dried samples and sun-dried samples were depicted by using SEM micrographs. The elemental contents of osmo-treated dried and sun-dried mutton were determined by using ED-XRF measurement for the improvement of the process.

Keywords: Osmotic dehydration, osmotic solution, immersion time

Introduction

Meat may be part of a balanced diet contributing various nutrients that are benefits to health. Meat and meat products contain important level of protein, vitamins, minerals and micronutrients essential for growth and development (Filipovi et al., 2012). Meat, fishes, fruits and vegetables are quickly perishable products in nature which can be rapidly deteriorated as a result of the biochemical activities. Further meat processing offers the opportunity to add value, reduce prices, improve food safety and extend the

[1] Assistant Lecturer, Department of Industrial Chemistry, Dagon University
[2] Professor & Head, Department of Industrial Chemistry, East Yangon University
[3] Professor (Retired), Department of Industrial Chemistry, University of Yangon

shelf-life. Some preserved methods for meat are smoking, salting, and drying (Oladele et al., 2008). Two major countercurrent flows take place simultaneously during osmotic processing. The first major one is water flow from the inside of the samples into the osmotic solution, and the second flow is the osmotic agent diffusion into the opposite direction that flows from solution into the product. The third flow, which is not much considerable, is the flow from food into osmotic solution (Khin et al., 2005). Osmotic dehydration process depends on some processing variables and parameters such as types of solute and osmotic solution, time of immersion, size and dimension, sample to solution ratio and osmotic temperature.

The process can be used to achieve meat samples with distinct characteristics, obtain foods with prolonged shelf life. It can be used as a previous step for further operations such as drying, freezing, canning, frying (Raoult-Wack, 1994). Basic purposes of food dehydration involve decreasing of water contents, minimizing rate of chemical reactions, facilitating for distribution (Fito, et al., 2003). The osmotic dehydration process followed by convective drying may prevent some objectionable structural changes on foods, promotes stabilization of color by reducing non-enzymatic browning reactions and increases flavor of food (Pereira, et al., 2006). The main objective of this study is to obtain the best dehydration condition of selected meat (mutton) by using osmotic solution containing salt, sugar and distilled water.

Materials and Methods

Raw Materials

Fresh meat samples (mutton) were purchased from Thein Gyi Market (obtained from Ywathargyi Slaughterhouse) Pabedan Township, Yangon Region. The parts of the meat used in the osmotic dehydration process were the leg of mutton. Sugar used in this research was the products of the Ministry of Agriculture, Livestock and Irrigation and salt was purchased from Sein Myittar Mon Salt Industry, Mingalar Taung Nyunt Township, Yangon Region.

Methods

Preparation of Raw Meat (Mutton)

First, adhering fatty materials from fresh meat were removed. Fresh lean meat samples (mutton) were washed and cut into slices of (5 x 5 x 0.5) cm^3. The prepared meat samples were weighed and used for osmotic dehydration process.

Osmotic Dehydration Process of Prepared Raw Meat Samples with Ternary Osmotic Solution

The prepared raw samples (mutton) were individually weighed and immersed in the ternary osmotic solution Type I (salt 20 g, sugar 10 g and distilled water) for 120 min. The weight ratio of sample to osmotic solution (1:5 w/w) was chosen for osmotic treatments. After the immersion, the samples were taken out from the osmotic solution and washed slightly with small amount of water. Then, the samples were blotted with absorbent paper to remove excessive water. The samples were reweighed and dried in a hot air oven at 80 °C for 3 hours. Then, the osmo-treated dried samples were taken out from the oven, cooled and reweighed. The weights of osmo-treated dried samples were recorded for the determination of weight reduction (WR), solute gain (SG), water loss (WL).

The same procedure was carried out by varying the types of ternary osmotic solutions (Type II (salt 25 g, sugar 15 g and distilled water), Type III (salt 30 g, sugar 20 g and distilled water), and Type IV (salt 35 g, sugar 25 g and distilled water), Type V (salt 40 g, sugar 30 g and distilled water)) while keeping the immersion time, size of samples, osmotic temperature (Room Temperature of 25-32°C), and sample to osmotic solution ratio (1:5 w/w) constant. The effect of types of ternary osmotic solution, size of samples, immersion time, osmotic temperature, and sample to osmotic solution ratio on weight reduction, solute gain, and water loss were also studied. These meat products were prepared by using the fabricated batch type steel reactor with temperature controller and heater as shown in Figure (1).

Determination of Weight Reduction (WR), Solute Gain (SG), Water loss (WL)

The percent of weight reduction (WR) was determined by the change in weight of samples, solute gain (SG) was determined by the change in total solids with the initial weight of samples, water loss (WL)

was calculated by the addition of (WR) and (SG) (Koprivica G., et al., 2011).

Determination of Physico-chemical Characteristics of Meat Before and After Osmotic Dehydration and Examination of Microbial Constituents in Osmo-treated Dried Mutton

Some physico-chemical characteristics such moisture content, crude protein content, crude fat content, crude fiber content, carbohydrate content, ash content, energy value and physical properties such as color density and total plate count of osmo-treated dried meat samples were determined by (AOAC 2000) method.

Determination of Organoleptic Properties

Organoleptic properties of osmo-treated dried mutton were determined by 9-Point Hedonic Scale Rating Test. These properties were based on the appearance, flavour, texture and overall acceptability of samples. Ten panelist were asked to rate each sensory attribute on a 9-point hedonic scale form 1 (dislike extremely) to 9 (like extremely) (1: extremely poor, 3: poor, 5: acceptable, 7: good; 9: excellent) (Naknean et al., 2012).

Scanning Electron Microscopy (SEM) and Energy Dispersive X-ray Fluorescence (ED-XRF) Technique

SEM was used to analyze the structural changes of osmo-treated and sun-dried products. It was conducted by using Electron Microscopy (JSM, 5610). The elemental content of osmo-treated dried mutton was determined by using ED-XRF measurement with EDX-720.

Results and Discussion

The results of osmotic dehydration of meat evaluated with respect to weight reduction (WR), solute gain (SG) and water loss (WL) are presented in Figures (2) to (6). The effect of each of the variables was shown by the plot for water loss and solute gain. Osmotic dehydration of meat were found to be directly related to compositions of osmotic solutions, thus showing that as solution concentration increases water loss also increases. The weight reduction is a dependent on the osmotic temperature and immersion time. The time of immersion had greater effect on water loss as observed in Figure (3) than solute gain. The kinetics of water loss and solute gain is markedly influenced by the type of osmotic solution.

Figure 1. Fabricated Batch Type Steel Reactor with Temperature Controller and Heater

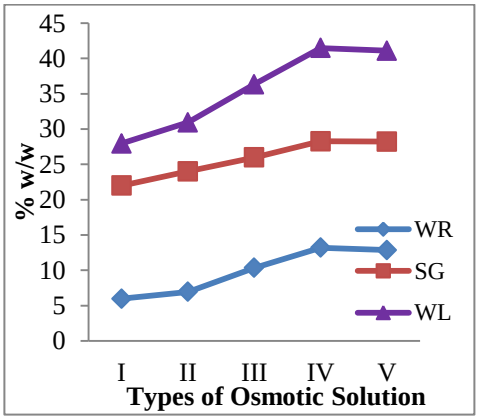

Figure 2. Effect of Compositions of Ternary Osmotic Solution on Weight Reduction, Solute Gain, and Water Loss for Osmotic Dehydration of Mutton

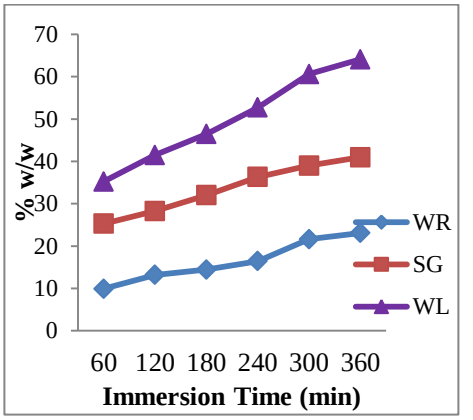

Figure 3. Effect of Immersion Time on Weight Reduction, Solute Gain, and Water Loss for Osmotic Dehydration of Mutton

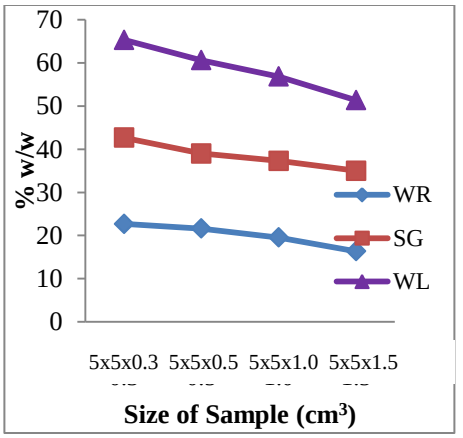

Figure 4. Effect of Size of Sample on Weight Reduction, Solute Gain, and Water Loss for Osmotic Dehydration of Mutton

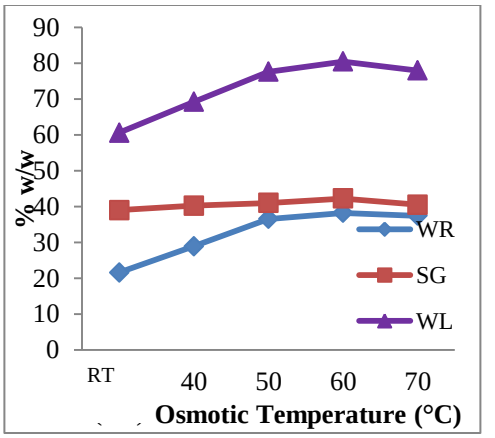

Figure 5. Effect of Osmotic Temperature on Weight Reduction, Solute Gain, and Water Loss for Osmotic Dehydration of Mutton

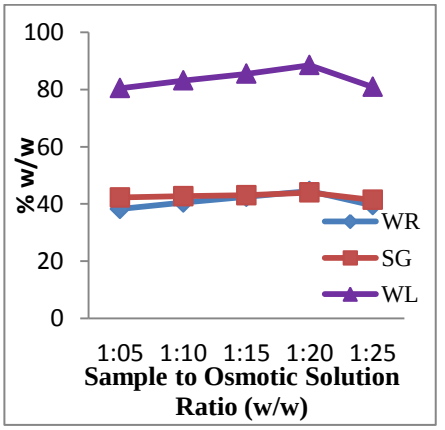

Figure 6. Effect of Sample to Osmotic Solution Ratio on Weight Reduction, Solute Gain, and Water Loss for Osmotic Dehydration of Mutton

(a) **(b)**

Figure 7. (a) Osmo-treated Dried (b) Sundried Mutton

From the results Figure (4), it was observed that the thicker samples gave the lower water loss and solute gain value. On the other hand, it was occurred that the thinner samples gave higher weight reduction and water loss. The size of the sample effects on the behavior of weight reduction, solute gain and water loss during the process. The effect of sucrose concentrations during the process was observed to be dependent on time to improve the degree of water loss. According to the Figure (5), the combined effects of solution compositions, immersion time, and osmotic temperature had significant effect on weight reduction and water loss than solute gain.

The ratio of water loss and solute gain is the indicator of the optimization of osmotic dehydration treatment. From the Figure (6), an increase of sample to osmotic solution ratio resulted in an increase in both solute gain and water loss in osmotic dehydration. A large ratio was used to avoid significant dilution of the medium during the process. It was found that the increase proportions of solute in osmotic solutions, temperature of the process and duration of the process had led to the increase of water loss. The osmotic temperature exhibited relevance on water loss and solute impregnation was enhanced at higher temperature.

The physico-chemical characteristics of raw, osmo-treated dried and sun-dried meat are shown in Table (1). It can be observed that the meat samples lose its moisture content on drying resulting in an increase in the concentration of protein and other nutrients per unit weight than in the fresh counterparts. Similarly, the crude fat contents in dried products also changed because of the heat treatment involved in this process. The colour of food product is the first attribute that affects the decision of consumer for purchasing any food products. Osmotic dehydration could improve dried food quality by stabilizing colour and allowed less colour loss of food by browning. The osmo-dried products were lighter in colour than sun-dried products.

With respect to the importance of the food drying process and obtaining a product with the desired quality and appropriate marketing, optimization of the conditions seems to be essential in order to produce dried products with minimum shrinkage and maximum rehydration capability. The rehydration ratio determines the ability of the sample to regain water without disintegration, which can be taken as a quality parameter. As the results of the Table (2), shrinkage also affects the

physical properties of materials. A study of shrinkage phenomena is thus important for a better understanding of the drying process and to control the characteristics of the product. In addition, bacteria will grow at water activity of 0.91 and fungi will grow at water activity of 0.71. It was obvious that water activity in the osmo-dried products were less than 0.91, these values were found to be in agreement with those of literature values.

Table 1. Physico-chemical Characteristics of Fresh, Osmo-treated Dried, and Sun-dried Meat (Mutton)

Sr. No.	Characteristics	Mutton		
		Fresh	Osmo-treated Dried	Sun-dried
1	Moisture (% w/w)	79.92	14.30	18.21
2	Protein (%w/w)	22.96	59.50	45.01
3	Fat (%w/w)	2.34	1.58	2.00
4	Crude Fiber (%w/w)	0.29	0.17	0.47
5	Carbohydrate (%w/w)	0.26	8.45	19.11
6	Ash (%w/w)	1.23	16.00	15.20
7	Energy Value (kcal)	111	286.02	274.48
8	Color Density	-	0.69	1.26

Table 2. Physical Properties of Osmo-treated Dried and Sun-dried Mutton

Sr. No.	Samples	Drying Rate (g/min)	Rehydration Ratio	Coefficient of Rehydration	Browning Intensity (at 420 nm)	Shrinkage Ratio	Water activity (a_w)
1	Osmo-treated Dried Mutton*	0.0139	1.56	0.49	0.592	0.540	0.536*
2	Sun-dried Mutton	0.0134	1.32	0.47	0.658	0.645	0.636

* Osmo-treated dried mutton was acceptable properties.

Table 3. Organoleptic Properties of Osmo-treated Dried, and Sun-dried Mutton

Sr. No.	Mutton	Sensory Scores for Hedonic Scale Rating Test			
		Appearance	Flavour	Texture	Overall Acceptability
1	Osmo-treated Dried	7.4	7.3	7.0	7.3*
2	Sun-dried	6.7	7.4	6.9	7.0

*Score about 7 was good quality products.

Table 4. Microbial Analysis of Osmo-treated Dried and Sun-dried Mutton during Storage Period

Sr. No.	Mutton	Total Plate Count (cfu/g) with Respect to Shelf- life	
		1 month	6 month*
1	Osmo-treated Dried	0	1×10^3
2	Sun-dried	1×10^3	3×10^8

* Shelf-life of osmo-treated dried mutton was 6 month period.

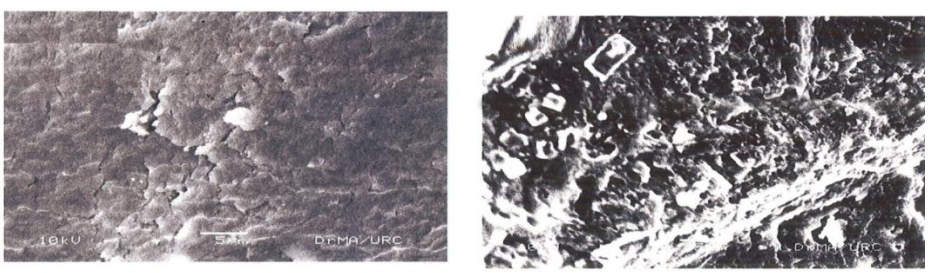

(a) Sun-dried (b) Osmo-treated Dried

Figure 8. SEM Images of Dried Meat (Mutton)

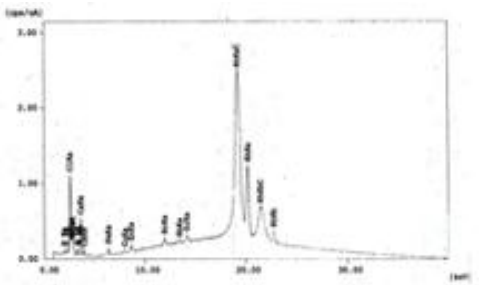

Figure 9. X-ray Fluorescence Spectra of Osmo-treated Dried Mutton

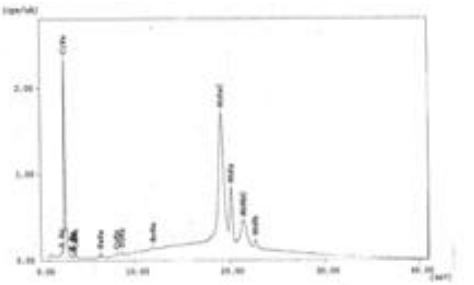

Figure 10. X-ray Fluorescence Spectra of Sun-dried Mutton

The sensory evaluation results are shown in Table (3). Higher mean scores of colour and texture were observed in the osmo-treated dried samples compared to the sun-dried samples. The sun-dried samples showed lower mean score of colour as compared to osmo-treated dried samples as it possessed brown colour. Thus, the use of osmotic solution reduced brown colour and hard texture of meat products. Then osmotic process could improve the sensory quality of dried meat products. It decreases the energy costs as the process could conduct at low temperature. In addition, osmo-dried meat has the improvements of colour, rehydration, organoleptic properties and less shrinkage properties. Sun drying process takes much more time to dry and the product give poor quality due to contamination of foreign matter. From the results of the TPC shown in the Table (4), it was observed that the plate count in osmo-treated dried products was lesser than the total plate count of the sun-dried products during storage period. The microbial profile of dehydrated mutton indicates that the osmotic dehydration is a hygienic process.

According to the SEM micrographs of Figure (8a) and Figure (8b), the effect of sucrose solution concentration on the microstructure of food during osmotic dehydration treatment can be observed. The osmotic pretreatment maintains the structure of samples from undesirable structural changes According to Figure (b), it was observed that the solute crystals were formed on the surface of the samples and the texture of the osmosed samples was softer than the sun-dried samples. The elemental contents of osmo-treated dried and sun-dried meat were determined by ED-XRF and their X-ray Fluorescence Spectra are shown in Figure (9) and Figure (10). It

was observed that Cl, K, Ca, contents were mainly found in osmo-treated dried meat products. The osmo-treated dried samples had higher contents of chlorine than that of sun-dried samples because osmotic solutions contain salt and sugar. ED-XRF is a precise and simple method to determine minerals contents in dried samples.

Conclusion

It can be concluded that the effect of sucrose concentration during the process was observed to be dependent on time to improve the degree of water loss. Therefore, best process temperature should be decided on the basis of the structure of food tissue. The sensory scores of osmo-treated dried mutton were greater than 7, thus the products were good quality products. Then osmo-treated dried samples had higher proteins and lower fat contents compared to sun-dried samples. It can be concluded that osmotic dehydration could produce valuable, sanitized and nutritious products, and could improve the sensory quality of dried products.

Acknowledgements

I would like to express my profound thanks to Professor Dr Khin Hla Mon, Head of Department of Industrial Chemistry, Dagon University, for their permission to submit this article. I would like to express my sincere thanks to supervisor Dr Pansy Kyaw Hla, Professor of Department of Industrial Chemistry (Retd.), University of Yangon, for her close supervision, invaluable suggestions, advice, encourages during this research. I would like to express my deeply grateful to my co-supervisor Dr Thin Thin Naing, Professor and Head, Department of Industrial Chemistry, East Yangon University, for valuable guidance, and helpful suggestions given to me while conducting this research work.

References

AOAC 2000. Official Methods of Analysis, 17th edition, Association of Analytical Chemists, USA.

Filipovic V S., Curcic B L., and Nicetin M R., 2012. Mass Transfer and Microbiological Profile of Meat in Dehydrated in Different Osmotic Solutions, Science Paper, Ind. 66 (5) 743-748.

Filipovic V., Levic L., Curcic B., Nicetin M., and Pezo L., 2014. Optimization of Mass Transfer Kinetics during Osmotic Dehydration, Ind. Chem. Eng. Q 20(3) 305-314.

Fito P, Chiralt A, 2003. Food Matrix Engineering: The use of water-structure functionally ensemble in dried food product development Food Science and Technology International, 9(3):151-156.

Khin MM., Weibiao Z., and Perera C., 2005. Development in the Combined Treatment of Coating and Osmotic Dehydration of Food: A Review, International Journal of Food Engineering.1-19.

Koprivica G.B, Jenovic N.M, 2011. Mass Transfer Kinetics during Osmotic Dehydration of Carrot Cubes in Sugar Beet Molasses, Original paper, Vol. 16 No. 6,201.

Naknean P., 2012. Factors Affecting Mass Transfer during Osmotiic Dehydration of Fruit. International Food Research Journal 19:7-18.

Oladele A.K, and Odedeji J.O, 2008. Osmotic Dehydration of Catfish (Hemisynodontis membranaceus): Effect of Temperature and Time, Parkiston Journal of Nutrition, 7, 57-61.

Peason D, June 2010. The Chemical Analysis of Food, Journal of Food Science Vol.4(6), pp. 303-324.

Pereira LM, Ferrari CC, and Mastrantonio SDS., 2006. Kinetic Aspects, Texture and Colour Evaluation of Fruits during Osmotic Dehydration. Int.,J, 24 (4) 475-484

Raoult-Wack, 1994. Recent Advances in the Osmotic Dehydration of Fruits, Journal of Food Science, 5, 255-260.

Effect of Solar Drying on the Characteristics of Dry Cat Food

Kyaing Thuzar Mon[1], Nwe Nwe Aung[2] & Pansy Kyaw Hla[3]

Abstract

In this study, dry cat food was prepared by mixing fish with soybean and undergone steaming, extruding and drying. Fish powder was prepared from low grade fish, Torpedo scad (Pyi-taw-thar) and White mouth croaker (Nga-khaung-pwa) which were collected from fish factory. Direct solar cabinet dryer was constructed for the preparation of fish powder and dry cat food. The nutritive value of dried fish powder was determined and compared with fish powder using hot air oven drying. The nutritive value, pH and size stability of dry cat food were also investigated and compared with dry cat food using hot air oven drying. To investigate the effect of solar drying on the characteristics of dry cat food, the comparison of nutritive value of fish powder and dry cat food by using two different drying methods (solar drying and hot air oven drying) was carried out. The results revealed that the protein content of fish powder with direct solar cabinet dryer was slightly higher than that of fish powder with hot air oven. In addition, it was noted that dry cat food with the least solar drying time of 2 hr was the most suitable dry cat food because the moisture content and protein content differences were under allowable limit. It was also found that the protein content and metabolizable energy of dry cat food using solar drying were significantly higher than that of dry cat food using hot air oven.

Keywords: Fish, fish powder, dry cat food, nutritive value, direct solar cabinet dryer

Introduction

Meat, meat byproducts, fish, poultry, cereals, fruits, and bones are used as the ingredients for the preparation of dry cat food. The energy, protein and other nutrients such as thiamine and niacin are supplied from cereals (Amir and Mona, 2013)**.** Fish protein helps build muscles and gives a great taste to the cats. A good source of calcium and phosphorus is also

[1] Lecturer, Department of Industrial Chemistry, University of Mandalay
[2] Professor, Department of Industrial Chemistry, Yadanabon University
[3] Professor (Retired), Department of Industrial Chemistry, University of Yangon

supplied from fish bones (Pet Food Manufacturers Association, 2010)**.** Used as the ingredient in the cat manufacturing, soybeans provide a source of protein and energy, omega 6, B vitamins, fibre and minerals (Potter,1996). Protein is crucial to maintain the total structure of the cat, which comprises of muscle, bone, ligaments and tendons. Dry foods are mostly the extruded products for the cats and they have a long shelf-life due to their low moisture content (Rivera, 1998). Solar drying has been used since time immemorial to dry plants, seeds, fruits, meat, fish, wood, and other agricultural, forest products. The working principle of direct solar crop drying is also known as a solar cabinet dryer. Solar drying is very simple and low-cost technology. Solar drying makes the process more efficient and protects the environments. It also saves energy, time, occupies less area, enhances product quality (Hii et al., 2012).

The objectives of the study are to investigate the effect of solar drying on nutritional value of fish powder and dry cat food, to evaluate the physico-chemical properties of dry cat food and to provide the import substitution of dry cat food.

Materials and Methods

Raw Materials

Pyi-taw-thar and Nga-khaung-pwa were collected as rejected fish from Ngwe Pin Lae Fish Factory, Ngwe Pin Lae Marine Industrial Zone, Hlaingthayar Township, Yangon Region. Soybean and salt were purchased from Nyaungpinlay Market, Lanmadaw Township, Yangon Region. Citric acid (Analar grade, BDH) was purchased from Academy Chemical Shop, 28th Street, Pabedan Township, Yangon Region.

Methods

Direct Solar Cabinet Dryer

In this study, direct solar cabinet dryer was constructed as a drying chamber with a transparent glass cover. The sides of the chamber were made of glass. The opening and bottom of the chamber were made of wood that was insulated with plastic sheet which also served as reflector sheet. Each edge of the dryer had a hole to allow the entrance of air to be heated for drying. The entering air left the groove between the glass plates. There were four metal trays in the direct solar cabinet dryer. The dryer is shown in Figure (3). The direct solar cabinet dryer was 0.79 m length, 0.34 m

breadth and 0.38 m height.

Efficiency of Direct Solar Cabinet Dryer

The effect of drying time on the drying rate of raw fish using direct solar cabinet dryer (November and December, 2018) and the system drying efficiency were determined.

Determination of Drying Rate Using Direct Solar Cabinet Dryer

Accurately 500 g of cut fish (1 to 2 cm) with known initial moisture content was evenly loaded on the tray. Then the tray was dried in the direct solar cabinet dryer. The dried fish was weighed every hour until the end of the drying process. The weight loss was converted as corresponding moisture loss for calculating the moisture content and drying rate.

$$\text{Drying Rate} = \frac{w_{\theta} - w_{\theta+\Delta\theta}}{A\,\Delta\theta}$$

where,

w_{θ} = Weight of total moisture in the sample at time θ

$w_{\theta+\Delta\theta}$ = Weight of total moisture in the sample at time $\theta+\Delta\theta$

A = Area of sample exposed to drying

Total moisture = Weight of wet material – Weight of dried material

Determination of System Drying Efficiency

This parameter is defined as the ratio of the energy required to evaporate the moisture to the energy supplied to the dryer.

$$\text{System drying efficiency} = \eta_d = \frac{W\,\Delta H_L}{I_d A_c}$$

where W = mass of moisture evaporated in time t, kg

ΔH_L = latent heat of evaporation of water, 2320 $kJkg^{-1}$

I_d = total daily insolation incident upon collector, 16272 kJm^{-2} per day

A_c = collector area (m^2) material

Preparation of Fish Powder Using Solar Drying

The 1:1 ratio of Pyi-taw-thar and Nga-khaung-pwa fish was cut into 1cm to 2 cm length and the cut fish was dried in a direct cabinet solar dryer at 50-64˚C for 4 hr. Afterwards, the dried fish was ground by using a meat grinder. And the ground meal was again dried by using a direct cabinet solar dryer for 2 hr in order to dehydrate. Finally, the dried fish meal was again ground into powder by using a grinder and screened with sieve (-14+20).

Preparation of Dry Cat Food Using Solar Drying (Fish and Soybean)

First of all, fish powder, soybean flour, citric acid and salt were thoroughly mixed and the mixture was pre-steamed at 90-95°C for 20 min. to gelatinize the starch. Then the mixture was thoroughly mixed with 50 ml. of distilled water. After that, the mixture was cooked with steam at 90-95°C for 20 min.. Next, the cooked mixture was extruded by using an extruder, dried using solar dryer at 58-70°C by varying the drying time 2 hr, 2.5 hr, 3 hr and 3.5 hr respectively and cut into 1.5 to 2.5 cm in length. Finally, the dry cat food was stored in air tight container. The moisture content, protein content and pH of the samples were investigated. From these results, the suitable dry cat food was selected and its nutritive value was determined.

Preparation of Fish Powder and Dry Cat Food Using Hot Air Oven Drying

To compare the nutritive value and physico-chemical characteristics of fish powder and dry cat food using solar drying with that of hot air oven drying, fish powder and dry cat food were also prepared by using hot air oven drying. The temperature for fish meal by hot air oven for the preparation of fish powder was 60° C for 2.5 hr. To prepare dry cat food, fish powder was mixed with soybean flour, citric acid and salt and pre-steamed at 90-95°C for 20 min.. Then the mixture was mixed with 50 ml. of distilled water and cooked at 90-95°C for 20 min. Finally, the mixture was extruded, dried using hot air oven at 60˚C for 3.5 hr and cut into 1.5 to 2.5 cm in length.

Analysis of Fish Powder

The nutritive values of fish powder such as moisture content (AOAC-2000 (934.01)), ash content (AOAC-2000 (942.05)), protein content (AOAC-2000 (920.152)), crude fibre content (AOAC-2000

(978.10)), crude fat content (Buchi Soxhlet Method), carbohydrate and energy value were determined.

Physico-chemical Characteristics of Dry Cat Food (Fish and Soybean)

The physico-chemical characteristics of dry cat food such as moisture content (AOAC-2000 (934.01)), ash content (AOAC-2000 (942.05)), protein content (AOAC-2000 (920.152)), crude fibre content (AOAC-2000 (978.10)), crude fat content (Buchi Soxhlet Method), carbohydrate and energy value, and pH, metabolizable energy and size stability were determined.

Determination of Metabolizable Energy of Dry Cat Food

To calculate the metabolizable energy, the percent of fat, protein, and carbohydrate in the dry cat food are then multiplied by their respective Atwater Factors, added together, and multiplied by 10.

$$ME\ (kcal/kg) = 10\ [(3.5xCP) + (8.5 \times CF) + (3.5 \times NFE)]$$

Where ME= Metabolizable Energy

CP= % crude protein

CF= % crude fat

NFE = % nitrogen-free extract (carbohydrate)

Determination of Size Stability of Dry Cat Food by Drop Test (ASTM 440-49)

Firstly, the dry cat food to be tested was added in a plastic bag and closed. And the plastic bag was held 1.83 m above the concrete floor, and it was dropped onto the concrete floor. Then the dry cat food was brought to the initial position from the concrete floor and dropped again. The drop test was made for six times to obtain size stability. Then the screen analysis on the dropped dry cat food was made and the size stability was calculated.

$$\text{Size stability percent} = \frac{S \times 100}{A}$$

where, A = average size of the dry cat food

S = average size of the dropped dry cat food

Statistical Analysis

t-test was applied for different drying methods on the protein value of dry cat food (fish and soybean) in the present study.

Figure 1. Pyi-taw-thar

Figure 2. Nga-khaung-pwa

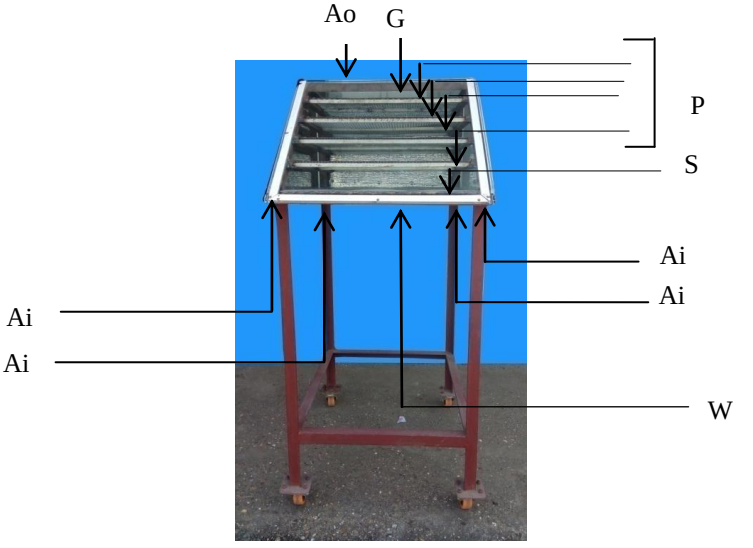

Figure 3. Direct Solar Cabinet Dryer

Ai = Air Inlet, Ao= Air Outlet, G = Glass Cover,
P = Plastic Coated Metal Trays,W = Wood, S = Plastic Sheet as Reflector and Insulator

Results and Discussion

To develop the manufacturing of dry cat food with low cost technology, direct solar cabinet dryer was used to dry the ingredients and cat food. The drying rate of fish was determined by using direct solar cabinet dryer in November and December and the results are shown in Table (1) and Figure (4), (5) and (6). In both months, the moisture content of fish was markedly decreased at drying time of 2 hr. Then the rate of drying was decreased with the moisture content of fish. It was also found

that the fish was dried for 10 hr in November to reduce nearly 280 g of weight of fish. In December, the fish was dried for 8 hr only. According to Figure (6), the moisture content was rapidly fallen at first; however, the rate of drying was reduced due to the loss of moisture content. According to Figure (7), the moisture content was found to be fallen as the transient early stage during drying of 8 hr.

Table 1. Effect of Drying Time on the Drying Rate of Raw Fish Using Direct Solar Cabinet Dryer (November and December, 2018)

Sr. No.	Drying Time (hr)	November			December		
		Weight of Sample (g)	Moisture Content (% w/w) (Wet Basis)	Drying Rate (g/hr sq.cm)	Weight of Sample (g)	Moisture Content (% w/w) (Wet Basis)	Drying Rate (g/hr sq.cm)
2	1	396.45	20.71	0.052	396.94	20.61	0.052
3	2	384.33	2.42	0.029	314.47	16.49	0.047
4	3	369.30	3.01	0.022	259.63	10.97	0.040
5	4	289.35	15.99	0.026	201.20	11.69	0.038
6	5	243.63	9.14	0.026	160.28	8.18	0.034
7	6	202.08	8.17	0.025	135.31	4.99	0.030
8	7	189.4	2.54	0.023	123.59	2.34	0.027
9	8	136.2	10.64	0.023	115.43	1.63	0.024
10	9	130.9	1.06	0.021	-	-	-
11	10	119.5	2.28	0.019	-	-	-

System drying efficiency of direct solar cabinet dryer was determined in November and December and the results are shown in Table (2). Direct solar cabinet dryer was found to have better drying efficiency in December than in November because of the ambient air condition.

Table 2. System Drying Efficiency of Direct Solar Cabinet Dryer during Drying of Fish

Sr. No.	Drying Period	System Drying Efficiency (%)
1	November	9
2	December	14

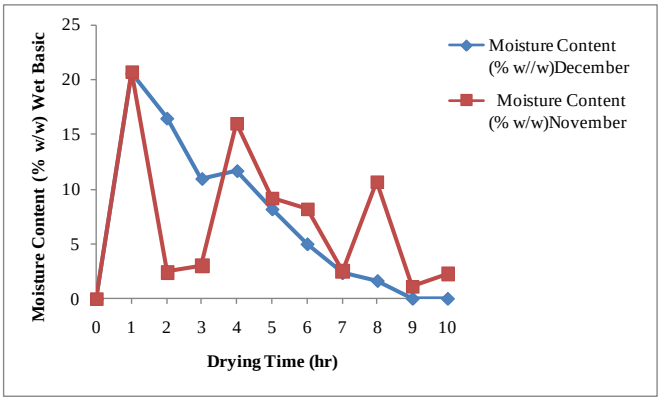

Figure 4. Drying Curve during Drying of Fish in November and December

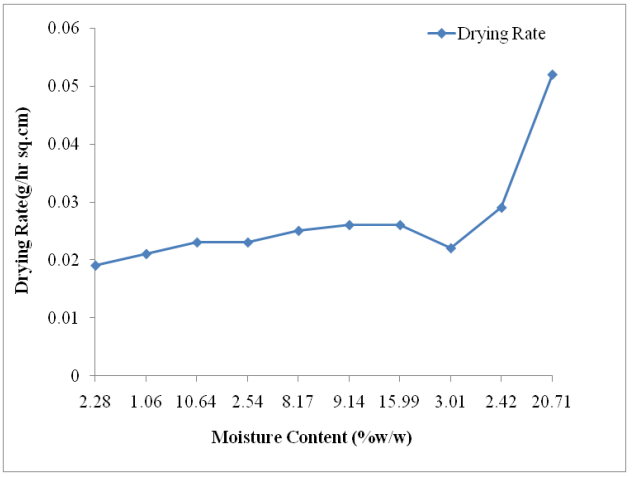

Figure 5. Drying Rate Curve during Drying of Fish in November

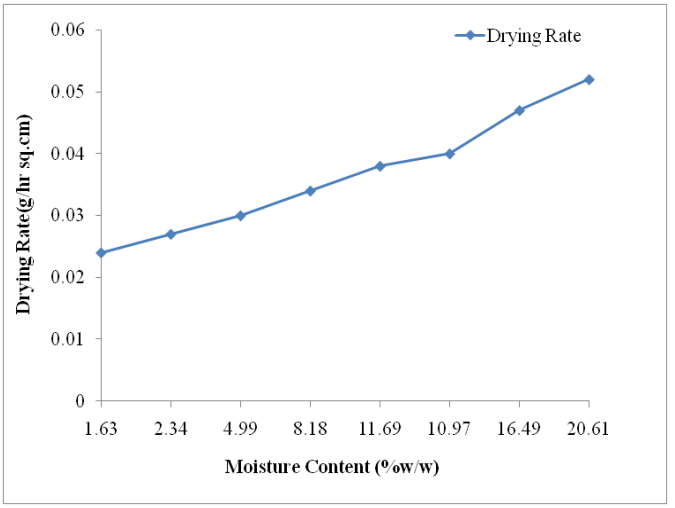

Figure 6. Drying Rate Curve during Drying of Fish in December

The effect of solar drying on nutritive value of fish powder was determined and compared with fish powder using hot air oven drying, and is shown in Table (3). It was observed that the protein content of prepared fish powder with solar dryer was slightly higher than that of fish powder with hot air oven because of the effect of drying temperature on the protein content. According to literature review, the most common factor affecting denaturation of protein is temperature.

Table 3. Effect of Different Drying Methods on Nutritive Value of Fish Powder

Sr. No.	Value of Sample	Solar Drying	Hot Air Oven Drying
1	Moisture Content (% w/w)	9.12±0.02	11.37±0.2
2	Ash (% w/w)	8.7±0.07	9.51±0.1
3	Protein (% w/w)	72.48	72.33
4	Crude Fat (% w/w)	0.06	0.09
5	Crude Fibre (% w/w)	3.20	4.08
6	Carbohydrates	6.35	2.31
7	Energy Value (kcal/100 g)	315.86	299.37

Table (4) shows the effect of solar drying time on the characteristics of dry cat food (fish and soybean) and the samples were coded as SFS_1 to SFS_4. The minimum solar drying time of 2 hr was selected for the preparation of dry cat food because all of the variables of the moisture content, protein content differences were very closer and all of the values were under allowable limit. The size stability percent of all the dry cat food was nearly the same.

Table 4. Effect of Solar Drying Time on the Characteristics of Dry Cat Food (Fish and Soybean)

Sr. No.	Sample	Drying Time (hr)	Moisture Content (%w/w)	pH	Protein Value (% w/w)	Size Stability (%)
1	SFS_1	2*	3.68±0.1	6.4	47.44	96.8
2	SFS_2	2.5	3.50±0.1	6.4	48.32	96.5
3	SFS_3	3	3.33±0.2	6.4	48.87	96.4
4	SFS_4	3.5	3.11±0.1	6.4	45.86	96.2

*Most suitable sample

SFS= Prepared dry cat food with solar drying (Fish and Soybean)

The effect of solar drying on physico-chemical characteristics of dry cat food was evaluated and compared with dry cat food using hot air oven drying, and presented in Table (5). It was evident that the protein content and metabolizable energy of dry cat food using solar drying were significantly higher and the crude fat and crude fiber content were also slightly higher than that of dry cat food using hot air oven. In addition, the cost of prepared dry cat food with solar drying was lower than the cost of dry cat food with hot air oven. According to t-test, t_0 =-10.41<-2.306 means the two drying methods are different.

Table 5. Effect of Different Drying Methods on Physico-chemical Characteristics of Dry Cat Food (Fish and Soybean**)**

Sr. No.	**Value of Sample**	**Solar Drying**	**Hot Air Oven Drying**
1	Moisture Content (% w/w)	3.68±0.1	10± 0.05
2	Ash (% w/w)	10.81± 0.19	13± 0.1
3	Protein (% w/w)	47.44	41.50
4	Crude Fat (% w/w)	15.20	14.89
5	Crude Fibre (% w/w)	3.92	3.13
6	Carbohydrates	18.95	15.98
7	Energy Value (kcal/100 g)	402.36	363.93
8	Metabolizable Energy (ME)(kcal/kg)	3615.65	3277.5
9	Estimated Cost (kyat) (400 g/bag)	1036	1175

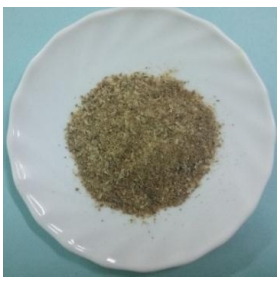

Figure 7. Fish Powder

Figure 8. Dry Cat Food (Fish and Soybean) Using Solar Drying

Conclusion

This research reveals practically how various low grade fish resources could be processed to high grade protein fish powder and dry cat food. This study also revealed the feasibility of using solar drying instead of hot air oven to produce dry cat food with the acceptable quality based on

the nutritive value and economic point of view and to support the import substitution. It was observed that the nutritive value of dry cat food using solar dryer was markedly higher than using hot air oven. The conclusion was that dry cat food could be produced by using direct solar cabinet dryer as constructed in this research work in some areas of country where solar radiation is abundantly available.

Acknowledgements

The researchers would like to express sincere appreciation to Dr. Soe Soe Than, Professor and Head, Dr. Khin Thet Ni, Professor and Head (Retired) and Dr. Cho Cho Oo, Professor and Head (Retired) of the Department of Industrial Chemistry, University of Yangon, for giving permission to perform this research work. The deepest gratitude is expressed to Dr.Than Htaik, Director General (Retired), Cottage Industry Department, Ministry of Cooperative for giving permission to perform the research, invaluable suggestions and helpful advice through the research work.

References

Asaro N.J., M.A. Guevara and K. Berendt (2017) "Digestibility is Similar between Commercial Diets That Provide Ingredients with Different Perceived Glycemic Responses and the Inaccracy of Using the Modified Atwater Calculation to Calculate Metabolizable Energy*", Journal of Veterinary Sciences*, pp. 1-12.

Amir H.M.S. and Z. Mona (2013) "Raw Ingredients in Cat Food Manufacturing", *Journal of TropicalResources and Sustainable Science*, Volume 1, University Malaysia Kelantan Publisher, pp. 1-12.

Brenndorfer, B., Kennedy, L., Bateman, C.O.O., and Trim, D.S., (1987). *Solar Dryers-their role in post-harvest processing,* Commonwealth Secretariat Publications, London.

Hii C.L., Jangam S.V., Ong S.P. and Mujumdar A.S. (2012) "Solar Drying: Fundamentals, Applications and Innovations", published in Singapore.

Pet Food Manufacturers Association (2010) "Ingredients in Pet Food".

Rivera J.A. (1998) "Petfood: physico-chemical characteristics and functional properties of meat by-products and mechanically separated chicken(MSC) in a high-moisture model system', *Dissertation, L*owa State University, pp.4-17.

Ruaud J., I. Guiller and A. Levesque (2011) "Method for producing highly palatable dry cat food", *International and National Patent Collections.*

WALTHAM (2003) "Feline Body Mass Index", *The world's leading authority on pet care and nutrition.*

A Study on the Processing of Brandy from Locally Available Wine Grapes

Mon Mon Maung[1], Thwe Linn Ko[2] & KhinThet Ni[3]

Abstract

This research work emphasized with the processing of brandy from locally to be had wine grapes. The physico-chemical characteristics of wine grape such as moisture content, ash content, fiber content, pH, acidity and soluble solids (˚Brix) was investigated. Red wine was firstly prepared with the variation of amount of sugar and fermentation duration for the manufacturing of brandy. The physico-chemical properties of prepared red wine and commercial wines were evaluated by the assurance of pH, acidity, total soluble solids, reducing sugar, colour, specific gravity and alcohol content. After seven week fermentation period, the highest alcohol content 14 %v/v was formed with 1: 0.16 mash to sugar ratio in prepared red wine. Prepared red wines were distilled to acquire brandy and the properties of brandies like pH, acidity, soluble solids (˚Brix), reducing sugar, colour, specific gravity and alcohol content were examined. It was found that alcohol content of the first distillate used to be 40 %v/v and 76.5 %v/v for the second distillate from red wine. The main constituents (ethanol) and fusel oils in prepared wines and these distillates were firmly resolved with the aid of gas chromatography. Prepared brandies from red wine were aged in oak cask to enhance colour, taste and odour.

Keywords: wine grape, ethanol, fermentation, distillation

Introduction

The name brandy comes from the Dutch word *brandewijn,* meaning "burnt wine" that is a spirit produced by distilling wine. Even as brandies are normally crafted from wine or different fermented fruit juices, it can be distilled from any liquid that consists of sugar. Wine is an alcoholic beverage produced by using the fermentation of sugars in fruit juices, mostly grape juice. In general, wines are classified into two types primarily based on alcohol content: table wines (7 percent to 14 percent, by volume)

[1] Lecturer, Department of Industrial Chemistry, University of Mandalay.
[2] Pro-rector, University of Pyay.
[3] Professor (Retired), Department of Industrial Chemistry, University of Yangon.

and dessert wines (14 percent to 24 percent, by volume). (Blue, Anthony., 2004)

A grape is a fruiting berry of the deciduous woody vines of the botanical genus *Vitis*. Grapes can be eaten raw or they can be used for making wine, jam, juice, jelly, grape seed extract, raisins, vinegar, and grape-seed oil. Fermentation biotechnology is an crucial industrial technique for the production of alcoholic drinks such as wine. . The method of fermentation in wine turns grape juice into an alcoholic beverage. During fermentation, yeast interacts with sugars within the juice to create ethanol, commonly referred to as ethyl alcohol, and carbon dioxide (as a by-product). (Anderson., and Hull., 1970)

Wine is made by means of crushing the grapes and then pressing them to extract the juice. This juice is then fermented, which means that the sugar contained within the juice turns to alcohol. But the end result is wine that will then be aged in various different ways before being bottled. In the process of making brandy, the grapes are picked, crushed and pressed, after which fermented. But it's after this stage where the big differences begin to become apparent. The fermented wine is then distilled twice in alembic pot stills. Within these stills the liquid is heated, and the various volatile components within the liquid are separated and eliminated. This concentrates the alcohol. The process is carried out twice, which is one of the unique aspects of brandy making. This is referred to as 'double distilled' (Eisenman., 1998).

Distillation is a typically used approach for purifying beverages and separating mixtures of liquids into their individual components. In practice, distillation may be carried out by way of either of two principal methods. After distillation, the brandy is aged in oak casks for 3 to 15 years or more. During aging, some of the ethanol and water seep through the oak and evaporate, so brandy is added periodically to compensate for this loss. Caramel coloring is introduced to offer the brandy a characteristic dark brown color. After aging, the brandy may be blended and/or flavored, and then chilled, filtered, and bottled (McCabe., et al., 2005).

The main objective of this present work was to make a study on processing of brandy from locally available grapes. The specific objectives of this study were to study the characteristics of wine grape and physico-chemical properties of prepared wines, to analyze properties of distillates for processing of brandy, to determine main constituent and fusel oils in

prepared wines, distillates and brandies by gas chromatography and compare the properties between processed products and commercial products.

Materials and Methods

Materials

Raw materials for processing of brandy, wine grapes and table grapes were collected from Saebauk Grape Farm, Kyaukpadung Township, Mandalay Region. Sugar (Mikko Brand, Myanmar) was purchased from City Mart supermarket, 8 miles, Mayangone Township, Yangon Region. Yeast (*saccharomyces cerevisiae*), ascorbic acid, potassium metabisulphite and potassium sorbateAnalar grade, BDH, England and these were purchased from KEMIKO chemical shop, 28th St., Pabedan Township, Yangon Region.

Methods

Fermentation and Distillation Process

Selected wine grapes were washed with water and seeds were removed. And then, grapes were crushed to make the must. To obtain high yield of wine, various ratios of grape must and sugar (1:0, 1:0.1, 1:0.16, 1:0.2 and 1:0.3) were used. Sugar was added in the form of syrup. After that yeast (*saccharomyces cerevisiae*) was added to enhance fermentation and water was introduced and stirred two times day by day at some point of the three weeks of fermentation time. On the stop of sugar fermentation that remaining for three weeks the liquid was separated from the stable substances through racking. After racking, prepared red wines were obtained and stored in the wine pot.

Prepared red wine was placed into a one necked .round bottomed flask. The distillation column, condenser and distillate collector were attached. Heating was applied to the round bottomed flask. The column top temperature was at 78^{o}C as the first distillate was being produced and the quantity of first distillate which turned into being collected If the first distillate was not being produced even the temperature was at 90^{o}C, heat supply was stopped and the final volume of first distillate was recorded. After the first distillation, which took about two hours, wine had been converted to concentrated liquid (not yet brandy) with an alcohol content of 40%. Second distillation was conducted as the same procedure and the second distillate was collected and amount of volume obtained was

recorded. The product of the second distillation had an alcohol content of around 76.5%. The brandy was not yet ready to drink after the second distillation and had been placed in oak casks and allowed to age. As the brandy ages, it absorbed flavors from the oak while it's owned structure softens, becoming less astringent.

Characteristics of Wine Grapes, Prepared Red Wines and Brandy

The physico-chemical characteristics of wine grape which include moisture content, ash content, fiber content, pH, acidity and soluble solids (˚Brix) was studied. The physico-chemical properties of prepared prepared wines and brandy were evaluated by the determination of pH, acidity, total soluble solids, reducing sugar, colour, specific gravity and alcohol content. Main constituent and fusel oils of prepared wines and brandy were analyzed through gas chromatographyat the Scientific and Technological Instrument Centers (STIC), Mae Fah Luang University, Chaing Rai, Thailand.

Results and Discussion

In Myanmar, wine grapes may be to be had though the whole season and are planted in very dry regions of Central Myanmar. These properties would be varied depending on the grape variety and climatic conditions of grape growing areas and ideal grape varieties have to be selected to get good wine and related beverages. The characteristics of wine grapes are shown in Tables (1).

Table 1. Characteristics of Wine Grapes

Sr. No.	Characteristics	Wine Grape
1	Moisture (%w/w)	72
2	Fiber (%w/w)	0.78
3	Ash (%w/w)	0.35
4	pH	3.0
5.	Acidity (%w/v)	1.01
6	Soluble solids (˚Brix)	18.25
7	Reducing sugar (mg/g)	1.92

Table 2. Physico-chemical Properties of Prepared Red Wine

Sr. No.	Property	Red Wine				
1	Ratio of grape pulp and sugar used	1 : 0	1 : 0.1	1 : 0.16	1 : 0.23	1 : 0.3
2	pH	3.5	3.2	3.3	3.4	3.5
3	Acidity (%w/v)	0.62	0.67	0.65	0.54	0.49
4	Specific gravity	0.99	0.98	0.97	0.98	0.98
5	Alcohol content (%v/v)	8.0	9.0	14.0	12.0	11.0
6	Soluble solids (˚Brix)	3.1	3.2	3.5	3.4	3.3
7	Reducing sugar (mg/g)	1.9	1.89	1.8	1.79	1.7
8	Colour (absorbance)	0.15	0.14	0.14	0.12	0.11

Red wine was prepared by varying the ratio of grape must and sugar (1:0, 1:0.1, 1:0.16, 1:0.2 and 1:0.3). The highest contents of alcohol, 14% v/v in red wines were obtained after 7 weeks fermentation period. To prepare brandy, initially higher alcohol concentration in wine should be selected and these data are shown in Table (2).

Table 3. Main Constituent and Fusel Oils in Prepared Red Wine by Gas Chromatography

Peak No	Retention Time (min)	Area%	Compound Name	% of Total
1	1.96	12.56	Ethanol$$ Ethyl alcohol	12.56
2	2.09	8.93	Ethanol$$ Ethyl alcohol	8.93
3	2.27	22.39	Ethanol$$ Ethyl alcohol	22.39
4	2.93	14.76	Ethanol$$ Ethyl alcohol	14.76
5	4.37	1.47	1-Pentanol $$ Amyl alcohol	1.47

Peak No	Retention Time (min)	Area%	Compound Name	% of Total
6	6.09	20.56	Not detected: Value of quality less than 60%	20.56
7	6.26	0.29	Acetic acid $$ Ethylic acid	0.29
8	6.33	0.08	Not detected: Value of quality less than 60%	0.08
9	6.44	0.17	1,2-Propanediol $$ Propylene glycol	0.17
10	6.52	1.50	2,3-Butanediol	1.50
11	6.77	0.14	cis-5-hydroxy-2-methyl-1,3-dioxane	0.14
12	6.82	0.03	trans-4-hydroxymethyl-2-methyl-1,3-dioxolane	0.03
13	6.89	0.14	Not detected: Value of quality less than 60%	0.14
14	7.19	0.27	Not detected: Value of quality less than 60%	0.27
15	7.41	0.64	Not detected: Value of quality less than 60%	0.64
16	7.48	0.33	Not detected: Value of quality less than 60%	0.33
17	7.66	0.85	Not detected: Value of quality less than 60%	0.85
18	7.90	2.01	2,3-Dihydro-3,5-dihydroxy-6-methy-4H-pyran-4-one	2.01
19	8.03	0.89	Not detected: Value of quality less than 60%	0.89
20	8.20	1.43	Not detected: Value of quality less than 60%	1.43
21	8.72	9.50	Not detected: Value of quality less than 60%	9.50

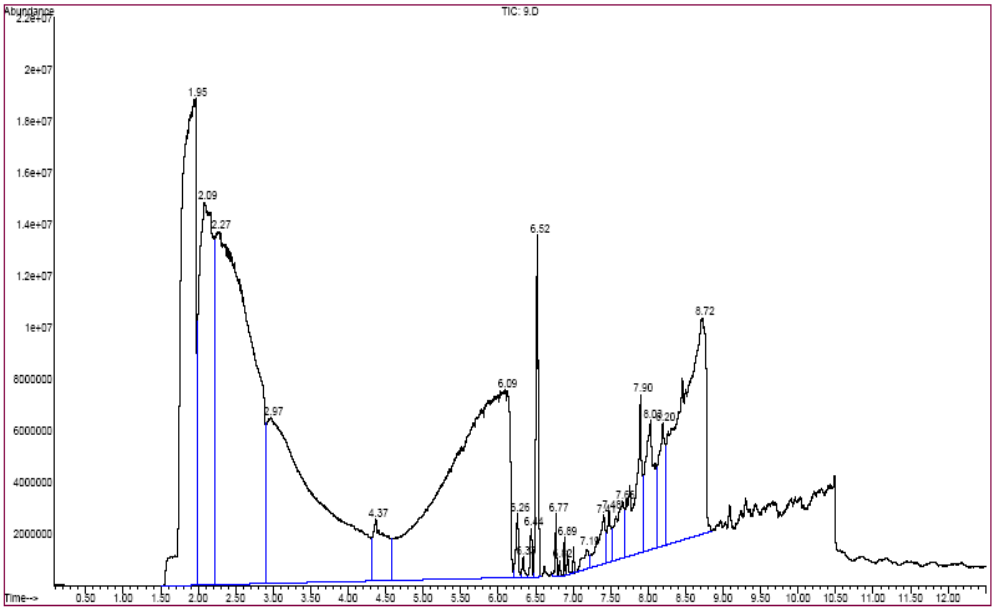

Figure 1. Gas Chromatography Spectrum of Main Consituent and Fusel Oils in Prepared Red Wine

Main constituent and fusel oils of prepared wines were analyzed by gas chromatography and the spectra are shown in Fig. (1) and their respective records are also presented in Tables (3). Analysis of wines by gas chromatography described that the main organic compounds in them was ethanol with other small amount of organic constituents. Fusel oil is a by-product of alcoholic fermentation and its composition can vary widely depending on the raw materials used. Fusel (higher) alcohols are quantitatively major volatile by-products of yeast fermentation and are thought to contribute to the aromatic complexity of wine. Quantitatively, the most important higher alcohols are the straight-chain alcohols – 1-propanol, 2-methyl-1-propanol (isobutyl alcohol), 2-methyl-1-butanol, and 3-methyl-1-butanol (isoamyl alcohol). Most straight-chain higher alcohols have a strong pungent odor. Many alcohols occured in wine, but only a few were present at sufficient concentrations to affect its characteristics.

Table 4. Properties of First Distillate from Red Wine Specific Temperature Range

Sr. No.	Temperature Range (˚C)	First Distillate from Red Wine		
		Specific Gravity	Soluble Solids (˚Brix)	Alcohol Content (%v/v)
1	78-80	0.9497	14.2	40
2	80-82	0.9511	13.5	37
3	82-84	0.9587	12.7	34
4	84-86	0.9627	12	31
5	86-88	0.9651	11.4	29
6	88-90	0.9687	10.4	26

Table 5. Properties of Second Distillate from Red Wine at Specific Temperature Range

Sr. No.	Temperature Range (˚C)	Second Distillate from Red Wine		
		Specific Gravity	Soluble Solids (˚Brix)	Alcohol Content (%v/v)
1	78-80	0.8704	19.4	76.5
2	80-82	0.8717	19.3	76
3	82-84	0.8730	19.2	75.5
4	84-86	0.8743	19.1	75
5	86-88	0.8756	19.0	74.5
6	88-90	0.8769	18.9	74

The properties of the first and second distillates from wines at specific temperatures are shown in Tables (4) to (5). First distillate 41mL.was distilled from 300 mL. red wine and second distillate 38 mL. was further distilled from first distillate. Only 2mL.of residue (2.62%v/v alcohol content) was retained after complete distillation. Distillation period 45 min. required to convert 300 mL. of red wine to first distillate 41mL. But distillation period for second distillation was 30 min. It was observed that, alcohol content of first distillate was 40 %v/v, whereas 76.5 %v/v for second distillate from red wine.

Table 6. Main Constituent and Fusel Oils in First Distillate from Red Wine Analyzed by Gas Chromatography

Peak No	Retention Time (min)	Area%	Compound Name	Quality	% of Total
1.	1.61	2.27	*Acetaldehyde	80	2.27
2.	1.85	92.50	Ethanol	86	92.50
3.	2.21	0.16	*Propyl alcohol	91	0.16
4.	2.60	0.20	*Ethyl acetate	91	0.20
5.	2.81	0.20	*Isobutyl alcohol	94	0.20
6.	4.13	0.09	*2,4,5-trimenthyl-1-3-dioxolane	83	0.09
7.	4.17	1.50	*1,1-diethoxyethane	83	1.50
8.	4.28	0.39	*Isoamyl alcohol	83	0.39
9.	4.32	0.21	*2-methyl-n-butanol	80	0.21

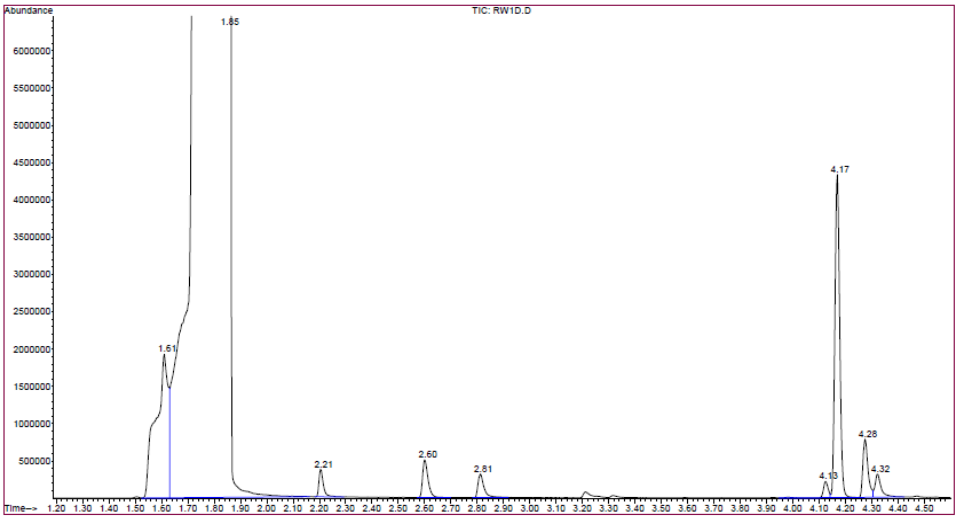

Figure 2. Gas Chromatography Spectrum of Main Consituent and Fusel Oils in First Distillate from Red Wine

Table 7. Main Constituent and Fusel Oils in Second Distillate from Red Wine Analysed by Gas Chromatography

Peak No	Retention Time (min)	Area%	Compound Name	Quality	% of Total
1.	1.61	2.22	*Acetaldehyde	80	2.22
2.	1.85	94.56	Ethyl alcohol	86	94.56
3.	2.21	0.15	*Propyl alcohol	91	0.15
4.	2.60	0.26	*Ethyl acetate	91	0.26
5.	2.81	0.18	*2-methyl-1-proponol	91	0.18
6.	4.13	0.09	*2,4,5-trimenthyl-1-3-dioxolane	83	0.09
7.	4.17	1.98	*1,1-diethoxyethane	83	1.98
8.	4.28	0.38	*Isoamyl alcohol	89	0.38
9.	4.32	0.18	*2-methyl-n-butanol	16	0.18

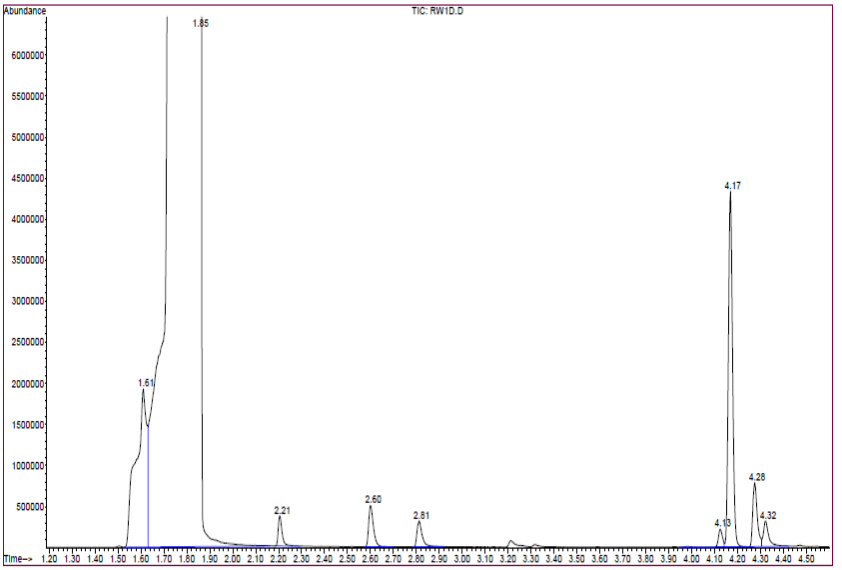

Figutr 3. Gas Chromatography Spectrum of Main Consituent and Fusel Oils in Second Distillate from Red Wine

Main constituent and fusel oils of first and second distillates were analyzed by gas chromatography and the spectra are shown in Fig. (2) to (3) and their respective data are also presented in Tables (6) to (7). From analysis by gas chromatography, it could be confirmed that the main organic compound in first and second distillates were ethanol. Minute trace quantity of other organic compounds were contained in these distillates. In brandy, fusel alcohols give some of their distinctive aromatic character. Although ethanol has a mild fragrance, the most significant aromatic alcohols are the fusel alcohols. Ethanol not only gives off an alcoholic odour but also acts as a carrier of other odour-active volatile compounds. The fusel alcohols impart a range of organoleptic attributes.

Conclusion

Alcohol content of finished wines depended upon the certain limit of the quantity of sugar and fermentation period and the stabilizers definitely affected on the finished wine's texture and sparkling. Despite the fact that alcohol content of prepared red wine was 14 %v/v, alcohol content of first distillate from red wine was 40%v/v and second distillate contained

76.5%v/v. Brandies from wines were colourless and odourless, accordingly so to imitate the effect of aging, caramel colour, 0.3-0.4g. consistent with 100mL.of brandy was suitable to feature. To obtain fine brandy, concentrated alcohol must be placed in oak casks and allowed to age for more than 5 years, an important step in the production process. Compounds released from wood into brandy depend on the factors such as type of wood, time of contact. As the brandy ages, it absorbs flavors from the oak while its own structure softens and becoming less astringent. Aging in the oak cask could support not only improved the taste, colour and odour of finished brandy but also eliminate the fusel oils. Moreover, by aging in the oak cask, brandy could also had interacting with air and oak barrel in which it evaporated and concentration would be dropped from 76%v/v to about 70% v/v.

Acknowledgements

I would like to express my greatest appreciation to Dr.Khin Hla Mon, Professor and Head, Department of Industrial Chemistry, Dagon University for her permission to submit this research paper, reviewing the manuscript and suggestions. I would like to express my profound respect and appreciation to my supervisor, Dr Khin Thet Ni, Professor and Head (Retired) of the Department of Industrial Chemistry, University of Yangon, for giving permission to perform this research, guidance, kind encouragement, invaluable suggestions and advice throughout this research work. I would like to express my sincere gratitude to my co-supervisor, Dr Thwe Linn Ko, Pro Rector, Pyay University for her patience, constructive criticisms and constant guideline throughout this research work until completion of my thesis.

References

Anderson, S. F., and Hull, R., 1970, “The Art of Wine Making”, New York.

Eisenman, L., 1998, “The Home Winemakers Manual”.

McCabe, W.L., et al., 2002, “Unit Operations of Chemical Engineering”, 5th Edition.

McCabe, W.L., et al., 2005, “Unit Operations of Chemical Engineering”, 7th Edition.

Perry, 1997,“Perry’s Chemical Engineers’ Handbook”, McGraw-Hill, Inc., 8th Edition.

Blue, Anthony ., 2004, “ The Complete Book of Spirits”. New York: HarperCollins. p. 239. ISBN 978-0-06-054218-4..

Extraction of Low Methoxyl Pectin from Banana Peels

Aye Aye Maw[1], Soe Soe Than[2] & Khin Hla Mon[3]

Abstract

The extraction of pectin from banana peels (Saba banana, *Musa 'saba',* pheegyan) was carried out by treatment with pectinase enzyme. The physico-chemical characteristics of banana peels such as moisture, ash, protein, crude fat, crude fiber, carbohydrate, pectin, sugar contents and pH were studied. During the enzymatic extraction, Box-Behnken Design was used to optimize the yield of pectin. The yield of pectin (1.8) g and methoxyl content of pectin 3.43 ± 0.18 (%w/v) were 0.04 (%w/v) of pectinase enzyme solution, 43 min extraction time and 33 ˚C extraction temperature. The physico-chemical properties of the resulting polysaccharide (pectin) such as moisture content, ash content, sugar content, pH, solubility, gel formation and precipitate formation were studied. The functional group of extracted pectin was analyzed by FTIR (Fourier Transformed Infrared Spectroscopy).

Keyword: banana peels, pectin, methoxyl content

Introduction

Banana peels constitute about 30% of the fruit and cause an environmental problem for solid waste. The use of banana peels as a source of high value compounds such as pectin, cellulose nanofibers, and phenolic compounds is interesting not only from an economic point of view, but also from an environmental perspective (Oliveira *et al*., 2015).

Pectin is a structural hetero-polysaccharide contained in the primary cell walls of terrestrial plants (Prashansa *et al*., 2017). The plant cell wall is consisted of polysaccharides and proteins. The wall polysaccharides are often classified into cellulose, hemicelluloses and pectin (Dong, 2010).

Pectin is the versatile stabilizers available. Its gelling, thickening and stabilizing properties provide an essential additive in the production of many food products. It was evaluated the differences in concentration, temperature and time on pectin extraction from banana peels using organic acids. Strong mineral acids are as cheap as and as effective as organic acids.

[1] Lecturer, Department of Industrial Chemistry, University of Yangon
[2] Professor and Head, Department of Industrial Chemistry, University of Yangon
[3] Professor and Head, Department of Industrial Chemistry, Dagon University

Organic acids are more interesting than strong acids from an environmental point of view (Oliveira *et al*, 2015).

Enzymatic extraction seems to be a promising alternative to chemical method for the extraction of pectin and has caught extensive attention in recent years. However, this method in turn results in modifying the physicochemical properties and lowering gel strength as compared to traditionally obtained pectin (ZaizhiLiu, *et al*, 2017).

Extracted pectin has more than 50% of the acid units esterified, and it is classified as high methyl ester (HM) pectin. The percentage of ester groups is known as degree of esterification. High methyl ester pectins are classified in groups according to their gelling temperature as rapid set to slow set pectin. Modification of the extraction process, or treated with acid, will yield a low methyl ester (LM) pectin with less than 50% methyl ester groups. Some pectin are treated during manufacture with ammonia to produce amidated pectin, which have particular advantages in some applications. They are called aminated pectin.

In this study, enzymatic treatment of banana peels was carried out using pectinase enzyme. Box–Behnken Design (BBD) was applied to obtain the optimal extraction conditions. Fourier transform infrared spectroscopy (FT-IR) was employed to evaluate the characterization of pectin.

Materials and Methods

Material

Banana peels were collected from Hledan Market, Kamayut Township, Yangon. Pectinase enzyme (HeFeiBoMei Biotechnology Co. Ltd, China) was purchased from Myanmar Supply Co.,Ltd, No.(244-246), Kon Zay Dan Street, Middle Block, Pabedan, Yangon. 95% Ethanol was purchased from Super Shell-Chemical Trading, No. (117), 27th street, Middle Block, Pabedan, Yangon.

Method

The physico-chemical characteristics of banana peels such as moisture, ash, crude fiber, crude protein, crude fat and carbohydrate content were determined according to (AOAC934.01), (AOAC930.05), (AOAC978.10), (AOAC 922.06) and (AOAC920.152) methods respectively. Carbohydrate content was determined by subtraction of 100 –

(Moisture + Fat + Protein + Fiber + Ash). pH of the sample was determined using a digital pH meter (pH 300, HANNA). Sugar content of the sample was determined by using a refactrometer (Milwaukee MA 871 Refractometer, Made in Romania) (Pearson, 1976). Protein, Crude Fat and Crude fiber were determined at food Industries Development Supporting Laboratory (FIDSL). UMFCCI Tower, Lanmadaw Township, Yangon Region.

Extraction of Polysaccharide (pectin) from Banana Peels

Banana peels were boiled in hot water at 90˚C for 15 minutes. The banana peels were then scrubbed with spoon. Banana paste was prepared using a motor and pestle. About (100) g of banana paste was thoroughly mixed with 50 mL of 0.04% pectinase enzyme solution at 33˚C for 43 minutes. The mixture was filtered through the filter paper (Whatman No 1). The filtrate was poured into 200 mL of 95% ethanol. Pectin was formed in ethanol solution. After that, pectin was filtered through the filter paper (Whatman No 1). The residue pectin was dried in a hot air oven at 60˚C for about (3-4) hours. And then, dried pectin was ground by using motor and pestle to obtain the fine powder (60 mesh). Finally, it was then packed into clean airtight plastic bag and stored at cool and dry place.

Optimization of Extraction of Polysaccharide (pectin) from Banana Peels

Box-Behnken Design was used for arrangement of 15 experimental runs response surface methodology (RSM). Levels of treatment time and treatment temperature, pectinase enzyme concentration are shown in Table (1).The experimental runs are shown in Table (2).

Table 1. Variables for the Enzymatic Treatment of Banana Peels

Sr. No.	Variables	Levels	
		Lower	Upper
1	Treatment Time (min)	30	60
2	Treatment temperature(˚C)	30	40
3	Enzyme Concentration (%w/v)	0.03	0.05

Table 2. Experimental Runs according to Box-Behnken Design

Run Order	Time (min)	Temperature (˚C)	Pectinase Enzyme Concentration (%w/v)
1	45	35	0.04
2	60	30	0.04
3	45	35	0.04
4	45	30	0.03
5	30	40	0.04
6	45	40	0.05
7	45	35	0.04
8	45	30	0.05
9	60	35	0.03
10	60	40	0.04
11	30	35	0.03
12	30	30	0.04
13	60	35	0.05
14	30	35	0.05
15	45	40	0.03

Characterization of Polysaccharide (pectin) from Banana Peels by Fourier Transform Infrared Spectroscopy (FTIR)

FTIR analysis (FTIR-8400, iD7ATR, Britain) was carried out to examine the functional groups of polysaccharide. FTIR analysis was carried out at the Physics Department, Dagon University.

Results and Discussion

The physico-chemical properties of banana peels are shown in Table (3). The results in Table (3) indicate that carbohydrate 13.88 (%w/w), pH 5.1 and 1 (%w/w) pectin present in banana peel. Carbohydrate is the main constituent of extracted pectin from banana peels. Enzymatic treatment of the more sensitive glycosidic linkages, like those involving the neutral sugar side chains, may lead to the increase of the galacturonic content and decrease of the neutral sugar content of the acid-treated pectin (Lees, 1975).

Pectin from banana peels was extracted with using pectinase enzyme treatment according to the experimental runs arranged in Box-Behnken design.

The second order polynomial equation obtained by using the statistical software (Design Expert, version 11, Stat Ease Inc..,) for the response function of methoxyl content is shown in Equation (1)

$$\text{Methoxyl content (\%)} = +3.43 + 0.3963x_1 - 0.03x_2 - 0.8938x_3 - 1.72\,x_1x_2 + 1.15\,x_1x_3 + 1.14\,x_2x_3 + 1.22x_1^2 + 1.76\,x_2^2 - 0.7658\,x_3^2 \qquad \text{Equation (1)}$$

To solve the equation (1) using MATLAB, the estimated value of pectin of methoxyl content was 3.43 %w/w of pectinase enzyme concentration, 43 min treatment time and 33 ˚C treatment temperature.

Figures (2), (3) and (4) showed the three dimensional response surface plots and three dimensional contour plots illustrating the interactive effect of extraction time and extraction temperature, extraction time and concentration of pectinase enzyme and extraction temperature and concentration of pectinase enzyme on the methoxyl content.

Under the optimum conditions, the maximum pectin content of 100 g of bananan peels (1.8) g has been resulted. The methoxyl content of pectin extracted from banana peel was (3.43 ± 0.18) and it was identified as low methoxyl pectin due to its methoxyl content of (3.43 ± 0.18) and DE <50%. The effect of extraction time, temperature and pectinase enzyme on the low methoxyl content and yield of pectin of polysaccharide are shown in Table (4). According to the result, it can be observed that the yield of pectin decreased when the less of the low methoxyl content was reached.

The physico-chemical properties of extracted pectin such as moisture, ash, sugar, methoxyl content, equivalent weight, solubility, gel formation, precipitate formation are shown in Table (5). Ash content and equivalent weight of the extracted pectin were slightly higher than that of commercial pectin but sugar content and methoxyl content of extracted pectin were lower than that of commercial pectin.

Table 3. Physico-chemical Properties of Banana Peels

Sr. No.	**Properties**	**Banana peels**	**Literature (Chongkhong, Doromae,2012)**
1	Moisture % (w/w)	81.22	86.01
2	Ash % (w/w)	1.69	1.75
3	Protein % (w/w)	0.56	1.27
4	Sugar (Brix)	5	-
5	Crude Fat %(w/w)	0.69	1.82
6	Crude fiber % (w/w)	1.96	2.28
7	Carbohydrate (%)	13.88	9.15
8	pH	5.1	5
9	Pectin % (w/w)	1	0.7-1.2

Table 4. Effect of Extraction Time, Temperature and Pectinase Enzyme on Yield of Pectin the Low Methoxyl Content

Run	Time(min)	Temp (˚C)	Pectinase Enzyme Concentration (%w/v)	Pectin (%w/w)	MeO (%w/w)
1	45	35	0.04	0.8	3.72
2	60	30	0.04	1.8	8.68
3	45	35	0.04	0.6	3.22
4	45	30	0.03	1.4	6.54
5	30	40	0.04	1.5	7.58
6	45	40	0.05	1.1	4.59
7	45	35	0.04	0.7	3.34
8	45	30	0.05	0.6	1.98
9	60	35	0.03	0.9	3.84
10	60	40	0.04	1.1	4.79
11	30	35	0.03	1.3	5.22
12	30	30	0.04	1.0	4.58
13	60	35	0.05	1.2	4.85
14	30	35	0.05	0.5	1.61
15	45	40	0.03	0.9	4.58

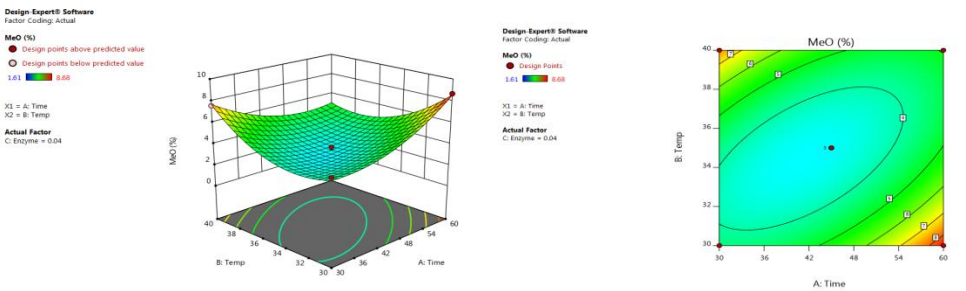

Figure 2. 3-D Response Surface Plot and Contour Plot for Methoxyl Content as a function of Time and Temperature

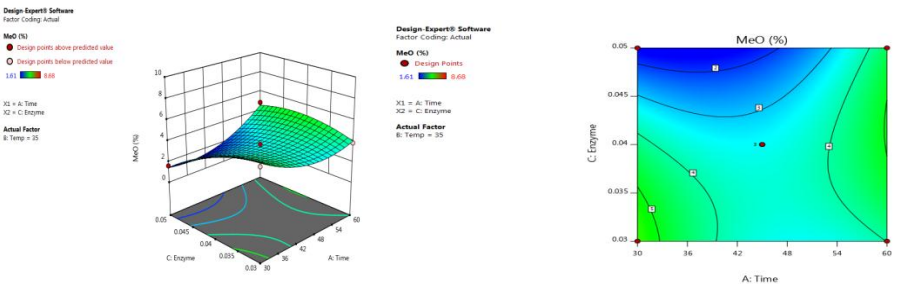

Figure 3. 3-D Response Surface Plot and Contour Plot for Methoxyl Content as a function of Time and Pectinase Enzyme Concentration

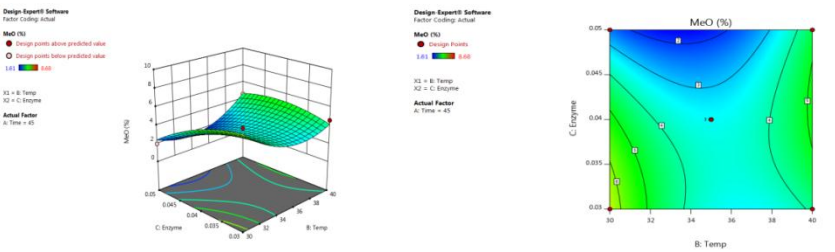

Figure 4. 3-D Response Surface Plot and Contour Plot for Methoxyl Content as function of Temperature and Pectinase Enzyme Concentration

Table 5. Physico-chemical Properties of Extracted Pectin

Sr. No.	Properties		Extracted Pectin	Commercial Pectin
1	Moisture (% w/w)		3.5	3.0
2	Ash (% w/w)		3.2	3.0
3	Sugar content (Brix)		2.5	3.0
4	pH		4	4
6	Equivalent weight		870	714
7	Methoxyl content (%)		3.43	4.83
8	Gel-formation		formation of slightly opaque gel	formation of translucent gel
9	Precipitate formation		colorless gelatinous precipitate	translucent gelatinous precipitate
10	Solubility	Hot water	+	+
		Ethanol	-	-

+ Soluble
- Insoluble

Figure (5) and Table (6) describe the FTIR spectra of extracted pectin obtained from banana peel and the reference commercial pectin. The FTIR spectra of both the extracted pectin and the commercial pectin showed characteristic peaks between 2500-3700 cm^{-1}, 2872-2962 cm^{-1}, 1715-1750 cm^{-1}, 1550-1650 cm^{-1} and 1000-1300 cm^{-1} and 1085-1150 cm^{-1} corresponding respectively, to -OH, -CH , C=O of ester and acid, COO- Asymmetric stretching vibration group, -COC- stretching of the galatouronic acid and C-O stretching vibration of ester group .The results of FTIR showed that the low methoxyl content of extracted pectin from banana peels was observed as the significant band at 3278.73 cm^{-1} for OH stretching vibration of alcoholic group, the weak peak at1731.40 cm^{-1} for C=O stretching vibration of ester group and the significant band at 1596.09 $cm^{-}1$ for COO-asymmetric stretching vibration group.

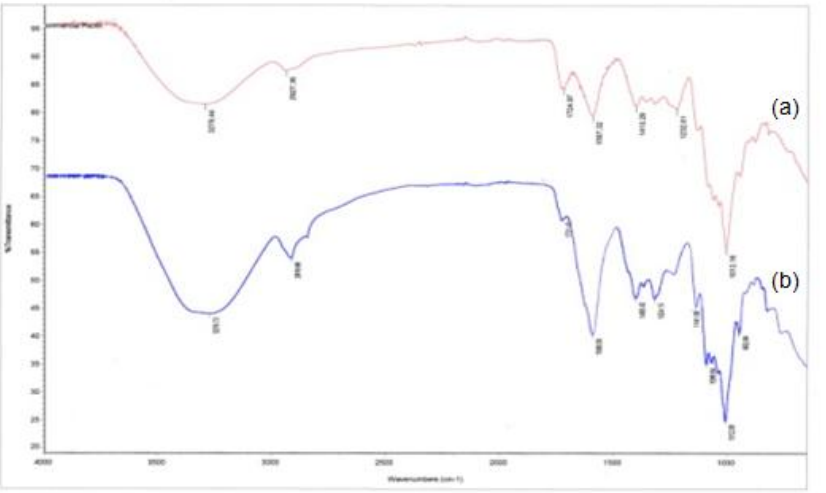

(a) Commercial Pectin

(b) Extracted Pectin

Figure 5. FTIR Spectra of Commercial Pectin and Extracted Pectin Powder

Table 6. Interpretation of FTIR Spectra of Extracted Pectin

Sr. No.	**Observed Frequency (cm^{-1})**		**Literature Frequency (cm^{-1})**	**Possible Assignments**
	Extracted pectin	**Commercial Pectin**		
1	3278.73	3278.44	2500-3700	-OH stretching vibration of alcoholic group and acid group
2	2919.96	2927.36	2872-2962	Aliphatic(C-H) stretching vibration group

Sr. No.	Observed Frequency (cm^{-1})		Literature Frequency (cm^{-1})	Possible Assignments
	Extracted pectin	Commercial Pectin		
3	1731.40	1724.97	1715-1750	C=O stretching vibration of ester group
4	1596.09	1597.32	1550-1650	COO- Asymmetric stretching vibration group
5	1232.61	1141.58	1000-1300	C-O stretching vibration of ester group
6	1012.16	1012.96	1000-1300	C- O stretching vibration of ester group

Conclusion

In this research, pectin from banana peels was extracted with pectinase enzyme according to the experimental runs in Box-Behnken design. The most suitable conditions of methoxyl content was 3.43 ± 0.18(%w/w) by using 0.037 (%w/v) enzyme, 43 min treatment time and 33˚C treatment temperature. Pectinase enzyme concentration, treatment time and temperature played a significant role for the yield of pectin. The results of FTIR spectrum showed that the low methoxyl pectin according to the weak peak at 1731.40 cm^{-1} which indicate the ester group.

Acknowledgements

The authors are greatly indebted to the ERC for editing and permission to submit this paper.

References

Imeson A., 1997. Thickening and Gelling Agents for Food, Second edition

Beli R. Thakur, Rakesh K. singh,and AvtarK.Handa,1997. Food Science and Nurition, 37(1):47-73

Castillo-Israel, K.A.T., Baguio, S.F., Diasanta, M.D.B., Lizardo, R.C.M., Dizon, E.I. and Mejico, M.I.F., 2015.*Extraction and characterization of pectin from Saba banana [Musa'saba'(Musa acuminatax Musa balbisiana)] peel wastes:* A preliminary study, International Food Research Journal 22(1): 202-207

ErmiasGirma1 and Mr. TeshomeWorku2, 2016. *Extraction and Characterization of Pectin From Selected Fruit Peel* Waste, International Journal of Scientific and Research Publications, Volume 6

Ensymm, Websites, 2017. *Pectin Production Abstract.* Retrieved March 14, 2017, from https://www.ensymm pectin production abstract .pdf

Kanmani P., E. Dhivya, J. Aravind and K. Kumaresan, 2014. *Extraction and Analysis of Pectin from Citrus Peels:* Augmenting the Yield from Citrus limon Using Statistical Experimental Design, Iranica Journal of Energy & Environment 5 (3): 303-312, 2014

Lope da Silva J.,A., and Rao M.,a.,2006, Food Polysaccharides and Their Applications, Page 354-377

Prashansa P. Bagde1, Sumit Dhenge2, SwapnilBhivgade3, 2017. *Extraction of pectin from orange peel and lemon peel,* International Journal of Engineering Technology Science and Research IJETSR, Volume 4

Poli A., Gianluca Anzelmo, Gabriella Fiorentino, Barbara Nicolaus, Giuseppina Tommonaro and Paola Di Donato, *Polysaccharides from Wastes of Vegetable Industrial Processing:* New Opportunities for their Eco-Friendly Re-Use.

Beguma R., M.G. Azizb, M.B. Uddinb, Y.A. Yusofa, 2014. *Characterization of Jackfruit (Artocarpusheterophyllus) Waste Pectin as Influenced by Various Extraction Conditions,* Agriculture and Agricultural Science Procedia 2 (2014) 244 – 251

Lees R., 1975. *Food Analysis*: Analytical and Quality Control Methods for the Food Manufacturer and Buyer.

Sohair A. El-Nawawi and Fadia R., Shehata, 1987. *Extraction of Pectin from Egyptian Orange Peel. Factors affecting the Extraction,* Biological Wastes 20, Page 281-290.

Sundari N., 2015. *Extraction of Pectin from Waste Peels:* A Review, RJPBCS 6(2), pp 1842-1248.

Parallel Implementation of Minimum Spanning Tree Algorithm on Windows Compute Cluster Server

Kyaw Moe Min*

Abstract

Minimum Spanning Tree (MST) problems are solved by using both sequential and parallel approaches. Parallelization was dealt with multi-tasks of multithreading and multiprocessing. MST problems by parallel computing are handled with equal loading of processors where communication among processes is necessary for exchanging the updated values of vertices and edges. The parallel approaches for calculating MST cost were taken by processing with the shared memory implementation using Open Multi-Processing (OpenMP), distributed memory implementation using Message Passing Interface (MPI) and *hybrid* implementation using both OpenMP and MPI. Distributed memory implementation and hybrid implementation programs were compiled and executed on Windows Compute Cluster Server 2003 with Microsoft Visual Studio 2008. *Execution time* was observed for each programming approach and *speedup* was shown against the sequential approach by other programming approaches.

Keywords: minimum spanning tree, multi-tasks, multiprocessing, OpenMP, MPI

Introduction

To create high-performance computing (HPC) clusters, the server is running with Microsoft Windows Server® 2003 x64 operating systems using a standard MPICH-based MPI library. Windows Compute Custer Sever (CCS) includes two components: the Windows Server 2003 Compute Cluster Edition Operating System and the Compute Cluster Pack (CCP). The CCP contains the necessary components to create server clusters, along with a job scheduler, MPICH, MPI library, and Microsoft Windows Remote Installation Services (RIS) extensions. Scalable parallel computing on PC clusters requires the use of a message passing system such as MPI, although

* Associate Professor and Head. Dr., Department of Computer Studies, National Management Degree College

OpenMP and other forms of thread-based parallelism may also be used on SMP nodes.

This paper presents a classic HPC development scenario centered around data parallelism, using Visual C++, OpenMP, MPI, Hybrid and Windows Server 2003 to develop high-performance, parallel solutions. Scientific computation is an obvious candidate for high-performance computing.

Parallel Implementation for finding MST with OpenMP

OpenMP is high-level approach for shared-memory parallel programming. Open Multi-Processing (OpenMP) is an open standard for platform-neutral parallel programming. OpenMP typically employs multi-threading for more efficient execution - this is certainly true on the Windows platform. OpenMP is easily enabled for Visual C++ in both Visual Studio 2005 and 2008. To use OpenMP, in any source code file, it is needed to include the header file <**omp.h**> as shown as the line code.

#include <omp.h>

So, every source code file in the application can use OpenMP. The following code is presented the data inputting which takes vertex_1, vertex_2 and their weights.

```
// Data Reading for v1, v2 and weight.
    #pragma omp parallel{
    #pragma omp for schedule (dynamic)
          for(count=0;count<edges;count++){   myFile>>v1>>v2>>weight;
           v1=((v1<1)?1:v1);          v1=((v1>vertices)?vertices:v1);
           v2=((v2<1)?1:v2);          v2=((v2>vertices)?vertices:v2);
           weight=((weight<=0)?0:weight);
           E[count].SetEdge(V[(v1-1)],V[(v2-1)],weight);
         }  }
```

The *#pragma omp parallel* pragma is inserted before the outermost loop. It is beneficial to insert the pragma at the outermost loop, since this

gives the most performance gain. The part of code is described to calculate minimum spanning tree problem by using Prim's algorithm.

```
#pragma omp for schedule (dynamic)
    for(i=0;i<vertices;i++){
        vertex_1[i]=0;   vertex_2[i]=0;
       edge_weights[i]=0;  }
```

The code of computation for the total cost (weights) of MST is also presented by using OpenMP.

```
// Calculation for resultant weights (cost).
#pragma omp parallel
{       #pragma omp for schedule (dynamic)
 for(count=0;count<(u_count-1);count++){
                    cost+=resultant_weights[count];
 if(count<(u_count-2))    cout<<resultant_weights[count]<<"+";
}}    cout<<resultant_weights[(count-1)]<<" =<<cost<<endl;
```

This code is written for showing processing time.

```
wtime = omp_get_wtime ( ) - wtime;
```

Parallel Implementation for finding MST with MPI

MPI (*Message Passing Interface*) is by far the most common approach for programming distributed-memory applications, given its flexibility, broad availability, and potential for high performance on a wide variety of hardware. MPI applications are thus run outside of Visual Studio using an MS-MPI command-line utility called *mpiexec*. This utility is responsible for launching the input matrix of the same program, one per socket/core. When combined with Windows HPC Server 2008, mpiexec launches processes across the cluster.

```
mpiexec -n 8 \\HNSERVER1\Apps\MPI_MST_Prim.exe
\\HNSERVER1\Apps\VEWeight10000.txt
\\HNSERVER1\Apps\outfile10000.txt
```

This tells mpiexec to launch **8 processors** of the cluster for MPI_MST_Prim.exe. In this MPI minimum spanning tree program, assume that the size of the matrix (edges) is divisible by the number of processes used. It will be distributed by rows across the processes (each process forming only those rows which it needs). The source code for this function is presented in the program, and some remarks are provided.

```
//Initializing the MPI program
        MPI_Init(&argc,&argv);
        MPI_Comm_rank(MPI_COMM_WORLD,&rank);
        MPI_Comm_size(MPI_COMM_WORLD,&numtasks);
        MPI_Status status;
        int cntloop=numtasks-1;// for loop processor
```

The following code is used for sending the size of edges to all processors.

MPI_Send(g, MAX_EDGES, structType, dest, tag, MPI_COMM_WORLD);

This code is used for receiving data from master node.

MPI_Recv(recv_g, MAX_EDGES, structType, source, tag, MPI_COMM_WORLD, &status);

Finally, the program terminates the MPI library with the following code.

MPI_Finalize();

Data sending and data receiving from other nodes are shown in figure 1.

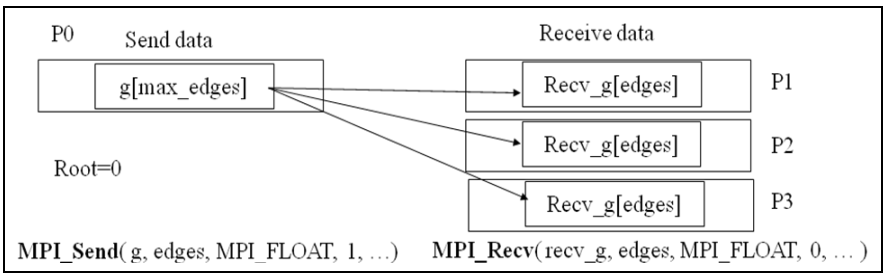

Figure 1. Data sending and data receiving from other nodes

Hybrid (OpenMP + MPI) Parallel Programming for Minimum Spanning Tree

The hybrid MPI-OpenMP model is a natural parallel programming paradigm for emerging parallel architectures. This section presents a hybrid implementation adapted for MST problems. Hybrid programming facilitates cooperative shared memory (OpenMP) programming across clustered SMP nodes because MPI facilitates communication among SMP nodes and OpenMP manages the workload on each SMP node. To use hybrid code (OpenMP + MPI), in any source code file, it is needed to include the header files <omp.h> and <mpi.h> as follows:

```
#include <omp.h>
#include <mpi.h>
```

To accomplish the algorithm presented, MPI functions, *MPI_ Send, and MPI_ Recv* are used as part of the Prim's algorithm. The source code for this function is written in the program for communication between nodes. To accomplish the algorithm is presented, ***OpenMP pragma Directives*** are used in the subpart of the algorithm. Then this program can be run with hybrid on the compute cluster.

The code "#pragma omp parallel" is used for **OpenMP.**

The following command function lines are to run the MPI Hybrid program on the compute cluster.

For no of processor =8;

```
mpiexec -hosts 1 HNSERVER1
1\\HNSERVER1\Apps\Hybrid_E_Alg.exe
\\HNSERVER1\Apps\VEWeight10000.txt \\HNSERVER1\Apps
```

For no of processor =12;

```
mpiexec -hosts 2 HNSERVER1 1 HNSERVER5 1
\\HNSERVER1\Apps\Hybrid_E_Alg.exe
\\HNSERVER1\Apps\VEWeight10000.txt \\HNSERVER1\Apps
```

For no of processor = 16;

```
mpiexec -hosts 2 HNSERVER1 1 HNSERVER6 1
\\HNSERVER1\Apps\Hybrid_E_Alg.exe
\\HNSERVER1\Apps\VEWeight10000.txt
\\HNSERVER1\Apps\outfile10000.txt
```

Results and Discussion

The problem of finding the minimum spanning tree using Prim's algorithm on the Head Node is considered. Most problem approaches for minimum spanning cost calculation are based on the computing over the input matrix such as no of vertices (V), no of edges (E) and their weights (W). As the matrix size (V, E) increases, more time consuming is needed. Calculation for minimum spanning cost is employed for the data-parallel processing approach to reduce the execution time. Both sequential implementation approach and parallel implementation approaches are described for minimum cost calculation by Prim's algorithm. The parallel approaches are adopted by processing with the shared memory implementation using OpenMP, the distributed memory implementation using MPI and the hybrid implementation with both OpenMP and MPI.

Table 1 shows the list of sample data-input (V, E, W). It is a medium scale size of vertices and edges (1000, 1000).

Table 1. Contents of data-input file

V1	V2	Weight
64	715	0.05034
64	837	0.05266
.	.	.
.	.	.
0	931	0.04934

When the program is run on the compute cluster node, it gets executing time for each data file included no of vertices and edges. No of vertices is 1000 for all inputted data files. Table 2 presents the results for executing time of C++ and parallel programming interfaces.

Table 2. Results for Executing Time of C++, OpenMP, MPI and Hybrid

No of Edges	Executing Time (s)			
	C++	OMP	MPI	Hybrid
1000	0.093	0.0804738	0.063834125	0.065665
2000	6.687	6.47852	**5.36243**	5.329765
3000	10.813	10.5888	**8.977629**	9.200348
4000	15.328	15.0385	13.8343556	13.27127
5000	19.391	18.9891	16.5705804	16.93961
6000	23.515	23.0529	20.460891	20.03564
7000	27.062	26.7239	24.7762099	23.48735
8433	32.562	32.126	30.5602206	29.08361

The relation between the time in second and the matrix size (edges) is shown in figure 2 for minimum spanning cost using Prim's algorithm by sequential (C++) and all parallel programming interfaces on the head node. A shared memory model such as OpenMP offers a more efficient parallelization strategy within an SMP node. The timing in Figure 5 demonstrates that the performance of parallel programming interfaces is superior to that of sequential (C++) for all the matrices tested here. The executing time of parallel programming interfaces is approximately 1.1 times faster than the sequential programming (C++) for all matrices sizes (edges). Here the hybrid is slower than other parallel programming (OpenMP and MPI) for no of edges 5000. But the hybrid is faster than other parallel programming for no of edges 6000 and above.

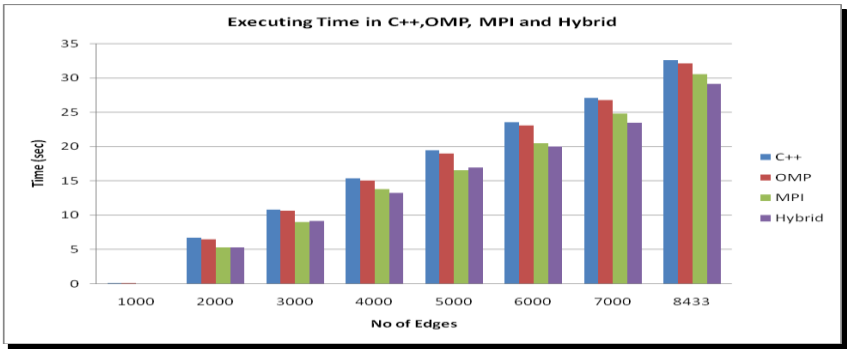

Figure 2. Comparison between executing time of C++, Open MP , MPI and Hybrid

Table 3 is described the Relation Between the **Speed Up** and Parallel Programming Interfaces on the Head Node with the Edges Size (1000 to 8433) for Computing MST Using Prim's Algorithm. The speedup depends on the efficiency of software, hardware and their application. In the proposed program of MST using Prim's algorithm on the head node, parallel programming (OpenMP) is approximately 1.1 times faster than sequential programming (C++), parallel programming (MPI) is approximately 1.2 times faster than sequential programming (C++). The hybrid parallel programming (OpenMP+MPI) is a bit faster than the parallel programming MPI.

Table 3. Relation between the **Speed Up** and Parallel Programming Interfaces on the Head Node with the Edges Size

Edges(1000-8433)	**C**	**OMP**	**MPI**	**HYBRID**
1000	1	1.15565563	1.456903844	1.4162796
2000	1	1.032180189	1.247009285	1.25465194
4000	1	1.01925059	1.107966315	1.15497613
6000	1	1.0200452	1.149265689	1.17365854
7000	1	1.012651597	1.092257456	1.15219469
8433	1	1.013571562	1.06550278	1.11959966

In order to Figure 3, parallel programming (OMP) is 1.15 times faster than sequential programming (C++), MPI is 1.45 times faster than C++ and Hybrid is 1.4 times faster than C++ for 1000 edges. When the no of edges is 2000, parallel programming (OMP) is 1.03 times faster than sequential programming (C++), MPI is 1.24 times faster than C++ and Hybrid is 1.25 times faster than C++.

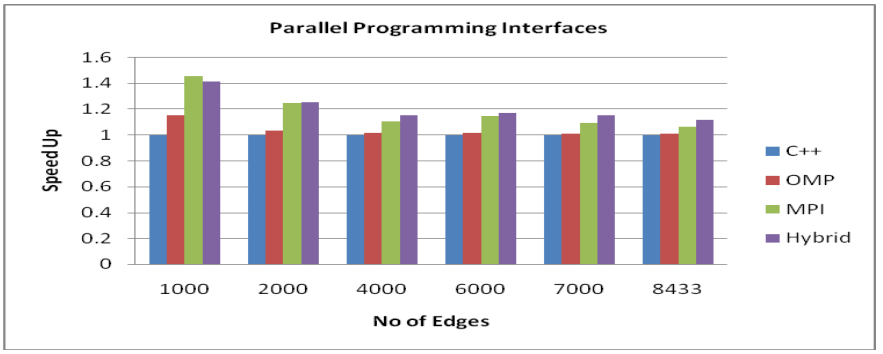

Figure 3. Relation Between the **Speed Up** and Parallel Programming Interfaces on the Head Node with the Vertices (1000) and Edges Size (1000 to 8433) for Computing MST Using Prim's Algorithm

For 8433 edges , parallel programming interfaces (OMP and MPI) are 1.01 and 1.06 times faster than C++. Then, Hybrid programming interfaces is only 1.12 times faster than sequential programming (C++). Communication (or network) latency is the time between sending and starting to receive data on a network link. Executing times for 1000 edges running on one processor and upto 16 processors is shown in Table 4.

Figure 4 is illustrated in Relation Between the **executing time** and Parallel Programming Interfaces on the Head Node with the Vertices and Edges Size (1000, 1000) for Computing MST Using Prim's Algorithm.

Table 4. Executing times for 1000 edges running on 1 to 16 processors

No of Processors	Time (s)
1	0.093
8	0.07969
10	0.077102
12	0.072994
16	0.044536

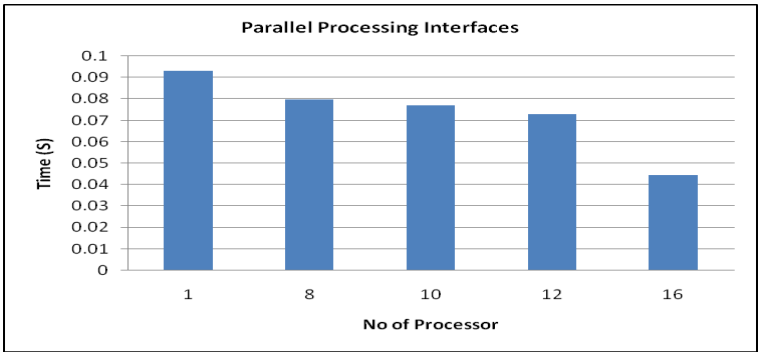

Figure 4. Relation Between the executing time and Parallel Programming Interfaces

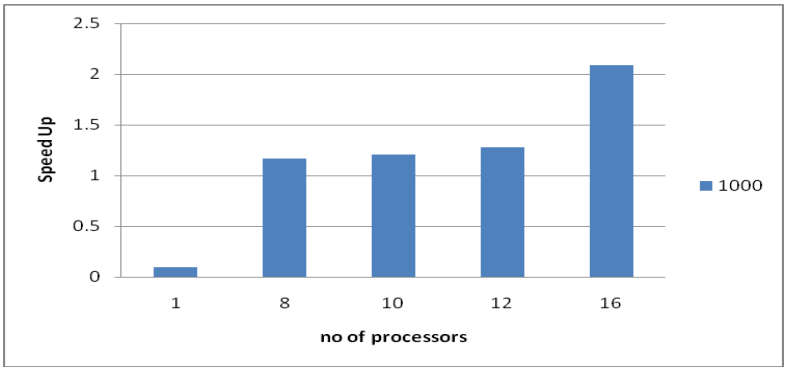

Figure 5. Speed Up of each processor finding MST cost for 1000 edges

In the proposed program of Prim's algorithm on the UY cluster with the matrix size (Vertices and edges) of (1000,1000), the processing time of parallel (MPI) by 12 CPUs is approximately 1.2 times faster than 1 CPUs, and by 16 CPUs is approximately 2.1 times faster than 1 CPUs. When the CPUs are more it can be seen that the speed up is a bit faster than one processor at the small scale size of matrix in Figure 5. The following data in table 5 is presented for a **large scale size** of vertices and edges (10000, 20000).

Table 5. contents of data-input file

V1	V2	Weight
0	1030	0.0187
0	1507	0.01714
…	…	…
1973	7450	0.00982
1973	7467	0.01228

The executing times are presented in the table 6 using sequential C++ and all parallel programming methods for the above inputting data that is no of vertices (10000) and no of edges (10000 to 13000).

Table 6. Result for executing times of C and all parallel programming methods

Edges	Executing Time (s)			
	C	OMP	MPI	HYBRID
10000	55.897	42.6392	33.25178	30.703861
11000	156.634	117.295	95.976544	39.7336
12000	265.381	195.593	161.92323	47.0589
13000	324.898	239.778	198.00992	56.9224

The timing in Figure 6 demonstrates that the performance of parallel programming interfaces is superior to that of sequential (C++) for all the

large scale matrices tested here. The executing time of all parallel programming interfaces is faster than the sequential programming (C++) for all matrices sizes (edges). The executing time of hybrid programming is the most faster than all programming interfaces in order to figure 6.

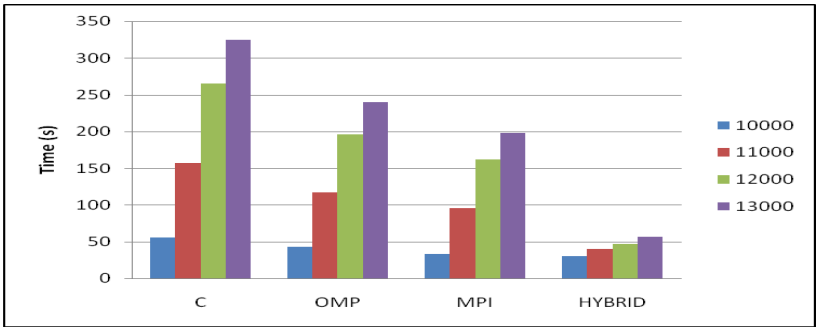

Figure 6. Comparison on execution time (s) taken by Sequential Version (C++) and all parallel programming methods among different edges sizes

The following table 7 is illustrated the Relation Between the **Speed Up** and Parallel Programming Interfaces on the Head Node with the Edges Size (10000 to 13000) for Computing MST Using Prim's Algorithm. In the proposed program of MST using Prim's algorithm for 10000 edges, parallel programming (OpenMP) is 1.31 times faster than sequential programming (C++), parallel programming (MPI) is 1.68 times faster than C++ programming. The hybrid parallel programming (OpenMP+MPI) is 1.82 times faster than C++. For 11000 edges and 12000 edges, the two parallel programming interfaces (OpenMP and MPI) are 1.33 and 1.63 times faster than sequential programming C++. It can be seen that the speed up of Hybrid programming is 5.63 times than C++ programming. Moreover the Hybrid parallel programming is 5.7 times faster than C++ programming at 13000 edges. So it can be seen that the speed up of parallel programming interfaces is faster than sequential programming at the large scale size of matrix (vertices, edges).

Table 7. Relation between the **Speed Up** and Parallel Programming Interfaces on the Head Node with the Edges Size

Edges (10000-13000)	**C**	**OMP**	**MPI**	**HYBRID**
10000	1	1.310929849	1.68102279	1.820520227
11000	1	1.33538514	1.63200292	3.942104415
12000	1	1.356802135	1.63893103	5.639337086
13000	1	1.354995037	1.64081677	**5.707735443**

Figure 7 presents the relation between the **speed up** and Parallel Programming Interfaces on the Head Node with the Vertices and Edges Size (10000, 13000).

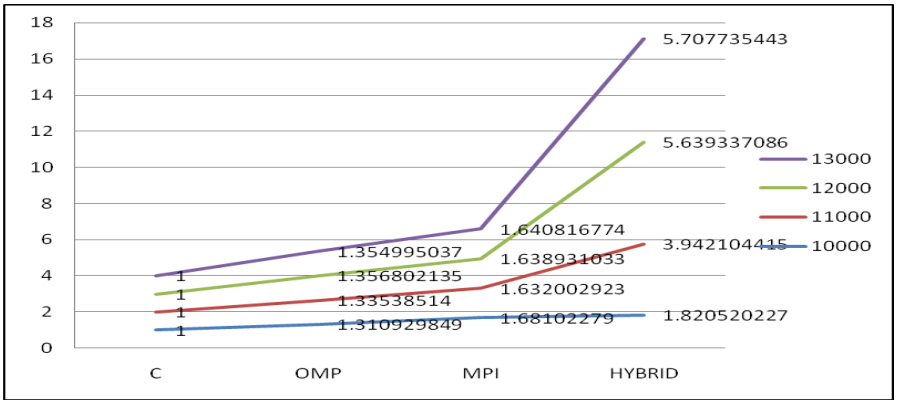

Figure 7. Relation between the ***Speed Up*** and Parallel Programming Interfaces on the Head Node

Conclusion

The efficiency of parallelization is affected by the type of parallel computers and the scale of a problem. The parallel approached for computing the cost of MST problems are processing using MPI and hybrid with both OpenMP and MPI.

The speedup depends on the efficiency of software, hardware and their application. For a medium scale size that is no of vertices and edges (1000, 1000), the executing time is ***1.2 times*** faster than one processor using

all parallelization methods by running on 12 Processors of the Dell® PowerEdge 2900 server Computer. The running time is ***2.1 times*** using hybrid programming on 16 processors. For a *large scale size* that is no of vertices and edges (10000, 13000), the executing time for MST algorithm is approximately ***5.7 times*** faster than one processor using Hybrid parallelization methods by running on 16 Processors on the Cluster.

When the matrix size (vertices and edges) is *large*, Hybrid parallel programming is more optimized to distribute and *less* memory implementation on each node. Thus, the highest speedup is achieved by hybrid for *large scale size* using OpenMP and MPI. Hybrid parallel programming is the *best method* and *highest speedup method* all of the parallel programming methods.

References

Joel Yliluoma, (2008), Guide into OpenMP, Easy multithreading programming for C++.

John Zollweg, (2009), Hybrid Programming with OpenMP and MPI, Introduction to Parallel Computing on Ranger based on material developed by Kent Milfeld, TACC, Cornell University Center for advanced Computing.

Myat Su Hlaing, (2012), Cluster Computing in Image Processing, Department of Computer Studies, Yangon University.

Pepper, R. and Mashayekhi, v., (2006), *Deploying Microsoft Windows Compute Cluster Server 2003*, Dell Power Solutions.

Quinn, J. M., (2004), *Parallel Programming in C with MPI and OpenMP*, McGraw-Hill Professional, ISBN 0072822562.

Shahzad,M.T., (2004), *C++ Program to implement the Prim's Algorithm to solve Minimum Spanning Tree Problem,* Government College University Lahore, Pakistan.

Than Than Wai,(2009), Parallel Computing Based On Cluster Computer By Using OpenMP And MPI, Myat Su Hlaing, *Universities Research Journal*,Vol.2, No.3, Page 385-398.

Feature Extraction Enhancement in Voice Recognition SMS Messaging System

Htet Yi Zaw[1], Wint Pa Pa Kyaw[2] & Khin Myo Sett[3]

Abstract

Voice recognition SMS messaging system is the mobile application with the process of writing hand-free SMS (Short Message Service) by dictating human voice to readable text. This paper describes the techniques to improve the accuracy of voice recognition SMS messaging system using Mel Frequency Cepstral Coefficients (MFCC). The main part of the system is the feature analysis of input acoustic signal. Feature extraction plays an important role in the performance and robustness of the voice recognition system. The purpose of this development is to benefit of both human voice recognition and easier and faster use of mobile devices by reducing typing time. Smart phone SMS messaging system will be completely based on voice recognition system.

Keywords: Feature extraction, MFCC, voice recognition, speech recognition, voice SMS

Introduction

Voice is the common form of communication method for people to interact with each other. As writing text by voice in SMS messaging with smart phone is faster than using keyboard, so people will prefer such system.

Voice recognition or speech recognition system can be classified in several different types by describing the type of voice utterance, type of speaker model and type of vocabulary that they have the ability to recognize. There are basically three types of speech recognition according to what types of utterance those are isolated speech recognition (ISR), continuous speech recognition (CSR) and spontaneous speech recognition (SSR). Isolated speech recognition usually requires each spoken word to have quiet on both side of the sample window. It accepts single word at a time. Continuous speech recognition consists of continuous utterance which

[1] Demonstrator, Department of Computer Studies, University of Mandalay

[2] Associate Professor, Dr. Department of Computer Studies, University of Yangon

[3] Professor (Head), Dr. Department of Computer Studies, University of Mandalay

is representative of real speech. Spontaneous speech is the type of speech recognition which is natural sounding and is not rehearsed. And then speech recognition is broadly into two main categories based on speaker models namely speaker dependent and speaker independent. The former systems are designed for a specific speaker and the latter are designed for variety of speaker. Speech recognition can generally function more efficiently with a small vocabulary size. As the number of words that need to be recognized increases, the amount of confusion and percentage of error can also increase.

The final result of voice recognition is the recognized words, as for applications such as voice dialing, call routing, simple data entry (e.g., entering a credit card number), preparation of structured documents (e.g., radiology report), voice to text processing. They can also serve as the input to further linguistic processing in order to achieve speech understanding. A voice recognition system involves several procedures in which signal modeling or what is known as feature extraction and classification are typically important. The process of feature extraction method transforms the input speech signal to the number of parameters. Feature extraction is a crucial step of the voice recognition process. The most commonly used feature extraction method is Mel Frequency Cepstral Coefficients (MFCC). The aim of this study is to apply MFCC algorithm in voice recognition SMS messaging system. This research will lead to the increasing need to develop a robust and accuracy of voice recognition system with MFCC features extraction algorithm.

After a brief introduction of voice recognition system, about the general architecture of voice recognition system is described and explained the step-by-step computation of Mel Frequency Cepstral Coefficients (MFCC) algorithm in detail are discussed. The implementation of voice recognition SMS messaging system and this result are displayed in final section. In conclusion, voice recognition SMS messaging system for Myanmar language have to develop to continue this research.

Overview of Voice Recognition System

The voice recognition system consists of two main parts. The first part is the processing acoustic signal which is captured by a microphone from smart phone. The second part is for interpreting processed signal to words. Generally, feature extraction, acoustics modeling, language

modeling and pronunciation dictionary are used to construct the voice recognition system.

In the voice recognition process, analog speech signal must first be digitized. The speech signal is analyzed in the intervals. The period of the interval is typically 20ms. This interval is considered the signal stationery support. The speech feature extraction of speech characteristics includes the formation of equal space discrete vectors. From the training database features vectors are used to estimate parameters of the acoustic model. Acoustic Model is used to establish the connection between the acoustic information and phonetics. Pronunciation dictionary is used to map words to their corresponding phonemes. Language model is used to figure out a speech recognizer how likely a word sequence is independent of the acoustics. The language model tries to capture the rules of a language and to predict the next word in a speech sequence by using the statistical information from different texts.

The preprocessing and feature extraction stages of a pattern recognition system serves as an interface between the real world and a classifier operating on an idealized model of reality. Firstly, Mel Frequency Cepstral Coefficients (MFCC) algorithm will be used to implement feature extraction process in which speech features are extracted for all the speech samples. Then all these features are given to pattern trainer for training and are trained by Hidden Markov Model (HMM) to create HMM model for each word.

Then HMM is used to find the log likelihood of entire speech samples. In recognition this likelihood is used to recognize the spoken word. After recognizing process, words are composed to get the sentence in text. Language model helps a speech recognizer figure out how likely a word sequence is independent of the acoustics. N-gram language model is used to find correct word sequence by predicting likelihood of the nth word, using the n-1 earlier words. The general architecture of the voice recognition system is shown in figure 1.

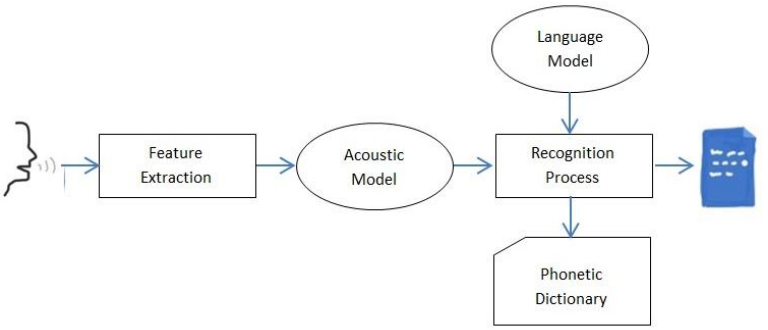

Figure 1. Architecture of Voice Recognition System

Mel Frequency Cepstral Coefficients for Feature Extraction

Mel Frequency Cepstral Coefficients (MFCC) algorithm is generally preferred as a feature extraction technique to perform voice recognition as it involves generation of coefficients from the voice of the user that are unique to every user. Human frequency bandwidth was important to hear from us. MFCC is based on the known variation of this. It uses to capture the important characteristics of speech. And then Mel frequency scale has a simple calculation, good ability of the distinction, anti-noise and other advantages. However, MFCC is the robust technique for feature extraction in clean speech or clean environment. Therefore, MFCC is the most suitable method for voice recognition SMS messaging system. The following is the feature extraction procedure of Mel Frequency Cepstral Coefficients (MFCC) algorithm.

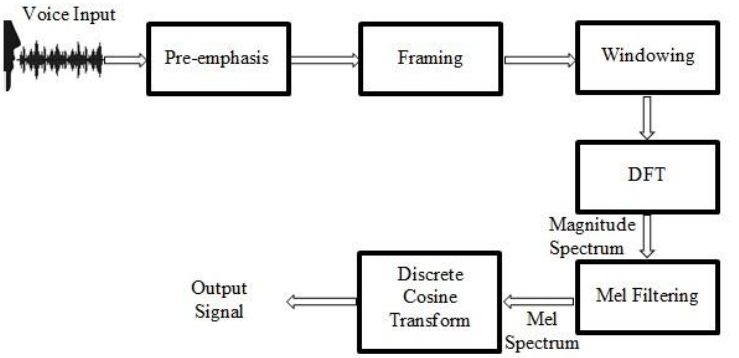

Figure 2. MFCC Block Diagram

As shown in Figure 2, MFCC consists of six computational steps. Each step has its function and mathematical approaches as discussed briefly in the following:

Pre-emphasis

In this step, the signal spectrums are pre-emphasized. Pre-emphasis allows cracking down for compensating part of the high-frequency during the human's voice production mechanism. The speech signal x(n) is sent to a high-pass filter :

$$y(n) = x(n) - a * x(n - 1) \quad (1)$$

y(n) is the output signal. The value of a is usually between 0.9 and 1.0. The Z transform of this equation is given by:

$$H(z) = 1 - a * z^{-1} \quad (2)$$

H(z) = high-frequency formants

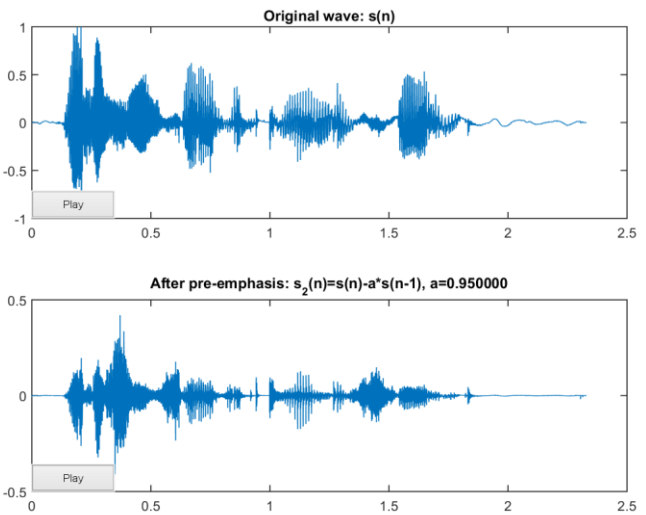

Figure 3. Effect of Pre-emphasis

Framing

The speech signal is normally divided into small duration blocks, called frames, and the spectral analysis is carried out on these frames. Because of the human speech signal is slowly time varying and can be treated as a quasi-stationary process. The input of the speech signal with the

50% of the size of the frame to the age of 15 ~ 20ms frame is segmented. If sample rate of 16 kHz and 256 sample points of frame size, then the frame duration is

$$256/16000 = 0.016 \text{ sec} = 16 \text{ ms} \quad (3)$$

The frame size, 256 sample points will become 128 points because of the 50% overlap. Overlapping is used to produce continuity within frames. Then the frame rate is

$$16000/(256-128) = 125 \text{ frames per second} \quad (4)$$

Windowing

After framing, each frame is multiplied by a window function prior to reduce the effect of discontinuity of the first and last points in the frame. Hamming window is commonly used, it decreases the frequency resolution of the spectral analysis while reducing the side lobe level of the window transfer function $y(n) = x(n) * w(n)$.

Hamming window is used for voice recognition task as:

$$w(n) = 0.54 - 0.46 * \cos(2\pi n/(N-1)) \text{ , where } 0 \leq n \leq N-1 \quad (5)$$

Different values of correspond to different curves for the hamming windows shown in figure 4:

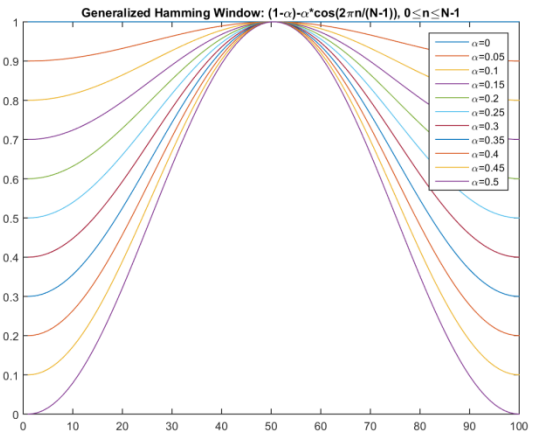

Figure 4. Hamming Window

Spectral Estimation

Spectral estimation is computing for each frame by applying Discrete Fourier Transform (DFT) to produce spectral coefficients. These coefficients are complex numbers comprising the two magnitude and phase information. Phase information is usually removed and only the magnitudes of the spectral coefficients are extracted. DFT can be defined as:

$$X(k) = \sum_{n=0}^{N-1} y(n) e^{-j\frac{2\pi}{N}} \qquad 0 \leq n, k \geq N-1 \qquad (6)$$

where *X(k)* are the spectral coefficients, and *y(n)* the framed speech signal

Mel Filtering

A group of triangle band pass filters that simulate the characteristics of the human's ear are applied to the spectrum of the speech signal. For Mel- scaling mapping is need to done among the given real frequency scales (Hz) and the perceived frequency scale (Mels). The frequency resolution is high in the low frequency region and low in the high frequency region. The Mel frequency is computed from the linear frequency as:

$$f_M = 2525 \times \log(1 + \frac{f}{7}) \qquad (7)$$

where f_M is the Mel frequency for the linear frequency *f*. The filter bank energy is obtained after Mel filtering.

$$E_i^X = \sum_{k-1}^{N} |X(k)|^2 . \ \psi_i(k) \qquad (8)$$

where |X(k)| is the amplitude spectrum, k is the frequency index, ψ_i are the i^{th} Mel band pass filter, $1 \leq i \leq M$, and M is number of Mel-scaled triangular band-pass filters E_i^X is the filter bank energy. The relationship between the mel and the linear frequencies is shown in figure 5:

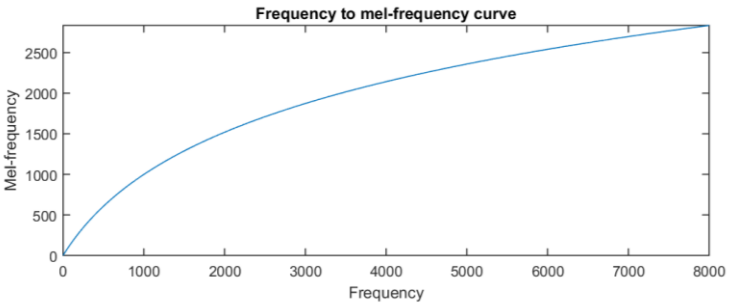

Figure 5. Mel Filtering

Discrete cosine Transform

The higher order coefficients represent the periodicity in the waveform**.** The lower order coefficients represent the smooth spectral shape. DCT can be defined as:

$$C_i^X = \sum_{i-1}^{M} \log(E_i^X)\, C\left[l.\frac{(2i-1)\pi}{2M}\right] \qquad (9)$$

In voice recognition systems, only the lower order coefficients (order<20) are being used, thus a dimension reduction is achieved. Another advantage of DCT is that the created cepstral coefficients are less correlated compared to log Mel filter bank coefficients.

Implementation of Voice Recognition SMS Messaging System

The implementation of the voice recognition SMS messaging system was based upon to generate voice to readable text on speaker independent recognition in SMS messaging system. Mel Frequency Cepstral Coefficients (MFCC) feature extraction technique was emphasized on this study. The main process of this system is to extract speech that is spoken by different speaker with applying MFCC algorithm. And then the extracted features are given to pattern trainer for training and are trained by Hidden Markov Model (HMM) to create HMM model for each word.

Main Activity Class of the Voice Recognition SMS Messaging System

In AndroidManifest.xml file, MainActivity.java is launched for starting. To use the speech recognizer, RecognizerIntent component from speech library must be imported. onCreate() method is called after starting the activity. Firstly, setContentView (R.layout.activity_main) is used to show the user interface view. The user interface is defined in res>layout>activity_main.xml. Voice recognition activity is started when the user pressing on the button. Then askSpeechInput() function is starting to launch. The process of onCreate() method is shown in the following code segment.

```
protected void onCreate(Bundle savedInstanceState) {
    super.onCreate(savedInstanceState);
    setContentView(R.layout.activity_main);
    voiceInput = (EditText) findViewById(R.id.sms_message);
    speakButton = (TextView) findViewById(R.id.btnSpeak);
    speakVoice = (ImageButton)
findViewById(R.id.voice_icon);
    speakVoice.setOnClickListener(new View.OnClickListener()
{
        public void onClick(View v) {
           askSpeechInput();
        }
    });
    checkForSmsPermission();
}
```

The process of askSpeechInput() function is shown in the following code segment.

```
private void askSpeechInput() {
    Intent intent = new
Intent(RecognizerIntent.ACTION_RECOGNIZE_SPEECH);
    intent.putExtra(RecognizerIntent.EXTRA_LANGUAGE_MODEL,
            RecognizerIntent.LANGUAGE_MODEL_FREE_FORM);
    intent.putExtra(RecognizerIntent.EXTRA_LANGUAGE,
Locale.getDefault());
    intent.putExtra(RecognizerIntent.EXTRA_PROMPT,"Speak
Something");
}
```

The input voice is recognized and the results of recognized text is sent back to voice SMS messaging system by calling the onActivityResult() callback. As the results of the voice recognition, the recognized text of the input spoken information is displayed in sms_message EditTextBox. The process of onActivityResult() function is shown in the following code segment.

```
protected void onActivityResult(int requestCode, int resultCode,
Intent data) {
    super.onActivityResult(requestCode, resultCode, data);
    switch (requestCode) {
        case REQ_CODE_SPEECH_INPUT: {
            if (resultCode == RESULT_OK && null != data) {
                ArrayList<String> result = data

.getStringArrayListExtra(RecognizerIntent.EXTRA_RESULTS);
                voiceInput.setText(result.get(0));
            }
            break;
        }
    }
}
```

XML Files of the Voice Recognition SMS Messaging System

The user interface view is created in activity_main.xml file. On mobile devices, Installing and launching applications are caused of AndroidManifest.xml. Every application must have an AndroidManifest.xml file in its root directory. The information about the android application is stored in the manifest. The system information must have in the manifest before it can run any code. It defines the activities required for the application and approval. There are restrictions that prevent access to some of data or code on mobile device. Permissions are used to remove the limit. For sending and receiving messages, SMS permission is called in AndroidManifest.xml file. Permissions are:

- android.permission.SEND_SMS.
- android.permission.RECEIVE_SMS.

The process of using permission for sending and receiving messages is the following code segment.

```
<uses-permission android:name="android.permission.SEND_SMS" />
<uses-permission android:name="android.permission.RECEIVE_SMS" />
```

The below code segment is SMS receiver to receive message in AndroidManifest.xml.

```
<receiver
    android:name="com.example.lenovo.voicesms.MySmsReceiver"
    android:enabled="true"
    android:exported="true">
    <intent-filter>
        <action
android:name="android.provider.Telephony.SMS_RECEIVED"/>
```

Results and Discussion

Voice SMS messaging system records the input spoken voice information of user and changes as text message. And then send this text as SMS message. When the user open Voice SMS application on mobile phone, user can see the microphone icon button which initiate voice recording process. User can input speech by pressing microphone button. Voice recognition process starts when communicate with Google's server by sending blocks of voice signal. The received speech signal is recognized on server. After the voice recognition process is done, the recognized text of input voice spoken information can be seen in SMS text box. User can customize these text messages. User can also write phone number in the contact textbox or can easily add contact number form the contact list on which message will be sent after pressing the send button.

The interface of voice recognition SMS messaging system is shown in figure 6.

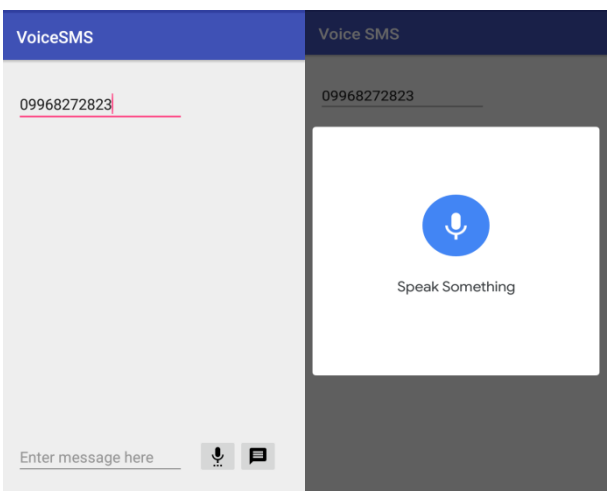

Figure 6. Voice SMS Messaging System

Conclusion

Voice recognition systems have been recently used in wide varieties of real applications especially after the enormous technological revolution where smart-phone within the reach of everyone. MFCC feature extraction techniques affect the accuracy of the voice recognition systems. Therefore, this voice SMS messaging system give easily and reducing typing time for user with more accurate result. But Myanmar language is not enriched with speech recognizers. In future, voice recognition SMS messaging system for Myanmar language can be developed on android platform to continue this research.

References

A. Majeed, H. Husain, S. A. Samad, and T. F. Idbeaa. *et al*, (2015, September), "Mel Frequency Cepstral Coefficients (MFCC) Feature Extraction Enhancement in the Application of Speech Recognition: A Comparative Study", Journal of Theoretical and Applied Information Technology, Volume 79, No. 1, September 2015, pp- 38-56, ISSN: 1992-8645, E-ISSN: 1817-3195.

S. Gupta, J. Jaafar, W. F. wan Ahmad, and A. Bansal, (August, 2013), "Feature Extraction Using MFCC", Signal and Image Processing: An International Journal (SIPIJ), Vol.4, No.4, August 2013, pp-101-108,DOI : 10.5121/ sipij.2013.4408

S. Primorac and M. Russo, (2012, May), "Android application for sending SMS messages with speech recognition interface," MIPRO, Opatija, Croatia, pp-2186-2190.

Z. Z. Tun, and G. Srijuntongsiri, (2016, May), "A Speech Recognition System for Myanmar Digits," International journal of information and electronics engineering, vol. 6, no. 3, pp. 210–213, 2016.

https://github.com/StackTipsLab/Android-Speech-to-Text-Example

http://practicalcryptography.com/miscellaneous/machine-learning/guide-mel-frequency-cepstral-coefficients-mfccs/

http://stacktips.com/tutorials/android/speech-to-text-in-android

Numerical Integration in Parallel by Cloud Computing

May Myint Thwe*

Abstract

Numerical solution techniques and the construction of mathematical models require a huge number of computing resources to perform large scale experiments or to cut down the computational complexity into a reasonable time frame. These needs have been initially addressed with dedicated high-performance computing (HPC) infrastructures such as clusters. Infrastructure services (Infrastructure-as-a-service, IaaS) offered by Cloud providers, allow any user to provision a large number of compute instances fairly easily. Whether leased from public Clouds or allocated from private Clouds, utilizing these virtual resources to perform data/compute intensive analyses requires employing different parallel or high performance computing (HPC) runtimes to implement such applications. Multi-dimensional Numerical Integration needs extra compute power and therefore is a good scientific application to be run in parallel on the HPC cluster installed in IaaS virtual machines (VMs) on the cloud. This paper is concerned with the calculation of numerical integrations in parallel for faster calculation time and better performance on a virtualized HPC cluster on the cloud. Numerical Methods in engineering may be implemented well using Excel/VBA(Visual Basic Application). VBA is the tool to develop programs that control Excel.

Keywords: Numerical Integration, High- Performance Computing, Parallel Processing, Cloud Computing, Virtual Machines.

Introduction

Scientific computing involves the construction of mathematical models and numerical solution techniques to solve scientific, social scientific and engineering problems. It requires the availability of a massive number of computers to perform large scale experiments. Traditionally, these needs have been addressed by using high-performance computing (HPC) solutions and installed facilities such as clusters and super computers. Cloud computing provides scientists with a completely new model of utilizing the computing infrastructure.[6] Cloud is a parallel and distributed computing system consisting of a collection of inter-connected and virtualized computers that are dynamically provisioned and presented

* Associate Professor, Department of Computer Studies, Yadanabon University

as one or more unified computing resources.[2] To get the faster calculation and good ability of a system, cloud computing is very useful. Cloud infrastructure services allow users to provision compute clusters fairly easily and quickly. IaaS refers to the practice of delivering IT infrastructure based on virtual resources as a commodity to customers. Utilizing cloud virtual resources to perform data or computing intensive analyses requires employing different parallel or HPC runtimes.

Multi-dimensional Integration is a scientific application to be run in parallel on the HPC cluster installed in IaaS virtual machines (VMs) on the cloud because it needs extra computing power. This work is parallel processing of numerical integrations for faster calculation time and better performance on a virtualized HPC cluster with Excel VBA on the cloud. It also implements Excel 2010 workbook calculation of Numerical Integration in Windows HPC Server 2008 R2 by using HPC on cloud VMs. Numerical Methods in engineering may be implemented well using Excel/VBA.[3]

High Performance Computing(HPC) with Clouds

HPC is the use of parallel processing for running advanced application programs efficiently, reliably and quickly. HPC uses supercomputers and computer clusters to solve advanced computation problems. The application and the data both need to be moved to the available computational resource in order for them to be executed. These infrastructures are highly efficient in performing compute intensive data movement.[7]

Cloud computing is the latest and perhaps the most dramatic trend in advanced computing paradigms since the introduction of commodity clusters, which have dominated HPC for more than a decade. Clouds offer an amorphous distributed environment of computing resources and services to a dynamic distributed user base. Like clusters, cloud computing exploits economies of scale to deliver advanced capabilities. Unlike clusters, cloud resources are nonspecific and provide basic capabilities.[7]

The Concepts of Cloud Computing

Cloud computing is considered the evolution of a variety of technologies that have come together to change an approach for building the IT infrastructure. The Internet is a necessary foundation for the cloud. The cloud can be both software and infrastructure. It can be an application to

access through the Web or a server and it can be also an IT infrastructure that can be used as per user's request. The cloud services can be categorized into software services and infrastructure or hardware services.[4]

Cloud Deployment Models

A deployment model defines the purpose of the cloud and the nature of how the cloud is located.[5] As shown in Figure 1, public cloud, private cloud, hybrid cloud and community cloud are four deployment models.

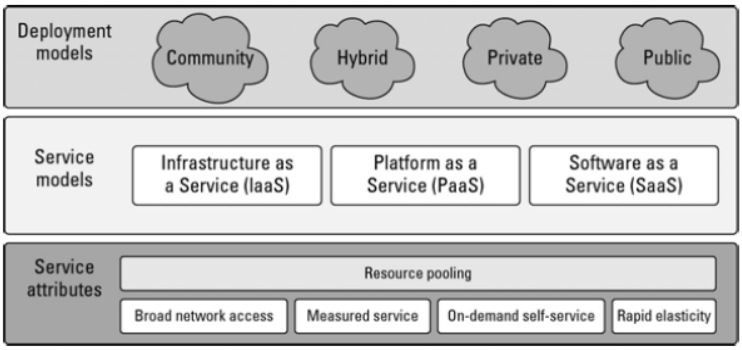

Figure 1. Cloud deployment models.

The public cloud infrastructure is available for public use alternatively for a large industry group and is owned by an organization selling cloud services. *The private cloud infrastructure* is operated for the exclusive use of an organization. The cloud may be managed by that organization or a third party. Private clouds may be either on- or off-premises. *A hybrid cloud* combines multiple clouds (private, community of public) where those clouds retain their unique identities, but are bound together as a unit. A hybrid cloud may offer standardized or proprietary access to data and applications, as well as application portability. *A community cloud* is one where the cloud has been organized to serve a common function or purpose. It may be for one organization or for several organizations, but they share common concerns such as their mission, policies, security, regulatory compliance needs, and so on. A community cloud may be managed by the constituent organization(s) or by a third party.[5]

Cloud Computing Services Offering

Cloud computing is typically divided into three levels of service offerings: Infrastructure as a Service (IaaS), Platform as a Service (PaaS),

and Software as a Service (SaaS).

Software as a Service **(SaaS):** Applications delivered to end users running from the provider's infrastructure. SaaS is used by business users for email, office automation, customer relationship management, business intelligence, enterprise resource planning and other related scenarios.

Platform as a Service **(PaaS):** Used by developers and application providers as a computing platform that typically includes operating system, programming language execution environment, database and web services.

Infrastructure as a Service **(IaaS):** IaaS is the foundational cloud platform layer. It is used by IT administrators for the provisioning of processing, storage, networks or other fundamental computer resources where users can run arbitrary software. Examples are GoGrid, Amazon's EC2 and S3.

Exploring the Cloud Computing Stack

Cloud architecture can couple software running on virtualized hardware in multiple locations to provide an on-demand service to user-facing hardware and software. Many descriptions of cloud computing describes it in terms of two architectural layers: A client as a front end. The "cloud" as a back end. Each of these two components is composed of several component layers, complementary functionalities, and a mixture of standard and proprietary protocols. A cloud can be created within an organization's own infrastructure or outsourced to another datacenter. While resources in a cloud can be real physical resources, more often they are virtualized resources because virtualized resources are easier to modify and optimize. A compute cloud requires virtualized storage to support the staging and storage of data.

The idea of Virtualization

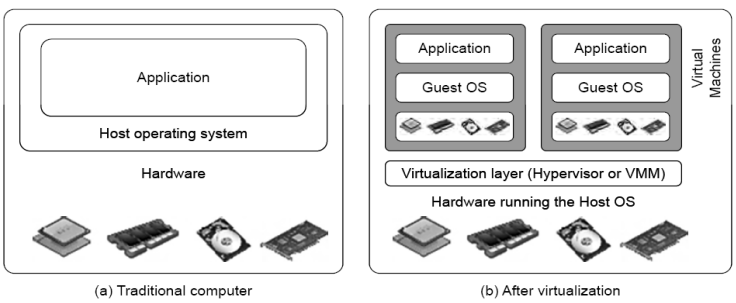

Figure 2.(a) Traditional computer Figure 2.(b) After virtualization

The idea of virtualizing a computer system's resources, including processors, memory, and I/O devices, has been well established for decades, aiming at improving sharing and utilization of computer systems. As shown in Figure 2(a) and 2(b), hardware virtualization allows running multiple operating systems and software stacks on a single physical platform. A software layer, the virtual machine monitor (VMM) mediates access to the physical hardware presenting to each guest OS a VM.

Hardware Requirements

Hyper-V requires a 64-bit processor that includes the following. Hardware-assisted virtualization is available in processors that include virtualization option_specifically processors with Intel Virtualization Technology (Intel VT) or AMD Virtualization (AMD-V) technology. Hardware-enforced Data Execution Prevention (DEP) must be available and enabled. Specifically, Intel XD bit or AMD NX bit must be enabled.

Software Requirements

Hyper-V includes a software package for supported guest operating systems that improves integration between the physical computer and the virtual machine. This package is referred to as integration services. Supported Windows Guest OS for Hyper-V in Windows Server 2008 R2 and Windows 8.1.

Implementation of Virtualized HPC Cluster

As shown in Figure 3, a virtualized HPC cluster composed of one head node, one broker node and three compute nodes was deployed on DELL Inspiron 14R laptop computer. VMM (Hyper V Manager; Version: 6.3) enables Windows 8(Version 8.1) and Windows HPC Server 2008 R2 operating system (OS).

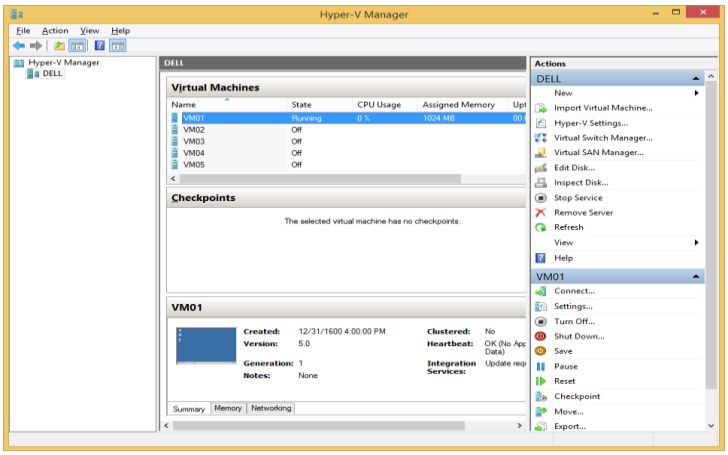

Figure 3. Virtualized HPC Cluster

Numerical Integration

Numerical methods are involved in almost every aspect of engineering. The solution of scientific and engineering problems sometimes requires integration of an expression. It may be difficult or even impossible to obtain an expression for the integral of a particular function. But by using numerical methods, a value for the definite integral can always be obtained.[1]

Numerical calculation for Fresnel Transform

Let $V_0(s, t)$ be the electromagnetic field on a point (p, q, z = 0) on a plane z = 0 and V(x, y, z) the electromagnetic field on point (x, y, z) as shown in Figure 4.

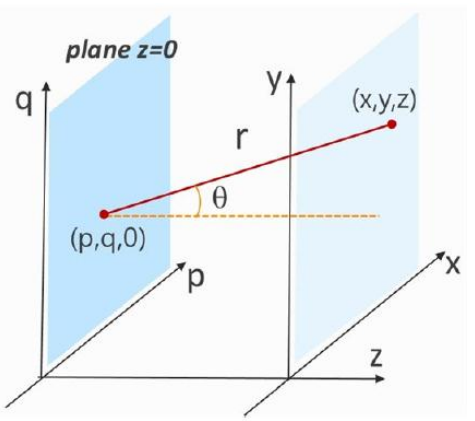

Figure 4. The electromagnetic field on point (x, y, z)

At distance z >> λ, the electromagnetic field V(x, y, z) is described with good approximation through the Fresnel transform:

$$V(x,y,z) = \iint V_0(p,q)e^{ikr}e^{\frac{i\pi}{\lambda z}((x-p)^2+(y-q)^2)}dpdq \qquad (1)$$

where $\cos\theta = \frac{z}{r}$; $r = [(x-p)^2 + (y-q)^2 + z^2]^{1/2}$; i is the imaginary unit.

By substitution of Euler's formula

$$e^{ikr} = \cos kr + i\ \sin kr$$

In Equation 1, the electromagnetic pattern V(x, y, z) on a plane (x, y, z) composed of real part and imaginary part:

$$V(x,y,z) = \iint V_0(p,q)(\cos kr + i\sin kr)\left[\cos\frac{\pi}{\lambda z}((x-p)^2+(y-q)^2) + i\sin\frac{\pi}{\lambda z}((x-p)^2+(y-q)^2)\right]dpdq \qquad (2)$$

$$Re(x,y,z) = \iint V_0(p,q)(\cos\ kr)\ \times\ (\cos\ \frac{\pi}{\lambda z}[(x-p)^2+(y-q)^2])\ dpdq$$

$$\mathrm{Im(x,y,z)} = \mathrm{i}\iint \mathrm{V_0(p,q)(\sin\ kr)} \times \left(\sin\frac{\pi}{\lambda \mathrm{z}}[\mathrm{(x-p)^2} + \mathrm{(y-q)^2}]\right)\ \mathrm{dpdq} \qquad (3)$$

In plane (p, q, z = 0) and in plane (x, y, z), consider a segment L_p centered around the p axis and L_q centered around the q axis, a segment X_m centered around the x axis and Y_n centered around the y axis. Consider N_p as the number of samples in the p axis, N_q as the number of samples in the q axis, N_m as the number of samples in the x axis, and N_n as the number of samples in the y axis.

$$V(x,y,z) = \iint V_0(p,q)(\cos kr + i\sin kr)\,[\,(\cos\frac{\pi}{\lambda z}[(x-p)^2+(y-q)^2]) + i\left(\sin\frac{\pi}{\lambda z}[(x-p)^2+(y-q)^2]\right)]dpdq$$

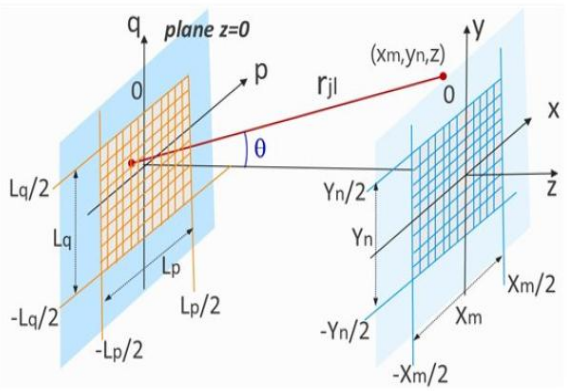

Figure 5. Sampling intervals on two planes

From the above Figure 5, the sampling intervals and the relative ranges

$$\Delta p = \frac{L_p}{N_p}\ ;\ j = -\frac{N_p}{2}, \dots, -1, 0, +1, \dots, \frac{N_p}{2}\ ; p_j = j\Delta p$$

$$\Delta q = \frac{L_q}{N_q}\ ;\ l = -\frac{N_q}{2}, \dots, -1, 0, +1, \dots, \frac{N_q}{2}\ ; q_l = l\Delta q$$

$$\Delta x = \frac{L_x}{N_x}\ ;\ m = -\frac{N_x}{2}, \dots, -1, 0, +1, \dots, \frac{N_x}{2}\ ; x_m = m\Delta x$$

$$\Delta y = \frac{L_y}{N_y}\ ;\ j = -\frac{N_y}{2}, \dots, -1, 0, +1, \dots, \frac{N_y}{2}\ ; y_n = n\Delta y \qquad (4)$$

In equation 4, there are the values such as Δp, Δq, Δx and Δy.

Δp: it is distance between two adjacency samples along the p axis.

Δq: it is distance between two adjacency samples along the q axis.

Δx: it is distance between two adjacency samples along the x axis.

Δy: it is distance between two adjacency samples along the y axis.

The distance r_{jl} between the sample (p_j, q_l, z = 0) and the sample (x_m, y_n, z) is shown in Equation 5:

$$r_{jl} = \left[\left(x_m - p_j\right)^2 + (y_n - q_l)^2 + z^2\right]^{1/2} \quad (5)$$

The discrete expressions for real and imaginary part of electromagnetic field are shown in the Equation (6) and (7);

$$R_e(x_m, y_n, z) = \sum_{l=-\frac{N_q}{2}}^{\frac{N_q}{2}} \sum_{j=-\frac{N_p}{2}}^{\frac{N_p}{2}} V_0\left(p_j, q_l\right)\left(\cos kr_{jl}\right) \times \left(\cos\frac{\pi}{\lambda z}\left[\left(\left((m\Delta x) - (j\Delta p)\right)^2 + \left((n\Delta y) - (l\Delta q)\right)^2\right)\right]\right)\Delta p\Delta q \quad (6)$$

$$I_m(x_m, y_n, z) = \sum_{l=-\frac{N_q}{2}}^{\frac{N_q}{2}} \sum_{j=-\frac{N_p}{2}}^{\frac{N_p}{2}} V_0\left(p_j, q_l\right)\left(\sin kr_{jl}\right) \times \left(\sin\frac{\pi}{\lambda z}\left[\left(\left((m\Delta x) - (j\Delta p)\right)^2 + \left((n\Delta y) - (l\Delta q)\right)^2\right)\right]\right)\Delta p\Delta q \quad (7)$$

The intensity I(x_m, y_n, z) of electromagnetic field is equal to the square of module of electromagnetic field V(x_m, y_n, z) ,

$$\mathrm{I}(\mathrm{x_m}, \mathrm{y_n}, \mathrm{z}) = \mathrm{Re}\ (\mathrm{x_m}, \mathrm{y_n}, \mathrm{z})^2 + \mathrm{Im}\ (\mathrm{x_m}, \mathrm{y_n}, \mathrm{z})^2 \quad (8)$$

The above equation (8) is the discrete expression of electromagnetic intensity.

Experimental Results on Virtualized HPC Cluster of Cloud

To evaluate the performance, the results for running many times with same input data but with different number of HPC cores are as follows;

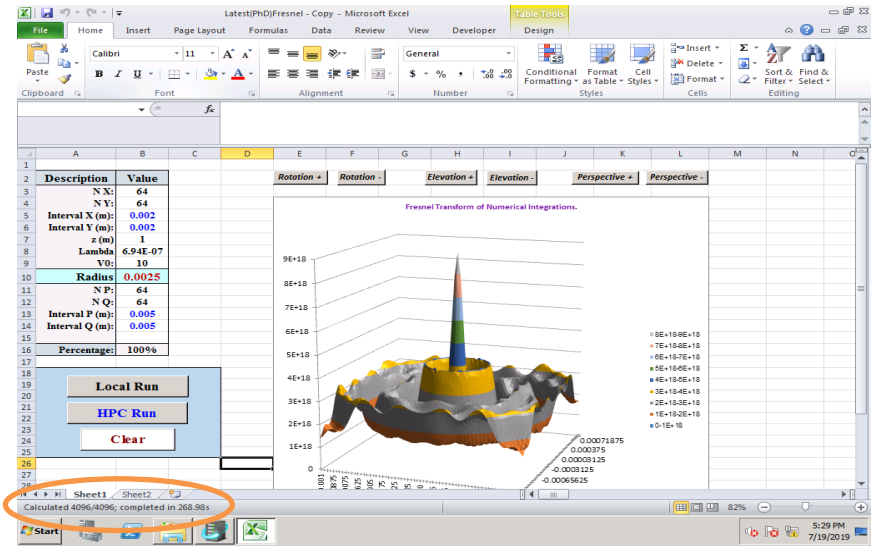

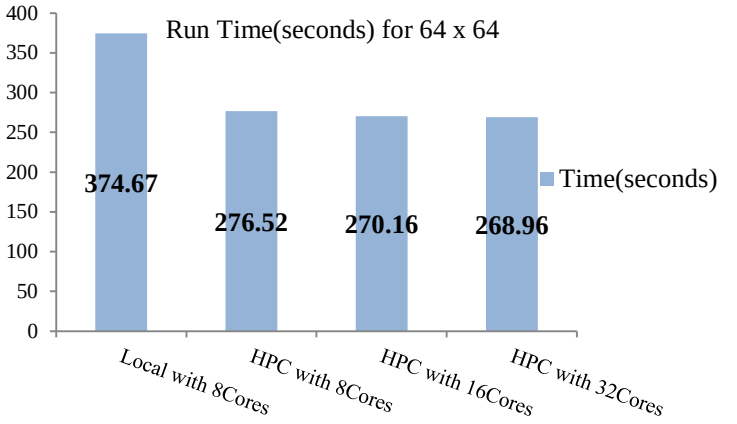

Figure 6. Run time of Local and Run time of HPC for 64 x 64

HPC with 8Cores is faster than Local with 8Cores by 98.15s. HPC with 16Cores is faster than HPC with 8Cores by 6.36s and faster than Local with 8Cores by 104.51s. HPC with 32 Cores is faster than HPC with 8 Cores by 7.56s, HPC with 16 Cores by 1.2 s and Local with 8Cores by 105.71s. HPC with 32 Cores can make Excel workbook run 1.4 times faster than Local with 8Cores. Therefore, HPC Services for Excel with a Windows HPC cluster can improve calculation performance.

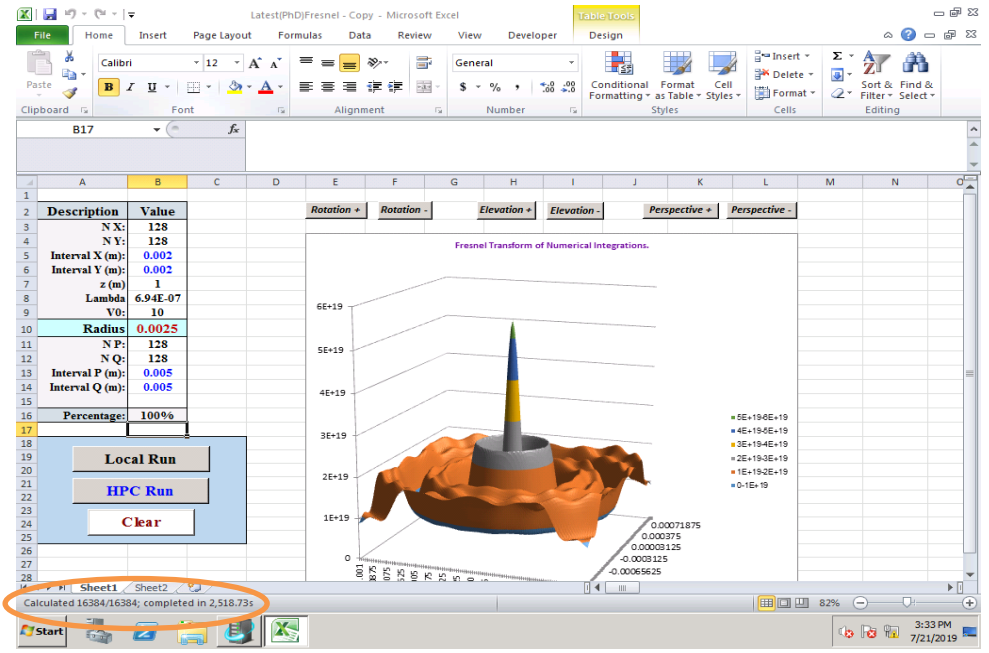

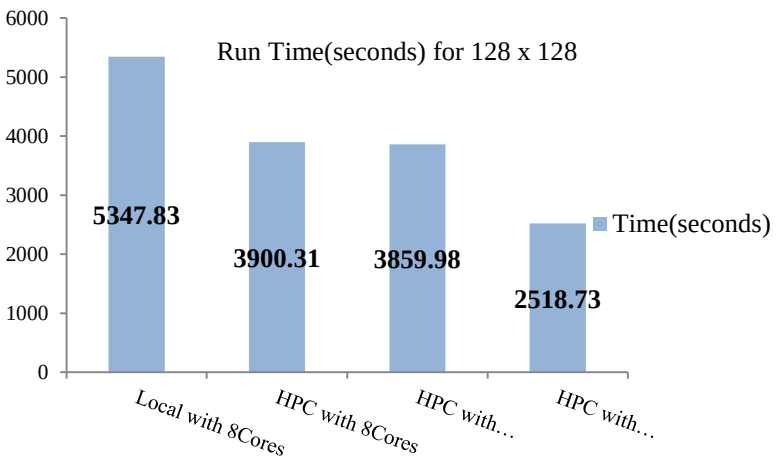

Figure 7. Run time of Local and Run time of HPC for 128 x 128

HPC with 8Cores is faster than Local with 8Cores by 1447.52s. HPC with 16Cores is faster than HPC with 8Cores by 40.33s and faster than Local with 8Cores by 1487.85s. HPC with 32 Cores is faster than HPC with 8 Cores by 1381.58s, HPC with 16 Cores by 1341.25s and Local with

8Cores by 2829.1s. HPC with 32 Cores can make Excel workbook run 2.12 times faster than Local with 8Cores. Therefore, HPC Services for Excel with a Windows HPC cluster can improve calculation performance.

Conclusion

By using numerical methods, a value for the definite integral is obtained. With the use of VMs on cloud, the need for several physical host machines is reduced in running multiple processes. The basic objective of this system is to get the faster calculation time and better performance of the Excel VBA program for numerical integration in parallel processing on cloud computing. Windows HPC Server 2008 R2 enables multiple instances of Office Excel 2010 run on HPC virtual machines. Faster execution of highly compute intensive tasks of multi-dimensional integration for advanced computation can be achieved by using HPC VMs. By using Windows HPC Server 2008 R2, the set-up of Virtualized HPC cluster on cloud, reduce calculation times for Excel 2010 workbooks. This work perform to reduce the calculation time required for long-running Spread-sheet Calculations and to get better accuracy for Numerical Integration by using HPC virtualized cluster on cloud. Therefore, this system is able to obtain improved calculation performance and faster calculation time for numerical integration by applying the Excel VBA on virtualized HPC cluster on cloud.

Acknowledgments

First of all, I wish to express my sincere thanks to Dr Thidar Win (Rector), Dr Tin Htun Aung (Pro-Rector), Dr Myint Zu Min(Pro-Rector), and Dr Min Min Yi (Pro-Rector), University of Mandalay, for their kind permissions for the submission of this research paper. I also wish to thank Professor Dr Khin Myo Sett (Head of Department) of Computer Studies, University of Mandalay) for her encouragement and support. Finally, I would like to express my sincere gratitude to Dr Pho Kaung, Rector, University of Yangon for his enthusiastic guidance and various suggestions.

References

Bill0, E.J, (2007), *Excel@ for Scientists and Engineers Numerical Methods*.

Buyya, R, Broberg, J, Gosci, A, John Wiley & Sons, Inc., Hoboken, New Jersey, (2011), *CLOUD COMPUTING Principles and Paradigms*.

David G. Lilley*, 48th AIAA Aerospace Sciences Meeting, Florida, (2010), *Some Useful Excel/VBA Codes for Numerical Methods in Engineering*.

Gamaleldin, A.M, Senior R & D Engineer-SECC, (2013), *An Introduction to Cloud Computing Concepts*.

Sosinsky, B, Wiley Publishing, Inc., Indianapolis, Indiana, (2011), *Cloud Computing Bible*.

Vecchiola, C, Pandey, S, and Buyya, R, The University of Melbourne, Australia, *High-Performance Cloud Computing: A View of Scientific Applications*.

Xiaotao, Y, Aili, L, Lin, Z, ISCSCT, China, (2010), *Research of High Performance Computing With Clouds*.

Parallel Chains in Markov Chain Monte Carlo Simulation

Wint Pa Pa Kyaw[1] & Soe Mya Mya Aye[2]

Abstract

Markov Chain Monte Carlo (MCMC) methods play an important role in scientific computation, especially when problems have a vast phase space. In the most general terms, the MCMC method is a statistical almost experimental approach to computing integral using random positions, called samples, whose distribution is carefully chosen. In this research an introduction to the MCMC method is given. It concentrates on how to obtain these samples, how to process them in order to approximately evaluate the pi, and how to get good results with as few samples as possible. MPI stands for the "Message Passing Interface" (MPI). This research also presents parallel communication schemes for simulated Markov chain using MPI.

Keywords: parallel processing, Message Passing Interface, Communication, Markov Chain

Introduction

A special kind of stochastic process (random process) is a Markov Chain (MC) method, where the outcome of an experiment depends only on the outcome of the previous experiment. MC method fluctuates in time because of random events. System can be in various states. MC method depicts movements between states. Andrei A. Markov graduated from Saint Petersburg University in 1878 and subsequently became a professor there. His early work dealt mainly in number theory and analysis, etc. He is particularly remembered for his study of MCs. These chains are sequences of random variables in which the future variable is determined by the present variable but is independent of the way in which the present state arose from its predecessors. MCs are used to analyze trends and predict the future (Weather, stock market, genetics, product success, etc.).

MPI (Message-Passing Interface) is a portable standard for programming parallel computers. MPI uses the message-passing paradigm which is well suited for computing on distributed-memory machines. Of

[1] Associate Professor, Dr., Department of Computer Studies, University of Yangon.
[2] Professor and Head, Dr., Department of Computer Studies, University of Yangon.

course, message-passing can also be used on shared-memory multiprocessors. The goal is to make use of the multi-core as well as multi-processor architectures to speed up large-scale data. This research also describes parallel algorithms and their MPI-based parallel implementation for Markov Chain Monte Carlo (MCMC) method.

For high-dimensional non-linear models, the only practical methods for analysis are based on MCMC techniques, and these are notoriously compute intensive, with some analyses requiring weeks of CPU time on powerful computers. It is clear therefore that the use of parallel computing technology in the MCMC computation is of great interest to many who analyze complex models using MCMC techniques. There are two essentially different strategies which can be used for parallelizing an MCMC scheme (though these may be combined in a variety of ways). One is based on running multiple MCMC chains in parallel and the other is based on parallelization of a single MCMC chain. There are different issues related to the different strategies, and each is appropriate in different situations. In this work, multiple MCMC chains are run in MPI environment.

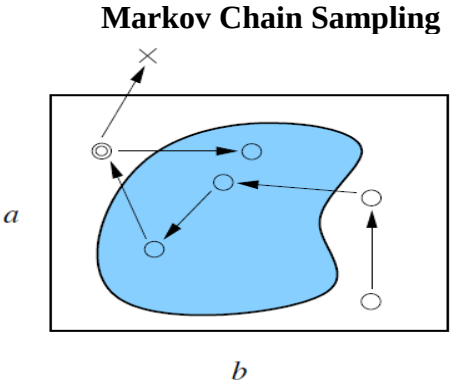

Figure 1. Illustration of Markov-Chain Monte Carlo.

A sampling approach is considered to estimate the area of a pond by throwing pebbles. If a pond is very large, it is impossible to throw pebbles randomly from one position. Thus simple MC approach is modified: one starts at a random location and throw a pebble into a random direction. One then walks to that pebble, pulls a new pebble out of a pebble bucket and

repeats the operation. This is illustrated in Figure.1. If the pebble lands outside the rectangular area, the thrower should go get the outlier and place it on the current position of the thrower, i.e., If a pebble lands outside the rectangular area (cross) the move is rejected and the last position recorded twice (double circle). Basically, it ensures that the MC is reversible. After many throws, pebbles are scattered around the rectangular area, with small piles of multiple pebbles closer to the boundaries (due to rejected moves).

A Serial Implementation of Markov Chain Program

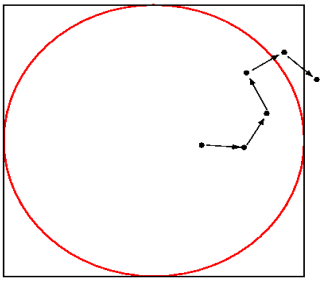

Figure 2. Movement of pebble

The new state is always derived from the previous state. At each step a pebble is thrown in a random direction, the following throw has its origin at the landing position of the previous one. This is illustrated in Figure 2.

If a pebble lands outside the rectangular area, the move is rejected and the last position recorded twice. It is assumed that the two independent random numbers in the program are uniformly distributed in the interval $[-\delta, \delta]$. δ is the "throwing range". It is intuitively clear that by starting somewhere on the pond and moving randomly (within the throwing range). All the (gray) pebbles should be counted. The pebble at $i = 3$ is counted twice, because there is a rejection. This is illustrated in Figure 3.

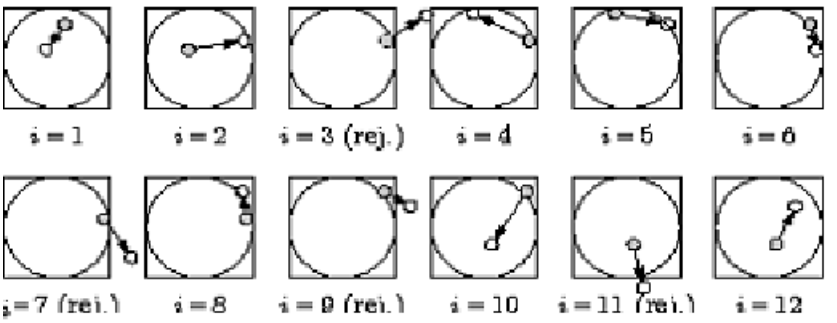

Figure 3. Rejecting movement of pebble

Pseudo Code for Serial Implementation

Above ideas can be used to estimate pi by MC sampling the unit circle. The following Pseudo code program describes MCMC for estimating pi:

```
procedure markov-pi
  N_hits←0; x←0.8; y←0.9
  for i=1,...,N do
        Δx←ran(-δ,δ)
        Δy←ran(-δ,δ)
        if(|x+Δx|<1.and.|y+Δy|<1) then
           x←x+Δx
            y←y+Δy
        endif
        if(x^2+y^2<1) N_hits←N_hits+1
   enddo
```

Message Passing Interface (MPI)

MPI has its own data types (e.g. MPI_INT). User defined data types are supported as well. MPI supports C, C++ and FORTRAN. It include file <mpi.h> in C/C++ and "mpif.h" in FORTRAN. An MPI environment typically consists of at least a library implementing the Application Programming Interface (API), a compiler and linker that support the library and a run time environment to launch an MPI program. Various implementations available Sun HPC Cluster Tools, MPICH, MVAPICH, LAM, Voltaire MPI, Scali MPI, HP-MPI, ... The MPI Programming

Model is shown in Figure.4. The MPI Execution Model is shown in Figure 5.

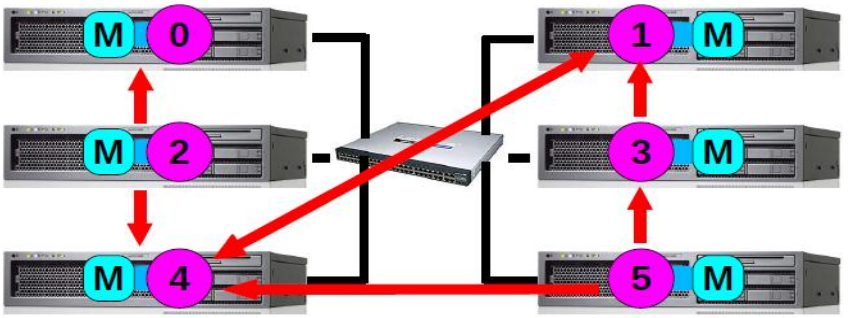

Figure 4: A Cluster of Systems

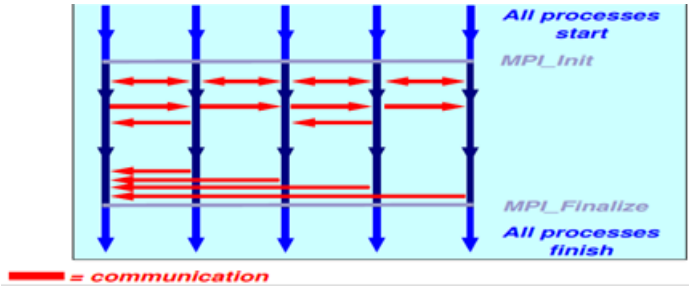

Figure 5. The MPI Execution Model

Perhaps the most advanced aspect of MPI is the concept of "communicators". These make it possible to isolate communication so that only those tasks which should take part in the message-passing can do so.

Implementation of Parallel Chains Markov Chain Monte Carlo

Parallel MCMC chains are run in an MPI environment. An independent chain is run on each processor. The parallel chains approach turns out to be surprisingly effective in practice. An important consideration in the parallel context is that of the starting point of the chain. Each chain could be started with an independent realization from the target distribution. A pragmatic solution is to initialize each chain at a random starting point that is in some sense “over-dispersed” relative to the target, and then burn-in until all chains have merged together.

The following Pseudo code program describes Parallel MCMC method for estimating pi:

```
procedure markov-pi
[MPI startup]
 IF(my_rank==server_rank)THEN
 CALL read_input(…)
 END IF
CALL MPI_ Send(…)
DO realization=1, number_of_realizations
CALL generate_random_realization(…)
CALL calculate_ realization_properties(…)
CALL calculate_local_running_hit(…)
END DO
IF (my_rank==server_rank)THEN
[collect properties]
ELSE
[send properties]
END IF
CALL calculate_ global_ pi from local_hit(…)
CALL output_overall_pi(…)
[MPI shutdown]
END PROGRAM markov-pi
```

Results and Discussion

The process generates random numbers in (-delta, delta) with the following code segments.

```
double delta_x = ( 2 * double(rand()) / RAND_MAX - 1 ) * delta;
double delta_y = ( 2 * double(rand()) / RAND_MAX - 1 ) * delta;
```

The process tests if we are still on the pond with the following code segments.

```
if ( fabs ( x + delta_x ) < 1 && fabs (y + delta_y) < 1 )
    {
       x += delta_x;
       y +=delta_y;
    }
   if ( x*x + y*y < 1 ) ++Nhits;
```

The process calculates pi with the following code segment.

```
cout << "pi = "<< double(Nhits) / N * 4 << endl;
```

The results of several runs are shown in Table 1 after four consecutive trials. During each trial, N = 4000 pebbles were thrown and δ = 0.1, 0.3, 0.35, 0.4, 0.45, 0.5, 0.7 are used.

Table 1. The results obtained after four consecutive trial runs with various δ.

N=4000	δ=0.1	δ=0.3	δ=0.35	δ=0.4	δ=0.45	δ=0.5	δ=0.7
1	3.0720	3.0500	3.1180	3.0880	3.1030	3.1710	3.1500
2	2.8570	3.2020	3.1070	3.2000	2.9770	3.1770	3.1190
3	2.8900	3.1150	3.1200	3.1370	3.0770	3.0970	3.1280
4	3.3000	3.2770	2.9880	3.2610	3.1490	3.1540	3.1260

The program starts from a given position in the space to be sampled [here (0.8; 0.9)] and generates the position of the new dot from the position of the previous one. If the new position is outside the square, it is rejected. A careful selection of the step size δ used to generate random numbers in the range [-δ; δ] is of importance.

From Table 1, through the compiling of the program written in C language, we see that the approximate value of pi is 3.149 at δ =0.45 by rounding off this value. This illustrates a general feature of MC method. The precision of the calculation is determined by carefully selecting the step size δ used to generate random numbers in the range [-δ; δ]. When δ is too small, convergence is slow, whereas if δ is too large many moves are rejected because the simulation will often leave the unit square. Therefore, a value of δ has to be selected such that consecutive moves are accepted approximately 50% of the times.

The simple-sampling approach has the advantage over the MC approach in that the different samples are independent and thus not correlated. In the MC approach the new state depends on the previous state. This can be a problem since there might be a “memory" associated with this

behavior. If this memory is large, then the autocorrelation times (i.e., the time it takes the system to forget where it was) are large and many moves have to be discarded. The MC approach should be followed because in the study of physical systems it is generally easier to slightly (and randomly) change an existing state than to generate a new state from scratch for each step of the calculation.

There are six basic MPI functions in parallel implementation. These functions are

1. Initialize MPI environment (mandatory)
   int MPI_Init(int *argc, char ***argv)
2. Clean up all MPI states (mandatory)
   int MPI_Finalize()
3. Returns the number of MPI processes in "size"
   int MPI_Comm_size(MPI_Comm comm, int *size)
4. Returns the MPI process ID ("the rank") in "rank"
   int MPI_Comm_rank(MPI_Comm comm, int *rank)
5. Send a message to "dest"
   int MPI_Send(void *buf, int count,
   MPI_Datatype datatype, int dest,
   int tag, MPI_Comm comm)
6. Receive a message from "source"
   int MPI_Recv(void *buf, int count, MPI_Datatype datatype, int source,
   int tag, MPI_Comm comm, MPI_Status *status)

The 7-th function: return the elapsed time in seconds

double MPI_Wtime()

The computational time of using the MCMC method on a data set is shown in Table 2.

Table 2. The results obtained after three consecutive trial runs with various samples.

Program	N=50000000	N=70000000	N=100000000
C	4.679824(sec)	6.537605(sec)	9.415152(sec)
MPI	1.794050(sec)	2.576539(sec)	3.764764(sec)

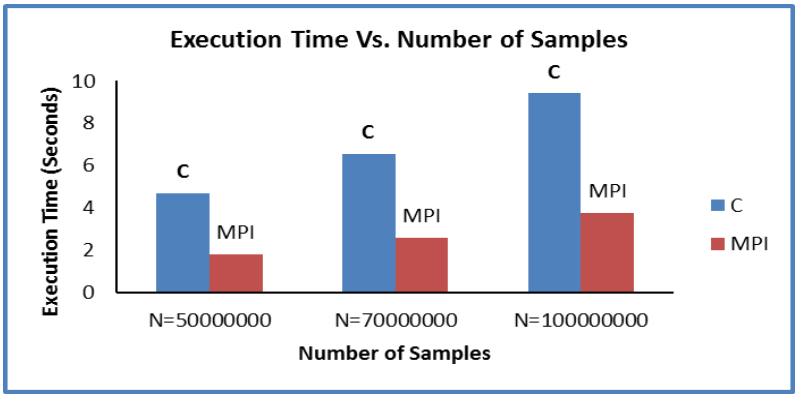

Figure 6. Variation of Execution time with Number of samples

When the program is executed with corei5 multiprocessor, the execution time for serial processing and the execution time for parallel processing are obtained for different processor. The results in Figure 6 show that the parallelized program with MPI runs rapidly. From Table 2 and Figure 6, it can be observed that parallel computing is more suitable for enormous data. The experimental results show that parallel algorithms using MPI achieve comparable accuracy and almost linear speedups over the traditional serial version.

Table 3. The results obtained after four consecutive trial runs with N=10000000.

Number of Processors	Execution Time(Sec)
2	0.519732
3	0.454756
4	0.358803
8	0.267789

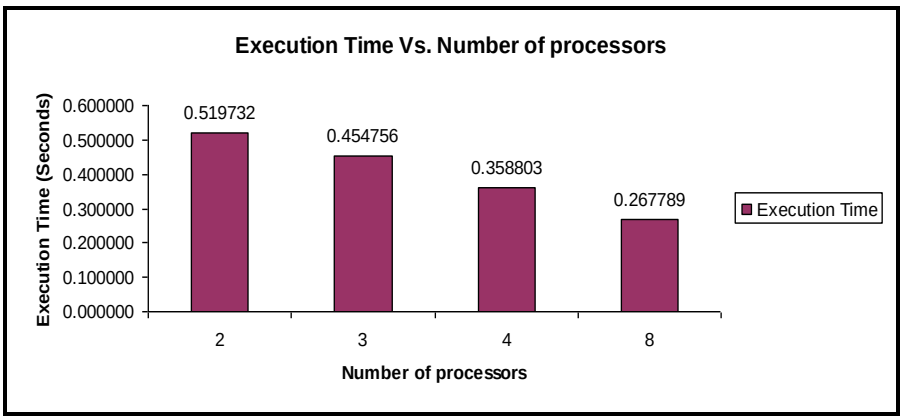

Figure 7. The relation of No. of Processors and Execution Time

When the program is executed with corei7 multiprocessor, the execution time for parallel processing are obtained for different processor namely two, three, four, and eight. The results in Figure.7 show that parallel execution time goes faster with increasing the number of processors. So running with number eight processor is faster than two, three, and four. From Table 3 and Figure.7, parallel computing gets speed up with more processors.

Conclusion

"Markov pi" is a basic MCMC algorithm. "Markov pi" concerns the choice of the throwing range δ. Every choice of δ should give the correct value of $\pi / 4$. Experiments show that δ is the best choice such that about 50% of proposed moves should be rejected, for best precision. This agrees to the famous one-half rule. It is only approximately valid, but it is very

general. The major advantages of MPI are four-fold. First, MPI can save time as it speeds-up the tasks. Second, it is cost-effective. Faster hardware devices are quite expensive but cheaper components can be used with MPI for parallel computing. Third, it can compute larger problems and bottlenecks like limited memory can be circumvented. Last, MPI can be combined with existing computational resources such that existing clusters can be used for parallel computing. From this research, it gets a good idea to explicitly specify the scope of all variables used in a parallel region. The performance of parallel processing is better than serial processing.

Acknowledgements

I would like to extend my sincere thanks to Dr Soe Mya Mya Aye, Professor, Head of Department of Computer Studies, University of Yangon, for her kind permission to carry out this work. I am utmost gratitude to Rector Dr Pho Kaung, University of Yangon, for introducing me to the field of Parallel Processing.

References

Allen, M., Tildesley, D. J., 1987, "Computer Simulation of Liquids",(Oxford :Clarendon Press)

Grama, A.; Gupta, A.; Karypis, G.; Kumai, V., 2003, "Introduction to Parallel Computing",2nd edition, (New York: Benjamin Cummings Publishing Company)

Karniadakis, G.E., and Robert, M.K., 2010,"Parallel Scientific Computing in C++ and MPI", (London: Cambridge University Press)

Landau, D. P., and Binder, K., 2000,"A Guide to Monte Carlo Simulations in Statistical Physics",(Cambridge :Cambridge University Press)

Some Aspects of Stationary Multiple Markov Gaussian Processes

Kyi Kyi Hlaing*

Abstract

In this paper, we first discuss the simple Markov Gaussian process $Y(t)$ which can be expressed as a product of additive process $U(t)$ and a real valued function $f(t)$. We define N-ple (multiple) Markov Gaussian process and we state it has an integral representation with Goursat kernel which is a factor of real valued functions $f_i(t)$ and $g_i(u)$ that are fundamental system of solutions of a certain linear differential equation of order N with constant coefficients and adjoint differential equation. Then we present differentiability and stationarity of kernel of N-ple Markov Gaussian process. In particular, the stationarity of a N-ple Markov process $X(t)$ $(= e^{-(2\alpha+1)t} X(e^{2t}))$ is proved.

Keywords: Gaussian process, simple Markov Gaussian process, multiple Markov Gaussian process

Introduction

In this paper we would like to study multiple Markov Gaussian processes by using the theory of representation. Throughout this paper, we will use the following properties for a Gaussian process $Y(t)$ with mean zero. Let M_t be the closed linear manifold generated by $\{Y(\tau): \tau \leq t\}$ and $M = \bigcup_{t \in T} M_t$ such that

(1. 1) M is *separable* as a sub-space of $L^2(\Omega)$,

(1. 2) $\bigcap_{t \in T} M_t = \{0\}$.

And we assume that M_t is *continuous in t*, i.e.

(1. 3) $\lim_{t \to t_0} M_t = M_{t_0}$.

A Markov process is a stochastic process that satisfies the Markov property; the predictions for the future of the process depend only on the

* Lecturer, Department of Mathematics, University of Yangon

present state of the system as well as past states are independent. That is, we can write,

$$P(X_{n+1}= j \mid X_n = i, X_{n-1} = i-1, \cdots, X_0 = i_0) = P(X_{n+1}= j \mid X_n = i),$$

and for the continuous parameter process $\{ X(t) : t \in T\}$, where T is a subset of **R**,

$$P(X_t(\omega) \le A \mid X_s, s \le t_0) = P(X_t(\omega) \le A \mid X_{t_0}).$$

Brownian motion and Poisson process are Markov processes in continuous time. Random walk and the Gambler's ruin problems are examples of Markov processes for the discrete parameter.

Simple Markov Gaussian Processes

We shall consider a simple Markov Gaussian process $Y(t)$. Since $Y(t)$ is Gaussian, the simple Markov property is usually defined as

$$(2.1) \quad E[Y(t) \mid \mathfrak{B}_s] = \varphi(t, s)Y(s), \text{ for } s \le t,$$

where $\varphi(t, s)$ is a real valued ordinary function of (t, s) and $t, s \in T$; T is a parameter space which may be $(-\infty, \infty)$ or $[0, \infty)$, however we will take $[0, \infty)$ in this paper . $\mathfrak{B}_s$ is the smallest Borel field of measurable sets with respect to which all $Y(\tau)$'s, $\tau \le s$ are measurable. Since $Y(t)$ is simple Markov process, $Y(t)$ satisfies the Markov property that is the relation between the past values and future values of a stochastic process are independent. In other words,

$$Y(t) - \varphi(t, s)Y(s)$$

is independent of every $Y(\tau)$, $\tau \le s$. Suppose that $Y(t)$ and $Y(s)$ are dependent, for $s \neq t$ and assume that

$$(2.2) \quad \Gamma(t, s) = E[Y(t)\, Y(s)]$$

never vanishes. Then

$$E[(Y(t) \mid \mathfrak{B}_s] = E[E(Y(t) \mid \mathfrak{B}_{s'}) \mid \mathfrak{B}_s] \quad \text{for } s \le s' \le t.$$

$$= \varphi(t, s')\, \varphi(s', s)Y(s).$$

and $\quad E[(Y(t) \mid \mathfrak{B}_s] = \varphi(t, s)Y(s).$

So we obtain

(2. 3) $\varphi(t, s) = \varphi(t, s')\,\varphi(s', s)$ for $s \le s' \le t$

and $\varphi(t, t) = 1$,

since $E[Y(s)Y(s)] = \Gamma(s, s) \neq 0$. Thus $\varphi(t, s)$ never vanishes and

$$\varphi(t, s) = \varphi(s, t)^{-1},\ s > t.$$

Then we can write

$$(2.\ 4)\quad \varphi(t, s) = \frac{f(t)}{f(s)}$$

where $f(t) = \varphi(t, s_0)$ for some fixed s_0.

By using the Markov property,

$$\begin{aligned} E[f(t)^{-1}Y(t) \mid \mathfrak{B}_s] &= E[\varphi(t, s_0)^{-1}Y(t) \mid \mathfrak{B}_s], \text{ for } t < s_0 \le s. \\ &= \varphi(s_0, s)^{-1}Y(s) \\ &= f(s)^{-1}Y(s) \end{aligned}$$

If we put $U(t) = f(t)^{-1}Y(t)$ then $U(t)$ is an additive process. Thus we can see that the Borel fields of $U(t)$ is the same as that of $Y(t)$ since $f(t)$ never vanishes. Since $Y(t)$ satisfies the conditions (1. 1), (1. 2) and the multiplicity of $Y(t)$ is one, $Y(t)$ has a canonical representation. It follows that $U(t)$ has a canonical representation without discontinuity part. Hence

$$Y(t) = f(t)U(t) = f(t)\int_0^{\infty} dU(u).$$

Thus a simple Markov Gaussian process $Y(t)$ can be expressed in the above form where f(t) never vanishes.

By summing up, we obtain the following theorem.

Theorem 2.1 Let $Y(t)$ be a Gaussian process and satisfies the conditions (1. 1), (1. 2), (1. 3) and (2. 2). The process $Y(t)$ is a simple Markov process if and only if

$$(2.\ 5)\quad Y(t) = f(t)U(t) = f(t)\int_0^t dU(u) = \int_0^t f(t)g(u)\dot{B}(u)\,du,$$

where $U(t)$ is an additive process with the property,

$$(2.\ 6)\quad \lim_{t \to t_0} U_t = U_{t_0},$$

($dB(u)$ $(= \dot{B}(u)\,du)$ is a continuous random measure) and $f(t)$ never vanishes.

By using Theorem (2.1) we have the following Corollaries.

Corollary 2.2 Let $Y(t)$ be expressed in the form

$$Y(t) = f(t)\, U(t).$$

If $Y(t)$ continuous in the mean then $f(t)$ is continuous and $U(t)$ is also continuous in the mean.

In particular, if $T = [0, \infty)$ and $E[U(t)^2]$ is the second moment about the origin then $U(t)$ has continuous derivative. So $U(t)$ becomes an ordinary Brownian motion by the change of time scale. In other words, $Y(t)$ has canonical representation $(\dot{B}(t), M_t, F(t, u))$ with random measure $dB(t)$ $(= \dot{B}(t)dt)$ and proper canonical kernel $F(t, u)$.

Corollary 2.3 If $Y(t)$ is a stationary simple Markov process satisfying the above conditions (1. 1), (1. 2) and (2. 2) then the representation of $Y(t)$ has a version of the form

$$c\int_0^t e^{-\lambda(t-u)}\, \dot{B}(u)du, \quad \lambda > 0.$$

Multiple Markov Property for Gaussian processes with Continuous Parameter

In this section, we shall give the definition of multiple markov process and we will discuss its properties.

Definition 3.1 A Gaussian process $Y(t) = \{Y(t, \omega) : t \in T\}$ is called an ***N-ple* (i.e. *multiple*) *Markov Gaussian process*** if $E(Y(t_i) \mid \mathfrak{B}_{t_0})$, $i = 1, 2, \cdots, N$, are linearly independent for any $\{t_i\}$ with $t_0 \le t_1 < \cdots < t_N$ and if $E(Y(t_i) \mid \mathfrak{B}_{t_0})$, $i = 1, 2, \cdots, N, N+1$ are linearly dependent for any $\{t_i\}$ with $t_1 < \cdots < t_N < t_{N+1}$.

N-ple Markov Gaussian process $Y(t)$ is (N–1) times differentiable. A simple Markov process is a 1-ple Markov process if the covariance function of $Y(t)$ never vanishes. A 1-ple Markov Gaussian process $Y(t)$, $t \ge 0$, is a simple Markov process in the ordinary sense. That is

$$Y(t) = f(t)\int_0^{\infty} g(u)\, \dot{B}(u)du = f(t)U(t),$$

where $g(u)$ never vanishes and $U(t)$ is additive process.

Example 3.2 Let $\{B_1(t, \omega) : t \geq 0\}$ and $\{B_2(t, \omega) : t \geq 0\}$ be mutually independent Brownian motions and let $F(t)$ be monotonically increasing and absolutely continuous function on $[0, \infty)$. Then a Gaussian process $X = \{X(t, \omega) : t \geq 0\}$ defined by

$$X(t) = B_1(t) + F(t)B_2(t)$$

is a double Markov Gaussian process because for $0 \leq t_0 \leq t_1 < t_2 < t_3$,

$$E(X(t_i)\,|\,B_{t_0}) = B_1(t_0) + F(t_i)B_2(t_0),\ i = 1, 2, 3.$$

Consider

$$\mu E(X(t_1)\,|\,B_{t_0}(x)) + \alpha\, E(X(t_2)\,|\,B_{t_0}(x)) + \beta\, E(X(t_3)\,|\,B_{t_0}(x)) = 0$$

$$(\mu+\alpha+\beta)B_1(t_0) + (\mu F(t_1)+\alpha F(t_2)+\beta F(t_3))B_2(t_0) = 0$$

Since $\{B_1(t, \omega) : t \geq 0\}$ and $\{B_2(t, \omega) : t \geq 0\}$ be mutually independent,

(3. 1) $\mu + \alpha + \beta = 0$

(3. 2) $\mu F(t_1) + \alpha F(t_2) + \beta F(t_3) = 0$

From (3. 1), $\mu = -\alpha - \beta$. Then we obtain $\alpha = \beta\, \frac{F(t_3) - F(t_1)}{F(t_2) - F(t_1)}$.

Thus three conditional expectations are linearly dependent. But any two of them are linearly independent since

let $$\alpha_1\, E(X(t_1)\,|\,B_{t_0}(x)) + \alpha_2\, E(X(t_2)\,|\,B_{t_2}(x)) = 0$$

$$(\alpha_1+\alpha_2)\, B_1(t_0) + (\alpha_1 F(t_1) + \alpha_2 F(t_2))\, B_2(t_0) = 0$$

Since $\{B_1(t, \omega) : t \geq 0\}$ and $\{B_2(t, \omega) : t \geq 0\}$ be mutually independent,

$$\alpha_1 + \alpha_2 = 0 \text{ and } \alpha_1 F(t_1) + \alpha_2 F(t_2) = 0.$$

This implies coefficients of $F(t_1)$ and $F(t_2)$ are all zero. Hence X is double Markov Gaussian process. □

Theorem 3.3 Let $Y(t) = \{Y(t, \omega) : t \in T\}$ be a Gaussian process which satisfies the conditions (1. 1), (1. 2), (1. 3) and it has multiplicity one. If $Y(t)$ is an N-ple Markov process then its version $X(t)$ can be expressed as

$$(3.\ 3)\quad X(t) = \int_0^t \sum_{i=1}^{N} f_i(t)\, g_i(u)\, \dot{B}(u)\, du$$

with proper canonical kernel

$$(3.\ 4)\qquad \sum_{i=1}^{N} f_i(t)\, g_i(u),$$

where $\{f_i(t)\}$, i= 1, 2, ⋯ , N, satisfies

$$(3.\ 5)\quad \det(f_i(t_j)) \neq 0, \text{ for any } t_i \neq t_j \text{ for } i \neq j,$$

and $\{g_i(u)\}$, i = 1, 2, ⋯ , N, are linearly independent as the element of

$$L^2(\upsilon, t) = \{\varphi : \varphi \in L^2(\upsilon), \varphi(u) = 0 \text{ for } u > t\}.$$

Further the covariance function of $Y(t)$ can be written in the form

$$\Gamma(s, t) = \sum_{i=1}^{N} f_i(t)\, h_i(s), \text{ for } s < t,$$

where $\{f_i(t)\}$, i = 1, 2, ⋯ , N, are the same as above and $\{h_i(s)\}$, i = 1, 2, ⋯ , N, are linearly independent.

Proof of the above theorem is omitted according to the limited number of pages.

Stationary Multiple Markov Gaussian Processes

Let $Y(t)$, $t \in T$ be a stationary Gaussian process with mean zero and satisfies the conditions (1. 1), (1. 2) and $Y(t)$ is mean continuous. Then by theorem, $Y(t)$ has canonical representation such that

$$Y(t) = \int_0^t F(t - u)\, \dot{B}(u)\, du \quad \text{and} \quad E(\dot{B}(u)\, du)^2 = du,$$

where $F(t - u)$ is canonical kernel. This canonical kernel is unique and it is also proper canonical.

In order to study the stationarity multiple Markov processes, we will first study the canonical kernel $F(t-u)$.

Lemma 4.1 Let $\{f_i(t)\}$, i = 1, 2, ⋯ , N which satisfy $\det(f_i(t)) \neq 0$ and let $\{g_i(u)\}$, i= 1, 2, ⋯ , N be linearly independent in $L^2((-\infty, c])$ for every c. If a Goursat kernel

$$F(t, u) = \sum_{i=1}^{N} f_i(t)\, g_i(u)$$

is a function of (t – u) in the Domain $\overline{D} = \{(u, t) : u \leq t\}$, then $\{f_i(t)\}$ is a fundamental system of solutions of a certain linear differential equation of order N with constant coefficients and $\{g_i(u)\}$ is also a fundamental system of solutions of its adjoint differential equation.

Proof. Consider $F(t, u) = \sum_{i=1}^{N} f_i(t)\, g_i(u)$ in the region $\overline{D}$. Let $\mathcal{D}_0$ be the set of all C_0^∞ functions whose supports are in $[0, \infty)$. Then for every $\varphi \in \mathcal{D}_0$,

$$(F * \varphi)(t) = \int_0^\infty F(t - u)\, \varphi(u)\, du$$

is a C_0^∞ function over $[0, \infty)$. Next we will show that there exists functions $\varphi_j(u)$, j = 1, 2, ⋯ , N in $\mathcal{D}_0$ such that

(4. 1) $$\det((g_i, \varphi_j), i, j = 1, 2, \cdots, N) \neq 0,$$

where g_i and φ_j are in $L^2(T)$, $T = [0, \infty)$. There exists $\varphi_1(u) \in \mathcal{D}_0$ such that

$$(g_1, \varphi_1) \neq 0.$$

If not, $g_i(u)$ must vanish on $(0, \infty)$. By induction, we can assume that for $\varphi_1, \cdots, \varphi_n \in \mathcal{D}_0$ $(n \leq N)$,

$$\det((g_i, \varphi_j), i, j = 1, 2, \cdots, N) \neq 0.$$

For $\varphi_1, \cdots, \varphi_N, \varphi_{N+1} \in \mathcal{D}_0$, consider the determinant,

$$\det((g_i, \varphi_j)) = \begin{vmatrix} (g_1, \varphi_1) & (g_1, \varphi_2) & \cdots & (g_1, \varphi_{N+1}) \\ (g_2, \varphi_1) & (g_2, \varphi_2) & \cdots & (g_2, \varphi_{N+1}) \\ \vdots & \vdots & & \vdots \\ (g_{N+1}, \varphi_1) & (g_{N+1}, \varphi_2) & \cdots & (g_{N+1}, \varphi_{N+1}) \end{vmatrix}.$$

If $\det((g_i, \varphi_j), i, j = 1, 2, \cdots, N+1) = 0$, for $\varphi_j \in \mathcal{D}_0$ then we get

$$\Delta_1 (g_1, \varphi_{N+1}) + \Delta_2 (g_2, \varphi_{N+1}) + \cdots + \Delta_{N+1} (g_{N+1}, \varphi_{N+1}) = 0, \varphi_{N+1} \in \mathcal{D}_0,$$

where $\Delta_i(g_i, \varphi_{N+1})$ is the cofactor of $(i, N+1)^{th}$ element, $i = 1, 2, \cdots, N+1$.

Since φ_{N+1} is arbitrary,

$$\Delta_1 g_1(u) + \Delta_2 g_2(u) + \cdots + \Delta_{N+1} g_{N+1}(u) = 0 \text{ a.e. in } [0, \infty).$$

If $\Delta_{N+1} \neq 0$ (cofactor of (g_{N+1}, φ_{N+1})) then $\{g_i(u)\}$, $i = 1, 2, \cdots, N, N+1$ are linearly dependent. This gives a contradiction to the fact that $g_i(u)$, $i = 1, 2, \cdots, N, N+1$ are linearly independent. Thus $\det((g_i, \varphi_j)) \neq 0$, $i, j = 1, 2, \cdots, N, N+1$ and $\varphi_j \in \mathcal{D}_0$. So by induction hypothesis,

$$\{\varphi_j\}, j = 1, 2, \cdots, N, \text{ exists}$$

and $$\det((g_i, \varphi_j)) \neq 0, i, j = 1, 2, \cdots, N.$$

On the other hand,

$$(F * \varphi_j)(t) = \int_0^\infty F(t - u)\, \varphi_j(u)\, du$$

$$= \int_0^\infty \sum_{i=1}^{N} f_i(t) g_i(u) \varphi_j(u) du$$

$$= \sum_{i=1}^{N} (g_i, \varphi_j)\, f_i(t)$$

and $\det((g_i, \varphi_j)) \neq 0$, $i, j = 1, 2, \cdots, N$. So $f_i(t)$ is a linear combination of $(F*\varphi_j)(t)$. Since $(F*\varphi_j)(t) \in C_0^\infty((0, \infty))$, $f_i(t) \in C_0^\infty((0, \infty))$ for all i. This implies $F(t) \in C_0^\infty((0, \infty))$. Thus we can see that $g_i(u) \in C_0^\infty((0, \infty))$, for all i.

Next we assume that $\mathcal{D}_a = \{(u, t) \mid u \leq a, t \geq a\}$, $a \in T$. We can see that

$$f_i(\cdot), g_i(\cdot) \in C_0^{\infty}(T), \ i = 1, 2, \cdots, N.$$

So we have

$$\sum_{i=1}^{N} f_i^{(k)}(t)\, g_i(u) = \frac{\partial^k}{\partial t^k} F(t-u)$$

$$= (-1)^k \frac{\partial^k}{\partial u^k} F(t-u)$$

$$= (-1)^k \sum_{i=1}^{N} f_i(t) g_i^{(k)}(u), \quad k = 0, 1, \cdots, N.$$

Taking $u = 0$, we obtain

$$\frac{d^k}{dt^k} F(t) = (-1)^k \sum_{i=1}^{N} f_i(t) g_i^{(k)}(0), \ k = 0, 1, \cdots, N.$$

There exists $b_0, b_1, \ldots, b_N$ such that $\sum_{i=1}^{N} |b_i| > 0$ and that

$$b_0 F^{(N)}(t) + b_1 F^{(N-1)}(t) + \cdots + b_N F(t) = 0, \ t > 0.$$

So that

$$b_0 F^{(N)}(t-u) + b_1 F^{(N-1)}(t-u) + \cdots + b_N F(t-u) = 0, \text{ for } t > u.$$

$$b_0 \sum_{i=1}^{N} f_i^{(N)}(t) g_i(u) + b_1 \sum_{i=1}^{N} f_i^{(N-1)}(t) g_i(u) + \cdots + b_N \sum_{i=1}^{N} f_i(t) g_i(u) = 0$$

$$\sum_{i=1}^{N} \left(b_0 f_i^{(N)}(t) + b_1 f_i^{(N-1)}(t) + \cdots + b_N f_i(t) \right) g_i(u) = 0, \text{ for } t > u.$$

Since $\{g_i(u)\}$ are linearly independent in $L^2((-\infty, c])$,

$$b_0 f_i^{(N)}(t) + b_1 f_i^{(N-1)}(t) + \cdots + b_N f_i(t) = 0, \quad i = 1, 2, \cdots, N.$$

If $b_0 = 0$ then we get the system of linear differential equations of order (N–1),

$$b_1 f_i^{(N-1)}(t) + b_2 f_i^{(N-2)}(t) + \cdots + b_N f_i(t) = 0.$$

We can find $f_i(t)$ which satisfies

$$c_1 f_1(t) + c_2 f_2(t) + \cdots + c_N f_N(t) = 0, \ \sum_{i=1}^{N} |c_i| \neq 0.$$

These $f_i(t)$, $i = 1, 2, \cdots, N$ form a system of N solutions of linear differential equations at most order (N–1). This gives a contradiction to $f_i(t_j) \in C_0^{\infty}((0,$

∞)) such that $\det(f_i(t_j)) \neq 0$, for any N different t_j. Thus $\{f_i(t_j)\}$ is a fundamental solutions of system of Linear differential equations of order N with constant coefficients. By the same way, we can prove for $\{g_i(u)\}$. □

Remark 4.2 The above lemma shows that the canonical kernel $F(t, u) = F(t - u)$ of a stationary N-ple Markov Gaussian process is a Goursat kernel of order N expressed as a linear combination of the following functions

$$(t-u)^k e^{-\mu(t-u)},$$
$$t^k u^{n-k} e^{-\lambda(t-u)} \sin \mu(t-u) \text{ and} \quad (4.2)$$
$$t^k u^{n-k} e^{-\lambda(t-u)} \cos \mu(t-u),$$

for all $u \leq t$, $k = 0, 1, 2, \ldots, n(\leq N)$, μ being a constant with $\mathrm{Re}\ \mu > 0$.

Theorem 4.3 If $Y(t)$ is a stationary N-ple Markov process satisfying the conditions (1. 1), (1. 2) and $Y(t)$ is continuous in mean, then its canonical kernel is a linear combination of the functions described in (4. 2).

The proof of Theorem 4.3 is obvious so we omitted.

Corollary 4.4 Let $Y(t)$ be a Gaussian process given in Lemma 4.1. Then the Fourier transform $F(\lambda) = \frac{1}{\sqrt{2\pi}} \int_0^\infty e^{-i\lambda t} F(t)\, dt$ of canonical kernel $F(t)$ is being expressible as

$$F(\lambda) = \frac{Q(\lambda i)}{P(\lambda i)}, -\infty < \lambda < \infty, (\mu > 0),$$

where $P(\lambda i)$ and $Q(\lambda i)$ are polynomials in X, and having no roots in the lower half plane such that degree of P is N and the degree of Q is at most (N–1).

Some Special Multiple Markov Gaussian Processes

Consider a stationary N-ple Markov Gaussian process $Y(t)$ which is (N –1) times differentiable(with respects to $L^2(\Omega)$-norm). Assume that

$$Y(t) \sim X(t) = \int_0^t F(t-u)\, \dot{B}(u)\, du$$

with proper canonical kernel

$$F(t-u)=\sum_{i=1}^{N} f_i(t)\,g_i(u).$$

Theorem 5.1 Let $X(t)$ be a stationary N-ple Markov process. Then a necessary and sufficient condition that differentiability of $X(t)$ is $F(0) = 0$, in this case, there exists a complex number λ such that

$$(5.1)\quad e^{\lambda t}\frac{d}{dt}e^{-\lambda t}X(t),$$

exists and it is a stationary (N–1)-ple Markov process.

Proof. If $h > 0$, $\frac{1}{h}\{X(t+h)-X(t)\}$

$$=\frac{1}{h}\left\{\int_0^{t+h}F(t+h-u)\dot{B}(u)\,du-\int_0^{t}F(t-u)\dot{B}(u)\,du\right\}$$

$$=\frac{1}{h}\int_0^{t}\{F(t+h-u)-F(t-u)\}\dot{B}(u)\,du+\frac{1}{h}\int_t^{t+h}F(t+h-u)\dot{B}(u)\,du$$

Since $F(t-u)$ is analytic in $\mathcal{D}$, the second term of right hand side tends to zero (in the mean) as h tends to zero given that $F(0) = 0$. Thus

$$\lim_{h\to 0^+}\frac{1}{h}\{X(t+h)-X(t)\}\quad\text{and}\quad\lim_{h\to 0^-}\frac{1}{h}\{X(t+h)-X(t)\}$$

exist and

$$X'(t)=\int_0^{t}\frac{\partial}{\partial t}F(t-u)\dot{B}(u)\,du\,.$$

Conversely suppose that $X(t)$ is differentiable.

$$\frac{d}{dt}X(t)=\frac{d}{dt}\int_0^{t}F(t-u)\dot{B}(u)\,du$$

$$dX(t)=F(0)\dot{B}(t)\,dt+dt\int_0^{t}\frac{\partial}{\partial t}F(t-u)\dot{B}(u)\,du$$

will be order of dt, thus $F(0)=0$.

$f_i(t)$ is a solution of a linear differential equation with constant coefficients by Lemma 4.1. If λ is one of the characteristic roots of the differential equation then

$$(5.2)\quad e^{\lambda t}\frac{d}{dt}e^{-\lambda t}F(t-u)$$

is obviously a proper canonical Goursat kernel of order (N – 1). The existence and the stationary property of equation (5. 1) is obvious. In this case λ must be real or complex. If λ is real, equation (5. 2) is real valued process. If $\lambda = \lambda_1 + \lambda_2 i$, equation (5. 2) is complex valued process. But we have

$$e^{\lambda t}\frac{d}{dt}e^{-\lambda t}F(t-u) = e^{(\lambda_1+\lambda_2 i)t}\frac{d}{dt}e^{-(\lambda_1+\lambda_2 i)t}F(t-u)$$

$$= \{\, e^{\lambda_1 t}\cos\lambda_2 t\frac{d}{dt}e^{-\lambda_1 t}\cos(-\lambda_2 t) - e^{\lambda_1 t}\sin\lambda_2 t\frac{d}{dt}e^{-\lambda_1 t}\sin(-\lambda_2 t))\,\}F(t-u)$$

$$+ i\,\{\, e^{\lambda_1 t}\cos\lambda_2 t\frac{d}{dt}e^{-\lambda_1 t}\sin(-\lambda_2 t)) + e^{\lambda_1 t}\sin\lambda_2 t\frac{d}{dt}e^{-\lambda_1 t}(\cos(-\lambda_2 t)\}F(t-u)$$

Thus we can see that

$$f_\lambda(t)\frac{d}{dt}f_\lambda(-t)X(t) \quad \text{and} \quad g_\lambda(t)\frac{d}{dt}g_\lambda(-t)X(t),$$

are real valued stationary processes, where

$$f_\lambda(t) = e^{\lambda_1 t}\cos\lambda_2 t \text{ and } g_\lambda(t) = e^{\lambda_1 t}\sin\lambda_2 t.$$

If $F(t)$ satisfies the conditions $F(0) = F'(0) = F''(0) = \cdots = F^{(N-1)}(0) = 0$, then $X(t)$ is (N–1) times differentiable. Then we can take a sequence of complex numbers $\lambda_1, \lambda_2, \cdots, \lambda_{N-1}$ such that

$$e^{\lambda_i t}\frac{d}{dt}e^{(\lambda_{i-1}-\lambda_i)t}\cdots\frac{d}{dt}e^{(\lambda_1-\lambda_2)t}\frac{d}{dt}e^{-\lambda_1 t}X(t) \equiv X^{[i]}(t)$$

exists and it is a stationary (N – i)-ple Markov process. □

We shall now discuss a multiple Markov process with a homogeneous canonical kernel. A canonical kernel $F(t, u)$ is said to be ***homogeneous function of degree α*** if $F(ct, cu) = c^{\alpha}F(t, u)$, $c \in \mathbf{R}$. A multiple Markov process with homogeneous canonical kernel can be transformed into a stationary process by changing the time parameter.

Lemma 5.2 (P. Lévy) Let $X(t)$ be a Gaussian process can be expressed as

$$X(t) = \int_0^t F(t, u)\,\dot{B}(u)\,du,$$

with a proper canonical kernel $F(t, u)$ which is a homogeneous function of degree α. Then $t^{\alpha-\frac{1}{2}} X(t)$ is also a stationary process of log t.

Theorem 5.3 If N-ple Markov process $\{X(t): t \geq 0\}$ has a proper canonical representation with canonical kernel $F(t, u)$ which is a homogeneous function of degree α, then the process

$$\{ X(t) = e^{(2\alpha-1)t} X(e^{2t}) \}$$

is a stationary N-ple Markov process. Moreover, if $X(t)$ is an N-ple Markov stationary Gaussian process then

$$X(t) = \sqrt{t}\ X(\frac{\log t}{2})$$

is also an N-ple Markov Gaussian process with homogeneous kernel of degree zero by changing the time parameter from t to e^t.

Proof. Since $X(t)$ is a N-ple Markov process having a proper canonical kernel $F(t, u)$ which is a homogeneous function of degree α. i.e.

$$F(et, eu) = e^{\alpha} F(t, u).$$

Consider $X(t) = e^{(2\alpha-1)t} X(e^{2t})$. Then we have

$$X(\frac{\log t}{2}) = e^{(2\alpha-1)\frac{\log t}{2}} X(e^{2\frac{\log t}{2}})$$

$$= e^{\log t^{\frac{2\alpha-1}{2}}} X(e^{\log t})$$

$$= t^{\frac{2\alpha-1}{2}} X(t)$$

$$= t^{\alpha-\frac{1}{2}} X(t)$$

By Lemma 5.2, $X(t)$ is a stationary N-ple Markov process. Moreover,

$$\sqrt{t}\ X(\frac{\log t}{2}) = t^{\alpha} X(t).$$

If $\alpha = 0$ then $\sqrt{t}\ X(\frac{\log t}{2}) = X(t)$. This implies $X(t) = \sqrt{t}\ X(\frac{\log t}{2})$ is also an N-ple Markov Gaussian process with homogeneous kernel of zero degree. □

Acknowledgements

I gratefully acknowledge my supervisor Dr. Si Si, Emeritus Professor, Faculty of Information Science & Technology, Aichi Prefectural University Aichi-Ken, Japan for her support, help, insight, encouragement and guidance. My special thanks are extended to my Professor, Dr. Cho Win (Professor & Head), Department of Mathematics, University of Yangon for his permission to submit this paper.

References

T. Hida, Canonical representations of Gaussian processes and their applications, in: L. Accardi, H. H. Kuo, N. Obata, K. Saitô, Si Si, L. Streit, eds. *Selected Papers of Takeyuki Hida*, World Scientific Publishing Co. Pte. Ltd., (2001) 95 – 141.

T. Hida and M. Hitsuda, *Gaussian processes*. (English edition), Math. Monogaraphs **120**, American Math. Soc. 1993.

P. Lévy, A special problem of Brownian motion, and A general theory of Gaussian random functions, in: Jerzy Neyman, eds. *Proceedings of the Third Berkeley Symposium on Mathematical Statistics and Probability*. **2**, (1956) 133 – 175.

Characterization of $LaCo_{0.6}Fe_{0.4}O_3$ Nanocrystalline Powder by Citrate Sol-gel Method

Zar Chi Myat Mon[1], Mya Theingi[2] & Cherry Ohn[3]

Abstract

A facile transition metal Fe doping has been employed as an effective approach to alter the electrical and optical properties of $LaCoO_3$. $LaCo_{0.6}Fe_{0.4}O_3$ nanocrystalline powders were prepared by citrate sol-gel method. The prepared $LaCo_{0.6}Fe_{0.4}O_3$ nanocrystalline powders were characterized by modern techniques (Thermogravimetry/Differential Thermal Analysis, X-ray Diffractometry, Fourier Transform Infrared Spectroscopy, Energy Dispersive X-ray Fluorescence and Scanning Electron Microscope). The $LaCo_{0.6}Fe_{0.4}O_3$ powder obtained by citrate sol-gel method was calcined at different temperatures (500 ºC, 600 ºC and 700 ºC) for 4 hours. From the XRD analysis, it was observed that the crystallite size of the prepared $LaCo_{0.6}Fe_{0.4}O_3$ (300 ºC,500 ºC, 600 ºC and 700 ºC) are 22.20, 20.60 and 25.46 nm res?. From the TG-DTA thermogram of the prepared powders calcined at 600 °C, the weight loss percent of prepared sample is very low and therefore it has thermal stability. From FT IR spectral data, taken for the xerogel and the sample calcined at 600 ºC, confirm that stretching and bending vibrations of absorbed water molecule and stretching vibration of metal-oxygen chemical bond . Surface feature study of the prepared nanocrystalline powders were obtained from SEM. It was observed that highly porous nature and agglomerates.

Keywords: perovskites, lanthanum cobalt iron oxide, nanocrystalline powders, citrate sol-gel method

Introduction

The perovskite-type oxides have received much attention in the last decade because of their potential application as electrode materials in solid oxide fuel cells, as gas sensors, in various interesting reactions, such as in the steam reforming and in the dried reforming of hydrocarbons, in the catalytic combustion and as oxygen-permeable membrances. Such materials have various advantages as wide variety of composition and constituent elements keeping essentially the basic structure unchanged, bulk structure

[1] 2PhD Candidate, Department of Chemistry, University of Yangon
[2] Lecturer, Department of Chemistry, University of Yangon
[3] Lecturer, Department of Chemistry , West Yangon University

can be characterized well, their surface can be bulk structure, their valency, stoichiometry and vacancy can be varied widely and huge information on physical and solid-state chemical properties has been accumulated (Grace *et al*., 2010).

One of the most promising active phase for environmental applications is the perovskite group of materials (ABO_3) where A and B are cations of different sizes. The catalytic properties of perovskite type oxides depend mainly on the nature of the A and B ions and on their valence states (Supachai *et al*., 2012)

Goldschmidt's tolerance factor is an indicator for the stability and distortion of crystal structures. It was originally only used to describe perovskite structure, but now tolerance factors are also used for ilmenite. Alternatively the tolerance factor can be used to calculate the compatibility of an ion with a crystal structure. The first description of the tolerance factor for perovskite was made by Victor Moritz Goldschmidt in 1926. Ideal perovskites have the ABO_3 stoichiometry and the ratio of bond length between A-O and B-O maintains a constant value which is equal to $\sqrt{2}$. The deviation from this is taken as the tolerance factor and in terms of ionic radii, it assumes:

$$t = \frac{rA + rO}{\sqrt{2}\,(rB + rO)}$$

where r_A, r_B and r_O are the ionic radii of A and B cations and oxygen, respectively. If t >1 hexagonal or tetragonal, 0.9 < t < 1 cubic, 0.71 < t < 0.9 orthorhombic / rhombohedral, < 0.71 different structures, eg. trigonal (Liu *et al*., 2008).

$LaCo_{0.6}Fe_{0.4}O_3$ perovskite nanopowder was synthesized by citrate sol-gel method. $LaCoO_3$ based materials have interesting electrical and electro catalytic properties owing to their high electronic/ionic conductivity. These materials have been prepared by many techniques which includes mechanical-synthesis, co-precipitation, solution combustion or thermal decomposition, solid-state reactions, Pechini, hydrothermal and sol-gel method. Many new methods or improvement of synthesis conditions have been tried by the researchers as the properties of the end product strongly depend on the method of preparation technique used. Here we have used citrate sol gel auto combustion method, a modified Pechini method based on the polyesterification of citric acid and ethylene glycol for the synthesis

of the title compound. The method involves relatively easy synthesis route when compared to the other conventional processes. Low operating temperature and control over the end stoichiometry are the main advantages of this technique (Unikoth *et al*., 2014).

In the present work, the preparation of the perovskite base $LaCo_{0.6}Fe_{0.4}O_3$ nanocrystalline powders by citrate sol-gel method at different temperatures. The prepared calcined powders were characterized by XRD in order to investigate phase purification and structures. The characterization of the perovskite-based $LaCo_{1-x}Fe_xO_3$ ($0.1 \leq x \leq 0.4$) nanocrystalline powders were prepared at optimum temperature by citrate sol-gel method. The prepared nanocrystalline powders were also characterized by XRD, SEM, FT IR, EDXRF, TG-DTA techniques.

Materials and Methods

All of the chemicals used were analytical grade. $La(NO_3)_3.6H_2O$ was product from China.$Fe(NO_3)_3.9H_2O$, $Co(NO_3)_2.6H_2O$ and citric acid were products from India. Ethylene glycol was product from Germany.

Various conventional and modern instruments techniques were used throughout the experimental procedure. These include Thermogravimetry /Differential Thermal Analysis (TG-DTA), X-ray Diffractometry (XRD), Energy Dispersive X-ray Fluorescence (EDXRF), Fourier Transform Infrared Spectroscopy (FT IR).

Preparation of $LaCo_{0.6}Fe_{0.4}O_3$ Nanocrystalline Powders

$LaCo_{0.6}Fe_{0.4}O_3$ nanocrystalline powder was prepared by sol-gel method using $La(NO_3)_3.6H_2O$, $Fe(NO_3)_3.9H_2O$, $Co(NO_3)_2.6H_2O$, citric acid and ethylene glycol. The precursor solution was prepared by mixing metal nitrates, citric acid and deionized water. The solution was ultra-sonicated for complete dissolution of metal cations in solution. The molar ratio of citric acid to the metal cation was 2:1. The solution was well stirred using magnetic stirrer and heated to about 60 °C. Ethylene glycol was added to the above solution in the molar ratio as 3:1 with citric acid. The resultant solution was heated and stirred on the magnetic stirrer to about 90 °C and then transferred to oil bath at 120 °C in order to form gel and finally heated at 300 °C in the furnace. Dried gels were ground and then calcined at 400 to 700°C for 4 h in air. Finally the samples were ground smoothly in an

agate mortar. $LaCo_{0.6}Fe_{0.4}O_3$ sample was also prepared by the above same method (Zahra *et al*., 2016).

Characterization Techniques

Crystal structure and phase analysis of prepared powders were performed by X-ray diffraction (XRD) using XRD-2000 diffractometer, Enraf Nonius Co., Bohemin NY, Physics Department, Yangon University. Morphology of the prepared powder was recorded by scanning electron microscope (SEM) EVO-18, ZEISS, Germany. FT IR transmission spectra in the region from 400-4000 cm^{-1} were measured by using Perkin Elmer GX system FT IR spectrophotometer. The thermal decomposition behaviours of the $LaCo_xFe_{1-x}O_3$ precursors were examined by means of thermogravimetric and differential thermal analysis (TG-DTA) by using Simultaneous TGA-DTA (DTG-6OH), Thermal analyzer, Shimadzu, Japan. Energy dispersive X-ray fluorescence (EDXRF) analysis confirms the elemental compositions of the prepared sample by using Shimadzu model EDX-8000, EDXRF spectrometer.

Results and Discussions

Characterization of the $LaCo_{0.6}Fe_{0.4}O_3$ Prepared Sample

TG-DTA analysis

Thermal decomposition of the prepared $LaCo_{0.6}Fe_{0.4}O_3$ precursor powder heated at 300°C are shown in Figures 1 and thermal stability of the prepared $LaCo_{0.6}Fe_{0.4}O_3$ nanocrystalline powders calcined at 600°C are shown in Figures 2 and their total weight loss are listed in Table 1. It was found that the prepared sample calcined at 300 °C, an endothermic peak 389°C, an exothermic peak 443°C and the weight loss was 15.071 %. It was found that the prepared sample calcined at 600 °C, the weight loss was 0.620% and the compound has thermally stability.

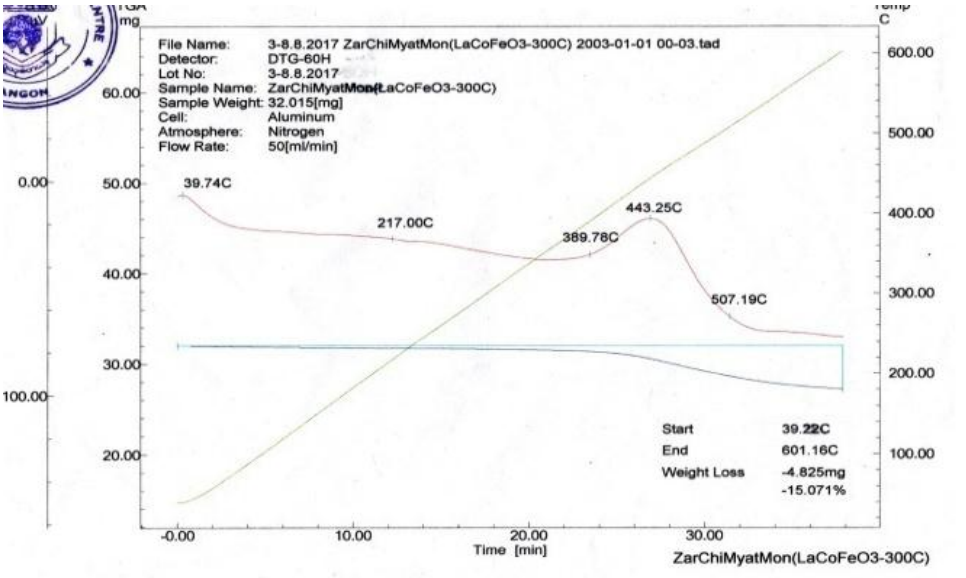

Figure 1. TG-DTA thermogram for the $LaCo_{0.6}Fe_{0.4}O_3$ heated at 300 °C

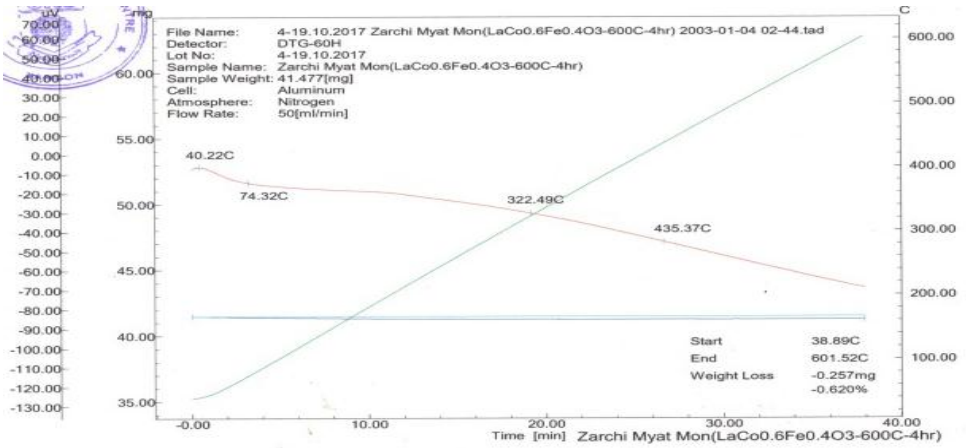

Figure 2. TG-DTA thermogram for the $LaCo_{0.6}Fe_{0.4}O_3$ calcined at 600 °C

Table 1. Thermal Analysis Data of $LaCo_{1-x}Fe_xO_3$ ($0.1 \leq X \leq 0.4$) Compounds Calcined at 600 °C for 4 Hours

Sample	Weight loss (%)
$LaCo_{0.6}Fe_{0.4}O_3$ (300 °C)	15.071
$LaCo_{0.6}Fe_{0.4}O_3$ (600 °C)	0.620

XRD analysis

The XRD patterns of the prepared samples calcined at different temperatures are shown in Figures 3-6 and XRD patterns of $LaCo_{0.6}Fe_{0.4}O_3$ powders calcined at 600°C are shown in Figures 4 and their lattice parameters and average crystallite sizes are summarized in Table 2. $LaCo_{0.6}Fe_{0.4}O_3$ was found that single phase perovskite structure was obtained after calcination at 500 °C. From XRD patterns, the prepared $LaCo_{0.6}Fe_{0.4}O_3$ powders calcined at 600 °C also showed single perovskite phase and good crystallinity. It was also found that crystal structure of the prepared samples were matched with those calculated from tolerance factor and they were found to have hexagonal crystal structure.

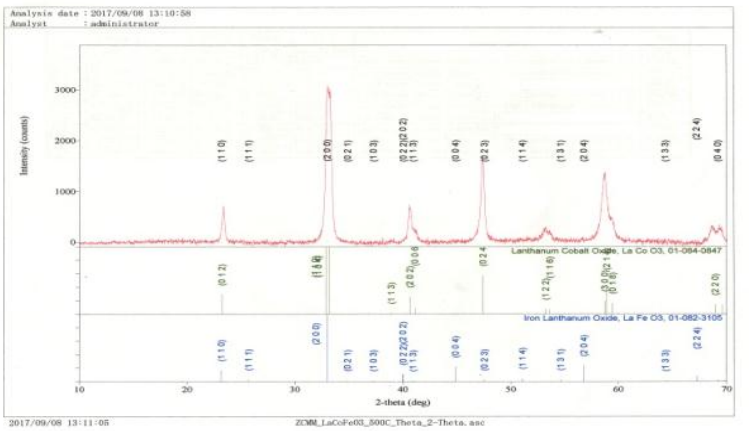

Figure 3. XRD patterns of $LaCo_{0.6}Fe_{0.4}O_3$ nanocrystalline powder calcined at 500 ° C

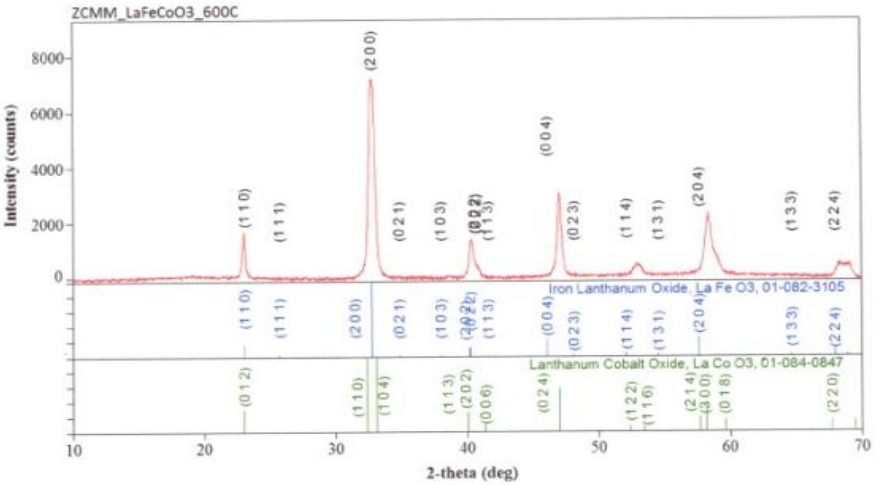

Figure 4. XRD patterns of $LaCo_{0.6}Fe_{0.4}O_3$ nanocrystalline powder calcined at 600 °C

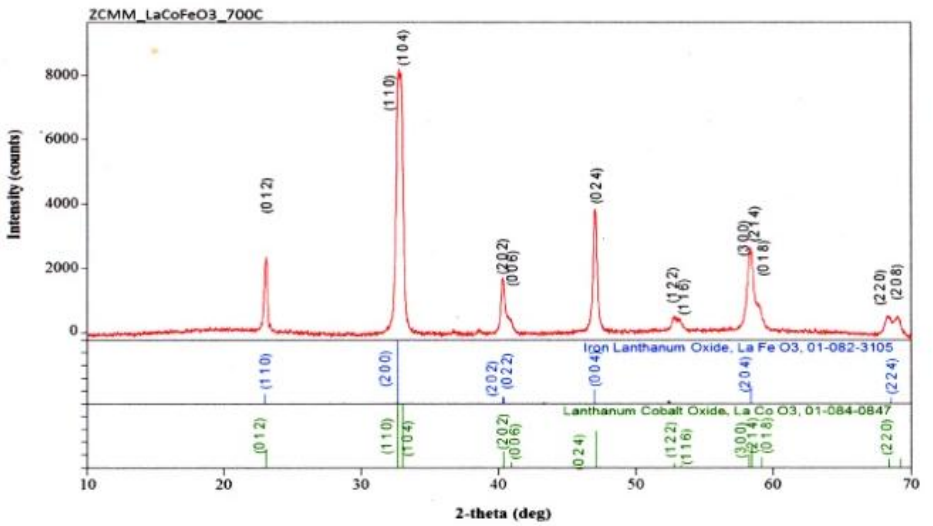

Figure 5. XRD patterns of $LaCo_{0.6}Fe_{0.4}O_3$ nanocrystalline powder calcined at 700 °C

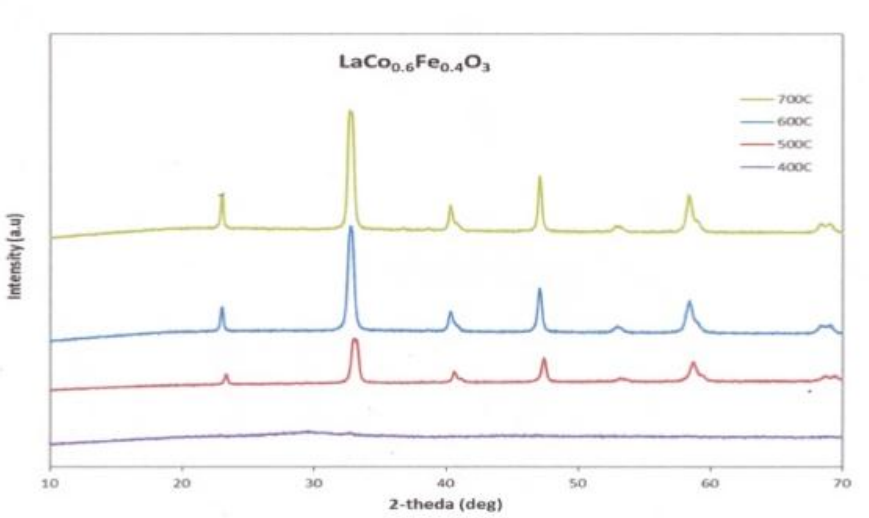

Figure 6. XRD patterns of $LaCo_{0.6}Fe_{0.4}O_3$ nanocrystalline powder calcined at different temperature

Table 2. Lattice Parameters (a and c) and the Average Crystallite Size (D) of $LaCo_{0.6}Fe_{0.4}O_3$ Powders Calcined at Different Temperature

Calcined Temperature (° C)	**Lattice Parameters**		**D / nm**
	a / Å	**c / Å**	
400	-	-	-
500	5.4438	13.1682	22.20
600	5.5281	13.0971	20.60
700	5.4822	13.2132	25.46

EDXRF analysis

The relative abundance of the elements in $LaCo_{0.6}Fe_{0.4}O_3$ nanocrystalline powders are described in Figure 7 and their relative

abundance of elements are listed in Table 3. In addition, all powder samples contain insignificant amount of other contaminating elements. On the basis relative abundance in the matrix of the samples indicate the samples contain high percentage of La, Co and Fe.

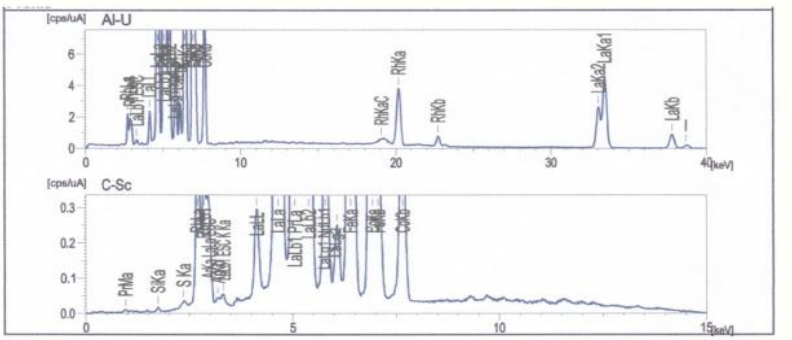

Figure 7. EDXRF spectrum of $LaCo_{0.6}Fe_{0.4}O_3$ nanocrystalline powder

Table 3. Relative Abundance of Elements in $LaCo_{0.6}Fe_{0.4}O_3$ Nanocrystalline Powders

Elements	**Relative Abundance of Elements in the Samples (%)**
La	60.818
Co	14.480
Fe	10.893

FT IR Analysis

FT IR spectrum of $LaCo_{0.6}Fe_{0.4}O_3$ nanocrystalline powders are presented in Figure 8. The small bands at 3446 cm^{-1} is assigned to stretching vibration of O-H group. The small band `due to the symmetric stretching vibrations of $–CH_2$ groups can be noticed at 2883 cm^{-1}. The characteristic band around 1633 $cm^{-1}$is assigned for C=O stretching in carboxyl or amide groups. The band 840 cm^{-1} is due to C-H bending. The bands around 650 and 400 $cm^{-1}$are characteristics of metal-oxygen bond stretching vibration.

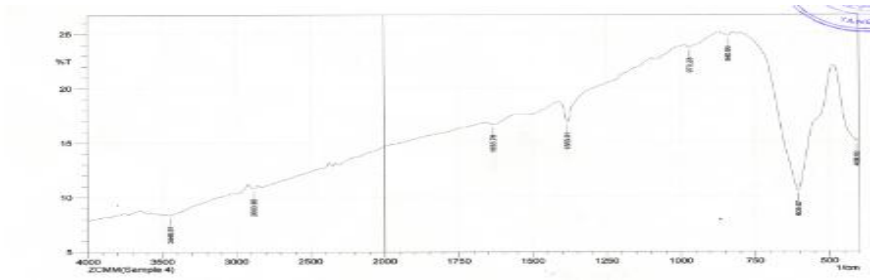

Figure 8. FT IR spectrum of the $LaCo_{0.6}Fe_{0.4}O_3$ nanopowders

SEM Analysis

SEM micrograph of the sample $LaCo_{0.6}Fe_{0.4}O_3$ is shown in Figure 9. Surface feature study of the prepared nanocrystalline powder was obtained from SEM. The microstructure of $LaCo_{0.6}Fe_{0.4}O_3$ sample was composed of small sized of grain with round shape and less agglomerates.

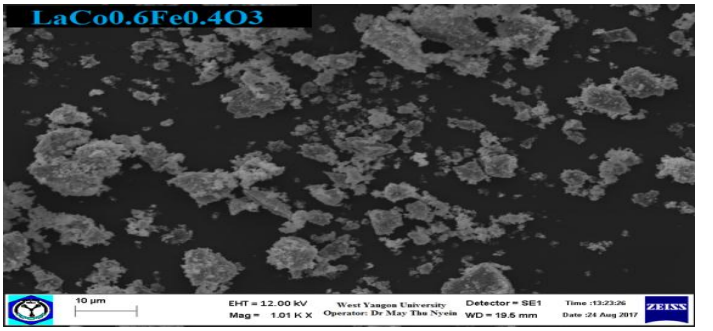

Figure 9. SEM micrograph of $LaCo_{0.6}Fe_{0.4}O_3$ nanocrystalline powder

Conclusion

$LaCo_{0.6}Fe_{0.4}O_3$ nanocrystalline powder was prepared by citrate sol-gel method at different calcination temperatures such as. XRD confirms the formation of perovskite structure and the average particle size confirms their nanosized nature. The average crystallite sizes are 22.20 nm at 500 °C, 20.60 nm at 600 °C and 25.46 nm at 700 °C. The optimum of calcination temperature was 600 °C because it had high crystallinity and average crystallite size was 20.60 nm. According to TG-DTA performance on $LaCo_{0.6}Fe_{0.4}O_3$ sample calcined at 600°C, there are no prominent weight losses observed in TG curves and there are also no prominent heat

absorbing or evolving processes found in DTA curves. From FT IR spectroscopy showed that strong absorption band appeared at 650 cm^{-1} and 400 cm^{-1} and this may be due to the stretching vibration Co-O, Fe-O and La-O group. Relative abundance of elements analysed by EDXRF showed the presence of lanthanum, cobalt and iron as major elements in the prepared samples. From the SEM micrograph, $LaCo_{0.6}Fe_{0.4}O_3$ was observed that agglomeration increase with high porosity. From above analyses, the prepared samples have desired phases, purity and structures. They will have potential for further applications.

Acknowledgements

We would like to express deep sense of gratitude to Rector Dr. Tin Maung Tun, West Yangon University for his kind provision of the research facilities. We also wish to express our profound gratitude to Dr Hlaing Hlaing Oo, Professor and Head of Chemistry Department, West Yangon University, Dr Mya Theingi, Lecturer of Chemistry Department, Yangon University and Dr Cherrt Ohn, Lecturer of Chemistry Department, West Yangon University for their encouragement and comment without which this work would not have been completed.

References

Grace, R. O. S., Santos, J. C., Martinelli, D. M. H., Pedrosa, A. M. G., Souza, M. J. B. and Melo, D. M. A. (2010). "Synthesis and Characterization of $LaNi_xCo_{1-x}O_3$ Perovskites via Complex Precursor Methods". *Materials Sciences and Applications*, vol.1, pp. 39-45

Liu, X., Hong, R. and Tian, C. (2008). "Tolerance Factor and the Stability Discussion of ABO_3-type Ilmenite". *Journal of Materials Science*: Materials in Electroncics, vol. 20(4), pp. 323-327

Supachai, S., Sricon, A. and Nuntiya, A. (2012). "Synthesis of Perovskite-Type Lanthanum Cobalt Oxide Powders by Mechanochemical Activation Method". *Science Asia*, vol. 38, pp. 102-107

Unikoth, M., Shijina, K. and Varghese, G. (2014). "Nanosized $LaCo_{0.6}Fe_{0.4}O_3$ Perovskite Synthesized by Citrate Sol-Gel Auto Combustion Method". *Processing and Application of Ceramics*, vol. 8(2), pp. 87-92

Zahra, D., Tamizifar, M., Arzani, K. and Baghshahi, S. (2016). "Synthesis and Characterization of $LaCo_xFe_{1-x}O_3$ ($0 \leq X \leq 1$) Nano-Crystal Powders by Pechini Type Sol-Gel Method". *Synthesis and Reactivity in Inorganic, Metal-Organic and Nano-Metal* Chemistry, vol. 46, pp. 25-30

Identification of Essential Oil and Some Biological Activities in the Leaves of *Citrus medica* L. (Shauk)

Myint Myint Kyi[1], Myo Min[2] & Hlaing Hlaing Oo[3]

Abstract

Citrus plants constitute one of the main valuable sources of essential oil used in food and medicinal purposes. The purpose of research work was to study some phytochemical constituents, to extract the essential oil, antimicrobial and antioxidant activities from leaves of *Citrus medica* L. (Shauk). The preliminary phytoconstituents were analysed in selected medicinal plant. The chemical constituents of essential oil from fresh leaves of *C. medica* were obtained by hydrodistillation and identified by gas chromatography-mass spectrometry (GC-MS) instrument. The results showed that the major components of the essential oil in *C. medica* leaves were limonene and citral compounds. Antimicrobial activity of crude extracts (ethanol and watery) and essential oil from *C. medica* leaves was determined against six strains of microorganisms such as *Agrobacterium tumefaciens*, *Bacillus subtilis*, *Escherichia coli*, *Pseudomonas fluorescens*, *Saccharomyces cerevisiae* and *Staphylococcus aureus* by agar disc diffusion method at Botany Department, Dagon University. All of these extracts were found to exhibit the highest inhibition zone against test organisms whereas essential oil showed the inhibition zone against *Agrobacterium tumefaciens.* The antioxidant activity was determined by using the DPPH radical scavenging method. In the screening of antioxidant activity, ethanol extract (IC_{50}= 44.39 µg/mL) was found to be more significant than watery extract (IC_{50}= 86.35 µg/mL) from the leaves of *Citrus medica* (Shauk). Both extracts showed moderate antioxidant activity when compare with standard ascorbic acid (IC_{50}= 2.68 µg/mL).

Keywords: *Citrus medica* L., phytoconstituents, essential oil, antimicrobial and antioxidant activities

Introduction

The interest in medicinal plant research has increased in recent years, especially for the treatment of pathologies of relevant social impact. Plants of the genus *Citrus* are primarily valued for their edible fruit, but

[1] Lecturer, Dr, Department of Chemistry, West Yangon University
[2] Associate Professor, Dr, Department of Chemistry, West Yangon University
[3] Professor (Head), Dr, Department of Chemistry, West Yangon University

they also have traditional medicinal value. *Citrus medica* Linn. from Rutaceae family had been used widely in Asian cuisine and also in traditional medicines, perfume and for religious rituals and offerings. The plant yields an edible fruit, though it is very acidic and is more commonly used as flavouring. The plant is occasionally cultivated in the tropics, subtropics and warm temperature zones (Xinmiao *et al*., 2015).

The fresh shoots, leaves, flowers, fruits and seeds of citron have all entered into a number of traditional medicine for the treatment of cancer, inflammation, asthma, arthritis, stomach-ache, diarrhoea, diabetes, alzheimer's diseases and intestinal parasites. Leaves of *Citrus* genus are promising source of vitamin C, carotenoids, coumarins and flavonoids. Vitamin C possesses antioxidant properties and reported on phytochemicals, pharmacological actions and health benefits of *Citrus* and its active components especially in cancer (Gurdip *et al.,* 1999). Citron fruit has been used since Roman times as a perfume, moth repellent and flavour foods. The major constituents in leaf oil are citronellal, citronellol, limonene, citronellyl acetate, citral and linallol. Limonene was the major constituent in the oil of leaves and peel while the content of the other constituents varied (Bhuiyan *et al*., 2009).

The aim of the present research is to investigate the some biological activities and extracting of essential oil from the leaves of *Citrus medica* (Shauk). This is accomplished through testing leaves extracts and essential oil for antimicrobial and antioxidant activities and identification of chemical compounds from leaves essential oil. Specific phytochemical constituents of the studied sample have been assessed as well.

Materials and Methods

The experimental works were performed at Chemistry Laboratory, in the Department of Chemistry, West Yangon University (WYU). The leaves of *C. medica* (Shauk) were collected from Alan Oak Village, Twantay Township, Yangon Region in March, 2019. Then, the samples were identified at Botany Department, WYU, Yangon. The fresh leaves were cleaned by washing with water and air dried at room temperature. Dry leaves samples were ground into powder and stored in air-tight container to prevent contaminations and kept for their phytochemicals and biological activity. All solvents and chemicals used were of analytical grade. The following instruments and materials were used for identification of

chemical compounds from essential oil and biological activity: GC-MS Autosampler (Trace 1300, ISQ-QD, Germany), Shimadzu UV-1800 Spectrophotometer, electric balance, shaker, quartz cuvette (4 mL), micropipette (1 mL), and beakers were obtained at Department of Chemistry, WYU.

Preparation of Crude Extracts

Dried leaves powdered sample (each 10 g) was separately extracted with 100 mL of ethanol and distilled water at their respective boiling point ranges for 3-4 hours by using hot extraction. Each extract was filtered through Whatman No.1 filter paper and the filtrate was concentrated under reduced pressure at 40°C. The crude extracts were kept at 4°C in storage vials for experimental use.

Phytochemical Screening

Phytochemical constituents such as alkaloids, flavonoids, phenolic compounds, organic acids, α-amino acids, carbohydrates, saponins, glycosides, tannins and reducing sugars were determined using standard procedures as described by Marini–Bettolo *et al*., 1981 and M-Tin Wa, 1972.

Extraction of Essential Oil

The fresh leaves of *Citrus medica* (100g) were used to extract the essential oil by hydrodistillation method using a round-bottomed flask at 100°C for 4 h. The oil was extracted with n-hexane in a separating funnel. The n-hexane was evaporated at 60-70°C to get the essential oil. The oil sample was stored at 0°C in air-tight container before going to GC-MS analysis. Then, The essential oil of *Citrus medica* leaves were analysed by GC-MS Autosampler.

Determination of Organic Compounds in Essential Oil from Shauk Leaves by GC-MS

Gas chromatography–mass spectrometry (GC-MS) is a method that combines features of gas chromatography and mass spectrometry to identify different substances with a test sample (Robert and Webster, 1998). Application of GC-MS includes identification and quantitation of volatile organic compounds in complex mixtures. Organic constituents in essential oil from the leaves of Shauk were detected by GC-MS Autosampler at

Chemistry Department, West Yangon University. Compound identification was done by comparing with library data and from the literature.

Screening of Antimicrobial Activity in the Leaves of Shauk (*Citrus medica* L.)

The antimicrobial activity of crude extracts (ethanol and watery) and essential oil in the leaves of *C. medica* was determined against six strains of microorganisms such as *Agrobacterium tumefaciens, Bacillus subtilis, Escherichia coli, Pseudomonas fluorescens, Saccharomyces cerevisiae* and *Staphylococcus aureus* by employing agar disc diffusion method (Madigan and Mattinko, 2005). The tests were screened at Botany Department, Dagon University.

Determination of Antioxidant Activity in Crude Extracts and Essential Oil by DPPH Free Radical Scavenging Assay

The antioxidant activity of crude extracts (ethanol and watery) and essential oil from *Citrus medica* leaves was determined by spectrophotometrically (Shimazu UV-1800) according to DPPH free radical scavenging assay (Marinova and Batchvarov, 2011). The control solution was prepared by mixing 1.5 mL of 0.002% DPPH solution and 1.5 mL of ethanol in the brown bottle. The blank solution was prepared by mixing 1.5 mL of sample solution and 1.5 mL of ethanol in brown bottle. The sample solution was also prepared by mixing 1.5 mL of 0.002% DPPH solution and 1.5 mL of test sample solution. These bottles were incubated at room temperature and were shaken on shaker for 30 min. After 30 min, the absorbance of different concentrations in tested samples was measured at λ_{max} 517 nm using spectrophotometer. Absorbance measurements were done in three times for each concentration and the mean value was obtained. The percentage of radical scavenging activity (% RSA) was calculated by the following equation.

$$\% \text{ RSA} = [A_{DPPH} - (A_{Sample} - A_{Blank})/ A_{DPPH}]x\ 100$$

Where, % RSA = % radical scavenging activity of test samples

A_{DPPH} = absorbance of DPPH in ethanol solution

A_{Sample} = absorbance of sample with DPPH solution

A_{Blank} = absorbance of sample in EtOH solution

The antioxidant power (IC_{50}) is expressed as the test substances concentration (µg/mL) that result in a 50% oxidative inhibition of the substance. IC_{50} values were calculated by linear regressive excel program. IC_{50} values of crude extracts from *C. medica* leaves are shown in Table 5 and Figure 8.

Results and Discussions

The crude extracts (ethanol and watery) in the leaves of *C. medica* L. were used to investigate for their phytochemical and biological activities. The phytochemical tests revealed that alkaloids, flavonoids, phenolic compounds, organic acids, carbohydrates, saponins, glycosides, tannins and reducing sugars were present in selected medicinal plant. α-amino acids were not detected in *C. medica* leaves.

Identification of Organic Compounds in Essential Oil from the Leaves of *C. medica* L. by GC-MS

The essential oil in fresh leaves of *C. medica* was analyzed by gas chromatography-mass spectrometry (GC-MS) Autosampler. GC-MS is the single most important tool for identification of unknown organic compounds by matching with reference spectra. The GC-MS chromatogram of essential oil from leaves of *C. medica* is shown in Figure1. Identifications were made by comparison of their retention time and m/z ratio indices with reference library data and from the literature. Chemical composition of essential oil from *C. medica* was shown in Table 1.

According to GC-MS chromatogram, the peak appear at the retention time 3.46 min with 100 % relative abundance. At this retention time, the GC-MS spectrum in Figure 2 shows the molecular ion peak at m/z 136, indicating the molecular weight of a compound to be 136 with the molecular formula $C_{10}H_{16}$. The ionic fragments of D-limonene from essential oil of *C. medica* leaves at retention 3.46 min are shown in Table 2. Therefore, it can be referred that the compound is D-limonene. Structure is shown in Figure 3.

At the retention 6.52 min, the GC-MS spectrum in Figure 4 shows the molecular ion peak at m/z 152 which indicate the molecular weight of a compound to be 152 with the molecular formula $C_{10}H_{16}O$. The ionic fragments of α-citral from essential oil *of C. medica* leaves at retention 6.52 min are shown in Table 3. Therefore, it can be referred that the compound

is α-citral in Figure 5. The GC-MS analysis of the essential oil in *C. medica* leaves showed that the major constituents are limonene and citral compounds. Citral was the key aroma component of citrus odor, flavour and content as indicative of essential oil quality.

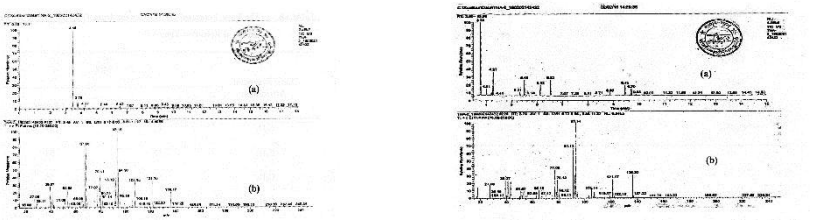

Figure 1. GC-MS chromatograms of essential oil from *Citrus medica* leaves according to (a) retention time and (b) mass to charge ratio

Table 1. Chemical Compositions of Essential Oil from Leaves of *Citrus medica* L.

Compound	Molecular Weight	Retention Time (min)
D-Limonene	136	3.46
α-Citral	152	6.52

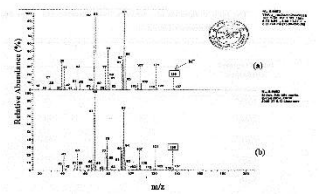

Figure 2. Mass spectra of D-limonene
(a) in leaves essential oil
(b) in library data at 3.46 min

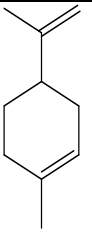

D-Limonene
Formula $C_{10}H_{16}$, MW 136,
CAS# 5989-27.5, Entry#8354
Cyclohexene, 1-methyl-4-(1-methylethenyl)-, (R):

Figure 3. Structure of D-limonene

Table 2. Ionic Fragments of D-limonene from Essential Oil of Shauk Leaves at 3.46 min

Ionic Fragment Attribution	Sample *m/z*	Library *m/z*
$C_4H_5^+$	53	53
$C_5H_8^+$	68	68
$C_6H_9^+$	93	93
$C_7H_{10}^+$	94	94
$C_9H_{13}^+$	121	121
$C_{10}H_{16}^+$	136	136

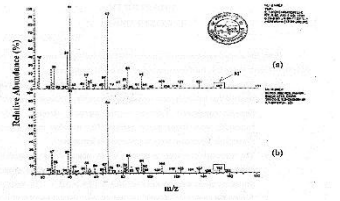

Figure 4. Mass spectra of α-citral
(a) in leaves essential oil
(b) in library data at 6.52 min

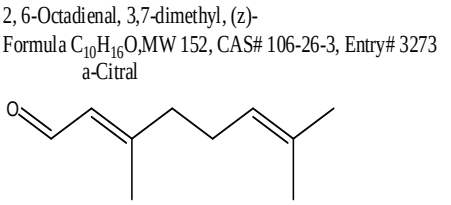

Figure 5. Structure of α-citral

Table 3. Ionic Fragments of α-citral from Essential Oil of Shauk Leaves at 6.52 min

Ionic Fragment Attribution	Sample *m/z*	Library *m/z*
C_2HO^+	41	41
$C_4H_5O^+$	69	69
$C_5H_8O^+$	84	84
$C_7H_9O^+$	109	109
$C_{10}H_{16}O^+$	152	152

Antimicrobial Activity of Crude Extracts and Essential Oil from the Leaves of *C. medica* L. (Shauk)

Screening of antimicrobial activity of crude extracts (ethanol and watery) and essential oil from leaves of *C. medica* was done by agar disc diffusion method. In this investigation, these extracts and essential oil were tested on six harmful microorganisms including *Agrobacterium tumefaciens*, *Bacillus subtilis*, *Escherichia coli*, *Pseudomonas fluorescens*, *Saccharomyces cerevisiae* and *Staphylococcus aureus*. In this experiment, the diameter of paper disc was 8 mm. The inhibition zones diameter of crude extracts and essential oil against six microorganisms tested are shown in Figure 6 and the observed data are summarized in Table 4. The larger zone diameter showed the higher antimicrobial activity of test organisms.

From these results, given in Table 4, it was observed that ethanol and watery extracts inhibited the respective test organisms inhibition zone diameters in the range between 12.06~26.02 mm and 11.54~26.36 mm against six strains microorganisms. Watery extract (26.36 mm) and ethanol extract (26.02 mm) of *C. medica* showed the largest inhibition zone diameter against *Agrobacterium tumefaciens*. Essential oil also showed the antimicrobial effect on *Agrobacterium tumefaciens* with inhibition zone diameter range 11 mm. From this investigation, it can be deduced that *C. medica* leaves may be used for the treatment of diseases infected microorganism such as fever, diarrhoea, boil, food spoilage and poisoning.

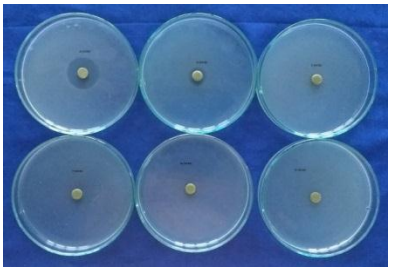

EtOH extract on test organisms

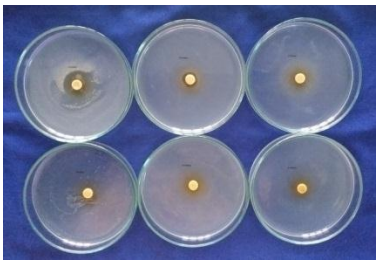

H_2O extract on test organisms

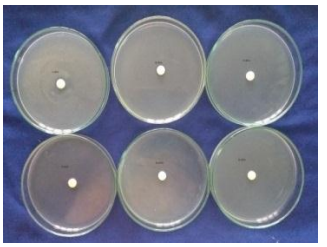

Essential oil on test organisms

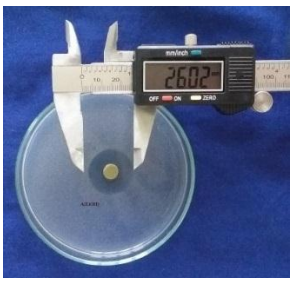

A. tumefaciens on EtOH

A. tumefaciens on H_2O

Figure 6. Photo records showing inhibition zone due to effect of extracts (EtOH and H_2O) and essential oil from leaves of *C. medica* L. (Shauk)

Table 4. Antimicrobial Activity from Leaves of *C. medica* Against Six Microorganisms

Organisms	**Inhibition Zone Diameter (mm)**		
	EtOH	**H_2O**	**EO**
Agrobacterium tumefaciens	26.02	26.36	11
Bacillus subtilis	15.42	14.62	-
Escherichia coli	13.04	14.02	-
Pseudomonas fluorescens	12.06	12.88	-
Saccharomyces cerevisiae	13.44	13.92	-
Staphylococcus aureus	-	11.54	-

EtOH = Ethanol extract ; H_2O = Watery extract ; EO = Essential oil

Antioxidant Activity of Crude Extracts from Leaves of *Citrus medica* L. (Shauk)

DPPH (2, 2-diphenyl-1-picrylhydrazyl) method is the most widely reported method for screening of antioxidant activity on many plant drugs. This method is based on the reduction of colored free radical DPPH in ethanol solution by different concentration of the samples. The antioxidant activity was expressed as 50 % oxidative inhibitory concentration (IC_{50}). In present study, seven different concentrations of each crude extracts in 95 % ethanol were measured at λ_{max} 517 nm according to the spectrophotometric method. The results of percent oxidative inhibition values of crude extracts are summarized in Table 5 and Figure 7. From the experimental results, it was found that crude extracts (EtOH and H_2O) in *C. medica* leaves had significant antioxidant activity and the concentrations were increased, the absorbance values were decreased, i.e increase in radical scavenging activity of crude extracts usually expressed in term of % inhibition. From the average value of % inhibition, IC_{50} values in µg/mL were calculated by linear regressive excel program. The IC_{50} values of ethanol and watery extracts were found to be 44.39 µg/mL and 86.35 µg/mL in the leaves of *C. medica*. Among these extracts, the lower IC_{50} showed the higher free radical scavenging activity, ethanol extract in *C. medica* leaves was found to be potent than watery extract. However, it was observed that these extracts have the moderate antioxidant activity than standard ascorbic acid (IC_{50}= 2.68 µg/mL) under condition. The antioxidant potential of crude extracts may be due to the difference in chemical structure of their phenolic and flavonoids compounds.

Table 5. Percentage of Radical Scavenging Activity (% RSA) of Crude Extracts in the Leaves of *C. medica* and Standard Ascorbic Acid

Sample	% RSA ± SD of different concentrations (µg/mL)							IC_{50} (µg/mL)
	1.5625	**3.125**	**6.25**	**12.50**	**25**	**50**	**100**	
Ascorbic Acid	45.71 ± 0.02	51.73 ± 0.02	62.85 ± 0.02	71.74 ± 0.02	78.28 ± 0.02	81.42 ± 0.03	90.57 ± 0.01	2.68

Sample	% RSA ± SD of different concentrations (µg/mL)							IC_{50} (µg/mL)
	1.5625	3.125	6.25	12.50	25	50	100	
EtOH	20.57 ± 0.02	23.14 ± 0.01	26.86 ± 0.03	31.14 ± 0.02	43.85 ± 0.02	51.78 ± 0.02	64.35 ± 0.01	44.39
Watery	11.71 ± 0.01	20.85 ± 0.01	24.17 ± 0.02	30.68 ± 0.02	33.94 ± 0.02	40.12 ± 0.01	53.71 ± 0.01	86.35

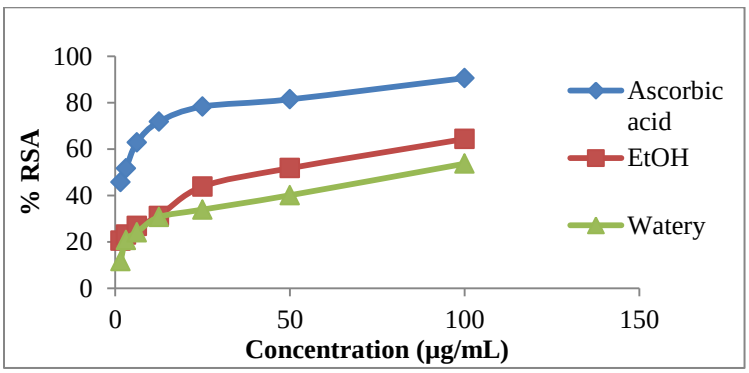

Figure 7. A plot of % RSA vs concentration (µg/mL) of crude extracts in *C. medica* leaves and standard ascorbic acid

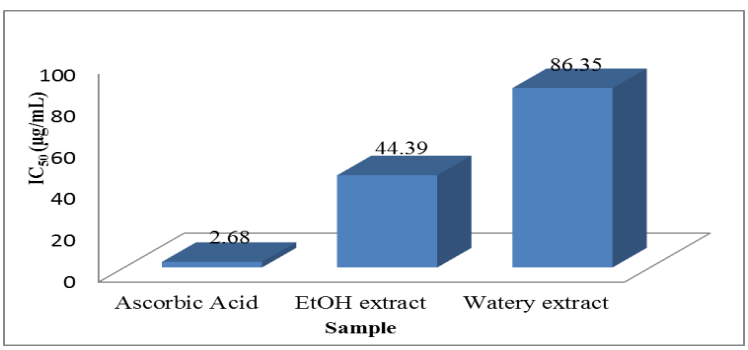

Figure 8. A bar graph of IC_{50} value of ascorbic acid and crude extracts in *C. medica* leaves

Conclusion

From the overall assessment of the chemical and biological investigation in *C. medica* leaves, following inferences could be deduced. Phytochemicals such as alkaloids, flavonoids, phenolic compounds, organic acids, carbohydrates, saponins, glycosides, tannins and reducing sugars were present in *C. medica* leaves.

The chemical constituents of essential oil from *C. medica* leaves were identified by gas chromatography-mass spectrometry (GC-MS) method. By GC-MS analysis, D-limonene (3.46 min) and α-citral (6.52 min) were found in essential oil of *C. medica* leaves. The mass fragmentations (*m/z* value) of each compound were compared with reference library data.

The antimicrobial activity of crude extracts (ethanol and watery) and essential oil in *C. medica* leaves was tested on six strains of microorganisms by agar disc diffusion method. According to the results, the higher antimicrobial activity was observed in ethanol and watery extracts in leaves of *C. medica* whereas essential oil possessed low activity on test organisms.

In vitro antioxidant activity of ethanol and watery extracts in *C. medica* leaves was performed by DPPH assay. According to the experiment, the IC_{50} value of ethanol and watery extracts were observed at 44.39 µg/mL and 86.35 µg/mL respectively. However, the antioxidant activity of crude extracts was observed to the moderate effect than standard ascorbic acid (IC_{50}= 2.68 µg/mL). Therefore, the results of the present study indicate that *C. medica* leaves can be used as raw materials for production of insecticides, medicines and flavouring ingredients.

Acknowledgement

The authors would like to express their profound gratitude to the Ministry of Education, Department of Higher Education, for provision of opportunity to do this research for allowing to present this paper.

References

Bhuiyan, M. N. I., J. Begum, P. K. Sardar and M. S. Rahman. (2009). Constituents of peel and leaf essential oil of *Citrus medica* L. *J. Sci. Res*. **1** (2) 387-92

Gurdip, S., I. P. S. Kapoor and P. S. Om. (1999). *J Essential Oil-Bearing Plants*. **2** (3), 119

Madigan M. and J. Mattinko (editors). (2005). *Brock Biology of Microorganisms*. New Jersey : 11th Ed., Prentice Hall, ISBN 0-13-144329-1

Marini-Bettolo, G. B., M. Nicolettic and M. Patamia. (1981). "Plant Screening by Chemical and Chromatographic Procedure Under Field Conditions". *J. Chromato*., **45**, 121-123

Marinova, G. and V. Batchvarov. (2011). "Evaluation of the Methods for Determination of the Free Radical Scavenging Activity by DPPH". *Bulg. J. Agric. Sci*., **17**, 11-24

M- Tin Wa. (1972). "Phytochemical Screening Methods and Procedures". *Phytochemical Bulletin of Botanical Society of America*, **5** (3), 4-10

Robert, M. S. and F. X. Webster. (1998). *Spectrometric Identification of Organic Compounds*. New York : 6th Ed., John Wiley & Sons, 367-370

Xinmiao, L., S. Zhao, Z. Ning, H. Zeng, Y. Shu, O. Tao, C. Xiao, C. Lu and Y. Liu. (2015). "*Citrus* Fruits as a Treasure Trove of Active Natural Metabolites that Potentially Provide Benefits for Human Health". *Chemistry of Central Journal*, **9**, 68

Investigation of Phytonutrients and Bioactive Properties of *Oroxylum Indicum* Linn. (Kyaung-Sha) Leaf

Aye Aye Than[1] & Myo Min[2]

Abstract

The present research deals with the some chemical nutrient and antimicrobial activity of *Oroxylum indicum* (Linn.)Vent. (Kyaung sha) leaves. Kyaun sha is known as one of the Myanmar indigenous medicinal plants. Preliminary qualitative phytochemical investigation of Kyaung sha leaf sample was carried out by Test Tube Methods. In the phytochemical tests, the presence of alkaloids, phenolic groups, carbohydrates, flavonoids, saponins, cyanogenic glycoside, glycosides, α-amino acids, reducing sugars, and tannins were found in the leaf sample. But the steroids were not observed. The semi-quantitative elemental analysis of the leaf samples were performed by ED-XRF methods. According to the elemental analysis, potassium and calcium were detected as the major constituents and Mn, Cu and Zn as minor trace elements in the leaf sample. *In vitro* antimicrobial activity of the different crude extract (MeOH, EtOAc, EtOH and H_2O) were screened by using agar well diffusion method against *Bacillus subtilis*, *Staphylococcus aureus*, *Pseudomonas aeruginosa*, *Bacillus pumilus*, *Candida albican*s and *Escherichia coli* species. The antioxidant activities of the ethanolic extracts from *Oroxylum indicum* Linn leaf were determined by DPPH method. The value of IC_{50} of the ethanolic extract was found as 4.25 μg / mL. The IC_{50} value of the ethanolic extract from the leaf sample was compared with that of standard ascorbic acid which has IC_{50} value of 3.8 μg / mL. Therefore, *Oroxylum indicum* Linn leaf possesses the rich antioxidant properties. According to the phytochemical and antioxidant properties, *Oroxylum indicum* leaf may be used not only food but also medicinal plant for human health.

Keywords: *Oroxylum indicum (Linn.), phytochemical analysis, ED-XRF, antimicrobial activity, antioxidant activity*

[1] Assistant Lecturer, Department of Chemistry, West Yangon University

[2] Associate Professor, Dr., Department of Chemistry, West Yangon University

Introduction

Oroxylum indicum (Linn) Vent. (Kyaung Sha)

Kyaung sha is known as one of the Myanmar indigenous medicinal plants. It's also known as Muhudie or Indian Trumpet flower. It is widely used by the Indians for the treatment of various ailments. The plant is known to be used in Haemorrhoids, Flatulence, as an expectorant, Leprosy, Diarrhoea, Dyspepsia, Cough, Vomitting, Abscess, Asthma, Migraine, Gynaecological diseases, improves appetite. It is so known as a potential anticancer medicinal plant (MaO, 2002).

The tree is also a night-bloomer and is pollinated naturally by bats. Additionally, after the large leaf stalks wither, they fall off the tree and collect near the base of the trunk, appearing to look like a pile of broken limb bones. Leaves of tree are very large (90-180cm long) and 2-3 pinnate. Leaflet rachis is very soft and swollen at the junction of the branches. Leaflets are in 2-4 pairs, ovate, elliptic or acuminate in shape and glabrous in texture (Colone, 1935).

Scientific Classification

Family	:	Bignoniaceae
Genus	:	Oroxylum Vent
Botanical Name	:	*Oroxylum indicum* (Linn.) Vent.
Myanmar Name	:	Kyaung Sha
English Name	:	Indian Trumpet flower, Muhudie

Figure 1. Fruits and leaves of *Oroxylum indicum* (kyaung sha)

Materials and Methods

Kyaung sha leaves were collected from Hlaing Thar Yar Township, Yangon Region. Firstly, phytochemical investigation of *Oroxylum indicum* (Kyaung sha) leaf was carried out by Test Tube method (Solomons, 1996). Then, semi-quantitative elemental analysis of the leaf sample was performed by EDXRF method (Griken, R.V, 1986). The nutritional values of the leaf sample were determined by AOAC method (AOAC, 2000). Antimicrobial activity of the sample was screened by agar well diffusion method (Mar Mar Nyein, *et al*., 1991).

Results and Discussion

Phytochemical Constituents of *Oroxylum indicum* (Kyaung Sha)

Kyaung sha leaf showed the presence of alkaloids, phenolic compound, carbohydrates, steroids, cyanogenic glycosides, glycosides, α-amino acids, flavonoids, saponnins, terpenoids, reducing sugars and tannins. But steroids were not observed in the leaf sample. The results were shown in Table 1.

Semi-quantitative Elemental Analysis of *Oroxylum indicum* (Kyaung Sha)

Mineral elements present in dried powder samples of leaf was determined by ED-XRF spectrometer (Shimadsu-EDX-8000). The resultant ED-XRF spectrum is illustrated in Figure 1. And the relative composition of the elements predominantly found in the sample is presented in Table 2. K and Ca which are bulk minerals and trace mineral elements.

Nutritional Values of *Oroxylum indicum* (Kyaung Sha) Leaf

The determination of nutritional values of leaf sample was carried out by AOAC method. It was found that the amount of moisture, carbohydrates and fiber were highest in the leaf sample. Protein is higher than fibre. The results are shown in Table 3.

Table 1. Results of Phytochemical Investigation of *Oroxylum indicum* (Kyaung sha) Leaf

No.	Constituents	Extract	Test reagent	Observations	Remark
1	Alkaloids	1% HCl	Dragendroff's reagent	Orange ppt,	+
			Mayer reagent	White ppt,	+
			Sodium picrate solution	Reddis hbrown	+
2	α-amino acids	H_2O	Ninhydrin	Purple spot	+
3	Carbohydrates	H_2O	10% α-naphthol, conc: H_2SO_4	Red ring	+
4	Cyanogenic glycoside	Dil H_2SO_4	Sulphuric acid, sodium picrate	No ppt	+
5	Flavonoids	EtOH	Mg turning, conc: HCl	Pink colour	+
6	Glycosides	H_2O	10% Lead acetate solution	White ppt	+
7	Phenolic compounds	H_2O	5% $FeCl_3$ solution	Green solution	+
8	Saponins	H_2O	Distilled water	Frothing	+
9	Steroids	PE	Acetic anhydride, conc: H_2SO_4	Green	-
10	Tannins	H_2O	2% gelatin solution	White ppt	+
11	Terpenoids	$CHCl_3$	Acetic anhydride, conc: H_2SO_4	Pink colour	+

(+) present, (-) absent

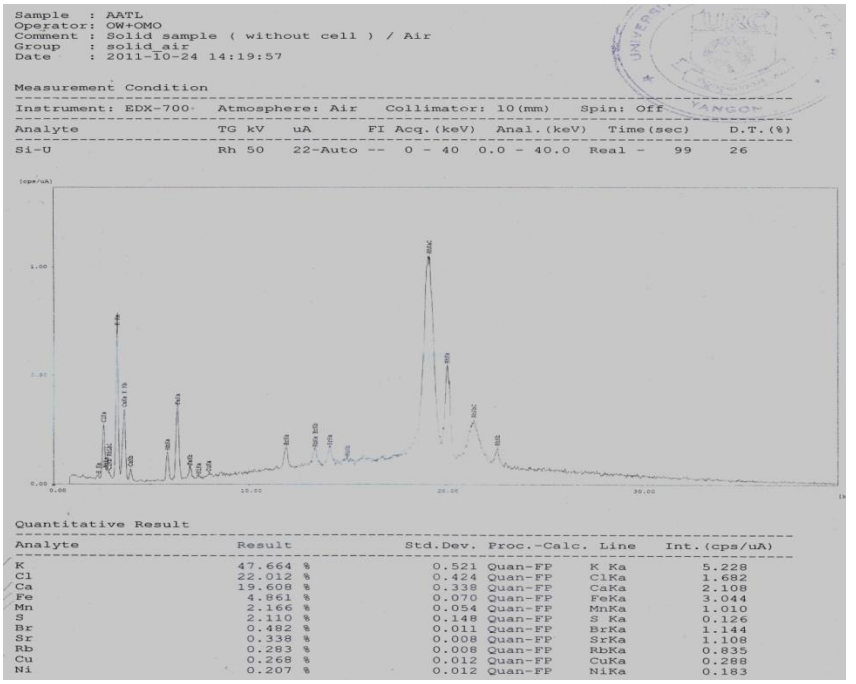

Figure 1. ED-XRF spectrum of *Oroxylum indicum* (Kyaung sha) leaf

Table 2. Relative Composition of Elements of *Oroxylum indicum* (Kyaung sha) Leaf

Analytes	**Composition (%)**
K	47.664
Ca	19.608
Mn	2.166
Fe	4.861
Cu	0.268

Table 3. Nutritional Values of *Oroxylum indicum* (Kyaung sha) Leaf

Nutrient	Content (%)
Moisture	7.7
Ash	1.86
Protein	4.31
Crude fiber	4.18
Crude fat	0.00
Carbohydrate	11.88

Antimicrobial Activity of *Oroxylum indicum* (Kyaung sha) Leaf

Antimicrobial Activities of MeOH, EtOAc, EtOH and H_2O extracts were screened by agar well diffusion method. In this investigation, the samples were tested on six species of microorganisms; *Bacillus subtilis, Staphylococcus aureus, Pseudomonas aeruginosa, Bacillus pumilus, Escherichia coli* and *Candida albicans* species.

H_2O extract did not show the activity on *Bacillus subtilis*. All other extracts showed antimicrobial activity with all microorganisms. Although all the extract possesses antimicrobial activity, they showed low activities. The results are shown in Figure 2 and Table 4.

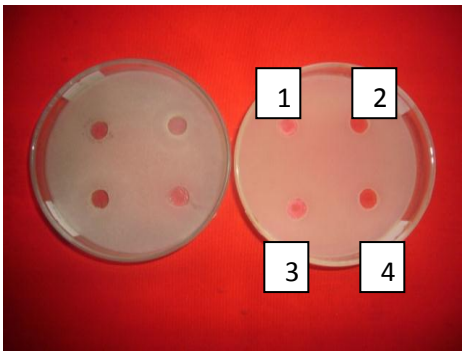

Bacillus subtilis

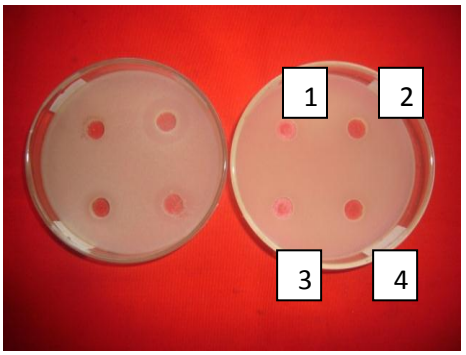

Staphylococcus aureus

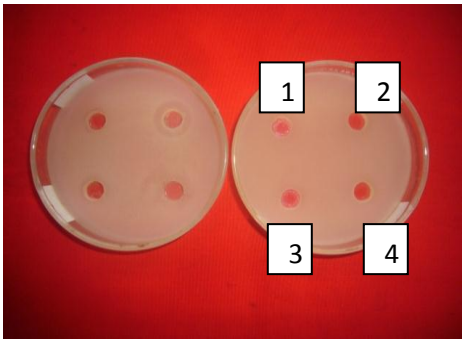

Pseudomonas aeruginosa

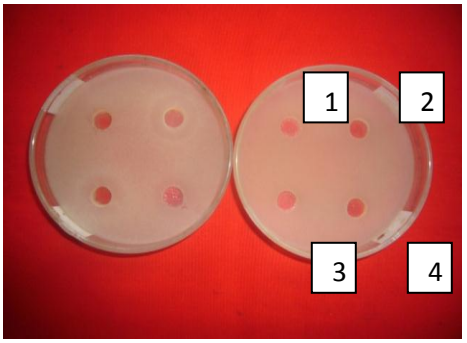

Bacillus pumilus

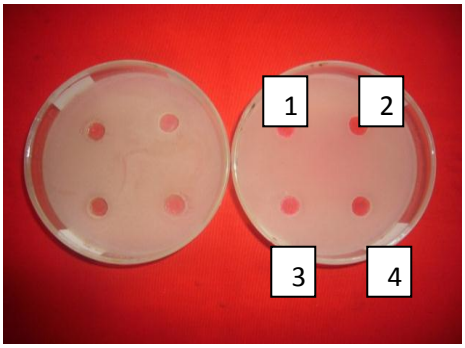

Escherichia coli

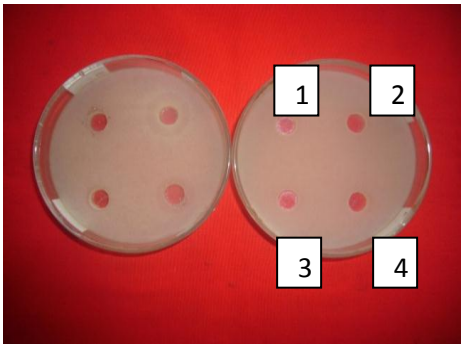

Candida albicans

(1) = MeOH extract (2) = EtOAc extract (3) = EtOH extract
(4) = H_2O extract

Figure 2. Antimicrobial activities of different extracts from kyaung sha leaf

Table 4. Antimicrobial Activities of Different Extracts from Kyaung Sha Leaf

Extract	*B. subtilis*	*S. aureus*	*P. aeruginosa*	*B. pumilus*	*E. coli*	*C. albicans*
MeOH	(+)	(+)	(+)	(+)	(+)	(+)
EtOAc	(+)	(+)	(+)	(+)	(+)	(+)
EtOH	(+)	(+)	(+)	(+)	(+)	(+)
H_2O	-	(+)	(+)	(+)	(+)	(+)

Agar well (diameter) ~ 10 mm, 10 mm – 14 mm = (+)

15 mm – 19 mm = (++), 20 mm – above = (+++)

Antioxidant Activity of Ethanolic Extract of *Oroxylum indicum* (Linn.) Leaf by DPPH Assay Method

70% ethanolic extracts of leaf samples of *Oroxylum indicum* Linn. were available for antioxidant activity by DPPH assay method. Ascorbic acid was used as standard sample. Five kinds of concentrations of leaf and bark samples; 0.625 μg mL^{-1}, 1.25 μg mL^{-1}, 2.5 μg mL^{-1}, 5 μg mL^{-1} and 10 μg mL^{-1} were prepared by dilution with ethanol as solvent. The absorbance values of standard ascorbic acid and the samples were described in Table 5 and Figure 3. Determination of absorbance of control solution, blank solutions, sample solutions and standard ascorbic acid solutions were carried out at wavelength 517 nm using spectrophotometer. The percent inhibition values of the leaf samples were described in Table 6 and Figure 4. From the values of % inhibition, IC_{50} values (50% inhibition concentration) were calculated by computer program. IC_{50} value of standard ascorbic acid was 3.8 μg / mL and IC_{50} value of leaf sample was 4.25 μg / mL respectively. It was found that both samples of 50% inhibition were larger than standard ascorbic acid so less potent antioxidant activity.

Table 5. % RSA of DPPH Free Radical by Ascorbic acid with Absorbance at 517 nm

Concentration (µg/mL)	%RSA	Absorbance	IC_{50} (µg/mL)
0.3125	10.099	0.242	3.8
0.625	15.198	0.226	
1.25	22.93	0.194	
2.5	45.183	0.162	
5	76.063	0.054	
10	99.407	0.023	

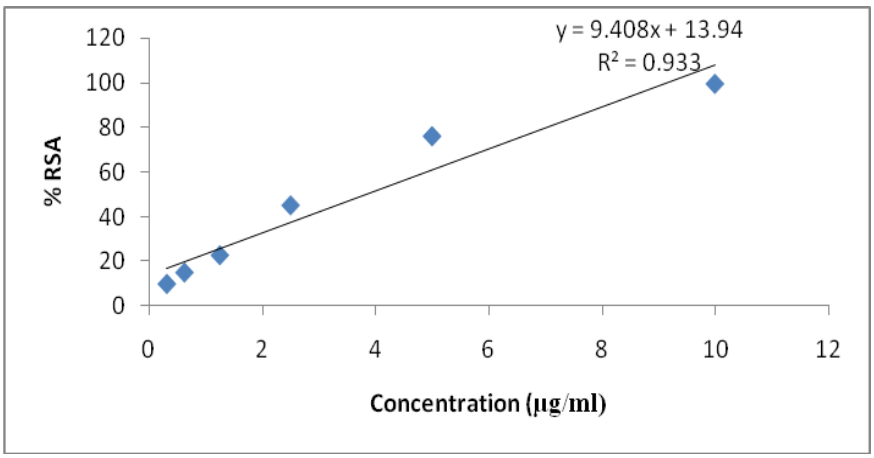

Figure 3. Correlation between DPPH radical scavenging activity and concentration of ascorbic acid at 517 nm

Table 6. % RSA of DPPH Free Radical by Ethanolic Extracts of *Oroxylum indicum* (Linn.) Leaf with Absorbance at 517 nm

Concentration (µg/mL)	%RSA	Absorbance	IC_{50} (µg/mL)
0.3125	48.37	0.399	4.25
0.625	50.12	0.348	
1.25	50.29	0.340	
2.5	56.8	0.315	
5	58.52	0.252	
10	64.74	0.209	

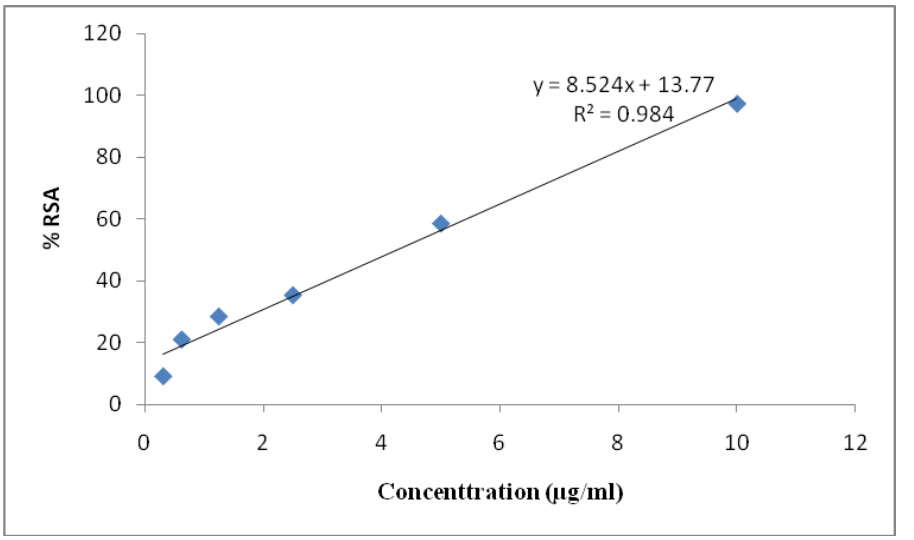

Figure 4. Correlation between DPPH radical scavenging activity and concentration of ethanolic extract of *Oroxylum indicum* (Linn.) leaf at 517 nm

Conclusion

From the phytochemical investigation, alkaloids, phenolic compounds, carbohydrates, flavonoids, cyanogenic glycoside, glycosides, α-amino acids, reducing sugars, saponins and tannins were observed to be present. Steroids were not found. So that, it can be observed that the above elements and phytochemical results may be important for human health. By using ED-XRF method, leaf sample contains K (47.66%), Ca (19.60%), P (9.17%), Fe (4.86%), S (2.11%), Cl (22.01%), Mn (2.16%), Br (0.48%), Sr (0.33%), Rb (0.28 %), Cu (0.46%) and Ni (0.20%) respectively. The element Potassium is an extremely important element in the human body. Calcium is important in building and maintaining strong bones and teeth. Kyaung sha leaf sample were found to contain moisture (7.7%), total ash (1.86%), protein (4.31%), crude fibre (4.18%), fat (0.00%), carbohydrates (11.88%) and energy values (65.84 kcal/100g) of energy respectively. From the antimicrobial activity of Kyaung sha leaf, H_2O extract did not show the activity on *Bacillus subtilis*. All other extracts showed antimicrobial activity with all microorganisms. Although all the extract possesses antimicrobial activity, they showed low activities. In the screening of antioxidant activity of the leaf sample, ascorbic acid was used as the standard. From the screening, IC_{50} values of standard ascorbic acid and leaf extract were 3.8 μg / mL and 4.25 μg / mL respectively. Therefore, *Oroxylum indicum* (Kyaung sha) leaf possesses the antioxidant property. Since *Oroxylum indicum* (Kyaung sha) leaf samples are rich in nutritional values. They also possess antimicrobial and antioxidant properties. Therefore, kyaung sha leaf may be used in the nutritional food and medicinal formulation for the human health.

Acknowledgement

We would like to express deep sense of gratitude to Rector Dr. Tin Maung Tun, West Yangon University for his kind provision of the research facilities. We also wish to express our profound gratitude to Dr Hlaing Hlaing Oo, Professor and Head of Chemistry Department and Dr. Myo Min, Associate Professor of Chemistry Department, West Yangon University for their encouragement and comment without which this work would not have been completed.

References

AOAC .(2000). Official methods of analysis of the Association of Official Analytical Chemists 15th Edition. Washington, DC.

Colonel K.R .(1935). "Indian Medicinal Plants", An I.C.S., **3**, 1839-1840.

Griken, R.V. (1986). "Energy Dispersive X-Ray Spectrometry", Department of Chemistry, University of Antwer (UIA), B2610 Antwerp, Wilrijk, Belgium.

Mar Mar Nyein, Chit Maung, Mya Bwin and Tha, S.J. (1991). "*In Vitro* Testing of Various Indigenous Plant Extracts on Human Pathogenic Bacteria", *Myanmar Health Science Research Journal*, **3**, 89-99.

MaO, A.A. (2002). "*Oroxylum indicum* Vent. A potential Anticancer Medicinal Plant", *Indian Journal of Traditional Knowledge* **1,** 17-21.

Solomons, T. W. (1996). "Organic Chemistry", John wiley and Sons, Inc., New York, 895.

Investigation of Tannins, Total Phenolics Contents, Flavonoids Contents, and Biological Properties of *Cleome viscosa* L. Leaves

Suu Suu Win[1], Moe Tin Khaing[2], Nyein Nyein Htwe[3] & Kathy Myint Thu[4]

Abstract

The main aim of this paper is to investigate the phytochemicals, contents of tannins, total phenolics, flavonoids, and biological properties including antimicrobial and antioxidant activities of *Cleome viscosa* leaves (Hingala-yine) which collected from Nyaung Kone Village, Sagaing Region, Myanmar. The sample was extracted with ethyl acetate, methanol and water.The phytochemicals investigation of collected sample was carried out by standard procedures. Tannin content was examined by titrimetric method and ethyl acetate, methanol and water crude extracts of total phenol content was determined by Folin-Ciocalteu Reagent (FCR). Then, total flavonoids contents of sample were determined by using the aluminium chloride colorimetric method. In addition, antimicrobial activity of five crude extracts of sample was examined by agar well diffusion method using selected six organisms. Moreover, antioxidant activity of ethyl acetate, methanol and water crude extracts of sample was performed by 2, 2-diphnyl-1- picrylhydrazyl (DPPH) radical scavenging assay. This investigation informs *Cleome viscosa* leaves which possess a potent source of bioactive constituents and natural antioxidant properties.

Keywords: *Cleome viscosa*, Tannins, Total phenolics, Total flavonoids, Antimicrobial and Antioxidant properties

Introduction

The collected sample, *Cleome viscosa* is a weed distributed throughout the tropics of all over the world and Myanmar. It is annual, sticky herb which obtains a height; up to 120 cm. This plant is prominent by its long slender pods and yellow flowers involving seeds that are similar to mustard with strong emitting odour.

[1] Associate Professor, Dr., Department of Chemistry, Sagaing University of Education
[2] Associate Professor, D., Department of Chemistry, Myitkyina University
[3] Lecturer, Dr., Department of Chemistry, Sagaing University of Education
[4] Professor and Head, Dr., Department of Chemistry, Sagaing University of Education

Moreover, flowering occurs from May to September and fruiting in August to November. The whole plant is sticky in nature and has a strong odour resembling asafoetida. In India, the natives and traditional healers use *C. viscosa* for many therapeutic purposes. This plant is used to treat various disorders containing diarrhoea, fever, inflammation, liver diseases, bronchitis, ulcers, skin diseases and malarial fever. Whole plant and its various parts such as leaves, seeds, and roots are widely employed in folkloric systems of medicine for the treatment of various ailments and rheumatism.

Fresh leaves of *C. viscosa* are used as vegetable and very effectively to treat respiratory tract infections, wounds and jaundice in the folk medicines. Leaves juice is also used to relieve piles, lumbago, earache and eyesore. The sap of leaves mixed with water or milk is applied to the eye in Java. Both leaves and seed oil is used for various veterinary. The seeds of *C. viscosa* are used in curries and are also mixed to tobacco to increase narcotic quality. The seeds consist of alkaloids, 18.3% oil, a mixture of amino acids, fatty acids, and sucrose, Linoleic, stearic, and oleic acids are found in the oil (Mali, 2010; Singh et al., 2015). So, the leaves of *Cleome viscosa* are chosen for this study.

Materials and Methods

Sample Collection and Preparation

Fresh leaves of C*leome viscosa* were collected from Nyaung Kone Village, Sagaing Region, Myanmar. The collected sample was washed thoroughly with distilled water to remove impurity. It was dried in air at room temperature and cut into pieces and grounded by electric blender. It was stored in a well-stoppered bottle and used throughout this research.

C*leome viscosa* was taxonomically identified by authorized Botanist, Professor, Dr. Soe Myint Aye, Botany Department, and University of Mandalay. (Figure-1)

Botanical description of selected sample

Family name	:	Cleomaceae
Scientific name	:	*Cleome viscosa* L.
Genus	:	*Cleome*

Species : *Cleome viscosa*
Myanmar name : Hingala-yine
Part used : Leaves

Figure 1. Plant of C*leome viscosa*

Determination of Phytochemical Constituents

Phytochemical test of C*leome viscosa* leaves was undertaken by using standard methods to know the presence or absence of alkaloids, flavonoids, phenolics, amino acids, carbohydrates, reducing sugars, glycosides, tannins, saponins, steroids, and terpenes, respectively (Harborne, 1998).

Determination of Tannins content

Tannins content of C*leome viscosa* leaves determination was done by titrimetric method using Indigo solution. Indigo carmine (0.6g), distilled water (50 mL) and concentrated sulphuric acid (5 mL) was mixed and shaken and then volume make up to (100 mL) with distilled water. (Atanassova & Christova-Bagdassarian, 2009)

Blank Titration and Sample Titration

Indigo solution (5 mL) was mixed distilled water (150 mL) and then titrated with 0.1N $KMnO_4$ solution until the green colour observed at end-point. Sample solution (5 mL), Indigo solution (5 mL) and distilled water (150 mL) were mixed and then titrated with 0.1 N $KMnO_4$ solutions until the golden yellow colour was observed at end-point. All samples are analysed three times. The tannins content (T%) in the sample can be calculated by using following equation:

$$T\% = \frac{(V\text{-}Vo) \times (0.004157 \times (250) \times (100)}{(5) \times g}$$

V = volume of 0.1 N $KMnO_4$ for the titration of sample solution

V_0 = volume of 0.1 N $KMnO_4$ for the titration of blank solution

(0.004157) = tannin equivalent in 1 mL of 0.1 N $KMnO_4$

(250) = mL of water to extract the sample

(5) = mL of extract sample solution for titration

g = mass of the sample taken for the analysis

Determination of total phenolics content

Ethyl acetate, methanol, and water extracts of C*leome viscosa* leaves were used for the determination of total phenolics content. Each solvent extract solution (0.2 mL) and Folin–Ciocalteu reagent solution (0.2mL) were mixed thoroughly. After 4 minutes, (1 mL) of 15% Na_2CO_3 was added, and then the mixture was allowed to stand for 2 hours at room temperature. The absorbance of this solution was recorded at 760 nm using Ultraviolet spectrophotometer. The concentration of the total phenolics was determined as mg of gallic acid equivalent by using an equation observed from gallic acid calibration curve. The evaluation of total phenolics in three solvent crude extracts was performed in triplicate and the results were averaged. (Eghdami & Sadeghi, 2010)

Determination of total flavonoids content

Total flavonoids contents of ethyl acetate, methanol, and water extracts of C*leome viscosa* leaves were determined by using the aluminium chloride colorimetric method with some modifications. Methanol extracts (0.5 mL), 10% aluminium chloride (0.1 mL), 1 M potassium acetate (0.1 mL) and distilled water (4.3 mL) were mixed at room temperature for 30 minutes. The absorbance of this mixture was measured at 415 nm using Ultraviolet spectrophotometer. Quercetin was used to show the calibration curve for the determination of total flavonoids. The determination of total flavonoids in three solvent crude extracts was done in triplicate and the results were averaged. (Eghdami & Sadeghi, 2010)

Determination of Antimicrobial Activity by Agar Well Diffusion Method (Valgas et al., 2007)

Antimicrobial activities of five crude extracts such as petroleum ether, ethyl acetate, ethanol, methanol and water extracts of C*leome viscosa* leaves were tested by agar well diffusion method against six microorganisms including *Bacillus pumilus, Bacillus subtilis, Escherichia coli, Pseudomonas aeruginosa, Staphylococcus aureus* and *Candida albicans*. Antimicrobial activity was examined at Pharmaceuticals and Food Research Department, Yangon. The antimicrobial activity was evaluated by measuring zone diameters of inhibition of microorganism's growth surrounding the sample extracts. (Valgas et al., 2007)

Determination of Antioxidant Activity by DPPH Radical Scavenging Assay

Preparation of DPPH solution

DPPH powder (2.346 mg) was added in (100 mL) of ethanol (Analar grade). This solution was thoroughly mixed at room temperature and it was stored in brown colored flask. This solution was kept for no longer than 24 hours. (Wojdylo et al., 2007)

Preparation of standard solution

Ascorbic acid (2mg) was dissolved in (20 mL) of ethanol (Analar grade). This solution was thoroughly mixed at room temperature to obtain (100 μg/mL) of standard solution.

Ascorbic acid solution (1 mL) and DPPH solution (3 mL) were thoroughly mixed for about 15 minutes at room temperature. The absorbance of the mixture was measured at 517 nm. The sample (0.004g) was dissolved in (20 mL) ethanol (Analar grade). This solution was thoroughly mixed at room temperature for (15) minutes to obtain (200 μg/ mL) of sample solution. The concentrations of standard solution (0.62, 1.25, 2.50, 5.00, 10.00, 20.00 μg/mL) were determined by using parallel dilution method. Sample solution (1mL) and (3) mL of DPPH solutions were thoroughly mixed for about 15 minutes at room temperature. The absorbance of the mixture was measured at 517 nm using UV Spectrophotometer. The capability of percent radical scavenging activity (%RSA) was calculated using the following equation:

$$\%RSA = \frac{A_{control} - A_{sample}}{A_{control}} \times 100$$

Where, $A_{control}$ = Absorbance of control DPPH solution

A_{sample} = Absorbance of sample solution

The antioxidant potency or IC_{50} (50% inhibitory concentration) values is evaluated by using the curve of %RSA values against concentration of test sample with linear regressive excel program. IC_{50} value is a measure of the effectiveness of a substance in inhibiting a specific biological or biochemical function.

Results and Discussion

Phytochemicals of *Cleome viscosa* Leaves

The experimental results of phytochemicals of *Cleome viscosa* leaves contained alkaloids, flavonoids, terpenes, tannins, glycosides, phenolics, reducing sugars, saponins, carbohydrates, and amino acids.

Tannins content of *Cleome viscosa* leaves

The yield percent of tannins content for *Cleome viscosa* leaves was found to be 2.19%. According to this result, the yield percent of selected sample (edible leaves) agrees with literature survey for edible fruits. So, *Cleome viscosa* leaves should be edible and used as useful medicine for human health. Result for yield percent of tannins content of *Cleome viscosa* leaves was described in Figure 2.

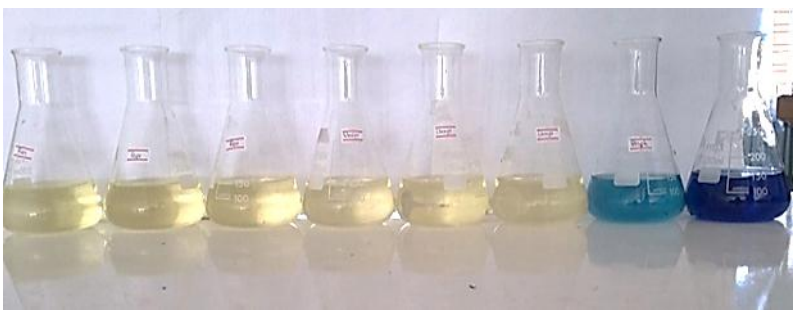

Figure 2. Result for yield percent of Tannins Content

Total Phenolics Content of Crude Extracts of *Cleome viscosa* Leaves

The total phenolics content of ethyl acetate, methanol and water extracts of *Cleome viscosa* leaves were examined using the diluted Folin-Ciocalteu Reagent (FCR). Standard curve of Gallic acid Figure 3 is needed to evaluate the total phenolics content. Because gallic acid is 3, 4, 5-trihydroxy benzoic acid and it is one kind of phenol compounds.

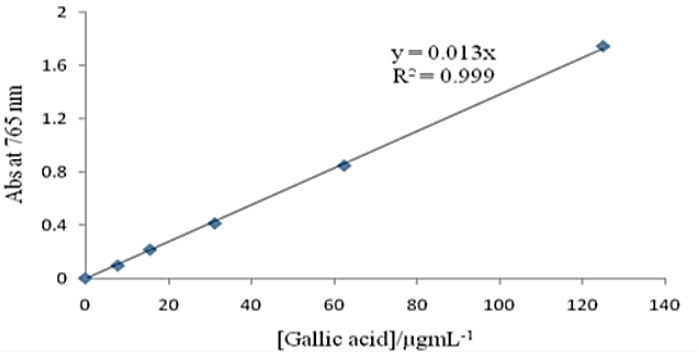

Figure 3. Standard curve of Gallic acid

The results of total phenolics contents for ethyl acetate, methanol and water extracts of *Cleome viscosa* leaves are displayed in Table 1.

Table 1. Total Phenolics Contents of Ethyl acetate, Methanol and Water Extracts of *Cleome viscosa* leaves by Folin-Ciocalteu Method

Sample	**TPC (µ g GAE ±SD) / mg**		
	Ethyl acetate	**Methanol**	**Water**
Leaves	35.12±1.37	32.13±2.81	28.23±0.81

Data showed as (µg Gallic Acid Equivalents GAE, (mean SD) in 1 mg of crude extract. According to experimental data, ethyl acetate extract of selected sample was found to be higher total phenolics content (35.12µg/mg) than methanol (32.13µg/mg) and water extract (28.23µg/mg) of sample which are represented in Figure 4.

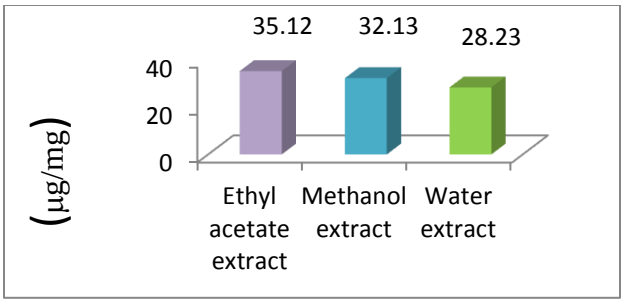

Figure 4. Bar graph for total phenolic content of ethanol and water extracts of *Cleome viscosa* leaves

Total flavonoids contents of *Cleome viscosa* leaves

The results of total flavonoids contents of three solvent extracts of *Cleome viscosa* leaves are tabulated in Table 2.

Table 2. Results of Total Flavonoids Content of *Cleome viscosa* Leaves

Extracts of sample	**Total flavonoids (mg quercetin/g)**
Ethyl acetate extract	43.12±0.3
Methanol extract	39.54±0.4
Water extract	36.98±0.5

The values are means ± SD of three replicates.

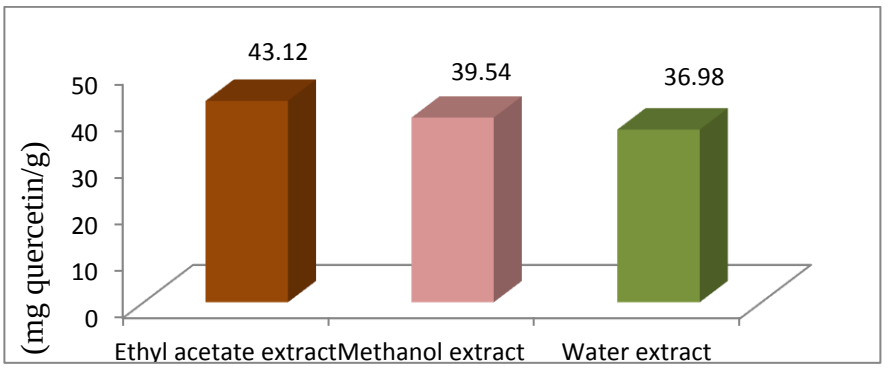

Figure 5. Bar graph for total flavonoids content of *Cleome viscosa* leaves

As shown in Figure 5, ethyl acetate extract of *Cleome viscosa* leaves indicates the highest total flavonoids content which compared with methanol and water extracts of selected sample.

Antimicrobial activity of *Cleome viscosa* Leaves

The results of antimicrobial activities with the inhibition zone diameters for *Cleome viscosa* leaves are revealed in Table 3.

According to these results, ethyl acetate extracts of *Cleome viscosa* leaves responded the highest activity on all tested organisms consists of *Bacillus subtilis, Staphylococcus aureus, Pseudomonas aeruginosa, Bacillus pumilus, Candida albicans,* and *Escherichia coli*. Petroleum ether extracts of sample found no activity on six selected organisms and methanol, ethanol and aqueous extracts indicated low antimicrobial activity describing the presence of phenolic compound. Thus, *Cleome viscosa* leaves contain bioactive phenol compounds.

Table 3. Results of Antimicrobial Activities of the Inhibition Zone for *Cleome viscosa* Leaves

		Inhibition Zone Diameters of Various Solvent Extracts of sample against six organisms					
Sample	**Solvents**	**I**	**II**	**III**	**IV**	**V**	**VI**
Leave	Methanol	+	+	-	-	+	-
	Ethyl acetate	+++	+++	+++	+++	+++	+++
	Ethanol	+	+	++	+	+	+
	water	++	-	++	+	+	+
	Petroleum ether	-	-	-	-	-	-

Diameter of agar well ~ 10 mm		Organisms	
10 mm ~ 14 mm	(+)	I	= Bacillus *subtilis*
15 mm ~ 19 mm	(++)	II	= *Staphylococcus aureus*
20 mm above	(+++)	III	= *Pseudomonas aeruginosa*
(+) = low activity		IV	= *Bacillus pumilus*
(++) = medium activity		V	= *Candida albicans*

(+++) = high activity VI = *Escherichia coli*,
(–) = absent

Antioxidant Activity of Ethyl acetate, Methanol and Water extracts of *Cleome viscosa* leaves by DPPH Radical Scavenging Assay

Antioxidant compounds in plants play an important role for human health. Researchers suggest that antioxidants reduce the risk for chronic diseases including cancer and heart disease. Primary sources of naturally occurring antioxidants are whole grains, fruits and vegetables. Plant sourced food antioxidants like vitamin C, vitamin E, carotenes, phenolic acids, phytate and phytoestrogens have been recognized as having the potential to reduce disease risk.

The extracts or their constituents when mixed with DPPH decolorized due to hydrogen donating ability. The radical scavenging activity of crude extracts was described by %RSA and IC_{50} (50% inhibitory concentration). These results are described in Table 4 and Figure 6.

Table 4. Radical Scavenging Activity (IC_{50}) of Ethyl Acetate, Methanol and Water Extracts of *Cleome viscosa* Leaves and Ascorbic Acid

Extracts of sample	**% RSA (mean ±SD) in different concentration (µg/mL)**						**IC_{50} (µg/ mL)**
	0.62	**1.25**	**2.50**	**5.00**	**10.00**	**20.00**	
Ethyl acetate	36.19 ±1.12	52.89 ±1.01	63.45 ±1.21	72.82 ±1.31	81.12 ±0.91	90.01 ±0.36	1.85
Methanol	21.98 ±0.81	29.52 ± 0.63	51.3 ± 1.91	57.76 ± 1.45	71.62 ± 0.51	75.81 ± 0.42	2.13
Water	18.92 ±0.91	27.37 ±0.77	39.75 ±1.71	52.89 ±1.79	69.54 ±1.89	71.81 ±1.91	3.68
Ascorbic acid	25.2 ± 1.4	53.58 ± 0.9	65.53 ± 1.1	74.82 ± 0.6	83.32 ± 0.8	91.21 ± 0.5	1.17

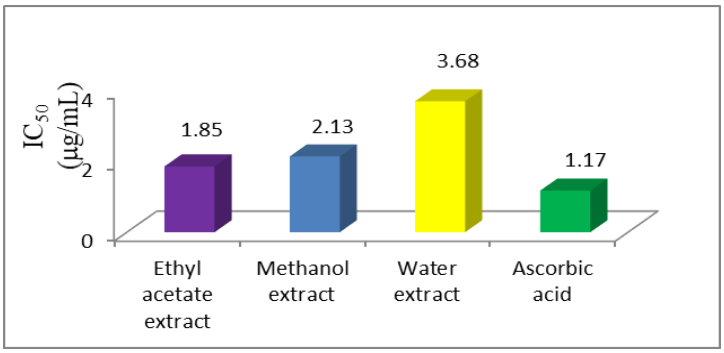

Figure 6. A bar graph of IC_{50} (µg/mL) values of ethyl acetate, methanol and water extracts of *Cleome viscosa* leaves and ascorbic acid.

According to experimental results of IC_{50} values, ethyl acetate extract of *Cleome viscosa* leaves exhibited the strong antioxidant activity compared with methanol, water extracts and standard ascorbic acid. Hence, *Cleome viscosa* leaves are suitable to eat for human health and use as traditional medicine.

Conclusion

Phytochemicals of *Cleome viscosa* leaves involve alkaloids, flavonoids, glycosides, phenolics, tannins, saponins, terpenes, reducing sugars, amino acid, and carbohydrates. The main constituents found in the extract were flavanoids, phenolics, and tannins. The presence of phenolics suggests the antioxidant activity of the extract. Ethyl acetate extract of sample for the total phenolics content was found to be higher than methanol and water extract of sample. Moreover, ethyl acetate extract of sample indicates high antimicrobial activities on all tested organisms and petroleum ether extract observed no antimicrobial activity. The strong potency of IC_{50} values of ethyl acetate, methanol and water extracts of sample were found to be (1.85 µ g/mL), (2.13 µg/mL) and (3.68µ g/mL) which compared by standard ascorbic acid. The investigation of *Cleome viscosa* leaves were provided bioactive and good source of antioxidant activities and better nutrition for human health. Therefore, bioactive new and novel compounds from the leaves of *Cleome viscosa* would be isolated and characterized for health benefits.

Acknowledgements

The authors would like to express special thanks to Dr Saw Pyone Naing, Rector, Dr Myat Myat Thaw, Pro-rector, Ethical Research Committee from Sagaing University of Education, and Professor Dr Kathy Myint Thu, Head of Chemistry Department, Sagaing University of Education for their ever encouragement, kind guidance, invaluable suggestion, and permission to submit this research paper. Thanks are also due to Honorable Professors and reviewers from Universities Research Journal for their acceptance and to publish this paper.

References

Atanassova, M., & Christova-Bagdassarian, V. (2009). Determination of tannins content by titrimetric method for comparison of different plant species. Journal of the University of Chemical Technology and Metallurgy, 44(4), 413–415.

Eghdami, A., & Sadeghi, F. (2010). Determination of total phenolic and flavonoids contents in methanolic and aqueous extract of Achillea millefolium. Organic Chemistry Journal, 2, 81–84.

Harborne, A. J. (1998). Phytochemical Methods A Guide to Modern Techniques of Plant Analysis (3rd ed.). Springer Netherlands.

Mali, R. G. (2010). Cleome viscosa (wild mustard): A review on ethnobotany, phytochemistry, and pharmacology. Pharmaceutical Biology, 48 (1), 105–112.

Singh, H., Mishra, A., & Mishra, A. K. (2015). Cleome viscosa Linn (Capparaceae): A Review. Pharmacognosy Journal, 7 (6), 326–329.

Valgas, C., Souza, S. M. de, Smânia. E. F. A., & Smânia Jr., A. (2007). Screening methods to determine antibacterial activity of natural products. Brazilian Journal of Microbiology, 38 (2), 369–380.

Wojdylo, A., Oszmia'nski, J., and Czemerys, R. (2007). Antioxidant activity and phenolic compounds in 32 selected herbs. Food Chem, 105 (3), 940-999.

Sorption of Acid Dye from Aqueous Solution by Using Modified Pomelo Peel

Htwe Htwe Mar[1], Khin Than Yee[2] & Thinzar Nu[3]

Abstract

In this study, modified pomelo peel was used as a sorbent for the removal of acid dye from aqueous solution. This research work is concerned with the preparation of acid modified pomelo peel (APP) powder. APP was characterized by modern techniques such as ED XRF, TG-DTA, SEM and FT IR analyses. The sorption capacities of APP were studied for the removal of Direct Fast Orange S (T) (acid dye) from aqueous solution with varying parameters of initial concentration, pH, dosage of sorbent and contact time. The removal percent of acid dye was found to be 91.193 % at 60 ppm of initial concentration, pH 6, 0.15 g of dosage and 3 h of contact time. In the adsorption isotherm studies, Langmuir isotherm indicated that the monolayer coverage value (Q_o) was found to be 52.083 mg g^{-1}. From the Freundlich isotherm studies, the adsorption capacity (K_f) was found to be 1.873. The experimental data fitted with both models. Waste pomelo peel could be applied in purifying the environmentally polluted wastewater.

Keywords: Adsorption, adsorption isotherms, dyes, pomelo peel, wastewater

Introduction

The effluents of textile wastewater contain different quantities of dyes. Many dyes are toxic to some organisms causing direct destruction of aquatic communities. Some dyes can cause allergic dermatitis, skin irritation, cancer and mutation in human beings and harmful to aquatic life (Bhanuprakash *et al*., 2015).

Due to the harmful effects of dye pollution in water, there is a pressing need to find efficient methods to combat this kind of pollution (Xiong *et al.,* 2014). Among the several dye removal techniques, adsorption is considered to give the best results as it can be used to remove different types of colouring materials and organic pollutants (Begum and Mahbub, 2013).

[1] Lecturer, Department of Chemistry, Sagaing University of Education
[2] Lecturer, Dr, Department of Chemistry, Myeik University
[3] Associate Professor, Dr, Department of Chemistry, University of Yangon

Pomelo peel is largely composed of cellulose, pectin, hemicellulose, lignin and other low molecular weight organic compounds. It can be used as an efficient and cost-effective bio adsorbent for removing dyes from aqueous solution (Tanzim and Abedin, 2015).

The objective of the present work was to explore the sorption capability of modified pomelo peel as a sorbent for removal of Direct Fast Orange S (T) (acid dye) from aqueous solution.

Materials and Methods

Sample Collection

The pomelo peels were collected from Tamwe Market, Tamwe Township, Yangon Region, Myanmar. The photograph of pomelo is shown in Figure 1.

Figure 1. Photograph of pomelo

Preparation of Acid Modified Pomelo Peel (APP) Powder

The collected pomelo peels were boiled with distilled water and the filtered. The peels were then dried in oven at 80 ˚C for 24 h. The dried peels were grounded to a fine powder by using blender and sieved through 100 mesh sieve. Finally, the grounded pomelo peel was packed in air tied container and labeled (Tanzim and Abedin, 2015).

The pomelo peel powder was soaked with 0.5 M sulphuric acid for 2 h. Then, it was washed several times with distilled water until pH 7.0. The sample was dried in oven at 110 ˚C for 8 h. Then, it was ground to a fine

powder by using blender and sieved through 100 mesh sieve. Finally, acid modified pomelo peel (APP) powder was obtained.

Characterization of APP

APP was examined by modern techniques such as ED XRF, TG-DTA, SEM and FT IR analyses (Stevulova *et al*., 2017, Silverstein *et al*., 2005 and Xu *et al*., 2013).

Sorption Studies for the Color Removal of APP

The sorption capacities of APP were studied for the removal of acid dye from aqueous solution with various parameters of initial concentration of dye solution, pH, dosage of sorbent and contact time.

Results and Discussion

Preparation of Acid Modified Pomelo Peel (APP) Powder

Acid modified pomelo peel (APP) powder was prepared as shown in Figure 2.

Figure 2. Acid modified pomelo peel (APP) powder

Characterization of APP

ED XRF analysis

The chemical constituents of APP were detected by using ED XRF analysis. Figure 3 shows ED XRF spectrum of APP. The resultant data were presented in Table 1. According to ED XRF spectrum, APP contains carbon which was the main component and others were trace constituents compare with carbon.

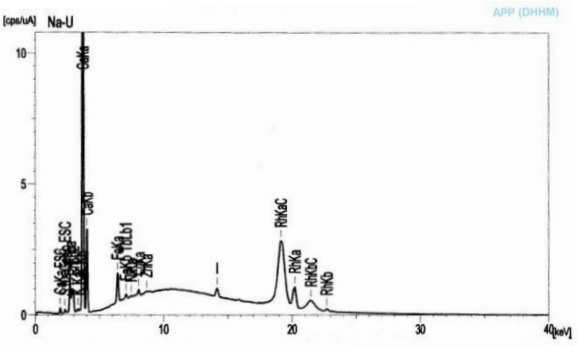

Figure 3. ED XRF spectrum of APP

Table 1. Relative Abundance of Elements in APP by ED XRF Analysis

Elements	Ca	S	K	Fe	Cu	Zn	Ni	COH
Relative abundance of elements (%)	2.011	0.088	0.031	0.014	0.002	0.001	0.001	97.853

TG-DTA analysis

Thermal stability of APP was determined by TG-DTA analysis under nitrogen atmosphere. The thermogram is divided into three stages. The thermal analysis results are shown in Figure 4 and Table 2.

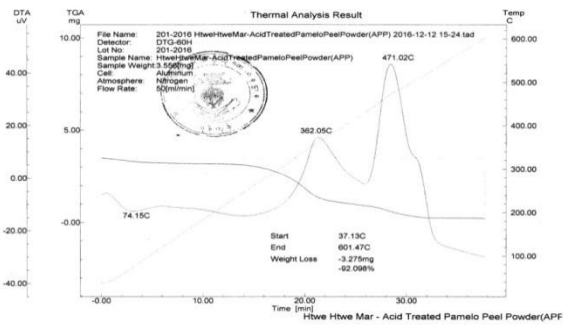

Figure 4. TG-DTA thermogram of APP

Table 2. Thermal Analysis Data of APP

Temp. range (˚C)	Wt. loss (%)	Peak's temp. (˚C)	Nature of peak	TG remark
36 - 120	7.47	74.15	endothermic	The weight loss is due to the dehydration of moisture and absorbed water.
120 - 380	58.59	362.05	exothermic	The weight loss is due to the decomposition of hemicellulose and pectin, carbonization of organic compounds.
380 - 600	26.04	471.02	exothermic	The weight loss is due to the decomposition and combustion of cellulose and lignin.

SEM analysis

The SEM photograph of APP is presented in Figure 5. The surface morphology of APP was showed well-developed porous structure.

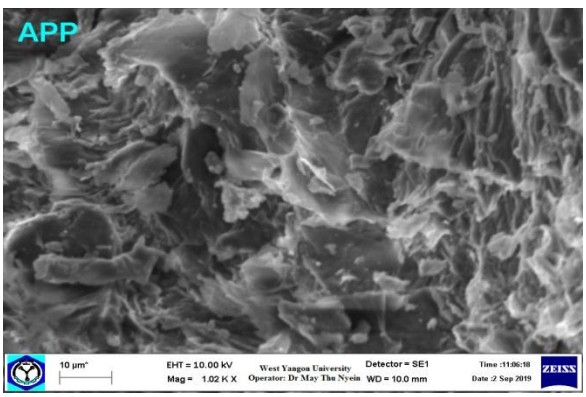

Figure 5. Scanning electron micrograph of APP

FT IR analysis

The FT IR spectrum of APP is shown in Figure 6. It can be observed that broad band at 3313 cm^{-1} attributed to O-H stretching. The peak appeared at 1031 cm^{-1} can be assigned to C-O, C=C and C-C-O stretching. Both peaks indicated the characteristic of cellulose, hemicellulose and

lignin. The peak located at 1982 cm^{-1} due to C-H bending of aromatic compound. The peak observed at 1629 cm^{-1} due to aromatic C=C bending. The peak appeared at 1320 cm^{-1} related to C-O of syringyl ring of lignin. The peak at 1156 cm^{-1} showed stretching of C-O-C due to cellulose and hemicellulose. The peak observed at 664 cm^{-1} can be assigned to O-H bending.

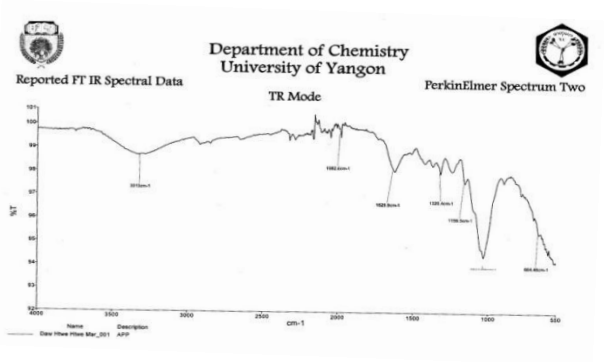

Figure 6. FT IR spectrum of APP

Sorption Studies for the Color Removal of Acid Dye by APP

Effect of initial concentration

Removal of acid dye by APP was determined by varying the initial concentrations from 20 to 100 ppm of dye solution. 0.10 g of APP was added to 25 mL of dye solution and was allowed to equilibrate for 2h in a shaker. The equilibrium concentration was determined spectrophotometrically at its corresponding λ_{max} at 490 nm. The results are shown in Table 3 and Figure 7. It can be seen that as the removal percent decreases with increase in initial concentration. This is related to the availability of active sites on the sorbent surface. After the equilibrium time, the removal percent was 81.223 % with respect to initial concentration (60 ppm) in 25 mL of dye solution.

Effect of pH

The effect of pH was carried out over the pH range from 2 to 10. pH was adjusted with HCl and NaOH. 0.10 g of APP was added to dye solution (60 ppm) and was allowed to equilibrate for 2h in a shaker. The results are shown in Table 4. Removal percent versus pH are shown in Figure 8. From these results, increase in pH, the removal percent also increase up to pH 6.

Beyond pH 6, the removal percent decreases with increasing pH. Almost all the active sites of the sorbent might have been saturated at pH 6. Thus, pH 6 was chosen as the optimum for sorption of sample. The removal percent was 81.587 % at optimum pH.

Effect of dosage

The color removal of dye solution was determined by various dosage of APP from 0.05 to 0.30 g under the optimum conditions. The results are shown in Table 5. Removal percent with respect to sorbent dosage are shown in Figure 9. It can be seen that the removal percent increases with increase in sorbent dose. This is due to increase in sorbent dosage attributed to increase in surface area and availability of sorption site. According to their data, 0.15 g was taken as the suitable sorbent dosage. The removal percent was 88.940 % at optimum dosage.

Effect of contact time

The effect of contact time was investigated for different periods of time from 1 to 6 h by keeping optimum conditions. The results are shown in Table 6 and Figure 10. Sorption percent increases significantly around 3 h and then increased slowly. Thus, 3 h was chosen for optimum contact time. The removal percent of dye being adsorbed was 91.193 % at 3 h.

Table 3. Effect of Initial Concentration on the Removal of Acid Dye by APP

Initial concentration (ppm)	Final concentration (ppm)	Removal percent (%)
20	2.009	89.955
40	5.066	87.335
60	11.266	81.223
80	23.319	70.851
100	34.934	65.066

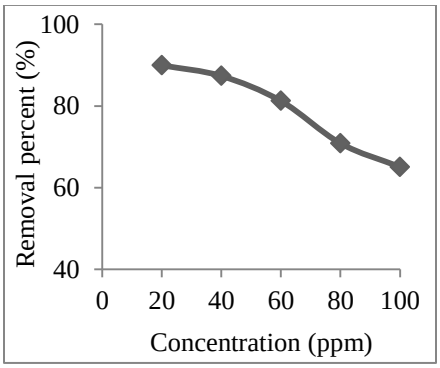

Figure 7. Removal percent of acid dye by APP as a function of initial concentration

Table 4. Effect of pH on the Removal of Acid Dye by APP

pH	Final concentration (ppm)	Removal percent (%)
2	20.873	65.212
3	19.651	67.248
4	16.638	72.270
5	13.450	77.583
6	11.048	81.587
7	11.179	81.368
8	12.140	79.767
9	13.057	78.238
10	13.799	62.590

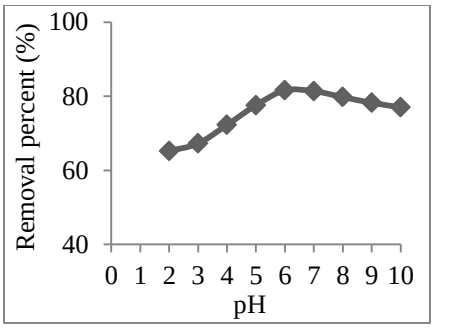

Figure 8. Removal percent of acid dye by APP as a function of pH

Table 5. Effect of Dosage of APP on the Removal of Acid Dye

Dosage (g)	Final concentration (ppm)	Removal percent (%)
0.05	20.306	66.157
0.10	11.048	81.587
0.15	6.638	88.940
0.20	5.022	91.630
0.25	4.061	93.232
0.30	3.406	94.323

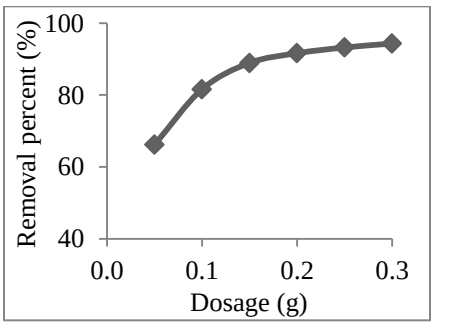

Figure 9. Removal percent of acid dye by APP as a function of dosage

Table 6. Effect of Contact Time on the Removal of Acid Dye by APP

Contact time (h)	Final concentration (ppm)	Removal percent (%)
1	12.009	79.985
2	6.769	88.718
3	5.284	91.193
4	4.934	91.777
5	4.803	91.995
6	4.498	92.505

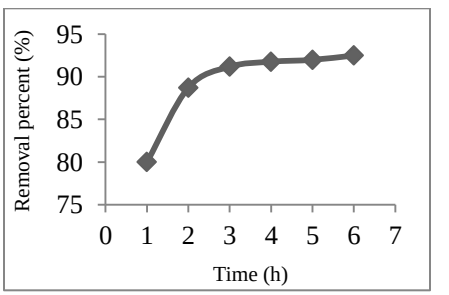

Figure 10. Removal percent of acid dye by APP as a function of contact time

Adsorption Isotherms

Langmuir isotherm

The Langmuir isotherm assumes that sorption occurs at specific homogeneous sites in the adsorbent and the adsorption capacity of the adsorbent is finite.

Langmuir sorption equation is $x/m = \frac{Q_o\, b\, C_e}{1+ b\, C_e}$.

The linearized Langmuir equation is given as:

$$C_e / x/m = (1 / Q_o\, b) + (C_e / Q_o)$$

where x/m is the amount of sorbate adsorbed per unit mass of sorbent (mg g^{-1}), C_e is the equilibrium concentration of adsorbate (mg L^{-1}), Q_o is the maximum monolayer coverage capacity (mg g^{-1}) and b is Langmuir constant (L mg^{-1}) (Nethaji *et al*., 2013).

Langmuir isotherm for sorption of acid dye by APP is shown in Figure 11. From the slope and intercept of the linear plot of the Langmuir isotherm, Langmuir constants and separation factor were obtained. The values of Q_o and b with the correlation coefficient (R^2) are listed in Table 7.

Based on the effect of separation factor on isotherm shape, the R_L value is in the range of $0 < R_L < 1$, which indicates that the sorption of dye solution on APP was favourable.

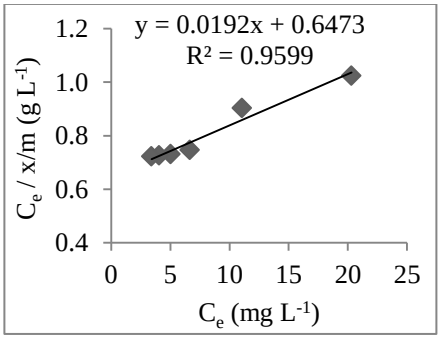

Figure 11. Langmuir isotherm: Sorption of acid dye by APP

Table 7. Langmuir Parameters for the Sorption of Acid Dye by APP

Langmuir parameters			R^2
Q_0 (mg g^{-1})	b (L mg^{-1})	R_L	
52.083	0.03	0.357	0.9599

Freundlich isotherm

The Freundlich isotherm model assumes that the uptake of dyes occurs on a heterogeneous surface by multilayer adsorption and that the amount of adsorbate adsorbed increases infinitely with an increase in concentration.

Freundlich sorption equation is $x/m = K_f C_e^{1/n}$.

The linearized Freundlich equation is given as:

$$\log x/m = \log K_f + 1/n \log C_e$$

where x/m is the amount of sorbate adsorbed per unit mass of sorbent (mg g^{-1}), C_e is the equilibrium concentration of adsorbate (mg L^{-1}), K_f is Freundlich constant (mg g^{-1}) and n is adsorption intensity (L mg^{-1}) (Nethaji *et al*., 2013).

Freundlich isotherm for sorption of acid dye by APP is shown in Figure 12. Figure showed the straight line. The values of K_f and n with the correlation coefficient (R^2) are listed in Table 8. The adsorption intensity (n) value of dye sorption for APP lies between 1 and 10, thus indicating a favourable.

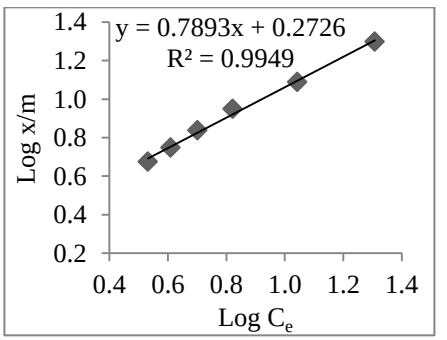

Figure 12. Freundlich isotherm: Sorption of acid dye by APP

Table 8. Freundlich Parameters for the Sorption of Acid Dye by APP

Freundlich parameters		
K_f (mg g^{-1})	**n**	**R^2**
1.873	1.267	0.9949

Conclusion

Acid modified pomelo peel (APP) powder was prepared for the removal of Direct Fast Orange S (T) (acid dye) from aqueous solution. In ED XRF spectrum, APP contains carbon which was the main component. From TG-DTA thermogram of APP, three stages of weight loss were observed. Corresponding functional groups were observed in FT IR spectrum. According to these results, APP has organic compounds including cellulose, pectin, hemicellulose and lignin. From SEM image, the surface pattern of APP was showed well-developed porous structure. Above four characterization techniques, it can be seen that APP can be used as a sorbent for removing dyes from aqueous solution. The effects of various parameters on APP were investigated in sorption process. From the results, it was found that initial concentration of 60 ppm, pH 6, 0.15 g in 25 mL dosage and 3 h contact time as the optimum conditions. The maximum removal percent of Direct Fast Orange S (T) (acid dye) from aqueous solution by APP was observed 91.193 %. From Langmuir isotherm studies, monolayer coverage value (Q_o) was found to be 52.083 mg g^{-1}. From Freundlich isotherm studies, adsorption capacity (K_f) was found to be 1.873 mg g^{-1}. According to equilibrium data, dye sorbent system fitted both models and indicated that the sorption conditions were favourable. The results showed that waste pomelo peel could be used as a sorbent for purifying the environmentally polluted wastewater.

Acknowledgements

The authors would like to express their profound gratitude to Department of Higher Education, Ministry of Education, Yangon, Myanmar, for provision of opportunity to do this research. We are deeply indebted to Rector Dr Saw Pyone Naing and Pro Rector Dr Myat Myat Thaw from Sagaing University of Education, for giving permission to submit this paper. We also thank to Professor and Head Dr Kathy Myint Thu, Department of Chemistry, Sagaing University of Education, for her kind encouragement.

References

Begum, H. A. and Mahbub M. K. B. (2013). "Effectiveness of Carboxymethyl Cellulose for the Removal of Methylene Blue from Aqueous Solution", *Dhaka Univ. J. Sci.*, **61** (2), 193-198

Bhanuprakash, M., Belagali S. L. and Geetha K. S. (2015). "Removal of Dyes from Aqueous Solution Using Coral Wood Tree Legume as Natural Adsorbent", *An Int. Quarterly J. of Environ. Sci*., **9** (1 & 2), 123-126

Nethaji, S., Sivasamy A. and Mandal A. B. (2013). "Adsorption Isotherms, Kinetics and Mechanism for the Adsorption of Cationic and Anionic Dyes onto Carbonaceous Particles Prepared from *Juglans Regia* Shell Biomass", *Int. J. Environ. Sci. Technol*., **10**, 231-242

Silverstein, R. M., Webster F. X. and Kiemle D. J. (2005). *Spectrometric Identification of Organic Compounds*, New York: 7th Edn., John Willey & Sons, Inc., 1 - 550

Stevulova, N., Estokova A., Cigasova J., Schwarzova I., Kacik F. and Geffert A. (2017). "Thermal Degradation of Natural and Treated Hemp Hurds Under Air and Nitrogen Atmosphere", *J. Therm. Anal. Calorim*., **128**(3), 1649-1660

Tanzim, K. and Abedin M. Z. (2015). "Adsorption of Methylene Blue from Aqueous Solution by Pomelo (*Citrus maxima*) Peel", *Intl. J. Sci. and Technol. Res.*, **4** (12), 230-232

Tanzim, K. and Abedin M. Z. (2015). "A Novel Bioadsorbent for the Removal of Methylene Red from Aqueous Solutions", *IOSR J. Environ. Sci., Toxicol. and Food Technol.*, **9** (12), 87-91

Xiong, J., Jiao C., Li C., Zhang D., Lin H. and Chen Y. (2014). "A Versatile Amphiprotic Cotton Fiber for the Removal of Dyes and Metal Ions", *J. Cellulose*, **21**, 3073-3087

Xu, F., Yu J., Tesso T., Dowell F. and Wang D. (2013). "Qualitative and Quantitative Analysis of Lignocellulosic Biomass Using Infrared Techniques: A Mini-Review", *J. Appl. Energy*, **104**, 801-809

In vitro Cytotoxicity of Three Medicinal Plants: *Mimusops elengi* L. (Kha-yay), *Desmodium triquetrum* (L.) DC.(Lauk-thay) and *Tradescantia spathacea* (Mee-kwin-gamone)

Yin Yin Myint[1], Thwe Thwe Oo[2], Naw Yadanar Htwe [3] & Kay Zin Hlaing[4]

Abstract

In this study, phytochemical constituents of stem barks of *Mimusops elengi*, aerial parts of *Desmodium triquetrum* and *Tradescantia spathacea*; flavonoids, phenolic compounds, carbohydrates , glycosides, phytosterols, terpenes and saponins were determined by standard and simple methods. The cytotoxicity of ethanol extracts of stem barks of *Mimusops elengi*, aerial parts of *Desmodium triquetrum* and *Tradescantia spathacea* was proved by brine shrimp lethality assay which is a rapid, inexpensive and simple bioassay. LC_{50} values of *Mimusops elengi*, *Desmodium triquetrum* and *Tradescantia spathacea* were found to be 261.28 μg/mL 111.16 μg/mL and >1600 μg/mL. LC_{50} value of caffeine was 1513.60 μg/mL and it was used as a positive control.

Keywords: *Mimusops elengi* , *Desmodium triquetrum*, *Tradescantia spathacea*, brine shrimp lethality, LC_{50} values

Introduction

Plants have been a major source of highly effective conventional drugs for the treatment of many forms of cancer and while the actual compounds isolated from the plant frequently may not serve as the drug, they provide leads for the development of potential novel agents such as vinblastine, vincristine, camptothecin, topotecan, irinotecan, etoposide and paclitaxel were acquired or developed from phytochemicals (Khushbum, et al., 2014). Plant derived natural products have received considerable attention, due to their diverse pharmacological properties including cytotoxic and cancer chemopreventive effects. The toxicity of the plants may originate from different contaminants or from plant chemical compounds that are part of the plant. Various assays are used for the research of potential toxicity of herbal extracts based on different biological models, such as in vivo assays on laboratory animals. According to the

[1] Associate Professor, Department of Chemistry, Pathein University
[2 3,4] MSc Students, Department of Chemistry, Pathein University

reported cytotoxicity studies, they employed efforts for alternative biological assays that include species of *Artemia salina*, *Artemia franciscana*, *Artemia urmiana* and *Thamnocephalus platyurus*. These toxicity tests are considered a useful tool for preliminary assessment of toxicity (Hamidi,et al., 2014). Brine Shrimp Lethality Assay is a convenient system for monitoring biological activities of various plant species. Although this method does not provide any adequate information regarding the mechanism of toxic action, it is a very useful method for the assessment of the toxic potential of various plant extracts (Gadir, 2012 and Naidu et al., 2014). This method provides preliminary screening data that can be backed up by more specific bioassays once the active compounds have been isolated (Pisutthanan, et al., 2004). In the present study, three traditional medicinal plants, namely *Mimusops elengi* L(Kha-yay), *Desmodium triquetrum* (L.) DC. (Lauk-thay) and *Tradescantia spathacea* (Mee-kwin-gamone) they were selected for cytotoxicity test (Table 1).

Table 1. Scientific Name, Family, English Name, Parts of Used and some Medicinal uses of Selected Plants

Scientific Name	**Family**	**English name**	**Part of use**	**Uses**
Mimusops elengi L.	Sapotaceae	Bullet wood, Sapanish cherry	Stem barks	treatment of diarrhoea, dysentery, gum inflammation, toothache, gonorrhoea, snakebites, fevers, wounds, scabies and eczema
Desmodium triquetrum (L.)DC.	Fabaceae	Trefle gros	Aerial parts	tea substitute, treatment of stomach discomfort, lumbago,chronic coughs, tuberculosis, kidney complaints
Tradescanta spathacea	Commelinaceae	Oyster plant	Aerial parts	treatment of sore throat, whooping cough, nasal bleeding,

Materials and Methods

Plant materials

Mimusops elengi, and *Tradescantia spathacea* were collected from from Mawlamying-gyun township, and *Desmodium triquetrum* from Kyonpyaw township, Ayeyarwaddy Region. hese plants were scientifically identified at Botany Department, Pathein University. All selected parts of plants were separately cut into small parts and washed. After being air dried at room temperature for two weeks, each sample of these parts was made powder by using grinding machine and stored in air-tight container to prevent moisture changes.

Preparation of plant extracts

Each 50 g of dried powder samples were extracted three times with 200 mL of 95% ethanol for about one week by maceration. After filtration, each of filtrate was concentrated to get ethanol extract with evaporation.

Phytochemical Screening

The various leaves and stem barks extracts were screened for the presence of alkaloids, α-amino acids, carbohydrates, phenolic compounds, flavonoid, glycosides, Starch, steroids, saponins, tannins, and terpenoids using the simple and standard methods. The qualitative results are expressed as (+) for the presence and (−) for the absence of phytochemicals.

Preparation of Seawater

Sea salt (without iodine) 38mg was weighed, dissolved in 1L of distilled water and filtered off to get clear solution.

Hatching of Brine Shrimp

Artemia salina leach (brine shrimp eggs) collected from aqurium shops was used as the test organism. Seawater was taken in the small tank and shrimp eggs were added to one side of the tank and then this side was covered. Two days were allowed to hatch the shrimp and to be matured as nauplii. Constant oxygen supply was carried out through the free from egg shell was collected from the illuminated part of the tank. The nauplii was taken from the fish tank by a pipette and diluted in fresh clear sea water to increase visibility and 10 nauplii was taken carefully by micropipette.

Brine shrimp Lethality Assay

The cytoxicity of plant extracts was determined by Mayer, et al., 1982 with slightly modification. Each of the test samples (32 mg) were taken and dissolved in 200µL of pure dimethyl sulfoxide (DMSO) and finally the volume was made to 20 mL with sea water. Thus the concentration of the stock solution was 1600 µg/mL. The solution was serial diluted to 800, 400, 200, 100, 50 µg/mL with sea water. Then 2.5 ml of plant extract solution was added to 2.5 ml of sea water containing 10 nauplii. Control groups were used in cytotoxicity study to validate the test method and ensure that the results obtained were only due to the activity of the test agent and the effects of the other possible factors were nullified. Positive control in a cytotoxicity study is a widely accepted cytotoxic agent and the result of the test agent is compared with the result obtained for the positive control. In the present study caffeine was used as positive control. Caffeine produce multiple physiologic effects throughout the human body, many of these effects could potentially modulate the activity of anticancer therapy. The negative control group was prepared by mixing 50 µL of DMSO with each of three premarked vials containing 4.95 mL of simulated sea water and 10 nauplii . If the brine shrimps in these vials show a rapid mortality rate, then the test is considered as invalid as the nauplii died due to some reasons other than the cytotoxicity of the compounds in the plant extracts. After 24 hours, the vials were inspected using a magnifying glass against a black background and the number of survived nauplii in each vial was counted. In these studies, each experiment has been conducted in triplicate. The percent (%) of motility of the brine shrimp nauplii was calculated for each concentration.

$$\% \text{ Motality} = \frac{\text{no.of death of nauplii}}{\text{no.of death of nauplii+no.of lives of nauplii}} \text{ X } 100\ \%$$

LC_{50} values were estimated using a probit regression analysis with Finney's statistical method, which enable computerized calculations of LC_{50} with confidence intervals (plotted probit value against log. concentration). These calculations may not give the exact lethal concentration of the examined compound or extract that kills 50% of the population, but without doubt it represents a significant preliminary data for further toxicity testing assays (Finney, 1971).

Results and Discussion

Phytochemical Screening

Alkaloids, α- amino acids, carbohydrates, flavonoids, glycosides, phenolic compounds, saponins, starch, phytosterols, tannins and terpenoids were detected for selected parts of three plants see in Table 2. Althouhg the most of tested phytochemical constituents were present in the tested parts of plants but α- amino acids *in M. elengi* ,carbohydrates in *D. triquetrum* and alkaloids in *T. spathacea were absent*. The contents of phytochemical contents such as tannins, flavonoids, phenolic compounds and saponins is a correlation with biological properties of herbal plants.

Table 2. Phytochemical Constituents of *M. elengi*, *D. triquetrum* and *T. spathacea*

No	Type of compounds	Result		
		M. elengi	***D. triquetrum***	***T. spathacea***
1	Alkaloids	+	+	-
2	Saponins	+	+	+
3	α-Amino acid	-	+	+
4	Phenols	+	+	+
6	Flavonoids	+	+	+
7	Carbohydrate	+	-	+
8	Glycosides	+	+	+
9	Phytosterols	+	+	+
10	Terpenes	+	+	+

(+) presence (-) absence

Brine Shrimp Lethality Assay

Brine Shrimp Lethality Assay is a convenient and easy to observe for biological activities of various natural products from plants and microbes, etc. Although this method does not provide any adequate information regarding the mechanism of toxic action, it is a very useful method for the

assessment of the toxic potential of various plant extracts (Gadir, 2012 and Naidu et al., 2014). This method support the preliminary screening data that can promote the more specific bioassays and isolation of active biological constituents.

Table 3. % Motality and LC_{50} Values of Ethanol Extracts of *M. elengi D. triquetrum*, *T. spathacea and* Caffeine

Plants	**Concentration (µg/mL)**	**Log conc.**	**% Motality**	**Probit***	**LC_{50} (µg/mL)**
M. elengi	50	1.6989	10	3.96	261.28
	100	2.0000	30	4.61	
	200	2.3010	30	4.61	
	400	2.6020	40	4.87	
	800	2.9030	60	5.39	
	1600	3.2041	100	7.58	
D.triquetrum	50	1.6989	20	3.96	111.16
	100	2.0000	40	4.87	
	200	2.3010	50	5.13	
	400	2.6020	70	5.67	
	800	2.9030	90	6.04	
	1600	3.2041	100	7.58	
T. spathacea	50	1.6989	0	3.36	>1600
	100	2.0000	0	3.36	
	200	2.3010	0	3.36	
	400	2.6020	10	3.96	
	800	2.9030	10	3.96	
	1600	3.2041	20	4.33	

Plants	Concentration (µg/mL)	Log conc.	% Motality	Probit*	LC_{50} (µg/mL)
Caffeine	50	1.6989	0	3.36	1513.60
	100	2.0000	10	3.96	
	200	2.3010	10	3.96	
	400	2.6020	20	4.33	
	800	2.9030	30	4.61	
	1600	3.2041	50	5.13	

(*Finnery,1952)

The brine shrimp lethality of 95% ethanol extracts of *M. elengi*, *D. triquetrum* and *T. spathacea* was determined using the procedure of Meyer et al. The LC_{50} values of the brine shrimp obtained for extracts of these medicinal plants and positive control, caffeine are given in Table 3.

Classifying toxicity criterion for assessment of plant extracts are: LC_{50} value above 1000 µg/mL are non-toxic, LC_{50} of 500 - 1000 µg/mL are low toxic, extracts with LC_{50} of 100 - 500 µg/mL are medium toxic, while extracts with LC_{50} of 0 - 100 µg/ml are highly toxic by Clarkson et al., 2004. According to the Clarkson's toxicity criterion (Clarkson, *et al.* 2004), as the LC_{50} values of *M. elengi* and *D. triquetrum* are within 100-500 µg/mL these two plants seem to be medium toxic and *T. spathacea* is found to be non-toxic. There was an observed concentration dependent increment in the mortality rate of the brine shrimp; this is considered an indication of proof the cytotoxic effect of the plant extracts. The cytotoxicity of plant extracts it is an indicative of the presence of cytotoxic components which warrants further investigation.

Conclusion

Various herbal plant species have contributed to their pharmacological activities in folk medicine and modern drug design. Moreover, the treatment with various plant constituents for some diseases may be associated with side effects or harmful effects. Therefore, the determinant of concentration of a substance is needed to prevent side effects from drugs. LC_{50} values from preliminary cytoxicity data of *M. elengi*, *D.*

triquetrum and *T. spathacea* ethanol extracts which are proof for further toxicity studies and chemical analysis.

Acknowledgement

We would like to thank Dr Si Si Hla Bu, Rector, Dr Than Tun and Dr Nilar Myint, Pro-rectors, Pathein University, for their permissions and suggestions. I am grateful to Dr Ye Myint Aung, Professor & Head, and Dr Than Than Oo, Professor, for their encouragement.

References

Clarkson, C., V. J. Maharaj, N.R. Crouch, O.M. Grace, P. Pillay, M.G. Matsabisa, N.Bhagwandin, P.J. Smith and P.I. Folb. (2004). "*In Vitro* Antiplasmodial Activity of Medicinal Plants Native to or Naturalised in South Africa", *Journal of Enthopharmacology*, **92** (2),177-191

Finney, D. (1952). *Probit Analysis: A Statistical Treatment of the Sigmoid Response Curve*, Cambridge University Press, Cambridge.

Finney, D. (1971). *Probit analysis*, 3rd Ed. Cambridge University Press, Cambridge.

Gadir, S.A. (2012). "Assessment of bioactivity of some Sudanese Medicinal Plants Using Brine Shrimp (*Artemia salina*) Lethality Assay", *J. Chem Pharm Res*. **4**, 5145 5148.

Hamidi, M.R., B. Jovanova, and T. K.Panovska. (2014). " Toxicological Evaluation of the Plant Products Using Brine Shrimp (Artemia salina L.) Model", *Macedonian pharmaceutical bulletin*, **60** (1), 9 - 18

Khushbu N., A. K. Prasad, J. Nayak, S. V. Iyer, and S. Kumar.(2014)."Antioxidant and *In Vitro* Cytotoxic Activity of Extracts of Aerial Parts of *Cocculus hirsutus* (L) Using Cell Line Cultures (Breast Cell Line)", *The Journal of phytopharmacology.* **3**(6): 395-399

Naidu,J.R., R. Ismail and S. Sasidharan. (2014). " Acute Oral Toxicity and Brine Shrimp Lethality of Methanol Extract of *Mentha spicata* L. (Lamiaceae) ", *Trop J Pharm Res.,* **13**, 101-107.

Pisutthanana,S.,P, Plianbangchang, N. Pisutthanana,S. Ruanruaya, and O. Muanrit. (2004). "Brine Shrimp Lethality Activity of T Thai medicinal plants in the family Meliaceae", *Naresuan Uni J*., **12**, 13-18.

Investigation on Some Phytoconstituents and Antipyretic Activity of Fruit of *Aesculus assamica* Griff. (Yemyaw Thee)

Tet Tun[1], Hla Ngwe[2] & Saw Hla Myint[3]

Abstract

The aim of this research work was to investigate some phytoconstituents and the antipyretic activity of fruit of *Aesculus assamica* Griff. (Yemyaw Thee, YMT - Hippocastanaceae family). The preliminary phytochemical investigation revealed the presence of α-amino acids, carbohydrates, flavonoids, glycosides, phenolic compounds, saponins, steroids, tannins and terpenoids by using the standard methods. The soluble matter contents in petroleum ether (PE), ethyl acetate (EtOAc) and 95 % ethanol (EtOH) were found to be 0.92 %, 1.33 % and 4.53 % by using successive solvent extraction method. Curcumin (0.004 %, m.pt = 183 °C) was isolated from EtOAc crude extract of YMT. In the investigation of antipyretic activity of crude extracts on yeast induced rat models, YMT EtOH extract was found to reduce 38.39 % ± 4.60 ($p<0.05$) in rectal temperature of yeast induced rats after administration of YMT EtOH extract (400mg/kg bw dose) within one hour. Moreover, it was also observed that the effectiveness of the antipyretic potency of curcumin (85.17 % reduction ±2.04, $p<0.005$, 50 mg/kg bw oral dose, 1h) was found to be the best in all of the samples. Therefore, it can be inferred that higher antipyretic activity of YMT may be due to the presence curcumin. The findings from this research work will contribute to the scientific development of Myanmar traditional medicine, specifically for the treatment of fever.

Keywords : *Aesculus assamica* Griff., Yemyaw Thee, antipyretic activity, curcumin

Introduction

The role of traditional medicines in the solution of health problems is invaluable on a global level. As estimated by WHO, 80 % of population of underdevolped countries rely on the traditional system of medicine. A large number of ethnic plants including neem are used traditionally to cure pyrexia in many parts of the world (Sharma *et al*., 2010).

[1]Dr, Associate Professor, Department of Chemistry, Mawlamyine University
[2]Dr, Professor & Head (Retd.), Department of Chemistry, University of Yangon
[3]Dr, Professor & Head (Retd.), Department of Chemistry, University of Yangon

Aesculus assamica is a handsome deciduous tree with a wide spreading hemispherical crown 12-15 m tall. Flowers are creamish tinged with brown red. Seeds 2.5 cm across shining. Figure 1 represents the *A. assamica* flowers, plant and its fruits. *Aesculus assamica* is a widespread species in the tropical and subtropical monsoon forest zone from NE India (Sikkim) eastward to S China (Guangxi) and N Vietnam, Bangladesh, Bhutan, Laos, Myanmar, Thailand. The fruits of *Aesculus assamica* are used for phlebitis, inflammation, varicosity, haemorrhoids, leg ulcers, sports injuries, trauma, astringent. The pharmacological activities of *Aesculus assamica* are astringent, anti-inflammatory, reducing edema, antioxidant, antipyretic activities (Prakash *et al*., 1980).

(a) Flowers (b) Fruits (c) Plant

Figure 1. Photographs of (a) flowers, (b) fruits and (c) plant of *Aesculus assamica* Griff. (Yemyaw Thee)

Chemical Constituents of *Aesculus assamica* are saponins, a complex mixture known as aescin, composed of acylated glycosides of protoaesigenin and barringtogenol-C and including hippocaesculin, flavonoids, sterols, tannins (Prakash *et al*., 1980). Two triterpenoid aglycone together with one triterpenoid saponin and one coumarin glycoside were identified as protoaeseigenin(1), 21-angeloyl-protoaeseigenin(2), 21β- angeloyl- protoaeseigenin-3β-O-[β-D-glucopyranosyl(1-2)][β-D-glucopyranosyl(1-4)] β-D-glucopy-ranosiduronic acid(3), and isofraxoside(4). Compounds 1~4 were first identified from the seeds of *Aesculus assamica* (Liu *et al*., 2005). This research work focus the investigation of some phytoconstituents of *Aesculus assamica* Griff. (Yemyaw Thee) and its antipyretic activity.

Materials and Methods

Sample collection

The fruits of *Aesculus assamica* Griff. (Yemyaw Thee, YMT) were collected from Taunggyi Township in Shan State (South). After washing with water, the fruit samples were dried at room temperature. The dried samples were cut into small pieces and ground into powder by a grinding machine. These powdered samples were stored in air-tight container.

Identification of the sample

The sample was identified at the Department of Botany, Yangon University.

Preliminary phytochemical analysis

The preliminary phytochemical investigations were carried out on the fruits of the selected medicinal plant in order to determine the presence of alkaloids, α-amino acids, carbohydrates, cyanogenic glycosides, flavonoids, glycosides, organic acids, phenolic compounds, reducing sugars, saponins, starch, steroids, tannins and terpenoids (Harborne, 1984, Marini- Bettolo *et al.*, 1981, Robinson, 1983, Shriner *et al.*, 1980, Tin Wa, 1972- , Trease and Evans, 1980, Vogel, 1966).

Preparation of various crude extracts from fruits of *Aesculus assamica* Griff. (Yemyaw Thee)

The various crude extracts like PE, EtOH and EtOAc extracts from the dried powder of fruits of YMT were prepared by using successive solvent extract method. The resultant extracts were then stored and kept in the refrigerator for the isolation and screening of the antipyretic activity.

Isolation of some organic constituents from EtOAc crude extract of fruits of YMT

The EtOAc extract (2 g) of fruits of YMT was separated by silica gel column chromatography with PE:EtOAc gradient elutions (4:1, 2:1, 1:1 and EtOAc only) to give one terpenoid compound: (0.004%, orange amorphous crystals, M.pt = 183°C). Then the isolated compound was characterized by melting points, R_f values, solubilities and some chemical tests such as treating with 5% H_2SO_4, vanillin-H_2SO_4, anisaldehyde-H_2SO_4, Liebermann-Burchard reagent on TLC chromatogram followed by treating with 1% $FeCl_3$ solution.

Acute toxicity test

Usually the acute lethality of a compound is determined on the basis of deaths occurring in 24 hours but the survivors should be observed for at least seven days in order to detect delayed effects (Loomis, 1968). In this experiment, acute toxicity test was carried out on mice by treating with YMT 95% ethanol extract.

Screening of Antipyretic Activity

The antipyretic activity of EtOH and watery extracts of YMT as well as isolated compound was investigated by using yeast induced rat models.

Materials required

Rats of male sex (250-300g), Animal balance, Thermometer, Syringe (3ml, 1ml) Intragestric needle, Brewer's yeast (*Saccharomyces cerevisiae*), Aspirin (200 mg/kg bw), Paracetamol (200 mg/kg bw), YMT EtOH and H_2O extracts (100, 200, 400mg/kg bw), Isolated compound

Procedure

Antipyretic activity was carried out according to the method (RaO *et al*., 1997). Briefly pyrexia was induced in rats by injecting 20% (w/v) aqueous suspension of Brewer's yeast intramuscularly. After 18 hours, the animals developed 0.5° C or more rise in the rectal temperature (about 60% of the total number of animals injected.).They were distributed into different groups of three each and dry residue in the doses of 100, 200 and 400 mg /kg bw was administered orally. One group was administered with aspirin (200 mg/kg bw) and the other group with paracetamol (200 mg/ kg bw) orally. Control group was given 0.5 ml normal saline. At different time intervals 1, 2, 3 and 4 hr after drug administration, the temperature was measured. Similarly, over night fasted normal animals were divided into different groups of 3 each and the experiment was carried out in the same manner as described above. Percentage reduction in rectal temperature was calculated according to the following formula, % Reduction = $\frac{B - C_n}{B - A}$ x 100 by considering the total fall in temperature to normal level as 100 %.

Results and Discussion

Preliminary phytochemical investigations

In accord with the results of the preliminary phytochemical investigations, α-amino acids, carbohydrates, flavonoids, glycosides, phenolic compounds, saponins, steroids, tannins and terpenoids were found to be present in YMT.

Preparation of various crude extracts

In this experiment, the soluble matter contents in PE, EtOAc and EtOH were found to be 0.92%, 1.33% and 4.53% for YMT. Based on these results, it could be noted that the polar constituents were higher amount than non-polar constituents in YMT.

Characterization of some phytochemical constituents

Some physico-chemical characteristics of the isolated compound (Figure 2) such as physical state, R_f value, melting point, solubility and the reactions with 1% $FeCl_3$, anisaldehyde, vanillin, 5%H_2SO_4 and Liebermann-Burchard reagents were compared with that of standard curcumin. The results were shown in Table 1. From the table, it was investigated that some physico-chemical characteristics of the isolated compound are identical with that of standard curcumin.

Therefore, it could be deduced that the isolated compound may be assigned as curcumin.

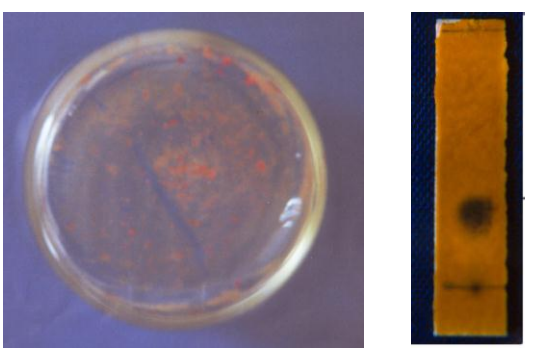

Isolated compound after treated with 1%$FeCl_3$

R_f = 0.45 (PE;EtOAc, 1:1,v/v)

Figure 2. Photographs of isolated compound from YMT and its TLC chromatogram

Table 1. Comparison of some Physico-chemical Characteristics of Isolated Compound and Standard Curcumin

Physicochemical Characteristics		**Isolated compound**	***Curcumin**
Physical state		Orange crystals	Orange crystals
R_f value		0.45 (PE:EtOAc = 1 : 1,v/v)	0.45 (PE:EtOAc = 1 : 1,v/v)
M.pt (°C)		183	183-184
Solubility in	PE	–	–
	EtOAc	+	+
	EtOH	+	+
	MeOH	+	+
	$CHCl_3$	+	+
	H_2O	–	–
1% $FeCl_3$		Reddish brown colouration	Reddish brown colouration
Anisaldehyde		Dark-purple colour	Dark-purple colour
Vanillin		Purple colour	Purple colour
5%H_2SO_4		Pink colour	Pink colour
Liebermann-Burchard		Reddish brown colouration	Reddish brown colouration

*Tet Tun (2008)

Identification of isolated compound

FT IR spectral data – 3452, 3070, 3030, 2927, 2847, 1628, 1510, 1430, 1281, 1206, 1155, 1028, 962, 811

^{1}H NMR spectral data - δ 3.97(6H,s,2-OMe), δ 5.86 (1H,s,H-C=C-OH), δ 6.48 (2H,d,J=16 Hz), δ 6.94 (2H,d,J=8 Hz, δ 7.05 (2H,d,J=2 Hz), δ 7.12 (2H,dd,J=8/2 Hz), δ 7.59 (2H,d,J=16 Hz)

It was investigated that the FT IR spectral results of the isolated compound were compared with that of the standard curcumin. In addition, the ^{1}HNMR spectrum (400MHz, $CDCl_3$) of the isolated compound also occurred to be identical with that of standard curcumin (Tet Tun, 2008). From this comparison, it was found that the significant frequencies of the important functional groups of the isolated compound such as phenolic group, OCH_3 group and C=O with conjugated double bond systems were nearly the same as that of the standard curcumin. Therefore, according to FT IR and ^{1}H NMR spectral results, it can be inferred that the isolated compound may be identified as curcumin.

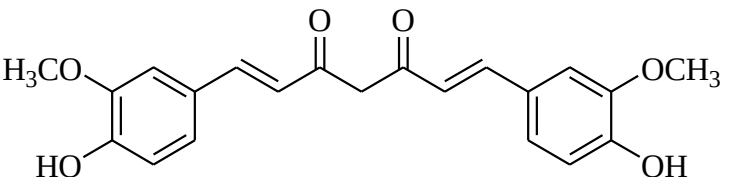

Curcumin

Acute toxicity study

No lethality of the mice was observed up to seven days, even with doses of the 2g/kg bw for YMT EtOH extract.

Investigation of Antipyretic Activity

The antipyretic activity of 95% EtOH and watery extracts of YMT as well as isolated compound (curcumin) was evaluated using Brewer's yeast – induced pyrexia in rats. The experimental rats showed a mean increase of about 0.5°C to 1.45°C in rectal temperature, 18 hrs after yeast injection. Aspirin and paracetamol (200 mg/kg bw dose) for oral administration were used as standard drugs in comparing the antipyretic action of those extracts and isolated compound. The rectal temperature of pyrexia was measured at 1 hour, 2 hour, 3 hour and 4 hour intervals after administration of extracts, compounds and standard drugs. The effects of YMT extracts on yeast-induced rats are described in Table 2 and 3. In addition, the % reduction in rectal temperature of pyrexia was calculated to compare the antipyretic effects of various drugs. The resultant % reduction values are described in Table 4 and Figure 3.

The % reductions in rectal temperatures of febrile rats after administration of YMT EtOH extract in the doses of 100, 200 and 400 mg/kg bw were higher than that of YMT watery extracts (Figure 3). On the other hand, it can be inferred that most of the active compounds affecting the fever are present in the 95% EtOH extract of YMT. However, YMT EtOH extract has (% reduction = 30.53 ± 0.05, p< 0.005, 21.43 ± 1.15, p< 0.005,38.39 ± 4.60, p< 0.005, 1h) weak antipyretic action than standard aspirin and paracetamol.

Table 2. Effect of Yemyaw Thee EtOH Extract and Standard Drugs on Brewer's Yeast Induced Fever in Rats

Group No.	**Doses (mg/kg bw)**	**Average normal rectal temperature (˚C)**	**Average rectal temp. after yeast injection (˚C)**	**Average rectal temp. (after drug and extracts administration orally) /(˚C)**			
				1 h	**2 h**	**3 h**	**4 h**
Group I Control)	normal saline	36.18 ±.23	37.63 ±0.08***	37.56 ± 0.06	37.56 ±0.10	37.56 ±0.12	37.63 ±0.12
Group II	Aspirin (200)	36.07 ±0.34	37.52 ±0.24**	36.50 ± 0.29*	36.27 ±0.33*	36.17 ± 0.29**	36.15 ± 0.31**
Group XXVI	Paracetamol (200)	36.11 ±0.11	37.15 ±0.06***	36.28 ± 0.11***	36.20 ± 0.09***	36.13 ± 0.12***	36.13 ±0 .12***
Group IX	YMT (100)	36.30 ±0.28	37.44 ± 0.17**	37.09 ± 0.11*	36.65 ± 0.18**	36.55 ± 0.18**	36.43 ± 0.25**
Group X	YMT (200)	36.41 ±0.13	37.43 ± 0.12**	37.21 ± 0.06*	36.78 ±0.06**	36.63 ± 0.08**	36.43 ± 0.12**
Group XI	YMT (400)	36.56 ±0.12	37.52 ± 0.13**	37.15 ± 0.16*	36.85 ± 0.13**	36.70 ± 0.11**	36.65 ± 0.12**

* p< 0.05 , ** p< 0.005 , *** p< 0.0005

Table 3. Effect of Yemyaw Thee Watery Extract and Standard Drugs on Brewer's Yeast Induced Fever in Rats

Group No.	Doses (mg/kg bw)	Average normal rectal temperature (˚C)	Average rectal temp. after yeast injection (˚C)	Average rectal temp. (after drug and extracts administration orally) /(˚C)			
				1 h	2 h	3 h	4 h
Group I (Control)	normal saline	36.18 ±0.23	37.63 ±0.08***	37.56 ±0.06	37.56 ±0.10	37.56 ±0.12	36.18 ±0.23
Group II	Aspirin (200)	36.07 ±0.34	37.52 ±0.24**	36.50 ±0.29*	36.27 ±0.33*	36.17 ±0.29**	36.15 ±0.31**
Group XXVI	Paracetamol (200)	36.11 ±0.11	37.15 ±0.06***	36.28 ±0.11***	36.20 ±0.09***	36.13 ±0.12***	36.13 ±0.12***
Group XII	YMT (100)	35.96 ±0.03	37.20 ±0.35**	37.15 ±0.36	37.13 ±0.32	36.48 ±0.16*	36.10 ±0.06**
Group XIII	YMT (200)	36.22 ±0.30	37.37 ±0.22*	37.32 ±0.23	37.30 ±0.20	36.70 ±0.20*	36.37 ±0.26*
Group XIV	YMT (400)	36.19 ±0.32	37.13 ±0.08*	37.08 ±0.08	37.06 ±0.10	36.61 ±0.24*	36.30 ±0.27*

* $p < 0.05$, ** $p < 0.005$, *** $p < 0.0005$

Table 4. % Reduction in Rectal Temperature of Pyrexia Rats after Administration of Standard Drugs and Extracts of Yemyaw Thee

Group No.	Doses (mg/kg bw)	%Reduction in rectal temperature(mean±SD) after administration of drug and extract			
		1h	2h	3h	4h
Control	n-saline	5.28±2.91	4.96±1.62	5.10±2.78	5.28±2.91
Aspirin	200	70.45±1.05	86.57±1.01	93.88±2.57	94.82±0.93
Paracetamol	200	83.56±0.97	91.03±2.63	98.00±3.46	98.00±3.46
YMT(EtOH)	100	30.53±0.05	69.47±0.05	77.66±0.53	88.11±3.35

Group No.	Doses (mg/kg bw)	%Reduction in rectal temperature(mean±SD) after administration of drug and extract			
		1h	2h	3h	4h
YMT(H_2O)	100	4.81±1.47	6.05±0.68	57.83±0.48	88.93±0.44
YMT(EtOH)	200	21.43±1.15	63.85±0.95	78.25±0.99	98.37±2.82
YMT(H_2O)	200	4.98±1.59	6.32±1.11	57.91±1.23	86.62±1.78
YMT(EtOH)	400	38.39±4.60	69.33±4.93	84.83±2.36	90.44±3.40
YMT(H_2O)	400	5.91±1.56	7.72±2.13	54.48±4.26	88.91±3.92

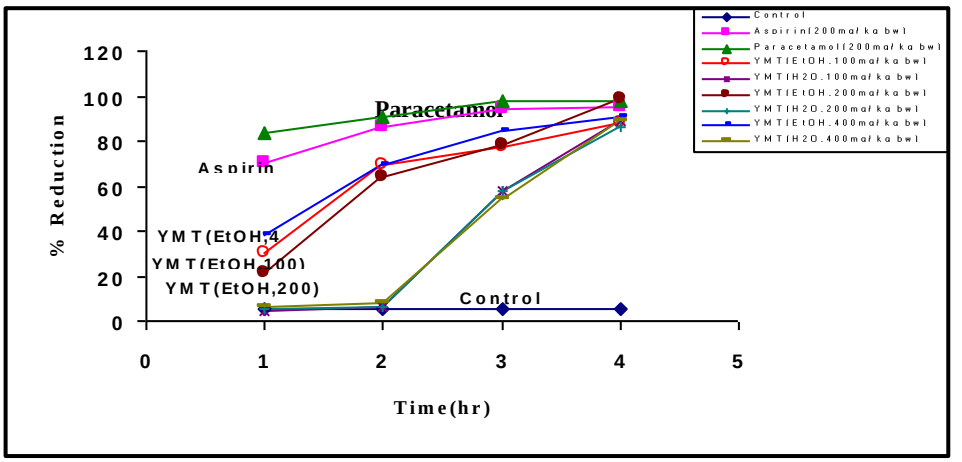

Figure 3. Comparison of antipyretic effects on yeast induced pyrexia rats after administration of Yemyaw Thee (EtOH and watery) extracts with respect to standard drugs

Table 5. Comparison of Effect of YMT EtOH Extract and Curcumin with Standard Drugs on Brewer's Yeast Induced Fever in Rats

Group No.	Doses (mg/kg bw)	Average normal rectal temperature (^{0}C)	Average rectal temp. (^{0}C)	Average rectal temp. (after drug and extracts administration orally) (^{0}C)			
				1 h	2 h	3 h	4 h
Group I (Control)	normal saline	36.18 ± 0.23	37.63 ±0.08***	37.56 ±0.06	37.56 ±0.10	37.56 ±0.12	37.56 ±0.06

Group No.	Doses (mg/kg bw)	Average normal rectal temperature (^{0}C)	Average rectal temp. (^{0}C)	Average rectal temp. (after drug and extracts administration orally) (^{0}C)			
				1 h	2 h	3 h	4 h
Group II	Aspirin (200)	36.07 ±0.34	37.52 ±0.24**	36.50 ±0.29*	36.27 ±0.33*	36.17 ±0.29**	36.15 ±0.31**
Group XXVI	Paracetamol (200)	36.11 ±0.11	37.15 ±0.06***	36.28 ±0.11***	36.20 ±0.09***	36.13 ±0.12***	36.13 ±0.12***
Group XI	YMT (EtOH,400)	36.19 ± 0.32	37.13 ±0.08*	37.08 ±0.08*	37.06 ± 0.10*	36.61 ± 0.24*	36.30 ±0.29*
Group XXI	Curcumin (50)	36.48 ±0.07	37.39 ±0.17**	36.61 ±0.06**	36.54 ±0.03**	36.50 ±0.06**	36.50 ±0.06**

* p<0.05, ** p<0.005, *** p<0.0005

Table 6. Comparison of % Reduction in Rectal Temperature of Pyrexia Rats after Administration of Standard Drugs and YMT EtOH Extract as well as Isolated Curcumin

Treatment	Doses (mg/kg bw)	%Reduction in rectal temperature(mean±SD) after administration of drug and extract			
		1h	2h	3h	4h
Control	n-saline	5.28±2.91	4.96±1.62	5.10±2.78	5.28±2.91
Aspirin	200	70.45±1.05	86.57±1.01	93.88±2.57	94.82±0.93
Paracetamol	200	83.56±0.97	91.03±2.63	98.00±3.46	98.00±3.46
YMT(EtOH)	400	38.39±4.60	69.33±4.93	84.83±2.36	90.44±3.40
Curcumin	50	85.17±2.04	94.32±5.38	98.21±3.09	98.21±0.34

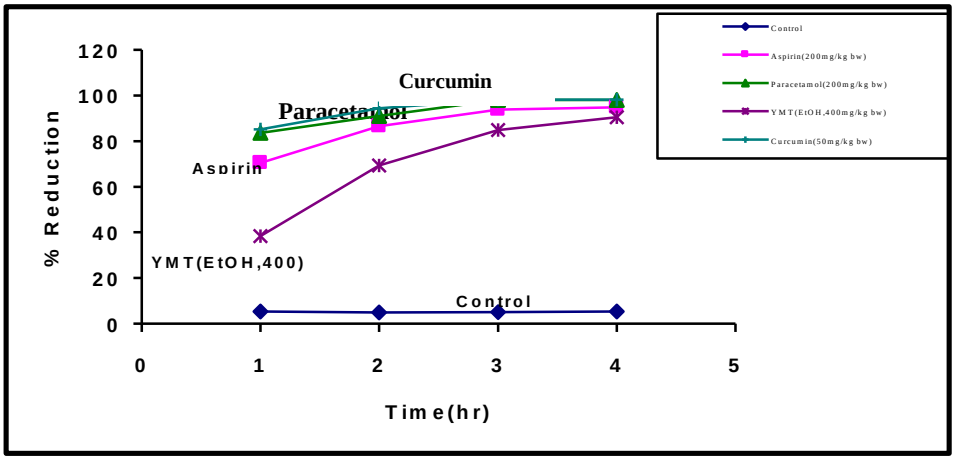

Figure 4. Comparison of antipyretic effects on yeast induced pyrexia rats after administration of YMT EtOH extract and Curcumin with respect to standard drugs

The antipyretic activity of isolated compound (curcumin) was also investigated on yeast-induced febril rats. As shown in Table 5, it was found that the rectal temperature of pyrexia was decreased significantly from 1 hour up to 4 hour later after administration of isolated compound, curcumin (50mg/kg bw). In addition, the % reduction in rectal temperature of pyrexia was also found to be comparable to that of standard drugs and higher than YMT EtOH extract (Table 6 and Figure 4).

Conclusion

From the overall assessment of this research work, it may be deduced that YMT EtOH extract and isolated compound, curcumin may be used as the antipyretic agents. In addition, EtOH extract is free from toxic effect since no lethality of mice within seven days. The findings from this research work will contribute to the scientific development of Myanmar traditional medicine, specifically for the treatment of fever.

Acknowledgements

I would like to express my deep appreciation to Rector Dr Aung Myat Kyaw Sein, Pro-rectors Dr Mie Mie Sein and Dr San San Aye, Mawlamyine University, Professor Dr Daw Mya Thaung, Professor and Head and Professor Dr San San Khin, Department of Chemistry, Mawlamyine University, for allowing this paper to print in Universities Research Journal.

References

Harborne, J.B. (1984). *Phytochemical Methods, A Guide to Modern Techniques of Plant Analysis*. London : 2nd Ed, **37**, 101

Liu, H.W., X.S. Yao, N.L. Wang and G.P. Cai. (2005). "Chemical Components of *Aesculus assamica"*. Zhongguo Tianran Yaowu, **3**(6), 350-353

Loomis, T.A. (1968). "Essentials of Toxicology". 1st Ed., Lea & Febiger, Philadelphia, 18-19

M-Tin Wa. (1972). "Phytochemical Screening, Methods and Procedures". *Phytochemical Bulletin of Botanical Society of America Inc*., **5(3)**, 4-10

Marini- Bettolo, G.B., M. Nicole Hic and M. Palamia. (1981)."Plant Screening by Chemical and Chromatographic Procedure under Field Conditions". *J.Chromate*, **46**(2), 359-363

Prakash, D., G. Misra and S.K, Nigam. (1980). "Chemistry of *Aesculus punduana* Wall. (*A. assamic* Griff.) Seeds". Fitoterapia, **51** (6), 285-287

RaO, R.R., R.M. Babu, M.R.V. RaO, M.G.V. Babu. (1997). "Studies on Antipyretic, Analgesic and Hypoglycemic Activities of Root of *Gynandropsis gynandra* Linn". *Ind. Drugs*, **34**, 690-693

Robinson, T. (1983). *The Organic Constituents of Higher Plants*. North America: 5th Ed., Cordus Press, 63-68

Sharma, J.P., A. Srivastava, S.P. Thakur, P.K. Barpete and S. Singh. (2010). "Herbal Medicine as Antipyretic : A Comprehensive Review". *International Journal of Pharmacy and Life Science*, **1** (1), 18-22

Shriner, R.L., R.C. Fuson, D.Y. Curtin and T.C. Morrill. (1980). *The Systematic Identification of Organic Compounds, A Laboratory Manual*. New York: John Wiley and Sons, 15-20

Tet Tun. (2008). *Study on some Bioactivities and some Bioactive Constituents in Zingibercassumunar* Roxb. (Meik-tha-lin-oot), *Kaempferia pulchra* Ridl. (Shan-pan-oot) and *Aesculus assimica* Griff. (Yemyaw Thee). PhD (Dissertation). Department of Chemistry, University of Yangon, 97-104

Trease, G.E. and W.C. Evans. (1980). *Pharmacognosy*. London, 1st Ed., Spottiswoode Ballantyne Ltd, **104**, 529

Vogel, A.I. (1966). *A Text Book of Practical Organic Chemistry*. London: 3rd Ed, Longmans, Green & Co. Ltd., 112

Immobilization of Isoamylase from Pea Embryo (Pisum *sativum* L.)

Yu Yu Hlaing[1] & Kyaw Naing [2]

Abstract

Isoamylase enzyme (EC 3.2.1.68) was isolated from pea embryo (*Pisum sativum* L.). The purifications were done by ammonium sulphate precipitation and gel filtration chromatography (Sphadex G-100). The isoamylase from pea embryo has optimum pH of 4 and optimum temperature value of 60°C. In the pH stability study on the isoamylase, the enzyme activity decreased by 74, 61, 77 and 84 % of original activity at pH 3.6, 4.0, 4.6 and 5.6, respectively, for 5 hr incubation. In the thermostability study on the enzyme, the enzyme activity decreased by 57, 52 and 41% of original activity at 40, 50 and 60°C, respectively, for 5 hr incubation. Activation energy (E_a) of the isoamylase-catalyzed reaction was calculated to be 6.697 kcalmol^{-1}. The turnover number of isoamylase catalyzed reaction was found to be 4.71 x 10^{-2} min^{-1}. Metal ions such as Na^+, K^+, Ca^{2+} and Mg^{2+} showed the activating effect on isoamylase activity. The dissociation constant of enzyme inhibitor constants (K_i) of Hg^{2+} and Cu^{2+} ions were investigated and they behaved as competitive type. Heavy metal ions such as Hg^{2+}, $Cu^{2+}$and Co^{2+} showed the inhibitory effect on isoamylase activity. The immobilization of purified isoamylase was carried out by using oxycellulose as support. There was no difference for optimum pH and temperature between free and immobilized enzyme. However, in the case of storage stability, the immobilized enzyme was more stable than free enzyme. By using the crude isoamylase from pea embryo, preparation of maltose was carried out. Cassava is used as starch source and enzymic hydrolysis of starch was carried out by using crude isoamylase.

Keywords : Isoamylase, Pea Embryo, Maltose, K_i

Introduction

A pea is most commonly the small spherical seed or the seed-pod of the legume *Pisum sativum* L. The average pea weighs between 0.1 and 0.36 grams. Pea contains about 5.7 g natural sugar and 5.4g of protein. They do contain vitamin A, B, C and are well known for their laxative effect and

[1] Assistant Lecturer, Department of Chemistry, East Yangon University
[2] Lecturer, Department of Chemistry, University of Yangon

good digestive properties. Pea is also a good source of calcium, magnesium, phosphorus and potassium.

Isoamylase enzyme was carried out from pea embryo. Enzymes that cannot attack pullulan but can debranch amylopectin and its limit dextrins are known as isoamylase. Isoamylase is an extra cellular enzyme. The enzyme can be used in industrial production of high maltose syrup, high fructose syrup and amylose.

If starch is hydrolyzed by α-amylase and β-amylase together with isoamylase, a product containing 95-99% maltose can be generated. Metabolism of maltose by yeast during fermentation then leads to the production of ethanol and carbon dioxide. Chemical reduction of maltose produces maltitol. Maltitol is a sweeter with low caloric content and can be used in candy and barky industries to make improvement in quality.

Materials and Methods

All chemicals used were of analytical-reagent grade and were provided by Merck and BDH, unless stated otherwise, and all solutions were prepared using de-ionized water.

The apparatus used include a digital balance (A 200s, Sartorius service Hot Lines, Japan), a UV-visible spectrophotometer (Shimadzu UV 240), a pH meter with a *HANNA* instruments pH-EC-TDS meter (HI-9812), a homogenzer (nissei Excel Auto Homogenizer, model Dx-5, KOKUSAN ENSHINKI Co., Ltd, Japan) and a thermostatted water bath shaker (Model BKR-51, max tem 80°C, Yamoto scientific Co., Ltd, Japan).

The Isoamylase enzyme was isolated from pea embryo by using successive ammonium sulphate precipitation method and Gel-filtration chromatography method at 610 nm.

Enzymic properties (isoamylase activity, protein content, specific activity, optimum pH, optimum temperature, pH stability, thermostability, substrate concentration, enzyme concentration and reaction order) were done by using UV-visible spectroscopy. From the data obtained, the values of maximum velocity (V_{max}), Michaelis Menten constant (K_m) reaction order (n) and activation energy (E_a) were calculated.

Protein content was determined by Biuret Method and Molecular weight was determined by non-SDS-PAGE Electrophoresis Techniques.

Results and Discussion

Isoamylase Activity, Protein Content, and specific Activity at the Various Purification Steps

The isoamylase activity of the enzyme solution was 28.98 EU per gram of pea embryo at final purification step. The protein content of the final enzyme solution was 1.10 mg ml^{-1} and specific activity was 25.16 ΔA mm^{-1} mg^{-1} proteins. It was found that specific activity (relative purity) of enzyme increase about 7 fold from crude to final purification step (Table1). Figure 1 mention the chromatogram of crude isoamylase purified by Gel chromatography.

Optimum pH for Isoamylase Activity

The most favorable pH value the point where the enzyme is most active is known as the optimm pH (Bell, 1965). The optimum pH for pea embryo isoamylase activity was found to be pH 4.0 (Figure 2).

Optimum Temperature for Isoamylase Activity

Optimum temperatures vary greatly from enzyme to enzyme like most chemical reaction, the rate of enzyme catalyzed reaction increases as the temperature is raised (Harper, 1977). The optimum temperature for pea embryo isoamylase activity was found to be 60°C (Figure 3).

pH Stability of Isoamylase enzyme

In the pH stability study on the enzyme, the enzyme activity decreased by 74, 61, 77 and 84 % of original activity at pH 3.6, 4.0, 4.6 and 5.6, respectively, for 5 hr incubation (Figure 4).

Thermostability Stability of Isoamylase enzyme

In the thermostability study on the enzyme, the enzyme activity decreased by 57, 52 and 41% of original activity at 40, 50 and 60^{o}C respectively, for 5 hr incubation (Figure 5).

Reaction Order of Isoamylase-catalyzed Reaction

The reaction order (n) value was calculated from the plot of log $V/(V_{max}-V)$ *Vs.* log [S] for isoamylase using linear regression. The value of n was found to be 0.98, meaning that the reaction is of the first order (Figure 6).

Effect of Enzyme Concentration on Isoam|ylase-catalyzed Reaction

The enzyme activity was found to have a linear relationship with volume of enzyme solution taken (Chen, 1990) (Figure 7).

Effect of Substrate Concentration on Isoamylase-catalyzed Reaction

When the enzyme concentration is constant, the initial velocity of the reaction increase, as the substrate concentration is increased (Harda, 1968). The V_{max} and K_m values from the Michaelis-Menten plot can be regarded as apparent values so that the Lineweaver Burk, Eadie-Hofstee, Hanes Wilkinson and Eisenthal-Cornish Bowden (Direct Linear) plot were made to obtain accurate values (Figure 8).

Effect of Foreign Metal Ions on Isoamylase-catalyzed Reaction

Effect of metal ions (Na^+, K^+, Ca^{2+}, Mg^{2+}, Hg^{2+}, Cu^{2+} and Co^{2+}) on isoamylase activities were investigated. Metal ions (Na^+, K^+, Ca^{2+} and Mg^{2+}) showed the activating effect on isoamylase activity. Heavy metal ions (Hg^{2+}, Cu^{2+} and Co^{2+}) showed the inhibitory effect on isoamylase activity (Figure 9). The dissociation constant of enzyme inhibitor constant (K_i) of Hg^{2+} and Cu^{2+} ions were investigated and they behaved as competitive type.

Molecular Weight of the Purified Isoamylase Enzyme

The homogeneity of the purified isoamylase was confirmed as a single band by non-SDS-PAGE (Yamamoto,1988). The molecular weight of purified isoamylase was determined to be 79430 Dalton(Table 2 and Figures 10 and 11).

Immobilization of Isoamylase Enzyme on Oxycellulose

The purified of isoamylase was immobilized on oxycellulose support (Walsh, 1968). The pH and temperature profile of free and immobilized isoamylase enzyme was very similar optimum pH 4.0 and optimum temperature at 60°C. However, in the case of storage stability, the immobilized enzyme was more stable than free enzyme. During 16 day storage time at 4°C free isoamylase enzyme lost 9.01 %, whereas the immobilized enzyme lost only 3.84% (Figure 12).

Production of Maltose from Cassava by using Isoamylase from Pea Embryo

By using the crude isoamylase from pea embryo, preparation of maltose was carried out. Cassava is used as starch source and enzymic hydrolysis of starch was carried out by using crude isoamylase from pea embryo. The prepared maltose powder was qualitatively identified by FT-IR spectroscopy. The reducing sugar content (calculated as maltose) was 94.94 %. The glucose content in prepared maltose powder was 3.64 % (Figures 13,14 and15).

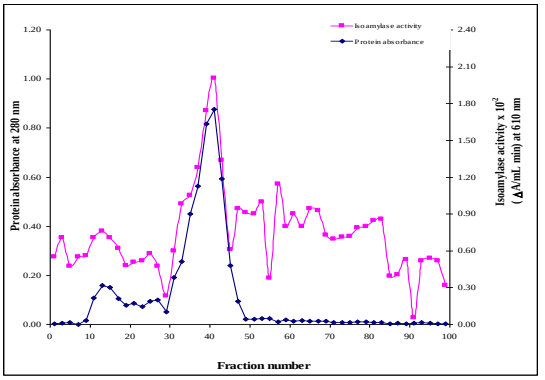

Figure 1. Purification of crude isoamylase enzyme by gel filtration chromatography

Table 1. Isoamylase Enzyme Activities, Protein Contents and Specific Activities of the Enzyme Solution at Different Purification Steps

No.	Main Steps Purification (mg/mL)	Protein content (mg / mL)	Isoamylase Activity (ΔA/mL min)	Specific Activity (ΔA/ min mg protein)	Protein Recovery (%)	Degree of Purity (fold)
1	Crude extract	13.71	48.293	3.552	100	1
2	After purification	8.982	40.967	4.561	65.5	1.295

No.	Main Steps Purification (mg/mL)	Protein content (mg / mL)	Isoamylase Activity (ΔA/mL min)	Specific Activity (ΔA/ min mg protein)	Protein Recovery (%)	Degree of Purity (fold)
	with 10% $(NH_4)_2SO_4$					
3	After purification with 80 % $(NH_4)_2SO_4$	3.532	8.961	8.961	25.76	2.544
4	After passing the Sephadex G-100 column	1.099	27.667	25.157	8.02	7.148

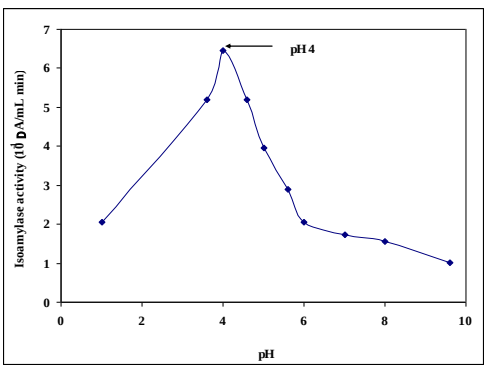

Figure 2. Plot of isoamylase activity as a function of pH of the solution

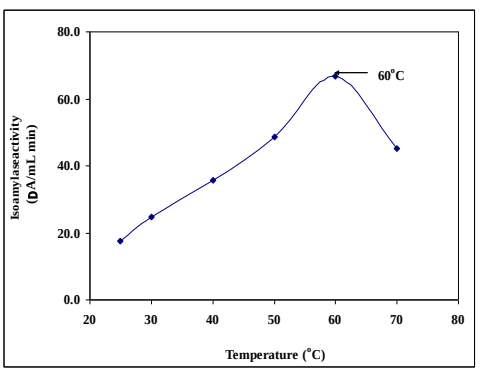

Figure 3. Plot of isoamylase activity as a function of temperature of the solution

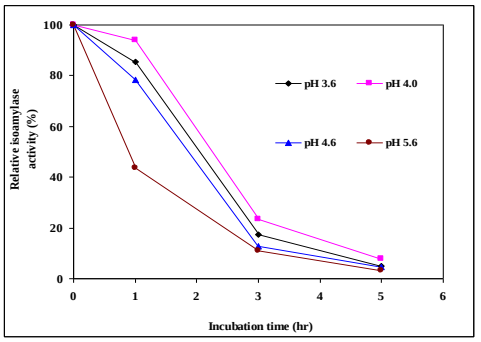

Figure 4. Plot of relative activity as a function of incubation time at different pH values

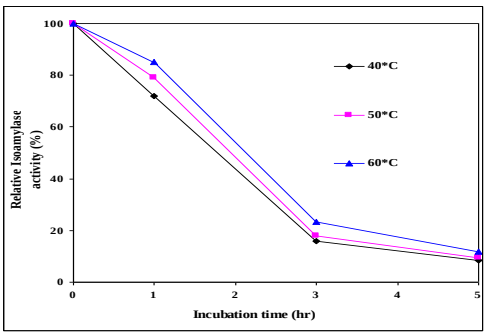

Figure 5. Plot of relative activity as a function of incubation time at different temperature

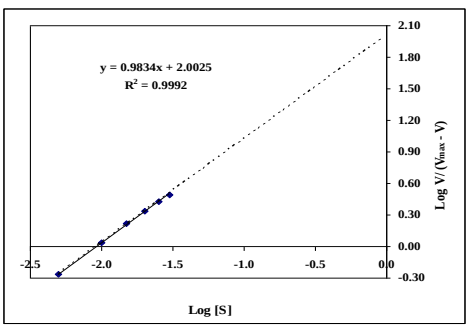

Figure 6. Plot of $\text{Log}\ \frac{V}{V_{max} - V}$ as a function of log[S] for isoamylase-catalyzed reaction

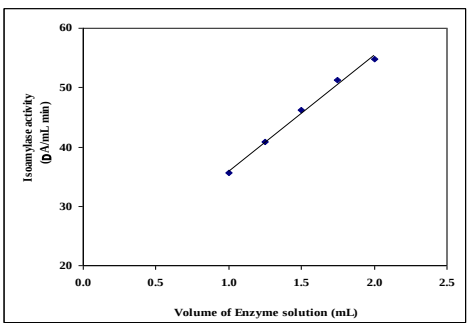

Figure 7. Plot of isoamylase activity as a function of volume of enzyme solution taken

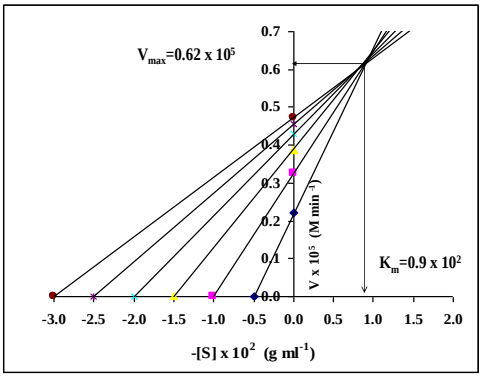

Figure 8. Eisenthal-Cornish Bowden plot of V vs. – [S] used for graphic evaluation of V_{max} and K_m for isoamylase enzyme

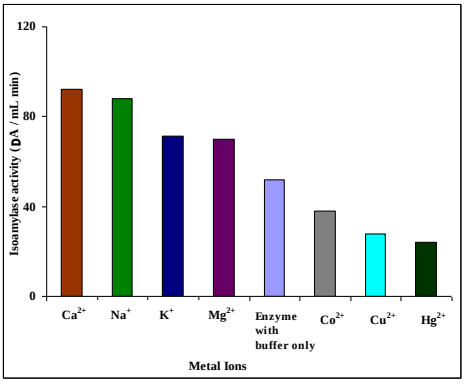

Figure 9. Changes of isoamylase activities with various metal ions

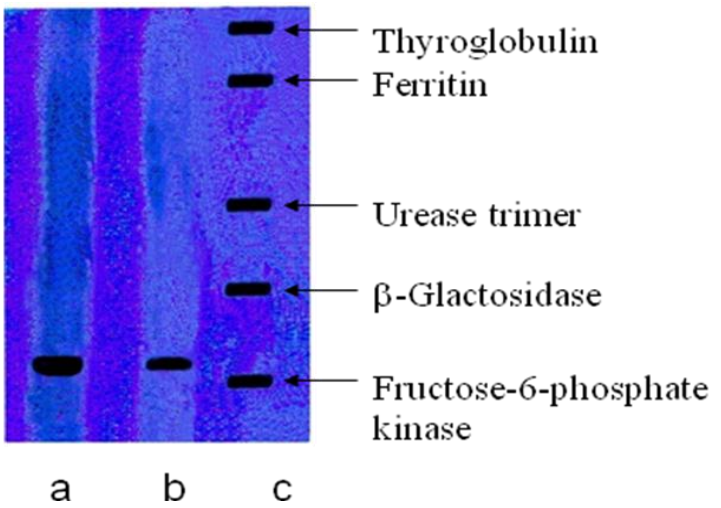

Figure 10. Photograph of non-sodium dodecyl sulphate polyacarylamide gel electrophoresis

(a) Purified isoamylase fraction obtained from Sephacryl S-200
(b) Purified isoamylase fraction obtained after successive purifications with Sephacryl S-200 and Sephadex G-100
(c) High Molecular Weight Marker Protein

Table 2. Relationship between Log of Molecular Weight of Standard Marker Proteins and Relative Mobility (R_f) Values Obtained from non SDS-PAGE

No.	Standard HMW marker proteins	MW (Dalton)	Log of MW	R_f
1	Thyroglobulin	667500	5.8244	0.054
2	Ferritin	439000	5.6425	0.171
3	Urease trimer	230000	5.3617	0.441
4	β-Glactosidase	139000	5.1430	0.621
5	Fructose-6-phosphate kinase	66500	4.8228	0.864

The R_f value of isoamylase was found to be 0.82 so that the molecular weight was determined to be 79430 Dalton.

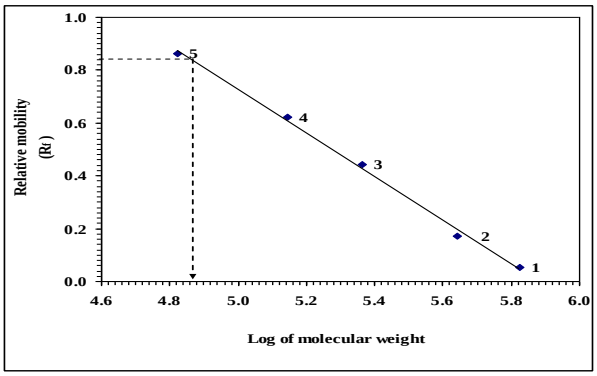

Figure 11. Plot of log of molecular weight of high molecular (HMW) marker proteins as a function of relative mobility (R_f) obtained from non-SDS-PAGE;
1. Thyroglobulin, 2. Ferritin, 3. Urease trimer,
4. b-Glactosidase and 5. Fructose-6-phosphate kinase

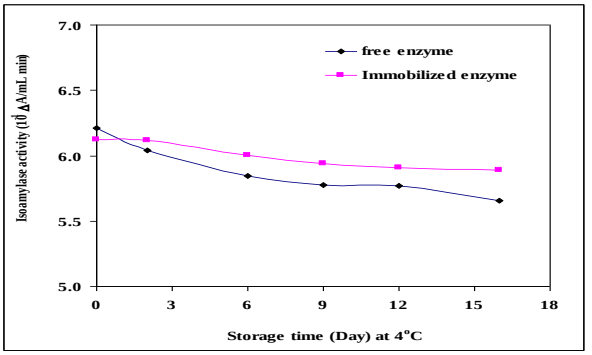

Figure 12. Plot of free and immobilized isoamylase activity as a function of storage time of the solution

Figure 13. Photographs of (a) cassava (b) soluble starch from cassava

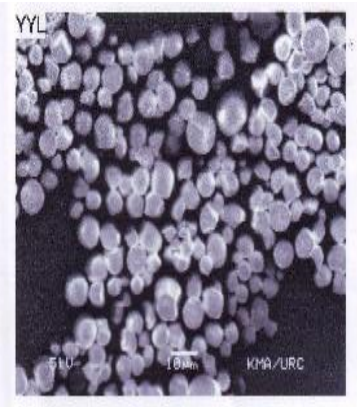

Figure 14. SEM microphotograph of soluble starch particles from cassava

Figure 15 Photograph of prepared maltose powder from cassava soluble starch

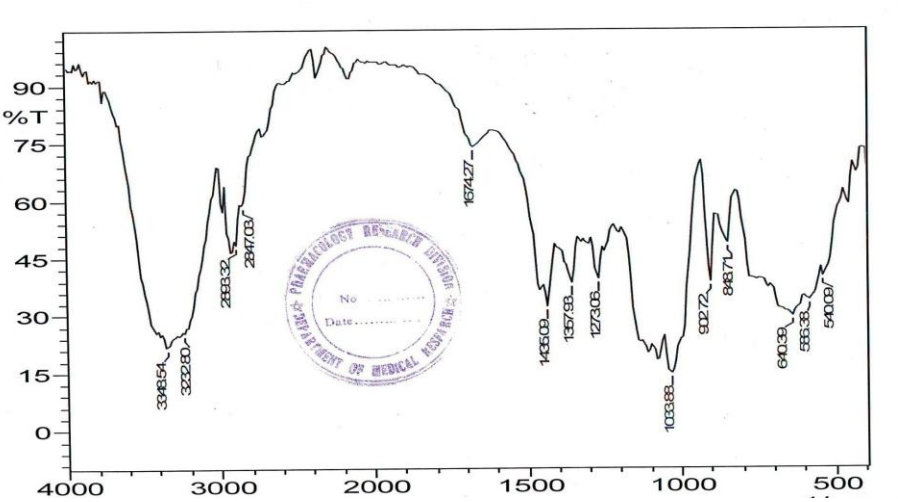

Figure 16. FT-IR spectrum of prepared maltose powder

Conclusion

The wavelength of maximum absorption of iodo-starch complex was formed to be 565 nm. Due to isoamylase action, the iodo-starch complex was decomposed and the λ_{max} shifted to 610 nm and significant decrease in absorbance value from 0.940 to 0.215. The isoamylase activity was found to be 28.98 EU per gram of pea embryo at final purification step. The homogeneity of the purified isoamylase was confirmed as a single band by non-SDS-PAGE. The molecular weight of purified isoamylase was determined to be 79430 Dalton. The optimum pH and temperature of the isoamylase enzyme was found to be pH 4 and 60^{o}C, respectively. The activation energy (E_a) of the isoamylase-catalyzed reaction was calculated to be 6.697 kcalmol^{-1}. The turnover number of the isoamylase-catalyzed reaction was found to be 4.92 x 10^{-2} min^{-1}. The reaction order was found to be first order (n = 0.98). By using the plot of Eisenthal-Cornish Bowden, the K_m and V_{max} values were found to be 0.90 x 10^{-2} gmL^{-1} and 0.619 x 10^{-5} Mmin^{-1}, respectively. The activation effects of Na^+, K^+ and Ca^{2+} were found 63.82, 51.15 and 81.56 %, respectively. Ca^{2+} has more activating effect than those of Na^+ and K^+ ions. The inhibitory effects of Hg^{2+}, Cu^{2+} and Co^{2+} ions on isoamylase activity were 73.73, 56.95 and 35.12 %, respectively. Hg^{2+} ion has more inhibitory effect than those of Cu^{2+} and Co^{2+} ions. The purified isoamylase was immobilized on oxycellulose support. The pH and temperature profile of free and immobilized isoamylase enzyme were same values of optimum pH 4.0 and optimum temperature 60°C. However, in the case of storage stability, the immobilized enzyme was more stable than free enzyme. During 16 day storage time at 4°C free isoamylase enzyme lost 9.01 %, whereas the immobilized enzyme lost only 3.84 %. The reducing sugar content (calculated as maltose) and glucose content in prepared maltose powder were 98.94% and 3.64 %, respectively.

Acknowledgements

The authors wish to express our deep gratitude to the Department of Higher Education, Ministry of Education, Yangon. We were also indebted to Dr. Kyaw Kyaw Khaung (Rector) and Dr. Nilar Aung (Pro-Rector), East Yangon University. We warmest thanks are also extended to Dr. Tin May San (Professor and Head), Department of Chemistry, East Yangon University for her effective suggestion, comments, encouragement and allowing for submission of this paper.

References

Bell, G.H., and Davidson, J.N., (1965), "Text Book of Physiology and Biochemistry", E. and S. Livingstone Ltd., London, 9

Chen, J.H., (1990), "Nucleotide Sequence and Expression of the Isoamylase Gene from Isoamylase-Hyper Producing Mutant, *Pseudomonas amylodermosa*", *JD 210, Biochim. Biophys., Acta*, **1087**, 309-315

Harda, T., Misaki, A., Alkai, H., and Yokobayashi, K., (1968), "Formation of Isoamylase by *Pseudomonas*", *Appl. Microbiol.*, **16**, 1439-1444

Harper, H.A., (1977), "Review of Physiological Chemistry", Lange Medical Pub., Tokyo, 128-129

Walsh, E.O.F., (1968), "An Introduction to Biochemistry", The English Universities Press, Ltd., London, 135-144

Yamamota, T., (1988), "Handbook of Amylase and Relative Enzyme", Pergamon Press, Oxford, 18-56